OUKA
Osaka University Knowledge Archive

Title	A Physico-Technical Step to ZnSe Blue Light Emitting Diode
Author(s)	Yodo, Tokuo
Citation	大阪大学, 1991, 博士論文
Version Type	VoR
URL	https://doi.org/10.11501/3086308
rights	
Note	

Osaka University Knowledge Archive : OUKA

https://ir.library.osaka-u.ac.jp/

Osaka University

A Physico-Technical Step to ZnSe Blue Light Emitting Diode

June 1991

Tokuo Yodo

A Physico-Technical Step to ZnSe Blue Light Emitting Diode

A Thesis

Submitted to College of Physical Science

of Osaka University

for the degree of

Doctor of Sciene

by

Tokuo Yodo

June 1991

Contents

Abstract 7

1. Introduction 10

1-1. Solid state properties required for blue light emitting diode (B-LED) 11

1-2. Background of B-LED fabricated using various materials 12

1-2-1. SiC 13

1-2-2. ZnSe and ZnS

1-2-3. GaN 15

1-2-4. Others 16

1-3. Why is ZnSe B-LED chosen as most hopeful material? 18

1-4. Purpose and significance of this study 20

1-5. Construction of this study 23

2. ZnSe epitaxial growth by metalorganic vapor phase epitaxy (MOVPE) 28

2-1. Heteroepitaxial growth

2-1-1. Layer thickness dependence 30

2-1-2. Reactor pressure dependence 35

2-1-3. Dependence of source gas mole ratio and gas velocity ratio on crystalline quality of ZnSe epitaxial layers (epilayers) grown by atmospheric pressure MOVPE 39

2-1-4. Growth temperature dependence 43

2-2. Homoepitaxial growth 48

2-2-1. ZnSe substrate preparation 50

2-2-2. ZnSe homoepitaxial growth 51

(A) Effect of heat treatment conditions of ZnSe substrate on crystalline quality of ZnSe homoepitaxial layer (homoepilayer)

(B) Origin of Self-activated (SA) emission in ZnSe homoepilayer 58

(c) Dependence of source gas mole ratio on crystalline quality of ZnSe homoepilayer 65

(D) Dependence of growth temperature on crystalline quality of ZnSe homoepilayer 75

3. Thermal stability of epilayer 148

3-1. Heteroepilayer 149

3-1-1. Effect of growth conditions on thermal stability of ZnSe epilayer 150

3-1-2. Effect of annealing conditions on thermal stability of ZnSe epilayer 151

3-1-3. Effect of ambient gases on thermal stability 154

3-2. Homoepilayer 156

4. p-type ZnSe by ion implantation 178

4-1. Li^+ ion implantation into ZnSe heteroepilayer 180

4-1-1. Effect of annealing conditions on crystalline quality of Li^+-implanted ZnSe heteroepilayer

4-1-2. Dependence of ion implantation and annealing conditions on crystalline quality, radiation damage and activation rate of acceptors in Li^+-implanted ZnSe epilayer 184

4-2. Na^+ ion implantation into ZnSe heteroepilayer 196

4-2-1. Effect of annealing conditions on crystalline quality of Na^+-implanted ZnSe heteroepilayer

4-2-2. Dependence of ion implantation and annealing conditions on crystalline quality, radiation damage and activation rate of acceptors in Na^+-implanted ZnSe epilayer 200

4-3. Li^+ ion implantation into ZnSe homoepilayer 204

4-4. Comparison of doping technique between vapor phase and ion implantation into ZnSe epilayer 207

5. Crystalline quality of ZnSe epilayer grown on Li^+-implanted ZnSe heteroepilayer and fabrication of ZnSe B-LED 255

5-1. Crystalline quality of undoped ZnSe epilayer on Li^+-implanted epilayer 256

5-2. Crystalline quality of n-type ZnSe epilayer on Li^{+}-implanted epilayer 261

5-2-1. Device structure and characteristics of ZnSe B-LED 262

5-2-2. Contrivance on device structure of ZnSe B-LED 268

6. Conclusion 291

7. Acknowledgement 294

8. References 295

9. Publication lists 303

Abstract

We discuss why ZnSe is chosen as one of the most hopeful materials for B-LED (blue light emitting diode) with high efficiency firstly. ZnSe is a difficult material to control electrical properties, particularly p-type conduction, because of the compensation effect inherent in II-VI compounds. Accordingly, the ZnSe B-LED with pn junction has never been fabricated. P-type ZnSe is hard to grow in general epitaxially. We have adopted metalorganic vapor phase epitaxy (MOVPE) to overcome the compensation effect. That is the sole possible technique that can be run at low temperature (250 ^{o}C). It is most important to grow the epitaxial layers (epilayers) with high crystalline quality. The crystallographic property should be excellent and the residual impurity concentration must be minimum. The crystalline quality is much related to lattice mismatching as well as growth conditions. We investigate the effects of growth conditions on the crystalline quality of both undoped ZnSe heteroepilayers and homoepilayers with complete lattice matching, and find the optimum growth conditions. Next, we examine thermal stability of the ZnSe epilayers grown at low temperatures to find that the crystalline quality of ZnSe epilayers is maintained even at 650 ^{o}C and still more to 700 ^{o}C by introducing Zn vapor in the ambience of annealing. We dope Li and Na impurities by ion implantation in the ZnSe epilayers and compare Li acceptor with Na acceptor in ZnSe. The result is that the radiation damage is related to activation rate of acceptor, generation rate of self-activated

centers and the crystalline quality. Li is superior to Na as p-type doping species in ZnSe because of the lightness of the radiation damage. We also dope Li impurities into ZnSe homoepilayers by ion implantation and try an n to p conversion. We fabricate the ZnSe B-LED with pn junction by growing n-type ZnSe on Li^+-implanted ZnSe and investigate the relation between the crystalline quality of n-type ZnSe and the properties of device. By improving the crystalline quality of n-type ZnSe, the blue light emission has been observed at 77 K from the B-LED. However, the EL emission is not seen at 300 K. It is suggested that the crystalline quality of Li^+-implanted ZnSe epilayers near the pn junction is much related to EL property, since the crystalline quality of the implanted epilayer fundamentally determines the crystalline quality of the over-epilayer. The crystalline quality of the epilayers should be improved near the pn interface. The fatal fault of the device structure using ion implantation is that pn interface is contaminated by the exposure to air at ion implantation, that degrades the crystalline quality at pn interface. We propose B-LED with a new device structure ("nipp-type"), by interposing an undoped ZnSe buffer epilayer on Li^+-implanted ZnSe before growing an n-type ZnSe epilayer. That is a method of devising the structure of the B-LED. We diffuse Li impurities into the buffer epilayer by sequent annealing to form a new pn interface (Li-diffused epilayer). Since the new pn interface is maintained relatively clean, the white-color EL emission is seen to eyes at 300 K with dominant blue spectrum. Thus keeping the crystalline quality near the pn interface is

found to be a key factor to emit the strong blue light at 300 K.

Unfortunately, the crystalline quality of the Li-diffused epilayer near the pn junction is not yet so good even in the nipp-type. It is therefore of vital importance to improve the crystalline quality near the pn interface all the more.

1. Introduction

II-VI compounds are materials produced massively from 1930's era as a luminous paint for the Braun tube of a television set [1]. Table 1.1 shows the general characteristics of typical II-VI compounds with those of other semiconductor materials. The II-VI compounds made by chemical reaction between II- and VI-family of elements have two characteristics: big ionic bonds and wide band-gap energies (E_g). In addition, the II-VI compounds have direct band structure, so that they have high transition probability of emitting and absorbing the visible light. Particularly, they are the most promising luminescence materials in visible spectrum we have ever known. Since the carrier mobilities of II-VI compounds are lower than those of other materials, however, they are not suitable materials for switching devices developed in Si, GaAs and InP. On the other hand, GaAs and InP of III-V compounds have direct band structure which Si does not have, and carrier mobility higher than that in Si. Therefore, the research of III-V compounds has been powerfully proceeded for the purpose of developing micro-opto electric materials.

Actually, E_g of Si and III-V compounds (GaAs and InP) is very small. Thus it is intentionally tried to enlarge E_g by alloying GaAs, AlAs and GaP. Red light emitting devices are already on the market. To develop the green light emitting devices with wavelength shorter than red, GaP of III-V compounds with device structure of pn junction is used. However, GaP is not suitable for emitting devices with high efficiency because of having indi-

rect band structure. Nevertheless, the efficiency of green light emitting devices is heightened by introducing isoelectric traps like nitrogen (N) in GaP, or localized impurities, thus delocalizing k-space of impurity levels, which extends to conduction and valence bands without accompanying phonons [2]. However, even E_g of GaP is too small to cover the visible spectrum. Other III-V compounds with wider band-gap like GaN is needed for emitting visible light. Since E_g of II-VI compounds coincides just with the visible spectrum, II-VI compounds are widely suitable for devices emitting the visible, and even ultraviolet spectra. In the absence of pn junction, however, such devices are not realized yet by II-VI compounds.

Generally, it is more difficult to control the electrical properties of p- and n-type of II-VI compounds owing to the increase in E_g, that makes the ionicity higher. It is needed to reexamine the crystal growth of II-VI compounds basically.

1-1. Solid state properties required for blue light emitting diode (B-LED)

Human visual sensitivity is greatly dependent on the wavelength (Fig. 1.1.). That for blue spectrum is about 10 times as small as one for green spectrum. Accordingly, development of B-LED with high luminescent efficiency is especially required.

One solid state property required for B-LED materials is that E_g has to be bigger than 2.6 eV (480 nm; blue spectrum region).

Developing a blue laser diode in the future, the material with direct band structure is very advantageous. In order to emit the blue light efficiently, the structure of the device needs to be discussed. Namely, it is important to lock the carriers up and to increase the efficiency of the injection by selecting the device structure. Moreover, controlling electrical properties of II-VI compounds is an essential factor for development of the B-LED. Controlling lattice constant and E_g is important for the crystal growth with high crystalline quality and the development of the B-LED with high efficiency.

In order to realize the B-LED, obtaining the large substrate with high crystalline quality is needed to grow the epitaxial layers (epilayers) with high crystalline quality. It means that the lattice matching is an important factor for fabricating devices with high efficiency like laser diodes. It is mainly because homoepitaxial growth with lattice matching is possible while keeping the crystalline quality of the epilayers. It is also important to fabricate the devices massively in the future to make the process easy.

1-2. Background of B-LED fabricated using various materials

SiC, ZnS, ZnSe, GaN, boron nitride (BN), diamond and I-III-VI_2 compounds (chalcopyrite type) are considered as hopeful materials for B-LED. In this section, we discuss the characteristics of these 7 materials from the viewpoint of developing the B-

LED with high efficiency.

1-2-1. SiC

Only SiC B-LED is on the market [3]. Both Si and C are IV-family elements, and join common bonds. However, SiC has an ionicity of about 12 % because of the difference in electrical affinity. Since SiC is chemically very stable and strong against mechanical force as well as radioactive rays, it is noted as a proof-device against environment. However, the SiC crystal has to be grown at a very high temperature of 2200 ^{o}C. It is known that some poly-type of SiC crystallite exist by the difference in piling atoms up. Therefore it was very difficult to obtain a uniform hexagonal SiC crystal with a single phase [4]. The E_g of SiC is 3.04 eV (408 nm; ultraviolet spectrum) at room temperature and the band structure is indirect transition type. The transition has to be accompanied by phonons and the probability is very low. In fact, the external quantum efficiency of SiC B-LED is about 0.02 %.

1-2-2. ZnSe and ZnS

Both ZnSe and ZnS are II-VI compounds and their characteristics are much analogous to each other. ZnS and ZnSe have E_g of 3.7 and 2.7 eV (457 nm and 335 nm), respectively. The band struc-

ture is direct transition type. Then, the B-LED using ZnSe or ZnS with high efficiency seems to be hopeful. In ZnS, the B-LED has to utilize the transition emission related to deep levels (they are well-known as self-activated (SA) centers.). In ZnSe, the band-edge emission is used as the main blue electroluminescence (EL) emission from the B-LED. It thus becomes important in the fabrication of the ZnSe B-LED to suppress the concentration of SA centers in ZnSe crystal growth. The hexagonal structure changes into cubic one at 1050 ^{O}C in ZnS when increasing the growth temperature [5]. The entropy difference between respective structure is very small, so that high concentration of poly-type of crystallite and stacking faults are easily generated during ZnS crystal growth [6]. The phase transition temperature is 1420 ^{O}C in ZnSe. Thus the low growth temperature is essential to grow bulk crystal with high crystalline quality, since the concentration of stacking faults becomes very low. Indeed, ZnSe or ZnS bulk crystal grown at 850 ^{O}C by iodine vapor transport method has no twins and a low density of stacking faults [7]. But the high density of iodine impurities (about 200 ppm) are included in the bulk crystal. Also the constituting elements and compounds themselves of II-VI compounds have very high vapor pressures [8-10] (for example, Zn; 0.1 Torr at 400 ^{O}C, Se; 10 Torr at 431 ^{O}C, ZnSe; 10^{-5} Torr at 600 ^{O}C, S; 10 Torr at 241 ^{O}C, ZnS; 10^{-5} Torr at 600 ^{O}C.). The high concentration of native defects (Zn, Se and S vacancies) occur in bulk crystal grown at high temperatures and easily make complexes (so-called SA centers) with impurities. The high density of SA centers compensate the impurities in the bulk

crystal and increase the resistivity of the bulk crystal drastically (it is well-known as self-compensation effect.). Therefore, it becomes impossible to control the electrical properties. Particularly, p-type ZnSe and ZnS cannot be grown, though n-type ones are grown. Thus the self-compensation is a phenomenon peculiar to II-VI compounds and much related to ionicity [11-17]. Comparing ZnS and ZnSe, ZnSe has a possibility of p-type conversion higher than ZnS because of its lower ionicity.

The ZnSe and ZnS epilayers with high crystalline quality have recently been grown at low temperatures (200-350 ^{o}C) by molecular beam epitaxy (MBE; [18-21]), metalorganic vapor phase epitaxy (MOVPE; [22-25]), metalorganic molecular beam epitaxy (MOMBE; [26,27]) and atomic layer epitaxy (ALE;[28]) under non-equilibrium conditions. The generation rates of native defects and SA centers are greatly repressed by low growth temperatures. Therefore, it is hoped that p-type ZnSe can be grown in the future.

1-2-3. GaN

E_g of GaN with direct band structure is 3.39 eV at room temperature and the crystal structure is hexagonal. Therefore, GaN B-LED has to use the transition emission related to deep levels. The melting point of GaN is 1727 ^{o}C and the deposition pressure of N sources is very high. The crystal growth of bulk crystal has been very difficult. Only the film growth has been reported by chemical vapor deposition (CVD) and MOVPE [29-31]. Generally,

NH_3 with high thermal stability is used as a N source, so that the growth has to be made at high temperature. This causes high density of N vacancies in the film. Certainly, n-type GaN is obtained easily, but p-type GaN not. The GaN B-LED with pn junction has not been fabricated yet. In order to repress the concentration of N vacancies, we have to grow GaN epilayers at such low temperatures as 300 ^{o}C. However, it is very difficult because of high thermal stability of N sources.

In this situation, Al_2O_3, SiC and GaP are also used as substrates in place of GaN. However, both the lattice mismatching between GaN and their substrates and the difference in the thermal expansion coefficient are very large. For example, in the Al_2O_3 substrate, the lattice mismatching is as large as 13.8 %. A high concentration of cracks are then created in GaN layers and it is difficult to grow uniform and smooth layers. GaN has been already reported to have a PL efficiency of 12 % because of direct band structure [32]. Also GaN B-LED with MIS structure has a high quantum efficiency of 0.3-1 % [29,33-36]. This indicates the advantage of direct band structure.

1-2-4. Others

As other materials for B-LED, BN, diamond and I-III-VI_2 compounds are hopeful. BN is grown under ultra high pressure as in the case of diamond and its solid state properties are known very little. All we know is that the E_g of BN is 7-8 eV and its

band structure is indirect transition type. The external quantum efficiency of the reported BN B-LED is about 0.001 %. Diamond has been thought to have a possibility of semiconductor material for two decades. Recently, natural II_b- type of diamond shows p-type conduction. The E_g is 5.5 eV and the band structure is indirect transition type. It has recently been shown that the layer growth of diamond is possible by vapor phase under reduced pressure. Though both p-type and n-type diamond is grown, the resistivity of n-type diamond is about 10^3-10^5 Ω·cm and the doping efficiency of n-type dopant is very low compared with p-type doping. The solid state property is needed to be investigated basically. The reported emission voltage of diamond B-LED with pn junction is about 150 V. $CuAlS_2$ and $CuAlSe_2$ of I-III-VI_2 compound have direct band structure with peak energies near 2.5 eV. Indeed both the ionicity and melting point of I-III-VI_2 compound are lower than those of II-VI compounds, so that it is advantageous for the crystal growth. But, high concentration of twins are generated in the bulk crystal and the crystal is poly-crystallized since the stiffness of I-III-VI_2 compounds is softer than that of II-VI compounds. Moreover, as the phase changes from zinc-blend to chalcopyrite, numberless fine cracks occur in bulk crystal by the directional thermal expansion during the crystal growth. Kukimoto points out that it is difficult to develop the blue laser diode (B-LD) only by II-VI compounds because of lattice matching and band gap energy. He suggests that I-III-VI_2 compounds are required for the B-LD from the wide feasibility of lattice constants and band-gap energies of alloys.

1-3. Why is ZnSe B-LED chosen as most hopeful material?

In section 1-2, we have discussed the research circumstances on seven hopeful materials for B-LED. We will give reasons why ZnSe is chosen as most hopeful in this section.

Since SiC, BN, I-III-VI_2 compounds and diamond are possible to form pn junction, it is easy to fabricate the B-LED. However, the development of B-LED with high efficiency using all these materials except I-III-VI_2 compounds will be limited in the near future since they have indirect band structure. It is time that the strength of the green light emission of GaP LED with indirect band structure has increased by 4 times in a decade by the introduction of isoelectric traps. But the external quantum efficiency remains only 0.3 %. The BN and diamond with pn junction have recently been reported. The p-type and n-type of BN crystal with a low resistivity is not obtained yet, however. Special and expensive machines are required for the crystal growth. Diamond layers are recently grown under the reduced pressure by microplasma CVD. The mechanism why diamond is grown under the reduced pressure is not known yet. Furthermore, even the physical properties of chalcopyrite type of I-III-VI_2 compounds are not well known yet. On the other hand, SiC B-LED with pn junction is already on the market. But it is not widely used because of the indirect band structure. The efficiency of the blue light emission is too low. It has to be increased by 5-6 times at least for a wide use. Isoelectric traps in SiC have been looked for the development of SiC B-LED with high efficiency. Be that as it

may, the material with indirect band structure is not hopeful after all. GaN of III-V compounds, ZnSe and ZnS of II-VI compounds have the direct band structure. It is expected that B-LED with high efficiency using these materials will be fabricated. Unfortunately, crystal growth with p-type conversion is not realized. Thus the device structure of the B-LED is not with pn junction but with metal-insulator-semiconductor (MIS) structure. The device structure required in the future, however, should be a device with pn junction, in view of a possible extension to the development of B-LD.

We have to judge which of these materials will be the first to realize the crystal growth with p-type conduction. In the crystal growth of GaN, temperature higher than 900 ^{o}C is needed for thermal stability of N sources. It is impossible to grow at 300 ^{o}C to avoid N vacancy in the crystal. ZnS has a wide band gap. The blue light emission from ZnS B-LED has to utilize transitions related to SA center levels. Meanwhile E_g of ZnSe corresponds to the energy of blue light; then ZnSe B-LED may utilize transitions of band-edge emission without SA emissions. It seems that ZnS is more difficult than ZnSe to grow material with p-type conduction. The crystal growth of ZnS and GaN bulk is too difficult to grow homoepilayers with high crystalline quality. In addition, these two materials do not have good substrates lattice-matched with the layers. The electrical properties of ZnS and GaN layers thus cannot be controlled well. ZnSe, on the other hand, has a GaAs substrate with a small lattice mismatching of 0.27 %. ZnSe is in a delicate position from the calculation under

thermal equilibrium conditions whether p-type material can be grown or not. Furthermore, ZnSe has recently been grown epitaxially at low temperatures (200-350 ^{o}C). It has been reported that the generation rate of native defects is completely suppressed by low temperature growth techniques like MBE, MOVPE, MOMBE and ALE [37].

From these points, we choose ZnSe as a hopeful material for B-LED and investigate ZnSe from the crystal growth in this research.

1-4. Purpose and significance of this study

Here we state the purpose and significance of this study. First we clarify the problems of ZnSe epitaxial growth and show the way to solve them in order to develop B-LED.

It is required to grow epilayers with high crystalline quality and to dope acceptors into the epilayers without creating native defects. To the first place, we introduce MOVPE epitaxial growth and control the concentration of native defects as well as residual impurities by making growth at low temperatures. Then we try to grow undoped ZnSe epilayers with high crystalline quality as a body to realize p-type ZnSe. To the second place, we discuss the effects of lattice mismatching on the crystalline quality and the optimum growth conditions for growing ZnSe homoepilayers with high crystalline quality. To the third, we discuss the thermal stability of ZnSe epilayers grown at low temperatures. And we

find the high temperature annealing conditions with keeping a good crystalline quality. We apply the result to post-annealing after ion implantation of p-type dopants in order to activate acceptor level efficiently without creating SA centers.

The significance of this study is fourfold. Firstly, ZnSe epilayers with mirror-like surface morphologies are grown at 250 ^{o}C using dimethylzinc (DMZ) and hydrogen selenide (H_2Se) as source gases in MOVPE. It has been widely accepted that the source gases would, even at room temperature, react chemically during the transportation to degrade the crystalline quality and the surface morphology drastically. As Se sources, accordingly, other Se alkyls (such as dimethyl selenide (DMSe) or diethyl selenide (DESe)), which do not react chemically with DMZ in the vapor phase, are used in place of H_2Se to grow ZnSe epilayers with excellent surface morphologies. Since Se alkyls have the high deposition temperature, however, ZnSe epilayers are not grown at temperatures less than 500 ^{o}C. As a result, a high concentration of native defects are generated in the epilayers grown using Se alkyls. Thus repressing chemical reaction in the vapor phase is inconsistent with the epitaxial growth at low temperature.

Secondly, one has to investigate the evil influence of lattice mismatching and to report ZnSe homoepitaxial growth with complete lattice matching as the most reasonable solution. In this study, we discuss the optimum conditions for ZnSe homoepitaxial growth, which has never been reported so far. Therefore, it is significant to report the systematic growth conditions on

homoepitaxial growth. Since the ZnSe substrates ($10x10x0.7$ mm^3) used in this study are grown at relative by low temperature (850 ^oC) by iodine transport, they have no twins and low etch pit density ($2x10^4$ cm^{-2}) despite a high concentration of iodine impurities included in bulk crystal.

Thirdly, the fabrication process of ZnSe B-LED is required for the formation of electrodes etc. If ion implantation is used as one of p-type doping techniques, moreover, the post-annealing is needed to recover the crystalline quality and to activate the impurities electrically. The thermal stability of ZnSe epilayers grown at low temperatures (250 ^oC) has never been discussed, however. We will discuss the relation between the thermal stability and the growth conditions. We find the optimum annealing conditions without generating SA centers at 700 ^oC and even apply them to post-annealing after ion implantation for the realization of p-type ZnSe. Furthermore, this result can be undoubtedly applicable to post-annealing after ion implantation of n-type dopants.

Fourthly, we will discuss ion implantation of Li^+ and Na^+ ions as p-type dopants. Ion implantation into ZnSe epilayers with high crystalline quality has never been reported before, though ion implantation into ZnSe bulk crystal with a high concentration of SA centers was already reported more than a decade ago. In the p-type doping through vapor phase, the source of p-type dopant has to be of high purity despite the thermal instability at low temperatures around 200 ^oC. The ion implantation technique can dope impurities under non-equilibrium condition with high purity

and high concentration. On the other hand, the radiation damage is a main problem for ZnSe epilayers. We will discuss its effect on the crystalline quality, which has never been investigated.

Fifthly, we mention the crystalline quality of undoped and n-type ZnSe epilayers grown again on Li^+- implanted ZnSe epilayers, which is the first step of fabricating ZnSe B-LED.

Finally, we find the device characteristics much related to the degradation of crystalline quality of n-type ZnSe epilayers which is caused by propagation of radiation damage generated in the p-type ZnSe. We discuss the device structure to clarify that the efficiency and monochrome of the EL emission are related to the crystalline quality of epilayers near pn junction.

1-5. Construction of this study

Construction of this study is divided into 5 parts. In chapter 2, the epitaxial growth by MOVPE is discussed from the viewpoint of obtaining ZnSe epilayers (homo- and hetero-epilayers) with high crystalline quality. New growth techniques like MBE, or MOVPE etc. can produce ZnSe epilayers with high crystalline quality at low growth temperatures. Zn and Se atoms in ZnSe have vapor pressure higher than As atom in GaAs. It is an inevitable problem peculiar to II-VI compounds. Also ZnSe itself has the high vapor pressure of about 10^{-5} Torr at 600 ^{o}C. If not only the epitaxial growth but also thermal processes after the growth (for example, the annealing after ion implantation etc.) are made at

high temperatures, it would be feared that the epilayers are degraded due probably to the generation of many deep centers (or SA centers) or native defects. Details have little been reported on thermal stability of ZnSe epilayers grown at low temperatures yet, however. In chapter 3, we report the thermal stability of ZnSe epilayers (heteroepilayer: section 3-1.; homoepilayer: section 3-2.) and discuss the effect of the growth conditions on the crystalline quality and the optimum annealing conditions without generating SA centers even at high temperatures. We apply the optimum annealing conditions found in chapter 3 to the realization of p-type ZnSe doped by ion implantation in chapter 4. In chapter 3, the relation between thermal stability of the epilayers grown at 250 ^{o}C and growth conditions is discussed. The optimum annealing conditions not creating native defects are also investigated at temperatures higher than 650 ^{o}C. In chapter 4, ion implantation of Li^{+} and Na^{+} ions is discussed together with annealing conditions (temperature, period and atmosphere) in p-type doping. The activation rate and radiation damage are also discussed. In chapter 5, the crystalline quality of undoped and n-type ZnSe epilayers grown again on Li^{+}-implanted ZnSe epilayers is discussed. This is the first step of fabricating ZnSe B-LED. Indeed ZnSe B-LED is fabricated actually, and its device characteristics are investigated at various ion implantation conditions, each of which determines the crystalline quality of the epilayer. The device structure is discussed for maintaining the crystalline quality of the epilayers near pn junction. By adopting such a device structure, it is highly expected that the

device can emit blue light at 300 K.

Table 1.1. General characteristics of II-VI compounds and the other semiconductor materials.

Compounds	Energy gap(ev) (300K)	Type of transition	Electronic mobility ($cm^2 \cdot v^{-1} \cdot s^{-1}$) (300K)	Electronic effective mass	Ionicity
Ge	0.67	Indirect	4000	1.58, 0.08	0
Si	1.11	Indirect	1500	0.91, 0.19	0
GaAs	1.43	Direct	9000	0.065	0.31
GaP	2.3	Indirect	180	0.35	0.33
CdSe	1.73	Direct	650	0.13	0.70
ZnTe	2.25	Direct	100	0.11	0.61
CdS	2.42	Direct	350	0.20	0.69
ZnSe	2.67	Direct	200	0.17	0.63
ZnS	3.66	Direct	150	0.28	0.62

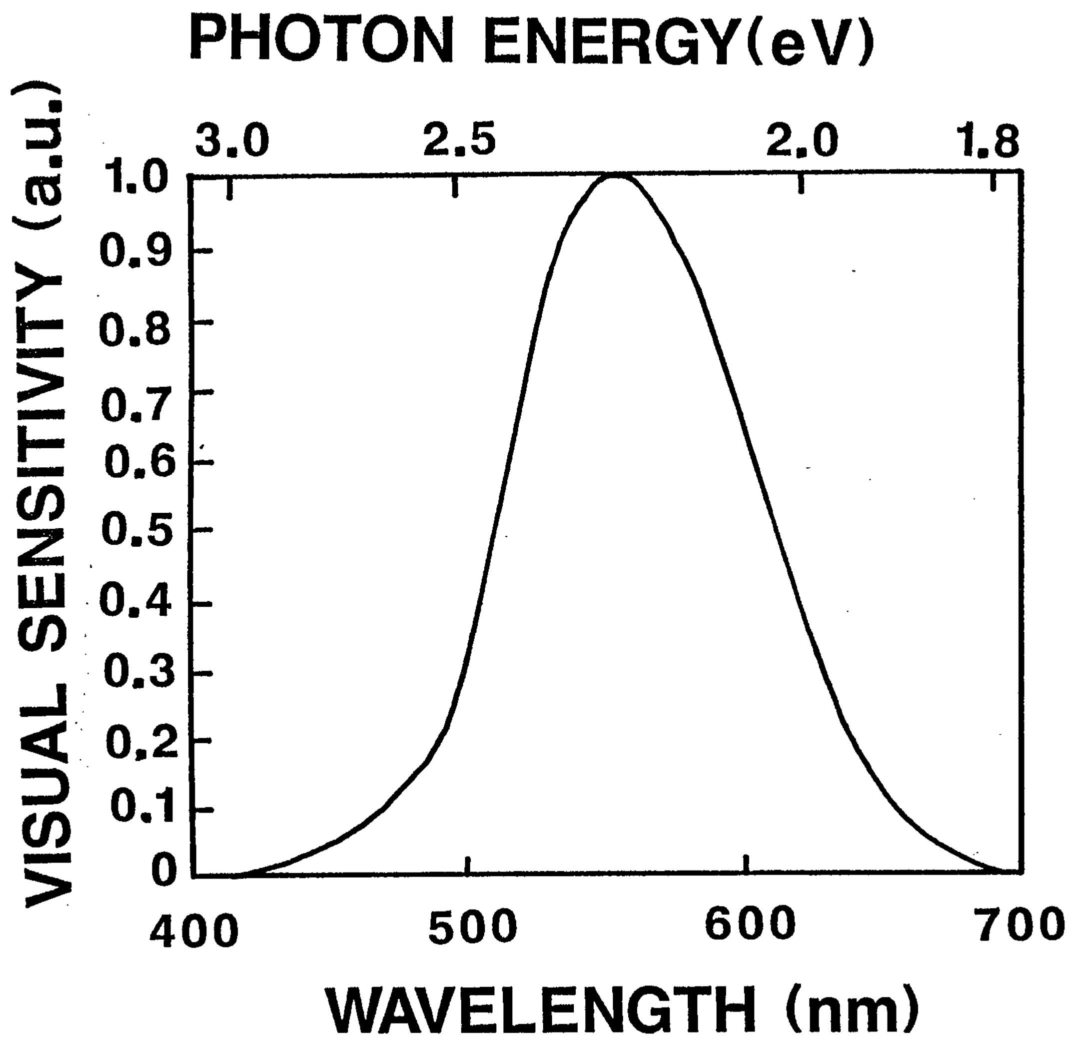

Fig.1.1. Human visual sensitivity is greatly dependent on the wavelength.

2. Epitaxial growth

In the past, several attempts were made to grow p-type ZnSe [38-40]. Few successful results have been reported so far. However, it is thought that an undoped ZnSe crystal contains both high density of residual impurities and native defects. These defects easily compensate the p-type impurities [12]. So it is most essential to reduce the density of the residual impurities during the epitaxial growth of undoped ZnSe. The crystal growth process in MOVPE is governed by chemical reaction, which is far from the thermal equilibrium situation, so that low temperature growth of II-VI compounds is possible. Low temperature growth processes in II-VI compounds are essential to grow the ZnSe epilayers with high crystalline quality for obtaining p-type conversion if the self compensation effect is to be suppressed.

Many investigators have been trying to fabricate the ZnSe B-LED with pn junction using several growth techniques for the past two decades. ZnSe single crystals with high crystalline quality were indeed epitaxially grown at low temperatures (250-350 ^{o}C) by MOVPE [38,41-49] and MBE [39,50,51].

2-1. Heteroepitaxial growth

In the MOVPE growth of ZnSe, two kinds of source combinations have been utilized [38-40, 41-46]. When zinc alkyls (for example, DMZ or diethylzinc (DEZ)) and H_2Se are used as source materials,

they react easily to form powder in the gas phase, even at room temperature, before the epilayer is grown on the substrate. Stutius [38], Fujita et al. [41] and Yoshikawa et al. [42] prevented such a chemical reaction by introducing zinc alkyls just above the substrate in the low pressure reactor (0.1 Torr), and the ZnSe epilayers could be grown at 300 ^{o}C with this source combination. The ZnSe epilayers grown in this manner, however, show poor surface morphologies characterized by hillocks along the <0$\bar{1}\bar{1}$> direction in epilayers thicker than 1 μm [10].

Recently, Kamata et al. [45] have reported that the ZnSe epilayers with mirror surface morphologies can be grown at 500 ^{o}C when Se alkyls, which are free from undesirable premature reactions, are used instead of H_2Se. In this case, however, it is difficult to obtain epilayers grown at temperatures lower than 500 ^{o}C, reflecting the thermal stability of Se alkyls. It is more than hard, accordingly, to grow ZnSe epilayers with both mirror-like surface morphologies and high crystalline quality at low temperatures (200-350 ^{o}C). Since the low growth temperature is an essential factor, we utilize DMZ and H_2Se as source gases for MOVPE and try to find the optimum conditions to grow the ZnSe epilayers with mirror-like surface morphologies.

We investigate the effect of the lattice mismatching on the crystalline quality first and discuss the importance of lattice matching. We report ZnSe homoepitaxial growth from the viewpoint of lattice matching and ZnSe heteroepitaxial growth, particularly effects of reactor pressure, growth temperature, source gas mole ratio and source gas velocity ratio on the over-all crystalline

quality including surface morphology of the ZnSe epilayers in this section.

2-1-1. Layer thickness dependence

The purpose of this section is to investigate the effects of lattice distortion due to the lattice mismatching on crystallographic, electrical and luminescence properties of ZnSe epilayers on GaAs substrates by examining the variation of those properties with epilayer thickness. In addition, we will discuss the importance of the lattice matching in the epitaxial growth.

The ZnSe epilayers were grown under the reduced pressure of 0.1 Torr at 300 ^{o}C and source gas mole ratio ([Se]/[Zn]) of 3 by MOVPE using DMZ and H_2Se (the respective flow rates are $3.1x10^{-5}$ and $9.3x10^{-5}$ mol/min.) as source gases. The MOVPE growth system used in this work is illustrated in Fig. 2.1.1. The reactor is of vertical design. The center tube carrying zinc alkyls extends to about 2-3 cm above the GaAs substrate on a SiC coated carbon susceptor. GaAs substrates were heated by a conventional electric furnace. Chemically polished Cr-doped semi-insulating (100) GaAs substrates were etched in a solution of H_2SO_4 :H_2O_2 :H_2O =4:1:1. The GaAs substrates were thermally annealed at 600 ^{o}C for 10 minutes at 0.1 Torr under the hydrogen (H_2) atmospheric gas just before growth. In order to investigate the effects of lattice mismatching on the properties of ZnSe/GaAs by MOVPE, ZnSe epilayers with different epilayer thickness were grown on Cr-doped

semi-insulating GaAs substrates. Under these condition, the growth rate was 3.0 μm/h and the epilayer thickness was easily controlled by choosing a suitable period of growth.

To characterize the epilayers, a Nomarski phase contrast interference microscope and PL were utilized to observe the surface morphology and to measure the PL properties. The PL spectra were measured at 4.2, 77 and 300 K, using a He-Cd laser (λ=325 nm) adjusted to a light power of 6 mW as the excitation source. All epilayers were mounted without adhesion to avoid the effects of strain.

Let us discuss the results of the crystallographic property of the ZnSe epilayers with various epilayer thickness. Figure 2.1.2 shows the variation of the X-ray rocking curve from (400) diffraction of ZnSe epilayer with epilayer thickness (t_g). In a thin epilayer (t_g=0.5 μm), CuK $_1$ and CuK $_2$ reflection peaks from both ZnSe epilayer and GaAs substrate are seen to be clearly resolved. The lattice parameter estimated from the position of CuK $_1$ peak for 0.5 μm is 5.681 A (a'_1), a value which is larger than that of bulk ZnSe (a_0=5.669 A) [52]. From this clear evidence, it is assumed that the epilayer suffers tetragonal distortion, since the lattice constant of GaAs (a_{GaAs}=5.653 A) is smaller than that of ZnSe. If the Poisson ratio $\nu=2C_{12}/C_{11}$ (C_{ij}: elastic constants) is taken as 1.2 for cubic ZnSe [53], the lattice parameter in a direction normal to the interface of the epilayer with perfect tetragonal distortion can be calculated as a_1=5.688 A. Then, a_1 is slightly larger than a'_1 for 0.5 μm, suggesting that the relief of the mismatching strain occurs

within the epilayers. As the lattice parameters in thick epilayers (t_g>2 μm) are almost the same as that of bulk ZnSe, it is reasonable to conclude that the strain due to lattice mismatching is relieved with increasing t_g and that the epilayer becomes almost free from the strain at a position farther than 2 μm away from the interface. Since the relief would occur with the creation of dislocation [50,54], they may be distributed with high density within the epilayer, where the strain is relieved.

Next let us see electrical properties of the ZnSe epilayers with different layer thickness. All the undoped ZnSe epilayers grown under the conditions employed here were highly n-type (a carrier concentration of $9x10^{16}$ cm^{-3}) except for thin epilayers (t_g<0.5 μm) which showed high resistivity. The electrical properties of the epilayers with different epilayer thickness are listed in Table 2.1.1, where the compensation ratio is seen to increase with reducing t_g. The temperature dependence of the Hall mobility (μ_H) of the epilayers as a parameter of t_g is indicated in Fig. 2.1.3. At 77 K, it is seen that μ_H is noticeably reduced with decreasing t_g, reflecting the increase in impurity concentration. Though quantitative impurity analysis has not been made here, such impurities as Al, Na and Li were detected by secondary ion mass spectroscopy (SIMS). The concentration of Al, roughly estimated, was of the order of 10^{17} cm^{-3}, while Na and Li were observed to be piled up over 0.2 μm from the interface. Main donor species possibly responsible for the high carrier concentration of the epilayers, therefore, could be considered to be Al which is probably included in the DMZ source. If one assumes that

impurities can be easily accumulated in the region where the dislocation density is high, the reduction in μ_H in the thin epilayers can be understood, since the high alkaline impurity concentration by contamination causes strong compensation. This supposition is consistent with the results in Table 2.1.1. On the other hand, the high Hall mobility for thick epilayers could be explained by taking into account the fact that the epilayers with low dislocation density are extended far from the hetero-interface.

Next let us discuss the photoluminescence (PL) properties of the ZnSe epilayers with different epilayer thickness. The PL spectrum of the epilayer varies with t_g as shown in Fig.2.1.4. It should also be noted in the MBE growth of ZnSe on GaAs that Yao [50] has noted an effect of thickness of the epilayer on the PL properties. Results similar to those in Fig.2.1.4 have been reported by Stutius [55], who observed a strong near band-edge (BE; the emission line is identified with free-to-bound transitions.) emission at 2.689 eV that predominated over the entire spectrum at 300 K. A noticeable feature in the thin epilayers (t_g=0.5 μm) is that several deep level emission bands appear with an appreciably strong intensity. For thick epilayers, on the other hand, only the so-called SA emissions peaking at around 2.08 eV in the low energy region appear, and their intensity is quite weak. On the basis of these facts, and the discussion in the crystallographic property, one may suggest that the two emission bands labeled D_1 and D_2 occurring at an energy region lower than 2.0 eV are related to deep complex centers caused by dislocations and/or

some impurities. Figure 2.1.5 shows 4.2 K spectra and FWHM of the I_x emission, excitonic emission bound to neutral donor, as a parameter of t_g. With reducing t_g, linewidth of I_x emission becomes much broader, suggesting the effects of impurity accumulation as well as strain [56].

In summary, the most interesting fact revealed by the present work is that the tetragonal distortion due to lattice matching is relieved with increasing the epilayer thickness and the epilayer becomes almost free from the distortion at a position of 1-2 μm away from the hetero-interface. With the assumption that the strain relief in the vicinity of the interface is caused by the production of some kind of dislocations [54,57], the variation with the epilayer thickness of the electrical properties and the photoluminescence could be interpreted in terms of impurity accumulation due to high dislocation density within a thin epilayer near the interface. It is thus evident that even a small lattice mismatching of 0.27 % between ZnSe and GaAs causes the degradation of the crystalline quality of the ZnSe epilayers. Indeed a heavy degradation is observed near the interface. To grow the ZnSe epilayers with crystalline quality high enough to dope p-type impurities, alloy growth of $ZnS_xSe_{1-x}/GaAs$ (x=0.06) with lattice matching, ZnSe homoepitaxial growth and ZnSe heteroepitaxial growth with thick epilayer thickness more than 10 μm should be tried. We shall discuss the ZnSe homoepitaxial growth in the next section 2-2.

2-1-2. Reactor pressure dependence

In this section, we discuss the dependence of reactor pressure at different growth temperatures on the crystalline quality of the ZnSe epilayers and find the optimum reactor pressure of growing the ZnSe epilayers with high crystalline quality. The growth conditions employed in this experiment were that the growth temperatures were 200-500 ^{o}C, [Se]/[Zn] was 3, the flow rate of DMZ ([DMZ]) was $3.2x10^{-5}$ mol/min and the reactor pressures were changed from 0.1 to 10 Torr. The MOVPE growth system used in this work is illustrated in Fig. 2.1.1. Generally, in the combination of DMZ/H_2Se, the chemical reaction in the vapor phase is repressed by reducing the reactor pressure. It is not yet clarified, however, whether the chemical reaction is completely controlled by lowering the reactor pressure, since it is also related to the design of reactor. The reactor pressure is controlled by adjusting the valve before the rotary pump.

Figure 2.1.6 shows the dependence of the reactor pressure on the growth rates of the ZnSe epilayers grown at different temperatures. As the reactor pressure increases, the growth rate increases and saturates at around 1 Torr. This reactor pressure dependence is almost independent of the growth temperature between 280 and 320 ^{o}C. Since the respective flow rates are kept constant, the increase in reactor pressure leads to decrease in respective flow velocities and to increase in concentration of the source gases. The saturating phenomenon is then thought to be due to the formation of some polymers in chemical reaction. The

saturation pressure is naturally dependent on the growth temperature. Actually, at 400 $^{\circ}$C, the saturation is not seen even at 10 Torr. Though the re-evaporation is prominent at 400 $^{\circ}$C and 0.1 Torr, it is repressed by increasing the reactor pressure to 10 Torr. The sticking coefficient of the source gases on the substrates is heightened. Though the chemical reaction at 400 $^{\circ}$C is rather serious, high crystalline quality is still maintained. Increase in reactor pressure does not always cause a degradation in crystalline quality.

Figure 2.1.7 shows surface morphologies of the ZnSe epilayers grown at 350 $^{\circ}$C and different reactor pressures (0.1 and 6.2 Torr). The directional hillocks along $\langle 0\bar{1}\bar{1}\rangle$ are observed independently of the reactor pressure. Namely, such a hillock structure is generated by other causes. The origin of the hillocks is not due to chemical reaction, but probably related to re-evaporation of VI-family of atoms. From the viewpoint of chemical reaction, it is imagined that the increase of the reactor pressure leads to the heavy chemical reaction and to increase the sticking coefficient of the source gases. The latter is possible to take effects on repressing the re-evaporation of IV-family of atoms from the epilayers. Thus the crystalline quality is heightened by increasing the reactor pressure. By increasing the reactor pressure, it is expected that the hillock structure disappears and the epilayers are grown with mirror-like surface morphologies and high crystalline quality. We will discuss the crystalline quality and surface morphologies of epilayers grown at the atmospheric pressure (760 Torr) in section 2-1-3.

Next let us discuss the crystallographic property of the epilayers. Figure 2.1.8 shows the dependence of the reactor pressure on the FWHM of (400) ZnSe diffraction patters in ZnSe epilayers grown at various growth temperatures and reactor pressures. When the growth temperatures are between 200 and 250 ^{o}C, the increase of the reactor pressure improves the crystalline quality drastically. It indicates evidently that the reactor pressure controls the stoichiometry of the ZnSe epilayers, namely the re-evaporation of the VI-family of atoms. At growth temperatures more than 300 ^{o}C, however, the reactor pressure is not effective on the crystalline quality. As the growth temperature decreases, the effect of the reactor pressure on the crystalline quality becomes more prominent. One may further keep the following fact in mind. The increase of the reactor pressure increases sticking coefficients of the source gases, the concentrations. It can easily form ZnSe lattice at same growth temperature.

Next we discuss electrical properties of these epilayers. Figure 2.1.9 shows the temperature dependence of electrical properties (n, ρ , μ_H) measured by Hall measurement of the ZnSe epilayers (T_g=300 ^{o}C, P_g=0.1 Torr and T_g=300 ^{o}C, P_g=7.4 Torr). Table 2.1.2 shows the list of electrical properties of epilayers grown at various growth temperatures and reactor pressures. Between 300 and 350 ^{o}C, the resistivity (ρ) and mobility (μ_H) increase, while carrier concentration (n) decreases as the reactor pressure increases. The Hall measurement also indicates that the crystalline quality is improved as the reactor pressure increases. For the growth temperature of 350 ^{o}C and 6.2 Torr,

mobility at 77 K becomes about 3000 $cm^2/V \cdot s$. The high value shows that impurities are repressed by increasing the reactor pressure. The total residual impurities in the epilayers are from both the source gases and the ambience. Namely, raising the reactor pressure increases the concentration of source gases, dilutes the contamination from the ambience and represses the diffusion of the impurities from the ambience. Though the crystallographic property is not appreciably improved by increase in reactor pressure at >300 ^{o}C, it is thought that the crystalline quality is really improved.

Figure 2.1.10 shows the dependence of reactor pressure on the PL ratio (ratio of the PL intensities of BE emission to SA emissions) at 77 K of the ZnSe epilayers grown at various growth temperatures. For growth temperatures less than 250 ^{o}C, the PL ratio increases as the reactor pressure increases. It indicates that the concentration of SA centers, which is the origin of the SA-PL intensity, is decreasing. On the other hand, between 300 and 350 ^{o}C, the PL ratio is decreasing drastically. It indicates that the concentration of SA centers increases and the crystalline quality is degraded. It is seemingly inconsistent with the result of Hall measurement. The inconsistency is explained by examining the absolute SA-PL intensity and by analyzing the temperature dependence of Hall measurement. Increasing the reactor pressure, it is estimated that the concentrations of SA centers, donor- and acceptor-like impurities are decreasing together. Particularly, the inclusion of acceptor-like impurities in the epilayers is limited by the reactor pressure, which is proba-

bly coming in from the ambience. The compensation ratio thus becomes lower as the reactor pressure increases.

The increase in the reactor pressure causes a raise in growth rate and improvement of the crystalline quality. The chemical reaction in the vapor phase does not always contribute to the epitaxial growth even if the reactor pressure increases. The residual impurity concentration is limited to that in source gases and carrier gas. By raising the reactor pressure, the flow rates of source gases and carrier gas, one can get free from the contamination due to the ambience. In the epitaxial growth under the atmospheric pressure, it is important to obtain the ZnSe epilayers with high crystalline quality and high purity. The carrier concentration of the ZnSe epilayers grown at 250 ^{o}C and 0.1 Torr is about $4x10^{17}cm^{-3}$. On the other hand, the carrier concentration of the ZnSe epilayers grown at 250 ^{o}C and 760 Torr is less than 10^{15} cm^{-3} as will be mentioned in the next section. The fact is the expectable results. We will further discuss the dependence of [Se]/[Zn] and $V_{Zn/Se}$ (the ratio of flow velocity of [DMZ] to that of [H_2Se]) on the crystalline quality of the ZnSe epilayers grown under the atmospheric pressure in detail there.

2-1-3. Dependence of source gas mole ratio and gas velocity ratio on crystalline quality of ZnSe epitaxial layers (epilayers) grown by atmospheric pressure MOVPE

In previous section, we have investigated the MOVPE growth of

undoped ZnSe epilayers under the reduced pressure and assured that the atmospheric pressure MOVPE is hopeful to grow the ZnSe epilayers with device quality. In this section, we report the ZnSe epilayers grown at growth temperatures of 220-300 ^{o}C, utilizing H_2Se and DMZ as source materials under the atmospheric pressure. The effects of the flow velocity of each source gas (V_{Zn} , V_{Se}) and [Se]/[Zn] on surface morphologies and stoichiometry of ZnSe epilayers will be examined.

The crux of this section shows that it is possible to vary the above growth parameters independently by adjusting the flow rate of each carrier gas according to the reactor configuration at the atmospheric pressure and to grow the ZnSe epilayers with smooth surface morphologies.

The MOVPE growth system used in this work is illustrated in Fig. 2.1.11 which is different from that in Fig.2.1.1. The reactor design is horizontal. It is because of the simple flow of the source gases and lack of the convection current in the horizontal reactor, which is important particularly at the atmospheric pressure. The center tube carrying zinc alkyls extends to about 2-3 cm above the GaAs substrate on a SiC coated carbon susceptor. GaAs substrates were heated by a conventional electric furnace or by an IR-radiant heater. Before growth, the GaAs substrates were preheated at 760 Torr under hydrogen atmosphere at 600 ^{o}C for 10 minutes. Growth conditions are listed in Table 2.1.3. V_{Zn} and V_{Se} were calculated from the size of the center tube and reactor, and were adjusted by varying the flow rates of the carrier gas. A typical growth rate for an epilayer

which exhibits excellent surface morphology was 8.2 μm/h., which was limited by the supply of DMZ.

The surface morphologies of ZnSe epilayers for various $V_{Zn/Se}$ ($=V_{Zn}/V_{Se}$) and [Se]/[Zn] were observed by a Nomarski phase contrast interference microscope. Figure 2.1.12(a) represents the familiar "orange peel" type of morphology with some hillocks as previously reported by Wright et al. [43]. As $V_{Zn/Se}$ increases, the "orange peel" type surface morphology disappears and induces a surface morphology with hillocks along the $\langle 0\bar{1}\bar{1} \rangle$ direction observed in a low pressure system (Fig. 2.1.12(b); $V_{Zn/Se}=180$) [58]. Such a surface morphology under these growth conditions is undoubtedly related to the elimination of premature reaction. A further increase in $V_{Zn/Se}$ simply reduces the growth rate. Figure 2.1.12(c) shows the surface morphology of an epilayer grown at a [Se]/[Zn] of 30 which is much higher than that ([Se]/[Zn]=3) of an epilayer shown in Fig. 2.1.2(b) with the same $V_{Zn/Se}$ ($V_{Zn/Se}=180$). The surface morphology is quite smooth with very little background texture, due probably to suppression of re-evaporating Se atoms in the ZnSe epilayer. This is analogous to the growth of the III-V compounds by MOVPE in that the growth conditions with a high [V]/[III] are necessary for suppressing the volatility of the group V constituents. Observation of cleaved cross sections of ZnSe epilayers (Fig. 2.1.12.) also shows that the flatness of epilayers grown under these growth conditions coincides well with the results of the surface morphologies. The surface morphologies of epilayers which were reported in the past become much poorer as the epilayer thickness

increases (Figs. 2.1.12(a) and 2.1.12(b).). This is probably because it is difficult in the low pressure system to vary these growth parameters independently.

Double crystal X-ray measurement is helpful in determining the crystalline quality of ZnSe epilayers accurately. The full-width at half maximum (FWHM) of the ZnSe(400) diffraction spectra of a ZnSe epilayer is about 125 sec regardless of the surface morphology (Fig. 2.1.13.).

The PL spectra are measured using a 6 mW He-Cd laser (λ = 325 nm) as the excitation light source. The PL spectrum at 77 K of a ZnSe epilayer (see Fig. 2.1.14.) grown on a (100) GaAs substrate consists of a narrow BE emission at 445 nm and SA emissions with very low intensities at longer wavelengths (at 560-600 nm). At room temperature (R.T.), the BE emission in the PL spectrum was not observed, due probably to the very low concentration of optically active donor species in the epilayers. It is also supported by SIMS measurement that the residual impurities is undetected and the concentration is at least less than 10^{15} cm^{-3} in ZnSe epilayers. As stated in section 2-1-2, it is probably because the ambience is diluted by the large quantity of H_2 carrier gas on the growth mechanism. Hall measurements also show that all the ZnSe epilayers grown under the atmospheric pressure have high resistivities and the carrier concentrations are below 10^{15} cm^{-3}. These results indicate that the ZnSe epilayers are purified to the purity of the source gases, as discussed in section 2.1.2, independently of source gas mole ratio and source gas velocity.

We have demonstrated that the ZnSe epilayers with an excellent mirror-like surface morphology can be grown on GaAs substrates by controlling the $V_{Zn/Se}$ and [Se]/[Zn] at the low growth temperatures of 220-300 ^{o}C. Premature reaction can be suppressed by the optimization of $V_{Zn/Se}$ even at the atmospheric pressure. The surface morphologies of ZnSe epilayers are improved with high [Se]/[Zn] (>10), which is probably related to the stoichiometry of ZnSe. Thus it is thought that the ZnSe epilayers can be grown with crystalline quality high enough to dope p-type impurities.

2-1-4. Growth temperature dependence

Next let us discuss the dependence of growth temperatures (200-400 ^{o}C) on the crystalline quality of undoped ZnSe epilayers grown under the atmospheric pressure in order to heighten the crystalline quality still more. The growth conditions except growth temperatures used in this section are almost the optimum ones ([Se]/[Zn]=12, $V_{Zn/Se}$=180, [DMZ]=15.5x10^{-6} mol/min.) mentioned in section 2-1-3.

Figure 2.1.15 shows the dependence of growth temperature on the growth rates of the ZnSe epilayers. The growth rate is independent of the growth temperature and dependent on the quantity of supply of the DMZ. The growth rate is about 6.5 μm/h under these growth conditions. Particularly, at 400 ^{o}C, the growth rate of ZnSe epilayers grown under the reduced pressure is decreased abruptly to less than 0.2 μm/h. It is because the chemical reac-

tion between DMZ and H_2Se in the vapor phase prevents the epilayers from being grown on the substrates. In the atmospheric pressure, the chemical reaction is suppressed by controlling the $V_{Zn/Se}$ and [Se]/[Zn]. Such a chemical reaction as decreasing the growth rate is very serious in the epitaxial growth. However, even when the growth rate is decreasing at the atmospheric pressure, it is thought that the crystalline quality or the surface morphology would be degraded also by other reasons than the chemical reaction.

Figure 2.1.16 shows the surface morphologies of the epilayers grown at different temperatures. In 200 ^{o}C, the surface morphology is very hazy and the crystalline quality is similar to polycrystal like. The surface morphology is mirror-like in 250 ^{o}C and gradually begins to worsen in 300 ^{o}C, being related to the stoichiometry.

Figure 2.1.17 shows the dependence of growth temperature on the FWHM of (400) ZnSe diffraction patterns. The FWHM is broad and the crystalline quality is bad in the growth temperature region of less than 200 ^{o}C and higher than 350 ^{o}C. However, the high crystalline quality of the epilayers is maintained between 210 and 300 ^{o}C. As the growth temperature increases, the surface morphology is worsened and the crystalline quality is degraded. The growth temperature dependence is much different from the case of the epitaxial growth under the reduced pressure. In the reduced pressure, the crystalline quality is not always related to the surface morphology.

Next let us discuss the PL properties. Figures 2.1.18 and 19

show PL spectra at 77 K of ZnSe epilayers grown at different temperatures. As seen in the figures, though the PL intensity of the BE emission is weak, the PL intensity of SA emissions (SA-PL intensity) is strong. Also the broad BE and Y emissions are seen. This is probably because the growth temperature is too low to maintain the crystalline quality. Furthermore, the reason why the PL intensity of the BE emission (BE-PL intensity) decreases drastically is thought that the sticking coefficient of impurity is decreasing at 200 ^{O}C. It indicates that the efficiency of drawing impurities into the epilayers is heightened by the degradation of the crystalline quality. At 250 ^{O}C, the BE-PL intensity increases by two orders of magnitude and the SA-PL intensity decreases. At 300 ^{O}C, the SA-PL intensity begins to increase again. At 350 ^{O}C, SA-PL intensity seems to increase dominantly. But it is because the BE-PL intensity decreases drastically in accordance with the variation of SA-PL intensity. The FWHM of the BE emission is very sharp and it shows that the crystalline quality is high. However, the result is inconsistent with the result of double crystal X-ray spectrometer. Since the BE-PL intensity of the ZnSe epilayer grown at 350 ^{O}C decreases drastically, n-type impurities are not included so dense in the epilayer probably by the decrease of the sticking coefficient of the impurities. The estimation by X-ray diffraction shows that the high density of dislocations would be generated in the epilayers.

Figure 2.1.20 shows the growth temperature dependence of PL intensities of BE, Y and SA emissions and PL ratio at 77 K. The SA-PL intensity is almost unchanged by the growth temperature.

The BE-PL intensity has a peak in the region of the growth temperature between 210 and 250 ^{o}C. A small change of growth temperature, from 200 to 210 ^{o}C, increases the BE-PL intensity by more than two orders of magnitude. As the growth temperature increases from 250 to 300 ^{o}C, the BE-PL intensity decreases drastically and its PL intensity at 350 ^{o}C is by about two orders of magnitude weaker than that at 250 ^{o}C. Furthermore, Y emission is observed only at 200 and 350 ^{o}C. The reason why the Y-PL intensity becomes strong at temperature lower than 200 ^{o}C is thought to be that the crystalline quality is worsened by being grown at too a low temperature. The degradation of the crystalline quality is also supported by the broadness of Y emission. Also the reason why the BE-PL intensity decreases at temperatures higher than 300 ^{o}C is thought to be that the sticking coefficient is decreasing or that the occurrence of Zn vacancy is related to the activation rate of the impurity in the epilayer. Also, the growth temperature dependence has the same tendency with that of the epitaxial growth under the reduced pressure.

Figure 2.1.21 shows PL spectra at 4.2 K near the band-edge region (435-460 nm) of the ZnSe epilayers grown at different temperatures. Clearly, E_X, I_X and I_V are seen with relative intense intensities. At 250 ^{o}C, the I_X-PL intensity is stronger than the E_X-PL intensity and it indicates that donor impurities are included in. At 300 K, the I_X-PL intensity decreases, though the E_X-PL intensity increases. It indicates that the epilayer is grown with high purity. At 350 ^{o}C, the I_X-PL intensity decreases more, while the I_V-PL intensity seems to increase reversely. It

indicates that the sticking coefficient of donor impurities is decreasing at temperatures above 300 $^{\circ}$C. Since the FWHM's of all these emissions are broad, it is evident that the crystalline quality is degraded by the increase of the growth temperature. Also, the origin of I_V is related to the dislocations, namely, the degradation of the crystalline quality.

All the epilayers have high resistivities, and the carrier concentration is lower than 10^{15} cm^{-3} as discussed in section 2-1-3. The result also indicates that the ZnSe epilayers are purified to the purity of the source gases, as discussed in section 2.1.2, independently of growth temperature. The kinetic energy required to form the ZnSe lattice determines the crystalline quality in the low growth temperature region (<210 $^{\circ}$C) and the generation rate of Zn vacancies determines the crystalline quality in the high growth temperature region (>300 $^{\circ}$C). Therefore, the optimum growth temperature is the region between 210 and 300 $^{\circ}$C.

2-2. Homoepitaxial growth

Next we will discuss the effects of lattice matching on the crystalline quality. A special attention is paid to the improvement of the crystalline quality by matching the respective lattice constants between the epilayer and substrate. The ZnSe epilayers have generally been grown on GaAs substrates whose lattice mismatching with ZnSe is 0.26 %. However, the lattice mismatching between ZnSe and GaAs causes misfit dislocations [45,54,57,59] which lead to deterioration of the epilayer as discussed in section 2.1.1. The difference in coefficient of heat expansion also worsens the quality of the epilayer and results in introduction of dislocations or defects, arising from the interfacial region [60]. Another inconvenience of heteroepitaxy is the diffusion of host atoms into the epilayer [61]. If Ga atoms diffuse into the ZnSe epilayer, they may compensate the p-type impurities. In order to eliminate the problem of mismatching, Mitsuhashi et al. [44] grew lattice-matched ZnS_xSe_{1-x} on GaAs substrates using DMZ, dimethylselenide (DMSe) and diethylsulfide (DES) at a growth temperature of 500 ^{o}C and obtained high-quality epilayers with a FWHM of 40 arc sec from double crystal x-ray measurement. Even in this case, however, exact lattice matching could not be completed due to the difference of thermal expansion coefficients. As the growth temperature is increased, the difference of the thermal expansion coefficients may contribute more to the degradation of the quality, and Ga atoms of donor species diffuse even more rapidly from the GaAs substrate into the epilay-

er.

The simplest method to solve these problems is to grow ZnSe epilayers on ZnSe substrates like homoepitaxial growth of III-V compounds such as GaAs epilayers on GaAs substrates. Thus homoepitaxy is quite attractive as a method to remove the above disadvantages of heteroepitaxy. For the purpose of homoepitaxy, high quality ZnSe bulk single crystal is required as substrate. We choose iodine vapor transport method as one of ZnSe bulk crystal growth and report ZnSe substrate preparation in section 2-2-1. In the past, several attempts were made for the homoepitaxy of ZnSe. For example, Werkhoven et al. [62] tried to grow undoped ZnSe epilayers by liquid phase epitaxy (LPE) on the ZnSe substrates provided by Eagle-Pitcher Industries, Inc. Blanconnier et al. [63] reported the MOVPE of the ZnSe using two kinds of ZnSe substrates grown by the Piper and Polish method and by iodine vapor transport. Recently, Park et al. [64] also grew the ZnSe epilayers by MBE on the Eagle-Pitcher's ZnSe substrates. They also investigated the effects of the orientation [(100), (110) and (111)] of the substrate on PL properties of epilayers and the effects of the argon ion sputtering as the pretreatment of the substrates before growth. It is found essential to epitaxial growth that the surface state of substrate greatly affects the crystalline quality of the epilayer. Nevertheless, it has never been discussed in ZnSe homoepitaxial growth. We will first report the effect of heat treatment of ZnSe substrate just before growth on the crystalline quality of the ZnSe homoepilayer in section 2-2-2(A) before discussing the ZnSe homoepitaxial growth systemat-

ically.

Menda et. al. [65] investigated the differences of the PL properties between the homoepilayer and the heteroepilayer in detail. The data of the ZnSe homoepilayer which indicates crystalline quality higher than the heteroepilayers has not been reported yet. The problem of out-diffusion of impurities from the substrate has not been sufficiently discussed either. We will report the ZnSe homoepitaxial growth in detail in sections 2-2-2(B), (C) and (D)., and discuss the systematic dependence of growth conditions (source gas mole ratio and growth temperature) on the crystalline quality and propose a new mechanism of out-diffusion of impurities and native defects into ZnSe homoepilayer from the ZnSe substrate (section 2-2-2(B).). At the end, we will compare the homoepitaxial growth with the heteroepitaxial growth.

2-2-1. ZnSe substrate preparation

ZnSe bulk crystal (20x14x14 mm^3) was grown by the iodine vapor transport method [66]. Then the ZnSe substrates (about (5-10)x10x0.5 mm^3) used in this work were cut and polished along the (100)+0.3^o orientation in Tsukuba Research Laboratory (Nippon Sheet Glass Co., Ltd.). Photographs of typical wafers are shown in Fig. 2.2.1. The substrates have no twins in the faces and the etch pit density is (2-7)x10^4 cm^{-2}. The FWHM of the ZnSe(400) X-ray diffraction peak of the substrate is 13 arc sec (see Fig.2.2.2.), which indicates the highest crystalline quality

ever reported. The PL spectrum at 300 K (see Fig. 2.2.3.) of the substrate, however, shows strong SA emissions at longer wavelength, which are ascribed to defects due to complex of Zn vacancy and iodine impurity [67,68]. The following procedures of chemically cleaning ZnSe substrates were adopted: (1) rinsing in trichloroethane; (2) rinsing in acetone; (3) rinsing in methyl alcohol; (4) etching in 1 % Br_2-CH_3OH for 5 minutes; (5) rinsing in DI water. Using this etching, the surface layer of about 12 μm was removed together with the amorphous and the strained layer generated by polishing.

2-2-2. ZnSe homoepitaxial growth

(A) Effect of heat treatment conditions of ZnSe substrate on crystalline quality of ZnSe homoepilayer.

In this section, we report the MOVPE growth of undoped ZnSe epilayers on (100) ZnSe substrates cut from ingots grown by iodine vapor transport method and try to raise the crystalline quality of the ZnSe epilayers by the homoepitaxial growth. At first, there is a serious problem how the pretreatment of the ZnSe substrates should be done to grow the ZnSe homoepilayers with high crystalline quality. This point has never been investigated. The purpose of the present section is to show the effects of the heat treatment of the substrates before the growth under various atmospheres on the morphological, crystallographic and

photoluminescence properties and the optimum cleaning procedure of the substrates to remove surface contaminants and oxide layers.

The source materials used in this work are DMZ and H_2Se. The undesirable premature reaction between source gases is completely prevented by controlling the flow velocity of each source gas (V_{Zn}, V_{Se}) even at the atmospheric pressure as mentioned in section 2-1 (heteroepitaxial growth). The V_{Zn} and V_{Se} are easily adjusted by varying flow rates of respective H_2 carrier gases.

Before growth, removal of the surface contaminants and the oxide layer on the substrate is critical to obtaining epilayers with high crystalline quality. We find the optimum conditions of treatment by investigating the characteristics of epilayers grown on ZnSe substrates pretreated under various atmospheres and temperatures. The conditions of the treatments are listed in Table 2.2.1. The parameters of the treatments are atmospheric gases (H_2, H_2Se and DMZ), the heating temperatures (300 - 650 ^oC) and the period of the treatments (10 - 30 min.). The growth conditions of all the epilayers are the same (the growth temperature is 250 ^oC, the reactor pressure is an atmospheric pressure, the flow rate of DMZ is $1.55x10^{-5}$ mol/min., the source gas mole ratio is 2.8, the total flow rate including the carrier gas is 3.3 l/min., the period of the growth is one hour and the epilayer thickness is about 6 μm.).

The surface morphologies of ZnSe epilayers grown on the substrates pretreated at various temperatures in a hydrogen atmosphere (the flow rate is kept 4 l/min.) are illustrated in Fig.

2.2.4. The epilayer (# 149) without heat treatment has a very rough morphology and shows countless triangular hillocks (see Fig. 2.2.4(a).). All homoepilayers grown on treated substrates at more than 300 ^{o}C for 30 minutes have no triangular hillocks and are mirror-like and smooth (see Figs. 2.2.4(b)-(d).). This phenomenon indicates that part of the contaminants adhering to the substrate can be removed by the heat treatment. Heat treatments made above 650 ^{o}C are likely to worsen surface morphologies of epilayers and the period of treatments also becomes the important factor (see Figs. 2.2.4(d) and (e).). This is probably due to the prominent re-evaporation of Se and Zn atoms from the ZnSe substrate at temperatures higher than 600 ^{o}C. The flow rate of H_2 carrier gas may also influence some effects at high temperature, but is not discussed here. Next, the effects of heat treatment under various atmospheres (H_2 only, H_2 plus H_2Se and H_2 plus DMZ) on the surface morphologies of the epilayers are shown in Figs. 2.2.5(a)-(c). The substrates are held under the controlled atmosphere for 20 minutes at 600 ^{o}C. All other growth conditions remain the same. The effects of the treatment in H_2 atmosphere including DMZ are similar to those in only H_2 atmosphere because of the small concentration of DMZ (see Figs. 2.2.5(a) and (c).). However, the heat treatment in H_2 atmosphere including H_2Se is very effective for obtaining homoepilayers with excellent surface morphologies (see Fig. 2.2.5 (b).). The homoepilayers are smoother than the similar heteroepilayers. Apparently, the introduction of additional H_2Se in the atmosphere prevents re-evaporation of Se atoms from the ZnSe substrate at a high temperature of 600 ^{o}C,

similar to substrate preservation process used in the epitaxial growth of III-V compounds.

We will next discuss the PL properties of the ZnSe homoepilayers with various pretreatment conditions of the ZnSe substrates just before growth. The PL spectra measured at 77 K are shown in Fig. 2.2.6 as a function of temperature of heat treatment of the substrates. The heat treatment just before growth is found to have a profound effects on the SA-PL intensity of the ZnSe epilayers. Heat treatment above 300 ^{o}C is an effective procedure for reducing the density of SA centers. The SA-PL intensity cannot be reduced below a level of the SA-PL intensity in the heteroepitaxial growth even if the temperature of the heat treatment is raised from 300 to 600 ^{o}C (see Figs. 2.2.6(b) and (c).).

The origin for generating SA centers is supposed to be two-fold. One would be the impurities in the epilayer. The substrates contain iodine impurities of about 200 ppm. It is supposed that they would diffuse from the substrate into the epilayer during growth or would be incorporated through the out-diffusion by re-evaporation of the constituents of ZnSe during heat treatment at high temperature. The SA-PL intensity remains independent of temperature. It is thought that the growth temperature of 250 ^{o}C is low enough for the iodine impurity to diffuse. Apparently, the SA-PL intensity is irrelevant to behavior of iodine impurities. The other origin would be native vacancies (Zn or Se vacancies). It is found that the SA-PL intensity becomes stronger as the source gas mole ratio is increased (see Fig. 2.2.7.). Apparently,

it is because Zn vacancy, which is one of the origin of SA emissions, diffuses into the homoepilayers from the substrates even at 250 ^{O}C and generates a SA center by combining the residual impurity in the homoepilayers. In the heteroepitaxial system, many dislocations originating near the interface due to the lattice mismatching would accelerate the out-diffusion of some impurities. However, no Zn vacancies are involved in GaAs substrate used in the heteroepitaxial growth.

Figure 2.2.8 exhibits the PL spectra measured at 4.2 K. The separation between I_X and E_X emissions becomes distinct and the FWHM's of I_X emission becomes sharper (0.8 meV; # 133) for higher temperature of heat treatment. The observed value of FWHM is the smallest that has ever been reported, indicating that the epilayer has a very high crystalline quality. Apparently, all the contaminants and oxide layer on the ZnSe substrate are completely removed by the heat treatments at high temperature (600 ^{O}C).

Let us now discuss the crystallographic property of the ZnSe homoepilayers with various pretreatment conditions of the ZnSe substrates just before growth. The double crystal x-ray diffraction patterns of ZnSe homoepilayers and a typical ZnSe substrate used in this work are illustrated in Fig. 2.2.9. The FWHM of ZnSe(400) diffraction pattern is 640 arc sec. Evidently, the crystalline quality is very bad when the ZnSe substrate is not pretreated before the growth. As the temperature of treatment is raised, the FWHM of ZnSe(400) diffraction patterns is sharpened to a value of 77 arc sec for the epilayer grown on the substrate treated at 600 ^{O}C. This value indicates that the ZnSe epilayer

has the highest crystalline quality which has ever obtained using any growth technique. The FWHM becomes broader (130 sec; # 139), however, when the temperature is raised from 600 to 650 ^{o}C. The treatment at 650 ^{o}C would worsen the surface state of the homoepilayers by the re-evaporation of constituents. The FWHM of the diffraction patterns of epilayers treated under various atmospheres is the same (77 arc sec), indicating little effect on the crystalline quality of the epilayers. Based on the results from double x-ray diffraction, the optimum conditions of heat treatment is found to be 600 ^{o}C and 20 minutes. This optimum conditions coincide well with the previous results of the surface morphology and the PL spectra.

In summary, undoped ZnSe homoepilayers have been grown on (100) ZnSe substrates at a low temperature of 250 ^{o}C by atmospheric pressure MOVPE using DMZ and H_2Se. Heat treatment of the ZnSe substrate just before the growth has a dramatic effect on the crystalline quality of epilayers. It is apparently by removing contaminants and oxide layer on the ZnSe substrate. The FWHM of ZnSe(400) diffraction of epilayers grown after heat treatment of 600 ^{o}C for 20 minutes is 77 arc sec and the FWHM of I_x PL measured at 4.2 K is 0.8 meV, while the typical values of the heteroepilayer are 150 sec and 1.2 meV, respectively. The above low values indicate that the homoepilayers have the highest crystalline quality ever reported. The surface morphologies of the homoepilayers become more excellent than those of heteroepilayers by the introduction of the additional H_2Se in H_2 atmosphere in the heat treatment. In the homoepitaxial growth of ZnSe, SA

centers are easily incorporated into the epilayer even at a low growth temperature, probably because of the fast out-diffusion of Zn vacancies.

Though the crystallographic property of the ZnSe homoepilayers is superior to that of the ZnSe heteroepilayers, the PL property is inferior to that of the ZnSe heteroepilayers. A ZnSe heteroepilayer has a density of SA centers by an one order of magnitude lower than a ZnSe homoepilayer. Since it is natural to expect that the ZnSe homoepilayer has crystalline quality higher than the ZnSe heteroepilayer, we discuss the origin of SA centers in the ZnSe homoepitaxial growth and the mechanism of generating the SA centers in ZnSe homoepilayers in the next section.

(B) Origin of Self-activated (SA) emissions in ZnSe homoepilayer

In this section, we report the growth of undoped ZnSe homoepilayers on (100) ZnSe substrates at 250 ^{o}C by atmospheric pressure MOVPE using DMZ and H_2Se and investigate the crystalline quality of the homoepilayers compared with that of the heteroepilayers. We will discuss the problem of the out-diffusion of impurities and native defects from the ZnSe substrate during crystal growth, which has never been treated, as the first step to heighten the crystalline quality.

The ZnSe substrates are thermally etched at 600 ^{o}C, for 20 minutes, under H_2(2 l/min.) atmosphere including H_2Se($4.6x10^{-4}$ mol/min.) in the reactor. The heat treatments just before the growth were done under the optimized conditions for removing the oxide layer and contaminants on the substrate as stated in section 2-2-2(A) [69]. The growth conditions are listed in Table 2.2.2. The sample named HETERO-1 is a ZnSe epilayer grown on a GaAs substrate under the same growth conditions as the homoepilayer (HOMO-1). Growth conditions of other samples (HETERO-2, 3 and HOMO-2, 3, 4, 5) are the same except for the source gas mole ratios ([Se]/[Zn]). Under the above growth conditions, the growth rate was about 6 μm/h independent of substrate material (ZnSe and GaAs) and [Se]/[Zn]. HOMO-3 had an epilayer thickness of 1μm. This was to investigate the effects of out-diffusion of impurities from the substrate on the crystalline quality of the homoepilayer by reducing the growth period from 20 min to 10 min.

On the other hand, HOMO-4 had an epilayer thickness of as large as 15.8 μm (growth rate was 31.8 μm/h with the period of 0.5 h.) lest impurities should diffuse from the substrate to near the surface in increasing the flow rates of both source gases by three times.

Let us next discuss the crystallographic property of the ZnSe homoepilayers. Figure 2.2.10 shows the diffraction patterns of ZnSe (400) measured by the double crystal x-ray spectrometer. To see crystallographic properties, it is very important to know the FWHM of the diffraction pattern. In the spectrum of HOMO-1, the diffraction patterns of ZnSe(400) from both the epilayer and the substrate overlap one another (see Fig. 2.2.9(a).). Judging from the sharpness (13 arc sec) of the FWHM of the substrate and the epilayer thickness (t_g=6 μm), a FWHM of 38 arc sec is regarded as being representative of the crystalline quality of the epilayer. In the case of heteroepitaxy (HETERO-1), the positions of ZnSe(400) and GaAs(400) diffraction patterns are different from each other by the lattice constants. The FWHM of HETERO-1 is as large as 250 arc sec (see Fig. 2.2.10(b).). This value is several times broader than that of HOMO-1 (38 arc sec). It shows that the homoepilayers, which have been grown, have little strain and low density of dislocations.

Next subject is the PL properties of the ZnSe homoepilayers. Figure 2.2.11 represents the PL spectra measured at 77 K. It is clear that the BE-PL intensity decreases to less than 1/100 as [Se]/[Zn] increases from 2.8 to 60. In this case, the absolute PL intensity of the deep centers remains the same. It means

either the concentration of donor impurities decreases or the crystalline quality degrades with increasing [Se]/[Zn]. In the heteroepilayer, such a dependence of [Se]/[Zn] on the PL properties was not observed yet (see Fig. 2.2.12.). We have no explanation for the phenomenon. Both the homoepilayer and the heteroepilayer have broad deep emissions near 560 nm (PL at 77 K). The PL intensity of deep emissions of the homoepilayer is several times more intense than that of heteroepilayer independent of [Se]/[Zn] (see Fig. 2.2.13.). Figure 2.2.14 shows PL spectra at 4.2 K of the homoepilayers at various [Se]/[Zn] in the near band-edge region. A strong and sharp I_X emission line near 2.7969 eV (the emission line has been reported at 2.7954 eV in the heteroepilayer [70].) becomes weaker and broader with an increase of [Se]/[Zn]. This basically outlines the degradation of the crystalline quality rather than the decrease of the donor concentration in the epilayer. The conclusion, however, is inconsistent with the crystallographic property of homoepilayers at the high source gas mole ratio. In addition to the I_X line, the E_X line is also observed at 2.8018 eV and the I_V line at 2.777 eV [70]. Figure 2.2.15 shows the PL spectrum of a heteroepilayer at 4.2 K. The I_2 line is also seen at 2.7981 eV. The line is probably assigned to the excitonic emission due to Ga atoms diffused from the substrate [70]. These excitonic emission lines are observed to be shifted by 0.5-0.7 meV upwards relative to heteroepilayers. Though the values are small compared with energy shift (3 meV) which Menda et al. [65] reported previously, the same energy shift upward is reasonably observed, so that it indicates the

absence of strain in the homoepilayers.

Next, we examine the out-diffusion of impurities from iodine doped ZnSe substrate in order to investigate the origin of deep emissions. There exist only a small amount of data on diffusion coefficients of impurities in bulk ZnSe [71-77]. Though the out-diffusion of iodine is thought to be an origin of deep emissions, no data on the diffusion coefficient of iodine are available.

Figure 2.2.16 shows PL spectra at 77 K of HOMO-3 and that of the substrate. Deep emissions near 520 nm and 600 nm are seen in the substrate, but HOMO-3 does not have these deep emissions. As seen from Fig. 2.2.13., the peak wavelengths (560 nm) of deep emissions are the same as those of heteroepilayers. Thus we conclude from these results that the origin of deep emissions is not diffused iodine impurities only. Another possibility is copper impurity diffused from the substrate with high diffusion coefficient. It is true that analysis by inductively coupled plasma (ICP) spectroscopy shows that the substrates contain copper impurities of less than 1 ppm (undetectable). But, it is well-known that the diffusion coefficient of copper impurity is extremely high in ZnSe [71-73]. Generally, the diffusion coefficient D, which depends on the temperature, is calculated by the following formula [78];

$$D=D_0 EXP(-\Delta E/kT_G), \qquad (1)$$

where D_0 is a temperature independent constant, ΔE an activation energy and T_G a growth temperature. The mean penetration depth

of diffusant is given by $2(Dt)^{1/2}$. In the case of copper, $D_0=1.7\times10^{-5}cm^2\cdot s^{-1}$ and $\Delta E=0.56$ eV [71,72] where t is the period of growth. T_G is 523 K (250 ^oC). Then, from equation (1), $D=6.9\times10^{-11}cm^2\cdot s^{-1}$. Since the period of growth is usually one hour, the mean penetration depth is about 10 μm. Namely, in all samples except HOMO-4, copper impurities could diffuse from the substrate to the surface of the homoepilayers. The distribution of impurities diffusing from the substrate is described by the following complementary error function [79,80];

$$C(x,t)= C_S \operatorname{erfc} [x/2(DT)^{1/2}], \quad (2)$$

where

$$\operatorname{erfc}(x)=1-\operatorname{erf}(x), \quad (3)$$

$$\operatorname{erf}(x)=(2/\pi^{1/2})\int_0^x \exp(-a^2)da. \quad (4)$$

C_S is the surface concentration of impurities in the ZnSe substrate and erf(x) denotes the error function. In the HOMO-1, 2 and 3, the surface concentration ($C(x=t_g,t)$) of copper impurities diffusing from the substrate can be calculated by equations (2)-(4) if we put C_S=1 ppm. And we put C(HOMO-1, 2, 3)=0.7 ppm, 0.7 ppm and 0.94 ppm, respectively. In the case of HOMO-4, since the growth rate is as high as 31.6 μm/h., the calculated value ($C(t_g,t)$=0.007 ppm) under the above conditions is too small to facilitate diffusion onto the surface of the epilayer.

Figure 2.2.17 shows PL spectra at 77 K of HOMO-3 and 4. As seen in the figure, the same deep emissions were observed with identical intensities. It means that there is not so large a difference in concentration of deep centers between the above two samples as is expected from the calculation. Moreover, the emission line of the bound exciton due to copper near 2.783 eV [80,81] in the 4.2 K PL spectra is observed in no sample (see Figs. 2.2.13 and 2.2.14.). This result shows that the out-diffusion of copper is unlikely. Thus we conclude that some impurities in the ZnSe substrate do not diffuse into the homoepilayer. The last possibility is the diffusion of Zn vacancies from the ZnSe substrates. But the bound exciton emission line due to the Zn vacancy itself near 2.783 eV (called I_1^d [81,82]) is not seen in our samples (see Fig. 2.2.14.). Since the origin of the deep emissions which are observed at 560 nm is supposed to be complexes between the Zn vacancies and impurities in the epilayer and the PL intensity in the homoepilayer is several times stronger than that in the heteroepilayer, we can imagine that the homoepilayer contains more Zn vacancies than the heteroepilayer. At this moment, the origin of Zn vacancies present in the homoepilayer is unclear. One possibility is that they diffuse from the substrate into the homoepilayer. They may easily combine with impurities without being isolated. Though there is little evidence that the Zn vacancy diffuses even at 250 ^{o}C, iodine-doped ZnSe contains a high density of Zn vacancies (see Fig. 2.2.16., the order of 100 ppm, probably.). Probably the Zn vacancy should have diffused from the ZnSe substrate. We cannot help suggesting that the out-

diffusion of the Zn vacancy is prominent in the ZnSe homoepitaxial growth. Namely, the deep emissions are thought to be SA emissions. If the Zn vacancies diffuse in the epilayer, the temperature independent coefficient of diffusion (D_0) would easily be calculated from the equations (1)-(4) in the sample of HOMO-4 to yield more than 10^{-4} $cm^2 \cdot s^{-1}$ at 250 ^oC. We plan to investigate the dependence of growth temperature in ZnSe homoepilayers on the generation rate of SA centers to verify the above suggestion in section 2-2-2 (D).

In summary, we have obtained ZnSe homoepilayers grown at 250 ^oC at a high value of [Se]/[Zn] with high crystalline quality (its FWHM is 38 arc sec.). From the PL properties, it is shown that the BE-PL intensity decreases drastically as [Se]/[Zn] increases. This phenomenon is quite different from the heteroepitaxial growth case. The reason has not been established yet. Broad deep emissions are seen at 560 nm and the PL intensity is several times stronger than that of the heteroepilayer. The origin of the deep emissions is identified with complexes between Zn vacancies and residual impurities in the epilayer. It is not impurities (iodine or copper) with high diffusion coefficient diffusing from the substrate. Thus we conclude that the deep emissions are SA emissions. It is suggested that the out-diffusion of the Zn vacancies is suspected to be the cause of generation of deep centers, and therefore it is important to control the behavior of the Zn vacancies, particularly in homoepitaxy. The generation mechanism of SA centers in the ZnSe homoepilayer is probably thought to be the out-diffusion of Zn vacancies from

the ZnSe substrate, which contains 200 ppm of iodine impurities and high density of SA centers. It would be suggested that a growth temperature lower than 300 ^{o}C decreases the generation of SA centers in the ZnSe homoepitaxial growth. That might prevent Zn vacancies from diffusing from the ZnSe substrate into the epilayer. The [Se]/[Zn] is much related to the generation rate of SA centers. It is expected that the concentration of SA centers will be controlled by investigating the [Se]/[Zn].

(C) Dependence of source gas mole ratio on crystalline quality of ZnSe homoepilayer

It is generally accepted that homoepitaxy is a reasonable way for reduction of defect densities. As discussed in section 2-2-2, however, the crystalline quality of the ZnSe homoepilayer is not always superior to that of the ZnSe heteroepilayer. One origin of SA centers in the ZnSe homoepilayer is assigned to be Zn vacancies generated in the epilayer. It is expected that the concentration of SA centers will be controlled by investigating the [Se]/[Zn] dependence. The [Se]/[Zn] is much related to the generation rate of SA centers in the ZnSe homoepitaxial growth.

The first purpose of the present section is to see the [Se]/[Zn] dependence on the morphological, crystallographic and PL properties of the ZnSe homoepilayers based on our previous work [69,83] and to see whether the crystalline quality of ZnSe epilayers can be heightened still more or not. We will discuss

the growth temperature dependence of the ZnSe homoepitaxial growth in the next section. The second is to compare homoepilayers with heteroepilayers and to discuss the differences of crystalline quality in detail.

The MOVPE system and procedures employed here are illustrated in section 2-1-3 [49]. After the chemical cleaning, the substrate was dried and quickly placed on a susceptor inside the preliminary chamber and carried into the reactor which had not been exposed to air. The substrates were preheated under hydrogen atmosphere (the flow rate was 4 l/min.) at 600 ^{o}C for 20 minutes just before growth and subsequently cooled down to the deposition temperature of 250 ^{o}C. The period of the growth was one hour at the atmospheric pressure and the epilayer thickness about 6 μm. Growth conditions are listed in Table 2.2.3. The flow rate of DMZ was kept constant (1.55×10^{-5} mol/min.) and the [Se]/[Zn] was controlled from 1 to 60, by changing the flow rate of H_2Se. In all cases, the total flow rate including carrier gas was constant in order to prevent the undesirable premature reaction as discussed in section 2-1-3 (V_{Zn} and V_{Se} were also constant.).

The surface morphologies of ZnSe homoepilayers for various [Se]/[Zn] are illustrated in Fig. 2.2.18. The surface morphology of the homoepilayer (# 1) grown at [Se]/[Zn] of 60 is very hazy to the eye and shows a very rough surface with no directional hillocks like poly-crystalline structure under the microscope. With decreasing [Se]/[Zn] , the surface roughness gradually disappears and the surface morphology becomes quite smooth with very little background texture. The homoepilayer (# 2) contains

some features of haziness observed in # 1 with the mirror-like surface morphology. In the homoepilayer (# 3; [Se]/[Zn]=6), they disappear completely and another type of hillocks appears. In the homoepilayer (# 4; [Se]/[Zn]=2.8), the surface morphology is entirely covered with their fine hillocks like the familiar "orange peel" type hillocks reported by Wright et. al. [58]. The homoepilayer (# 5; [Se]/[Zn]=1) shows a poor morphology with hillocks along <0$\bar{1}\bar{1}$> direction observed in heteroepilayers grown by the low pressure MOVPE. The phenomenon described above contrasts with the [Se]/[Zn] dependence in the heteroepitaxial system reported in section 2-1-3. Heteroepilayers (# 6 and # 7; [Se]/[Zn]>6) exhibit specular surface morphologies with very little background texture (see Figs. 2.2.19 (a) and (b).), while the heteroepilayer (# 8; [Se]/[Zn]<6) shows the same morphology with hillocks along the <011> direction as that of the homoepilayer (# 5; [Se]/[Zn]=1) (see Fig. 2.2.18 and Fig. 2.2.19 (c).). Thus, the hillocks observed along the <011> direction are caused by deficiency of Se atoms during the growth of the ZnSe epilayer. From these results, we conclude that the suppression of re-evaporation of Se atoms from the epilayer will be essential to improve the surface morphology of the epilayer in both homo- and hetero-epitaxial growth. The homoepitaxial growth at the [Se]/[Zn] (>30) is so much different from the heteroepitaxial growth and also different from the homoepitaxial growth of III-V compounds. Probably there exists a close relation between the complex behavior of the premature reaction dependent on the combination of source gases and the surface reaction on the ZnSe substrate at

low growth temperatures.

Next we discuss the crystallographic property of the ZnSe homoepilayers grown at various [Se]/[Zn]. Figure 2.2.20 shows the ZnSe(400) diffraction pattern of typical ZnSe homoepilayers under various [Se]/[Zn] measured by the double crystal x-ray diffraction spectrometer. Figure 2.2.21 shows the [Se]/[Zn] dependence on the crystallographic property of epilayers without and with heat treatments. As a reference, the crystalline quality of ZnSe heteroepilayers is also shown. We have already investigated the effects of pretreatment of ZnSe substrates before growth on characteristics of homoepilayers and found that the crystallographic property of homoepilayers (grown only at a [Se]/[Zn] of 2.8) is drastically improved by the heat treatment of substrates as shown in Fig. 2.2.22. The dependence of both [Se]/[Zn] and the temperature of heat treatment on FWHM of the ZnSe(400) diffraction spectra (the values are shown beside each point.) are shown systematically in Fig. 2.2.23. The abscissa and ordinate in the graph indicate the [Se]/[Zn] and the temperature of heat treatment of the substrate before growth, respectively. It is evident that the crystalline quality of the homoepilayers is remarkably improved by growing at high [Se]/[Zn] (> 15) , which is independent of conditions of treatment of the substrates. We have obtained the ZnSe homoepilayer with highest crystalline quality whose FWHM is 33 arc sec at a [Se]/[Zn] of 60. The surface morphologies of high [Se]/[Zn] (>15) are very hazy with a polycrystalline like structure. The crystalline quality of the homoepilayer is closely related not to the surface morphology but

to stoichiometry in the ZnSe epilayer. On the other hand, the crystalline quality of the heteroepilayers is little dependent on [Se]/[Zn]. It is probably because the crystalline quality is mainly influenced by many dislocations occurring from the interface due to the lattice mismatching. Furthermore, as seen in Fig. 2.2.21., the crystalline quality of the homoepilayer at high [Se]/[Zn] (>15) is not improved by the heat treatment. This result is different from the case of the low [Se]/[Zn] (=2.8) as shown in detail in Fig. 2.2.22. In the case of the low [Se]/[Zn], as reported previously [69], the crystalline quality of the homoepilayer is drastically improved by removing the oxide layer and contaminants from the ZnSe substrate just before growth. Though the reason is not clear yet why the crystalline quality of the epilayers at high [Se]/[Zn] is better even without heat treatment, two possibilities for this are suggested: 1) both oxide layer and contaminants on the substrate are naturally removed during the initial growth, or 2) they do not determine the crystalline quality of the homoepilayer at high [Se]/[Zn]. If the oxide layer and contaminants are naturally removed at high [Se]/[Zn] (>15), it is considered that the additional large quantity of H_2Se effectively causes their removal even at the growth temperature of 250 ^oC, by some chemical reaction at the first stage of the growth. From this end in view, we have tried the following experiment. The pretreatment of the substrate was done in the ambience of the same partial pressure of H_2Se as the growth conditions ([Se]/[Zn]=60 and the temperature of 250 ^oC for 60 minutes.). After that, a homoepilayer was grown at 2.8 of

[Se]/[Zn] and the crystalline quality was compared with that of a homoepilayer grown at 2.8 of [Se]/[Zn] without heat treatment. If the crystalline quality is improved, one can conclude that a large quantity of H_2Se remove the oxide layer and contaminants which adhere to the substrate. If it is not improved, it would be suggested either they will not be removed, or what they might be removed before the growth is not so important for improving the crystalline quality at high [Se]/[Zn]. In the latter case, it could be said that research on growth mechanism at high [Se]/[Zn] would be necessary. The result was that crystalline quality was not improved by above method. Namely, the H_2Se does not remove the oxide layer and contaminants (the FWHM was 640 arc sec.). This means that the crystalline quality of epilayers was unchanged. The oxide layer and contaminants are not removed or do not determine the crystalline quality of the homoepilayer at high [Se]/[Zn]. It is probably because the improving effect on the crystalline quality is hidden in the complex growth mechanism at high [Se]/[Zn]. The crystalline quality of a ZnSe homoepilayer grown at high [Se]/[Zn] seems not to be so good. This conclusion is also consistent with the result of surface morphology.

Next the PL property of the ZnSe homoepilayer grown with various [Se]/[Zn] will be discussed. Figure 2.2.24 shows the typical PL spectra at 77 K of ZnSe homoepilayers grown under various [Se]/[Zn]. At low [Se]/[Zn] (<10), the strong BE emission at 445 nm and weak deep emissions around 560 nm are observed. At high [Se]/[Zn] (>10), weak BE emission and strong deep emissions are observed. The change of the BE-PL intensity with [Se]/[Zn]

(from 3 to 60) is about one hundred times. This indicates that the concentration of donor impurities in the homoepilayer decreases at high [Se]/[Zn] (Se-rich condition). On the other hand, the PL intensity of deep emissions is almost unchanged with [Se]/[Zn]. Figure 2.2.25 shows the [Se]/[Zn] dependence of the PL ratio in both homo- and hetero- epilayers. As seen in the figure, the dependence in homoepilayers is quite different from that of the heteroepilayers. Figure 2.2.26 (a) shows 4.2 K PL spectra of homoepilayers in near band-edge region. At low [Se]/[Zn], the E_X emission line at 2.8018 eV, the strong I_X emission line at 2.7969 eV (this is recently thought to be an impurity replacing a Se atom [84] which appears at 2.7954 eV in heteroepilayers [85].) and the weak unknown I_V emission line at 2.777 eV (probably, a donor bound exciton line [70]) are observed. Furthermore, the FWHM of I_X line is smaller than that of heteroepilayer and it is easy to imagine that the homoepilayer has no strain and few dislocations. At high [Se]/[Zn], the broad I_X and I_V lines are observed with comparable intensities. The facts described above suggest that the concentration of donor impurity, which is the origin of not the I_V line, but the I_X emission line, is reduced at the Se-rich condition. Also it indicates that the crystalline quality is degraded. Figure 2.2.26 (b) shows PL spectra at 4.2 K of heteroepilayers, which correspond to homoepilayers in Fig. 2.2.26 (a). The source gas mole ratio dependence of the homoepilayer is evidently different from that of the heteroepilayer. This phenomenon probably indicates that since the crystalline quality of the heteroepilayer is determined mainly by the lattice

mismatching rather than by the growth conditions, the efficiency of taking impurities into the heteroepilayer does not change much at the growth condition, different from the case of the homoepilayer. It is suggested that the efficiency of taking residual impurities into the heteroepilayer is related to the crystalline quality of the epilayer. We assume that the crystalline quality of the homoepilayer at high [Se]/[Zn] is not so good. It is suggested that the degradation of crystalline quality of homoepilayer at high [Se]/[Zn] generates a high density of dislocations or/and non-radiative centers. Thus the [Se]/[Zn] dependence of the activation rate of donors rather than the efficiency of taking the donors is related to the crystalline quality of the homoepilayer. It is also suggested that the concentration of donors possible to substitute Se atoms is limited by the Se-rich condition in the homoepilayer.

Next, we discuss deep emissions around 560 nm. These appear at the same wavelength in both homo- and hetero-epilayers (see Fig. 2.2.27(a).). They are not emissions related to some impurities diffusing from the ZnSe substrate but emissions related to the complex of Zn vacancies and impurities in the epilayer. The impurities probably come from the source materials. The deep centers are assigned to be SA centers. Figure 2.2.28 shows PL spectra of heteroepilayers under various [Se]/[Zn] (measured at 77 K). The absolute SA-PL intensity in heteroepilayer is a monotonically decreasing function of [Se]/[Zn] as seen in Fig. 2.2.25. Such a tendency is not seen in the case of the homoepilayer. In homoepilayers, the absolute SA-PL intensity is almost

independent of [Se]/[Zn] (the BE-PL intensity decreases abruptly at high [Se]/[Zn].). This indicates that the homoepilayers have a density of SA centers higher than that in the heteroepilayers and have a new mechanism of generating SA centers different from heteroepilayers. It is shown that the SA-PL intensity is closely related to the stoichiometry of the epilayers independent of the species of substrates. Since the homoepilayer grown at low [Se]/[Zn] has almost the same SA-PL intensity as the homoepilayer grown at high [Se]/[Zn], the dislocations or/and non-radiative defects influence generation of SA centers very little.

For these results, the out-diffusion of Zn vacancies from the ZnSe substrate seems to be very likely. The out-diffusion of Zn vacancies has already been discussed from a different standpoint (section 2-2-2 (A) and (B)). In all samples, the I_1^{deep} line due to the Zn vacancy itself is observed near 2.783 eV [81,82]. It is not confirmed completely that Zn vacancies can diffuse in the homoepilayer even at 250 ^{o}C. The ZnSe substrates contain only about 200 ppm of iodine impurities and the iodine impurities can combine with high concentration of Zn vacancies (probably, it is of the order of 100 ppm.). We conclude that the substrate contains a high concentration of Zn vacancies and the out-diffusion of Zn vacancies from substrate is so remarkable that they easily make complexes with residual impurities.

In summary, the PL intensity of deep emissions of the homoepilayer is several times stronger than that of the heteroepilayer. Since the origin of the deep centers is considered to be due to the complex of the Zn vacancy and residual impurity in the epi-

layer, the deep centers are SA centers and it needs to be discussed on why, where and how SA centers are easily generated in the homoepilayer. It shows that homoepilayers have little dependence of [Se]/[Zn] on the concentration of SA centers and have deep centers several times more than heteroepilayers. It is shown that the generation rate of SA centers in the homoepilayer has nothing to do with both the stoichiometry and the crystallographic property. As a new mechanism of generating Zn vacancies, it will be concluded that the out-diffusion of Zn vacancies is marked in the homoepilayers. It shows that the control of the density of Zn vacancies will be essential to grow the ZnSe homoepilayers with device quality.

Thus the generation rate of SA centers in the ZnSe homoepilayers is not repressed only by controlling [Se]/[Zn] during the epitaxial growth. The Zn vacancies diffuse into ZnSe homoepilayers from the impure ZnSe substrates during the epitaxial growth. Accordingly, the growth temperature is thought to be an important parameter in controlling the concentration of SA centers and to grow the homoepilayers with high crystalline quality. In what follows, we will discuss the dependence of the growth temperature on the crystalline quality of the homoepilayers and try to improve the crystalline quality still more.

(D) Dependence of growth temperature on crystalline quality of ZnSe homoepilayer

In the section 2.2.2(B) and (C)., it is suggested that the origin of SA centers consists of Zn vacancies diffusing from the ZnSe substrate and residual impurities in the ZnSe homoepilayer. It is expected that the generation rate of Zn vacancies in the ZnSe homoepilayer can be reduced by lowering the growth temperature, so that the concentration of the SA centers will also be controlled at the same time in the ZnSe homoepilayer. The overall crystalline quality of the epilayers will be improved.

In this section, we report the characteristics of homoepilayers grown at low temperatures below 250 ^{o}C. Also we will make a comparison with the crystalline quality of heteroepilayers from the mechanism of epitaxial growth in detail.

The growth conditions are listed in Table 2.2.4. The growth conditions other than the growth temperature were kept as follows. The reactor pressure was atmospheric, the total flow rate was 3.3 l/min., the flow rate of DMZ was 11.5×10^{-6} mol/min., and the growth periods was one hour. And the [Se]/[Zn] was 10, which was the optimum for ZnSe homoepilayers with the best crystalline quality as reported in previous papers [46,86]. The growth temperature was changed between 190 and 250 ^{o}C. In the case of heteroepitaxy, the substrates were (100) HB-GaAs with the etch pit density of about 10^4 cm^{-2}. The ratio [Se]/[Zn] was changed from 20 to 40, which was the suitable condition for the heteroepitaxy [54]. The other growth conditions were all the same as

homoepitaxy.

Under the growth conditions listed in Table 2.2.4., all the epilayer thicknesses are about 4 μm and the surface morphologies are mirror-like. Figure 2.2.29 shows a typical surface morphology of the homoepilayer grown at 210 ^{o}C. Figure 2.2.30 shows the PL spectra (measured at 300 K) of the homoepilayers grown at various growth temperatures. No emissions are observed other than the BE emission which corresponds to the emission inherent to ZnSe with high crystalline quality. This apparently shows that the homoepilayers have little density of SA centers. The total PL intensity is very weak, since the concentration of residual impurities is very low (less than 10^{15}cm^{-3} from the Hall measurement) in the homoepilayers.

Figure 2.2.31 also shows the PL spectra (measured at 77 K) of the homoepilayers grown at various growth temperatures. Both BE and SA emissions are observed though SA emissions are not detected at 300 K as shown in Fig. 2.2.31. It indicates that the probability of occupation of trapped electrons in SA centers increases by lowering the measurement temperatures. It is necessary to measure the SA-PL intensity at suitably low temperatures in order to estimate the true concentration of SA centers in the epilayers. Figure 2.2.32 shows the dependence of the growth temperature on the PL ratio and on the absolute PL intensities of both BE and SA emissions. In order to compare them with the PL properties of the heteroepilayers grown at the same growth temperature, the PL ratios of the heteroepilayers are also plotted in Fig. 2.2.32. The PL ratio decreases above 250 ^{o}C, and also

below 200 ^{o}C abruptly. The growth temperature dependence shows that the generation mechanism of SA centers in the ZnSe homoepilayers is probably different from that in the region of the high growth temperature. A new generation mechanism of SA centers has been proposed in former sections 2-2-2(B) and (C). The generation mechanism requires that SA centers in the homoepilayers are generated by the out-diffusion of Zn vacancies from the highly iodine-doped ZnSe substrates during the growth. We assume that the out-diffusion of Zn vacancies is so heavy above 250 ^{o}C that SA emissions become very intense. Below 200 ^{o}C, on the other hand, the absolute PL intensity of the band-edge emission is abruptly decreasing, so that the PL ratio appears to be low. The reason is thought either the crystallographic quality of the ZnSe homoepilayers would become worse or the homoepilayer would be highly purified by growing at very low temperature. Let us discuss the reason. Though the small FWHM of ZnSe(400) diffraction pattern by the double crystal x-ray spectrometer seemingly shows that the crystallographic quality is most excellent of all the homoepilayers (the FWHM is 14 arc sec (see Fig.2.2.33.), which is comparable to the crystallographic property of the ZnSe [66] or GaAs substrates.), it is suggested from the observation of the hazy surface morphology that the homoepilayer grown at 190 ^{o}C is the layer with poly-crystalline quality. Because 190 ^{o}C is not a temperature high enough to form a complete ZnSe lattice. This inconsistency is analogous to the discussion on the degradation of crystalline quality of the homoepilayer grown at high [Se]/[Zn]. It is doubtful if the true crystallographic property

of the ZnSe homoepilayer is examined by the double crystal x-ray spectrometer. The crystallographic property cannot always determine the degree of purification in the epilayers, because, for example, the ZnSe substrates have such a small FWHM (about 10 arc sec), independent of the iodine-incorporation of about 200 ppm in the substrates. Figure 2.2.34 shows the dependence of the growth temperature on the crystallographic property of the homoepilayers examined by the double crystal x-ray spectrometer. The crystalline quality of the homoepilayer is independent of the growth temperature except for one grown at 190 ^{o}C. We thus conclude that the degradation of the crystalline quality of the ZnSe homoepilayer starts to occur at 190 ^{o}C. Also, it is very important to measure PL near the band-edge region at 4.2 K. One has to be aware to what degree the impurities are taken into the epilayers. Figure 2.2.35 shows the PL spectra (measured at 4.2 K) near the band-edge region of the homoepilayers grown at various growth temperatures. The total PL intensity of a homoepilayer grown at 190 ^{o}C is weaker than that of the homoepilayers grown at other temperatures. A broad donor bound exciton line appears at 2.7999 eV, which is probably assigned as I_X usually observed at 2.7974 eV in the heteroepilayers. The energy position of each line observed in homoepilayers shifts upwards. This line is a little broad and the E_X appears as a shoulder on the I_X line. It is obvious from this fact that all the homoepilayers have less strain compared with heteroepilayers. It is supported from the broadness of I_X that the crystalline quality of the homoepilayer grown at 190 ^{o}C is inferior to that of the homoepilayers grown

above 200 ^{o}C. The FWHM of the PL emission line becomes smaller with increasing growth temperature. It indicates that the crystallographic quality is reasonably improved by the raise of the growth temperature. The result is inconsistent with the result of the FWHM of ZnSe(400) diffraction pattern measured by the double crystal x-ray spectrometer in the homoepilayer at 190 ^{o}C. We have already reported a similar phenomenon [87] that the homoepilayers grown at 250 ^{o}C (and at high [Se]/[Zn]) seemingly have the high crystallographic property in spite of showing low PL ratios and having broad excitonic emission lines. The surface morphologies of the homoepilayers are also very hazy. Therefore, it is concluded that the true crystalline quality is not so good. It is suggested that the excellent crystallographic property of the ZnSe substrate, not the homoepilayer, is simply measured by the double crystal x-ray spectrometer as described before.

Let us now compare the crystalline quality of the ZnSe homoepilayers with that of the ZnSe heteroepilayers from the viewpoint of the crystal growth condition, particularly on the growth temperature dependence. Figure 2.2.36 shows the PL spectra (measured at 77 K) of the ZnSe heteroepilayers grown at various growth temperatures. Between 210 and 250 ^{o}C, the PL spectra show that the heteroepilayers have strong BE and very weak SA emissions. Below 210 ^{o}C, an abrupt change of the crystalline quality occurs in the heteroepilayers (see Fig. 2.2.32.). The BE-PL intensity of a heteroepilayer grown at 205 ^{o}C becomes by an order of magnitude less than that from a heteroepilayer grown at 190 ^{o}C and by two orders of magnitude less than that of the heteroepi-

layer grown at 210 ^{O}C , so that the PL ratio becomes very small (the PL emissions are not seen at 300 K.). This indicates that the crystallographic property of the heteroepilayer starts to degrade from the critical point (210 ^{O}C). The fact is also confirmed by the double crystal x-ray spectrometer (ZnSe(400) diffraction pattern is not observed at all.). Figure 2.2.37 shows the surface morphologies of the ZnSe heteroepilayers grown at 205 and 210 ^{O}C. It also shows that 210 ^{O}C becomes the critical temperature on the heteroepitaxial growth of ZnSe and the heteroepitaxial growth mechanism changes drastically at this temperature. This phenomenon is quite different from the case of the homoepitaxial growth as described before. In the homoepitaxy, the crystalline quality is not degraded even at 200 ^{O}C. The difference of the growth temperature dependence is telling that Zn and Se atoms can move around on the ZnSe substrates easier than on the GaAs substrates, so that the ZnSe homoepilayers can maintain the high crystalline quality even below 200 ^{O}C. We will discuss the behavior of Zn and Se atoms during the growth particularly at low temperatures. We further observe that if the high [Se]/[Zn] (>40) is chosen as the growth condition, the surface morphologies of the heteroepilayers grown at 210 ^{O}C become as hazy as that of the heteroepilayers grown at 205 ^{O}C (Fig. 2.2.37.) and the absolute PL intensity starts to decrease abruptly (Fig. 2.2.38.). This indicates that the high concentration of Se atoms on the GaAs substrate degrade the crystalline quality of the heteroepilayers during the growth. Moreover, we have reported in a previous paper [87] that even the homoepilayers grown at 250 ^{O}C have

very hazy morphologies similar to the one stated above if they were grown at a high [Se]/[Zn] (>30). Since it is generally accepted that the diffusion rate of Se atom on the substrate is lower than that of the Zn atom, the existence of immobile Se atoms on the GaAs substrates would obstruct the movement of the mobile Zn atoms especially at low growth temperatures or at high [Se]/[Zn]. Recently, a similar phenomenon is reported on the migration enhanced epitaxy of GaAs grown at the low growth temperature near 300 ^{o}C [88]. In that case, the migration of Ga atoms is enhanced by reducing the concentration of As atoms existing on the GaAs substrates at low temperatures. Probably, ZnSe is also grown according to a similar growth mechanism and, at the same time, Zn or Se atoms on the ZnSe substrates would be possible to move more easily than that on the GaAs substrates.

In summary, the homoepilayers with high crystalline quality were grown on the (100) oriented ZnSe substrates between 200 and 250 ^{o}C by the atmospheric pressure MOVPE. The SA-PL intensity of the homoepilayers is much related to the growth temperature. Above 240 ^{o}C, the SA-PL intensity increases gradually with increasing growth temperature. The reason is supposed that the Zn vacancies would diffuse from the highly iodine-doped ZnSe substrates into the homoepilayers above 240 ^{o}C to form SA centers. Below 240 ^{o}C, the SA-PL intensity of the homoepilayer becomes so weak that the PL ratio assumes a large value which is comparable to that of the best ZnSe heteroepilayer (particularly at 210 ^{o}C, the crystalline quality of the homoepilayer is superior to that of the heteroepilayer.). Below 200 ^{o}C, however, the PL

ratio appears to be reduced drastically because the BE-PL intensity is decreasing by two orders of magnitude. From the results of PL properties, we have obtained the ZnSe homoepilayers with very low concentration of SA centers. The growth temperature has been between 210 and 230 ^{O}C in both hetero and homoepilayers. The dependence of growth temperature on crystalline quality of homoepilayer is quite different from that of the heteroepilayer. In the heteroepitaxial growth, the crystalline quality starts to degrade below 210 ^{O}C (the critical temperature). The reason is perhaps that too many immobile Se atoms existing on the GaAs substrates would obstruct the movement of Zn atoms more than those on the ZnSe substrates, particularly at low temperatures.

Thus, as expected in sections 2-2-2 (A), (B) and (C), the concentration of SA centers in the ZnSe homoepilayers is drastically decreased by lowering the growth temperature. The crystalline quality is also improved then. Nevertheless, the crystalline quality of the ZnSe homoepilayers grown at the optimum conditions is still competing with that of the ZnSe heteroepilayers grown at the optimum conditions. It therefore indicates that the effect of lattice matching is not so clarified even by the homoepitaxial growth at present. It is not evident yet whether the ZnSe epilayer with higher crystalline quality are required, or the ZnSe epilayers with device quality are already grown independently of homo- and/or hetero-epilayers. We will further discuss whether the ZnSe epilayers are grown with the overall crystalline quality enough to try p-type doping in them and to develop the B-LED at the present stage.

Table 2.1.1. Electrical properties of MOVPE-grown ZnSe heteroepilayers.

Sample No.	Thickness (μm)	n_{300K} ($\times 10^{16}$ cm^{-3})	n_{77K} ($\times 10^{16}$ cm^{-3})	μ_{300K} (cm^2/V·s)	μ_{77K} (cm^2/V·s)	N_D ($\times 10^{17}$ cm^{-3})	N_A ($\times 10^{17}$ cm^{-3})	N_A/N_D [a]
SeB79	1.0	0.84	0.22	160	260	1.4	1.3	0.93
SeA64	3.0	9.0	2.3	310	540	1.8	0.9	0.50
SeB77	8.0	6.0	1.7	240	800	1.1	0.5	0.45
SeB93	14.0	1.2	0.35	300	2000	0.3	0.14	0.47

[a] These values were calculated using the Brooks–Herring formula and assuming $n_{300K} = N_D - N_A$.

Table 2.1.2. List of electrical properties of epilayers grown at various growth temperatures and reactor pressures.

T_g (℃)	P_g(Torr)	n ($\times 10^{16} cm^{-3}$)		μ_H($cm^2/V \cdot s$)	
		300K	77K	300K	77K
250	0.1	85	38	83	182
250	6.8	39	——	305	——
300	0.1	9.0	2.3	310	540
300	7.4	4.6	1.4	266	803
350	0.1	1.0	0.4	52	362
350	6.2	1.2	0.36	354	3004

Table 2.1.3. Growth conditions of ZnSe heteroepilayers by MOVPE.

Sample No.	Temperature (°C)	Flow rate (μmol/min.)		Mole ratio η_M((Se)/(Zn))	Flow velocity (cm/s.)		Flow velocity ratio $\eta_V(V_{Zn}/V_{Se})$	Growth rate (μm/h.)	Total flow velocity (cm/s.)
		(Zn)	(Se)		V_{Zn}	V_{Se}			
#17			46.5	3	0.9	0.9	1	3.9	2.8
#73	300	15.5	46.5	3	125	0.7	180	10.0	0.7
#35			465	30	125	0.7	180	8.2	0.7

Table 2.2.1. Heat treatment conditions.

Sample No.	Atmosphere	Temperature (°C)	Pressure (Torr)	Total flow rate (l/min.)	Period (min.)
149	– [a]	– [a]	– [a]	– [a]	– [a]
111	H_2	300	760	4.0	30
112	H_2	400	760	4.0	30
131	$H_2 + H_2Se$	600	760	2.0(H_2)+0.1(H_2Se)	20
133	H_2	600	760	4.0	20
135	H_2 + DMZ	600	760	2.0 (H_2)+DMZ (6.5 cm^3, −20 °C)	20
139	H_2	650	760	4.0	20

[a] No heat treatment.

Table 2.2.2. Growth conditions.

Sample No.	Temperature (°C)	Flow rate (μmol/min.) (Zn)	Flow rate (μmol/min.) (Se)	Mole ratio η_M	Total flow rate (ℓ/min.)	Growth rate (μm/h)	Layer thickness (μm)
HOMO-1	250	15.5	310	20	3.3	6.6	6.6
HOMO-2	250	15.5	43.4	2.8	3.3	5.5	5.5
HOMO-3	250	15.5	43.4	2.8	3.3	6.0	1.0
HOMO-4	250	46.5	46.5	1	3.3	31.6	15.8
HOMO-5	250	15.5	930	60	3.3	8.2	8.2
HETERO-1	250	15.5	310	20	3.3	6.4	6.4
HETERO-2	250	12	34	2.8	3.3	3.4	3.4
HETERO-3	250	12	720	60	3.3	3.5	3.5

Table 2.2.3. Growth conditions.

Sample No.	Substrate	Temperature (°C)	Flow rate (μmol/min.)		Mole ratio, [Se]/[Zn]	Total flow rate (l/min.)	Layer thickness (μm)
			Zn	Se			
1	(100) ZnSe	250	15.5	930	60	3.3	6.6
2	(100) ZnSe	250	15.5	186	12	3.3	5.3
3	(100) ZnSe	250	15.5	93	6	3.3	6.6
4	(100) ZnSe	250	15.5	43.4	2.8	3.3	5.5
5	(100) ZnSe	250	15.5	15.5	1	3.3	5.1
6	(100) GaAs	250	15.5	465	30	3.3	6.6
7	(100) GaAs	250	15.5	186	12	3.3	4.3
8	(100) GaAs	250	15.5	15.5	1	3.3	5.1

Table 2.2.4. Growth conditions.

Sample No.	Temperature (°C)	Flow rate (μmol/min.) (Zn)	Flow rate (μmol/min.) (Se)	Mole ratio	Total flow rate (ℓ/min.)
Homo-1	190	11.5	115	10	3.3
Homo-2	200	11.5	115	10	3.3
Homo-3	205	11.5	115	10	3.3
Homo-4	210	11.5	115	10	3.3
Homo-5	220	11.5	115	10	3.3
Homo-6	230	11.5	115	10	3.3
Homo-7	240	11.5	115	10	3.3
Homo-8	250	11.5	115	10	3.3
Hetero-1	190	11.5	230	20	3.3
Hetero-2	205	11.5	230	20	3.3
Hetero-3	210	11.5	230	20	3.3
Hetero-4	210	11.5	460	40	3.3
Hetero-5	250	11.5	230	20	3.3

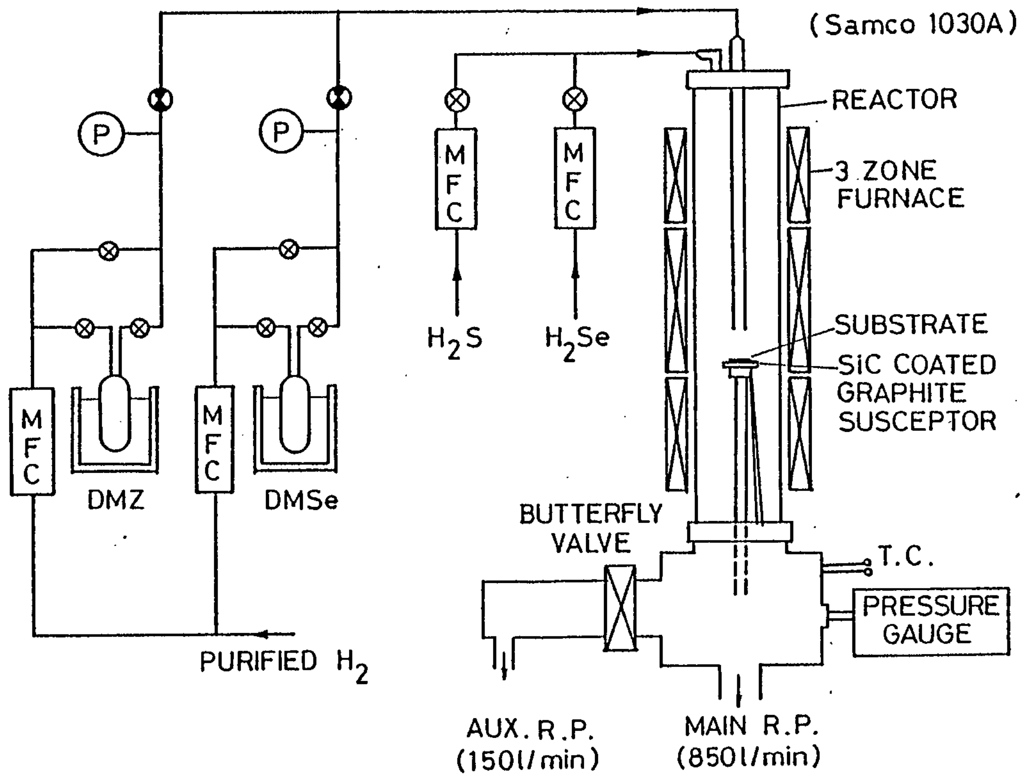

Fig.2.1.1. Illustration of MOVPE growth system used in this work.

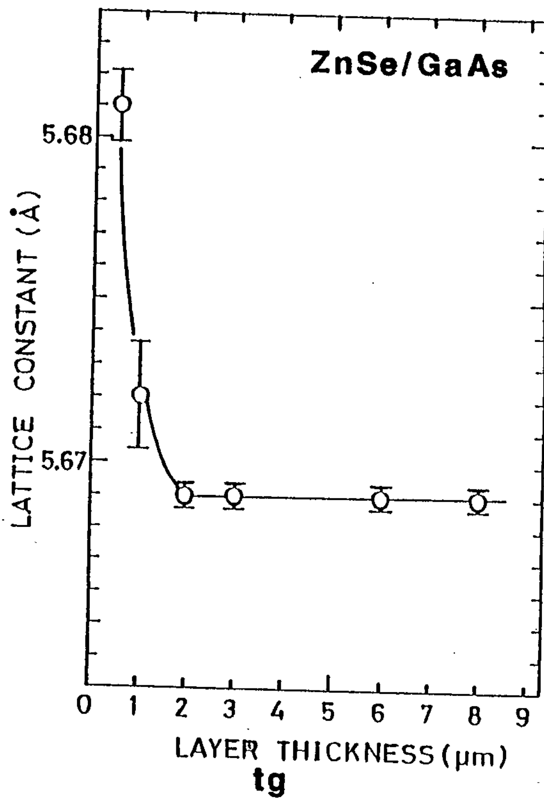

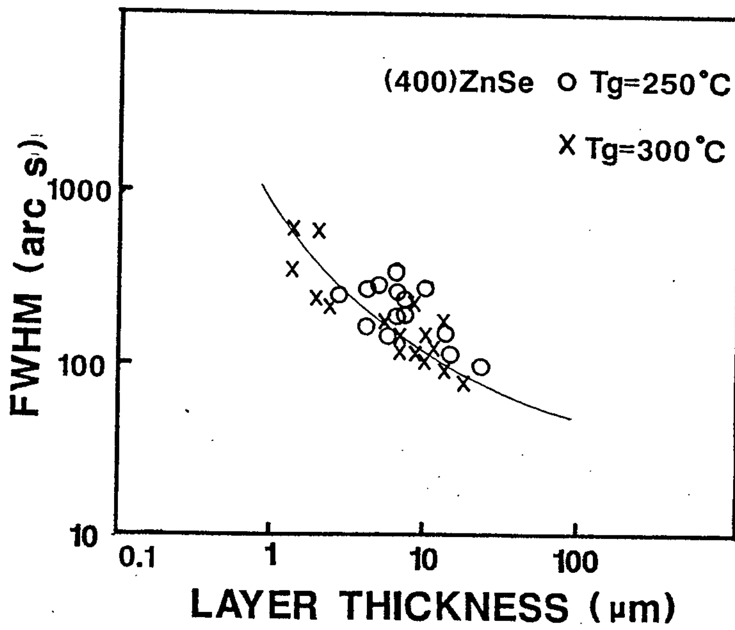

Fig.2.1.2. Variation of X-ray rocking curve with epilayer thickness.

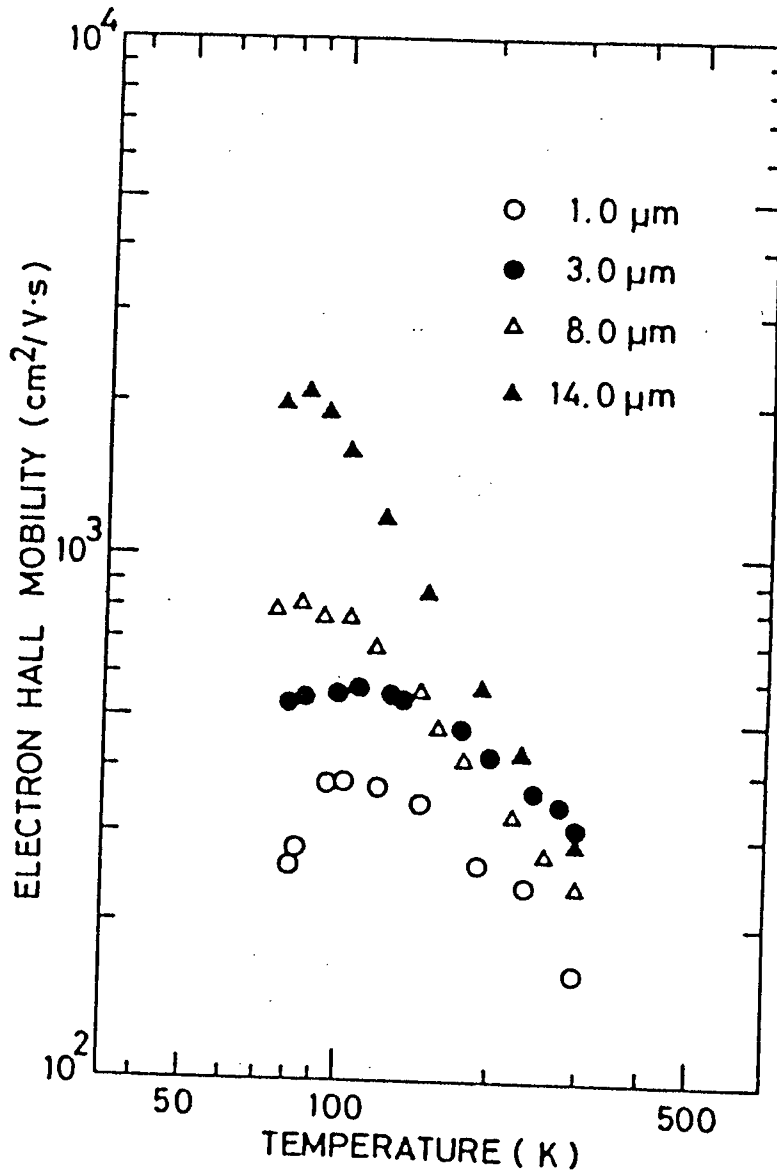

Fig.2.1.3. Temperature dependence of Hall mobility of ZnSe heteroepilayers as a function of epilayer thickness.

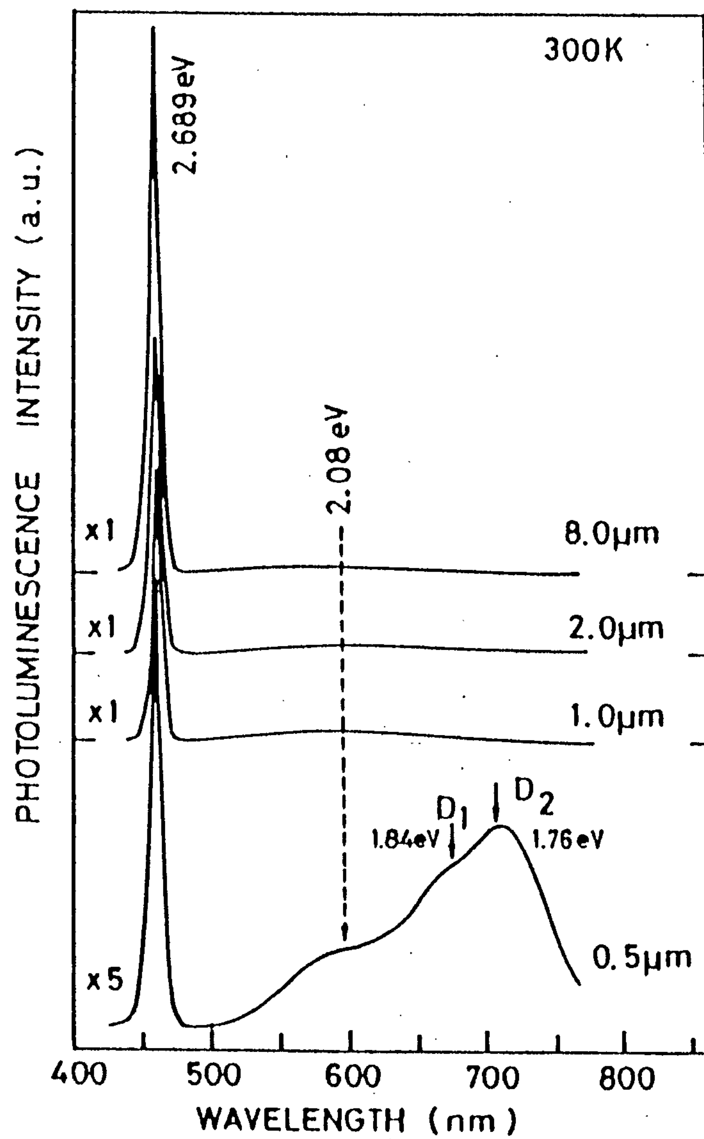

Fig.2.1.4. Variation of 300 K photoluminescence spectrum with epilayer thickness.

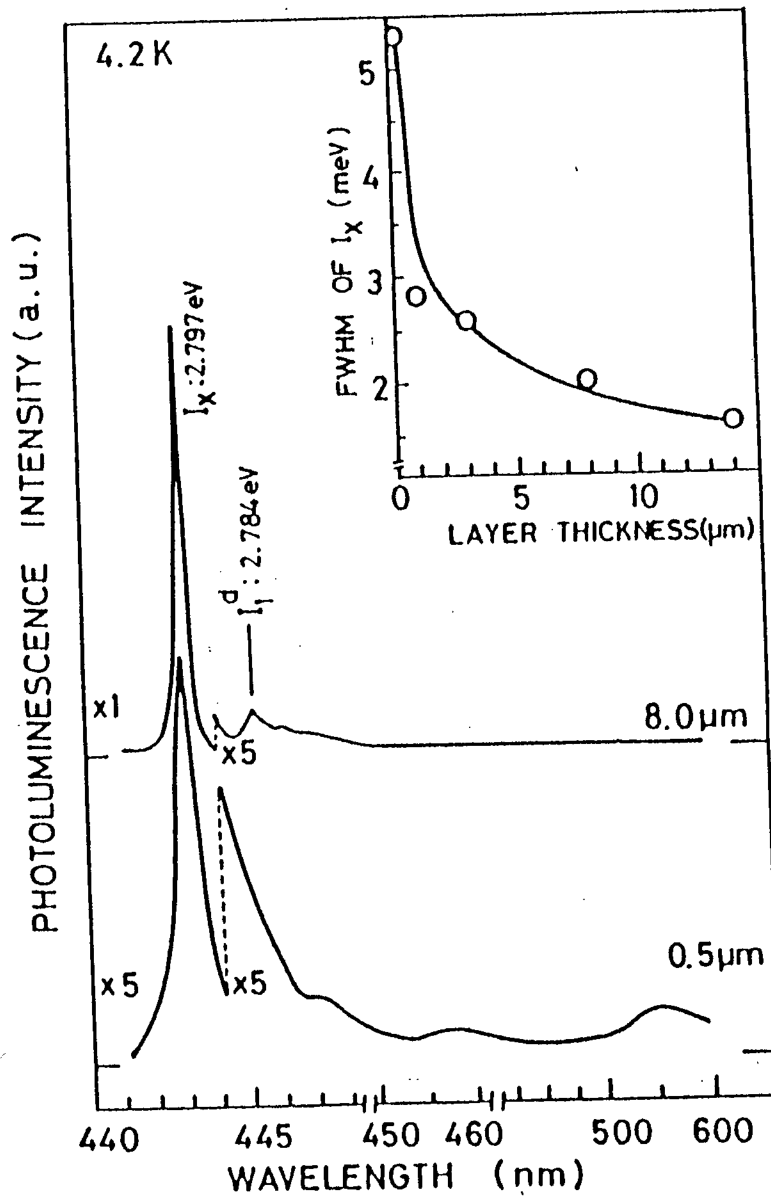

Fig.2.1.5. Photoluminescence spectra at 4.2 K of thin (0.5 μm) and thick (8.0 μm) heteroepilayers. The inset shows the variation of the linewidth of I_X with epilayer thickness.

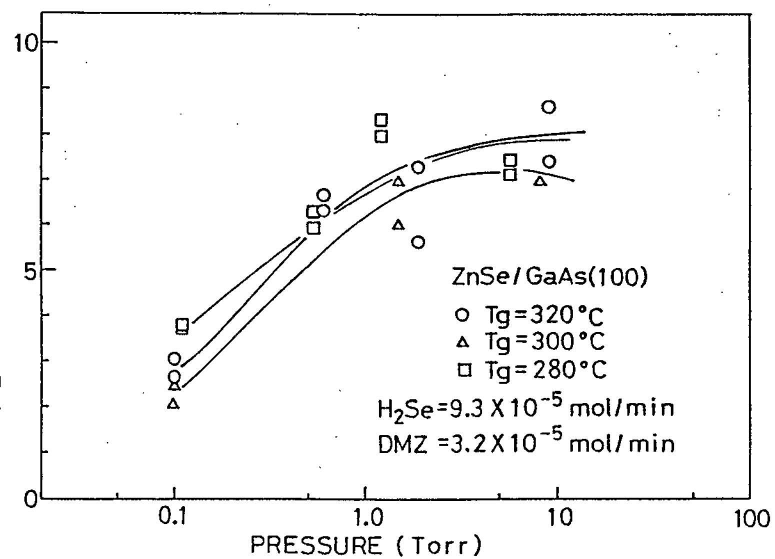

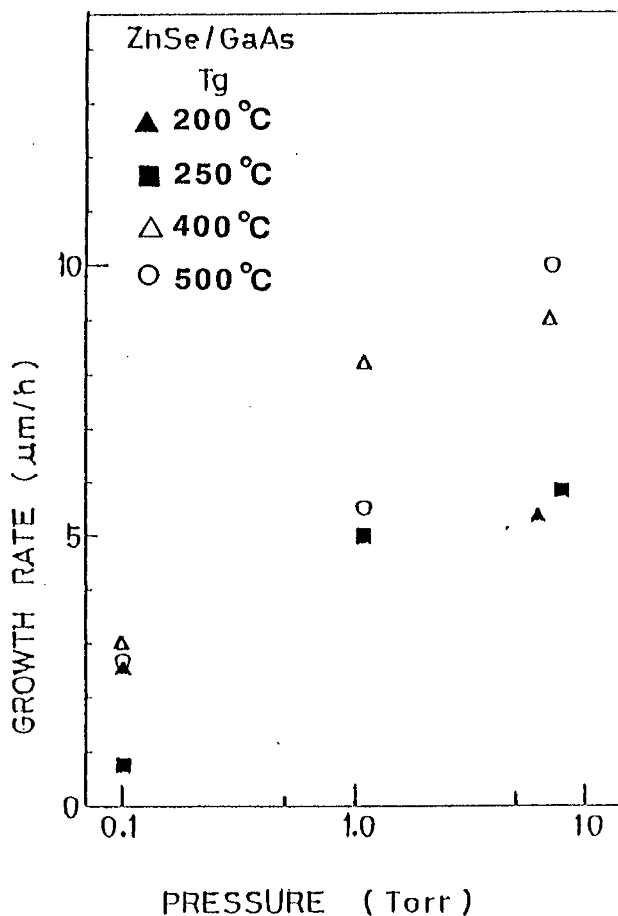

Fig.2.1.6. Dependence of the reactor pressure on the growth rate of the ZnSe heteroepilayers grown at different temperatures.

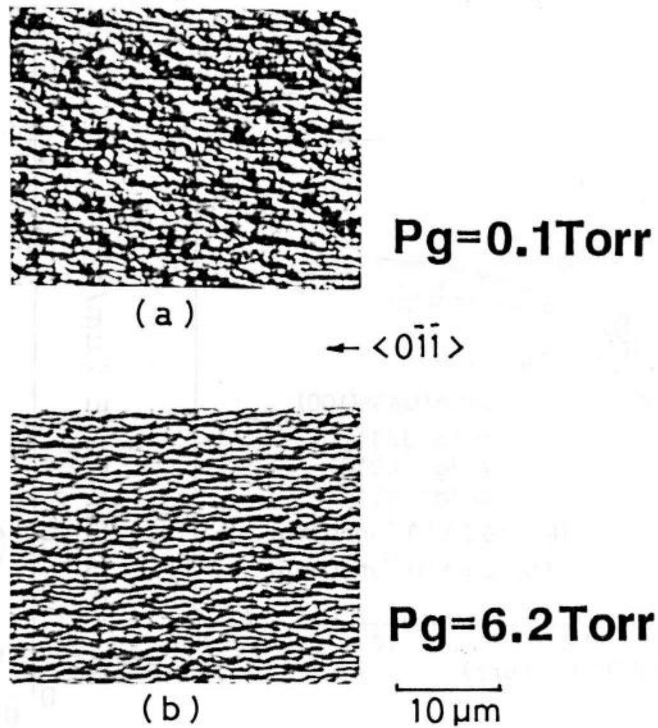

Fig.2.1.7. Surface morphologies of the ZnSe heteroepilayers grown at 350 ^{o}C and different reactor pressures (0.1 and 6.2 Torr).

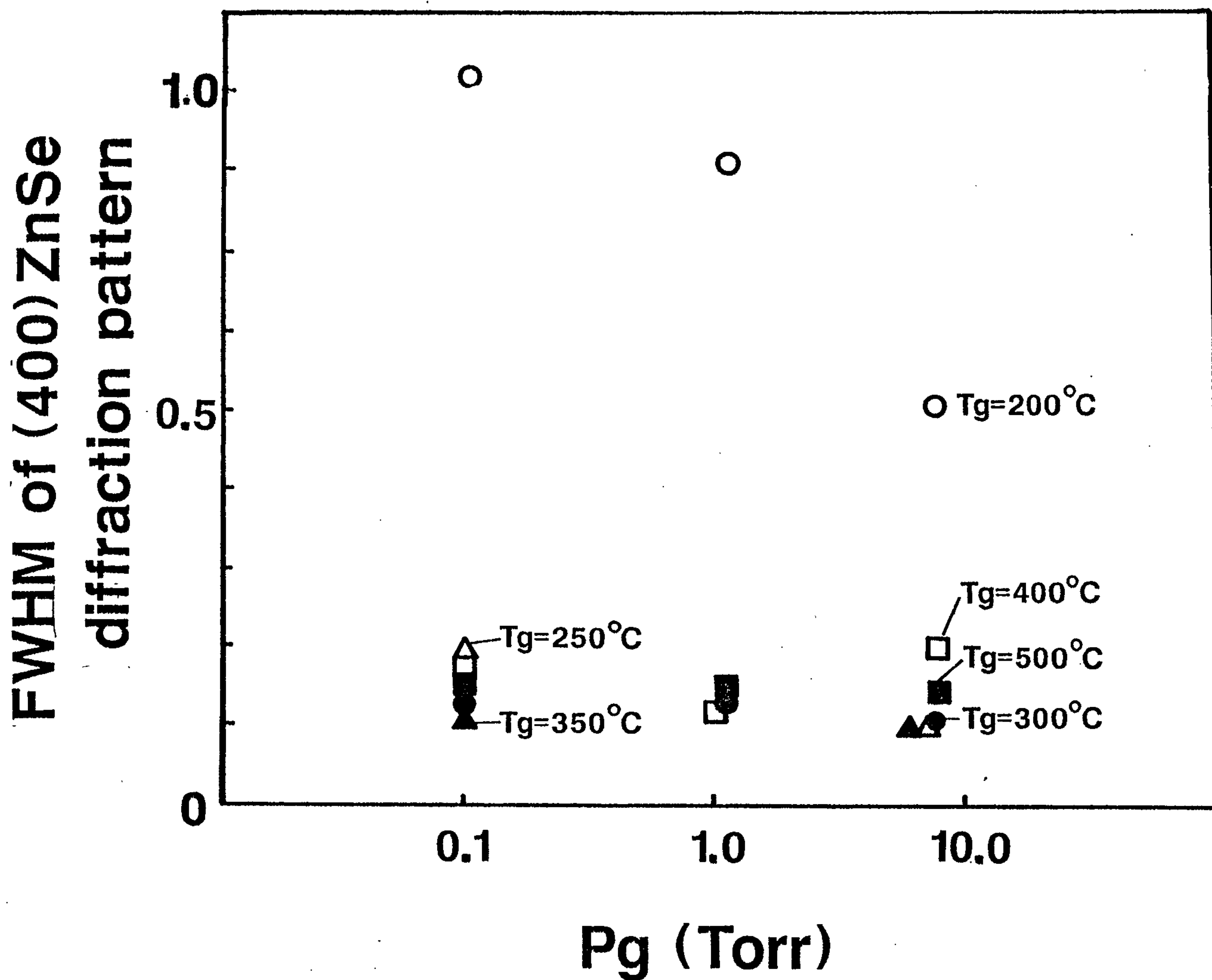

Fig.2.1.8. Dependence of the reactor pressure on the FWHM of (400) ZnSe diffraction pattern in ZnSe heteroepilayers grown at various growth temperatures and reactor pressures.

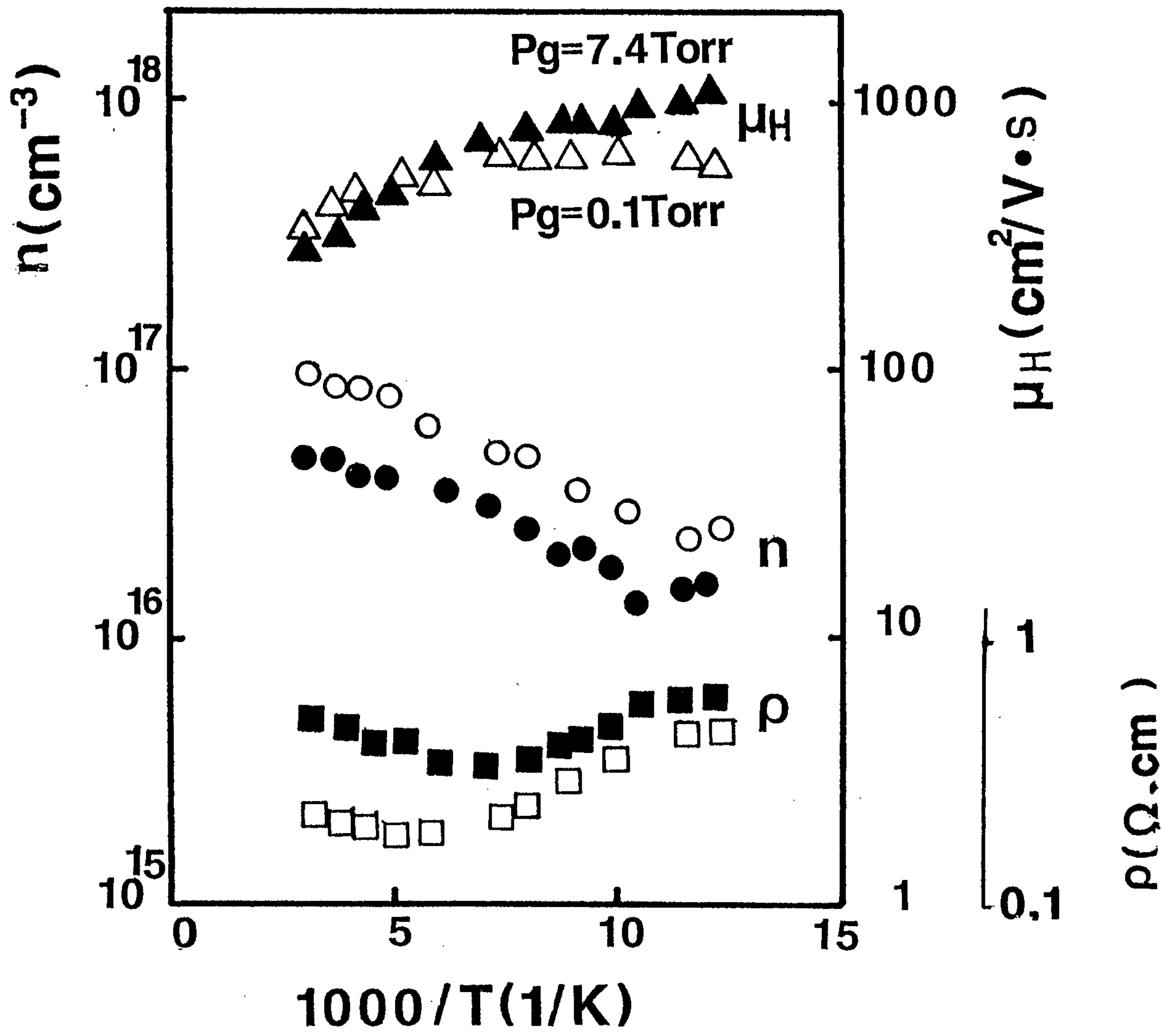

Fig.2.1.9. Temperature dependence of electrical properties (n, ρ, μ_H) by Hall measurement of the ZnSe heteroepilayer (T_g=300 ^oC, P_g=0.1 Torr and T_g=300 ^oC, P_g=7.4 Torr.).

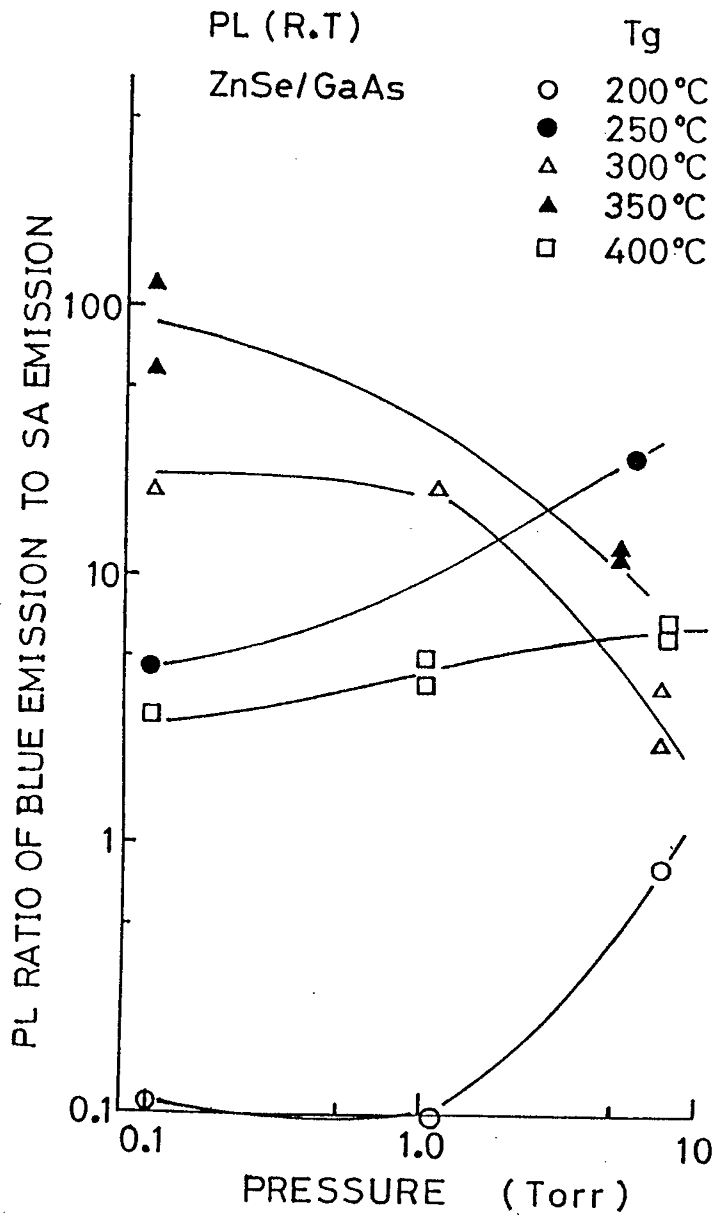

Fig.2.1.10. Dependence of reactor pressure on the PL ratio at 300 K of the ZnSe heteroepilayers grown at various growth temperatures.

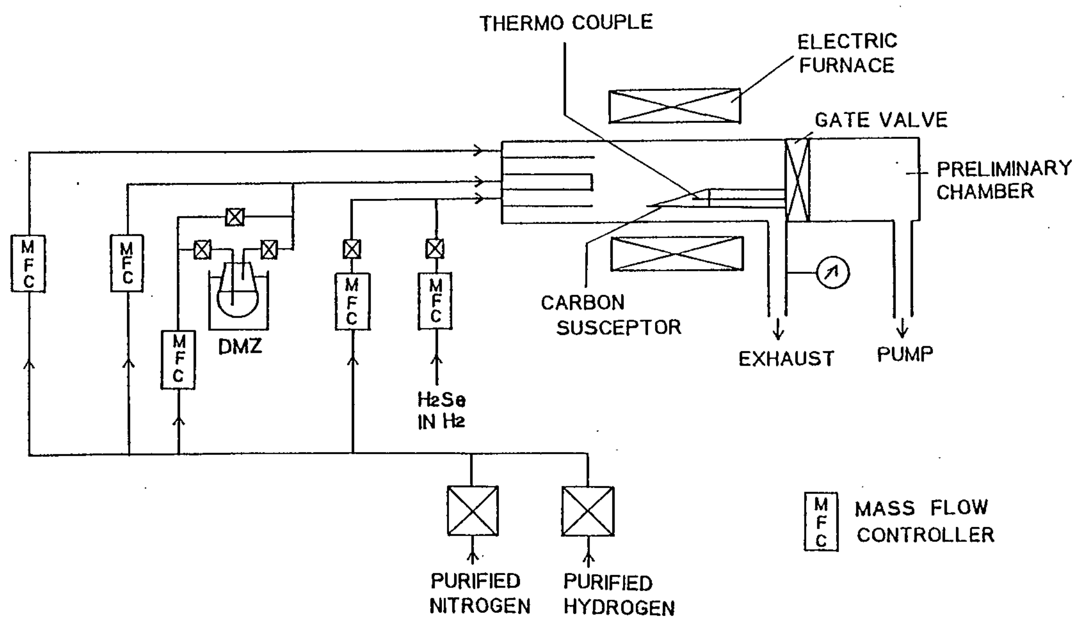

Fig.2.1.11. Illustration of MOVPE growth system used in this work.

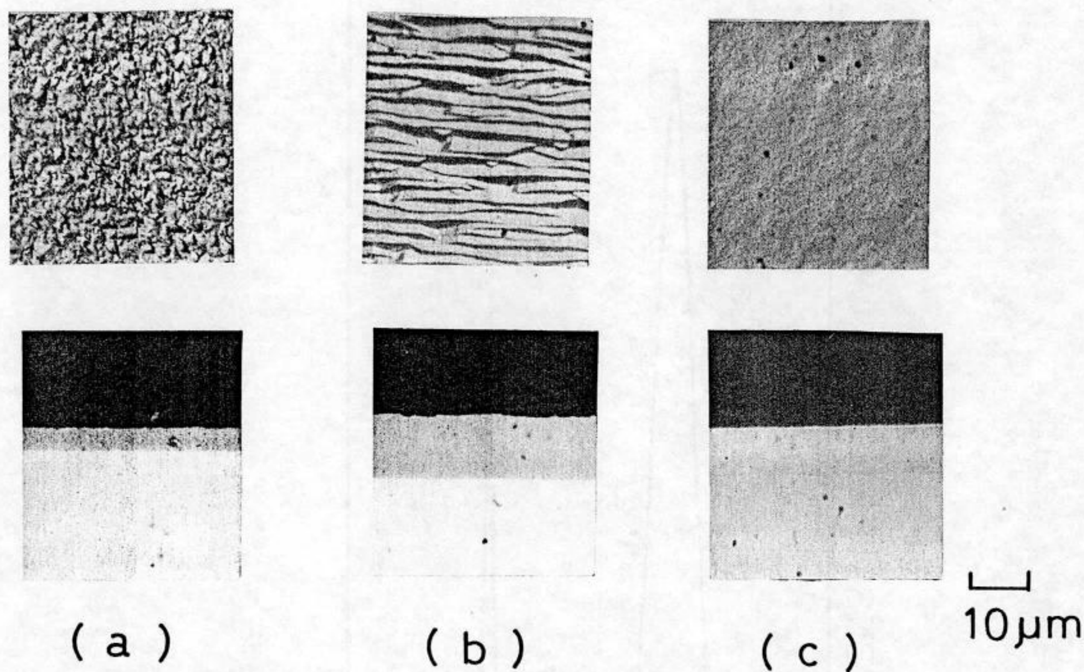

Fig. 2.1.12. Surface morphologies and cross sections of grown ZnSe heteroepilayers in relation to the [Se]/[Zn] and $V_{Zn/Se}$, as measured by a Nomarski phase interference microscope:

(a) [Se]/[Zn]=3 and $V_{Zn/Se}=1$; epilayer thickness (t_g) is 3.9 μm.

(b) [Se]/[Zn]=3 and $V_{Zn/Se}=180$; $t_g=10$ μm.

(c) [Se]/[Zn]=30 and $V_{Zn/Se}=180$; $t_g=8.2$ μm.

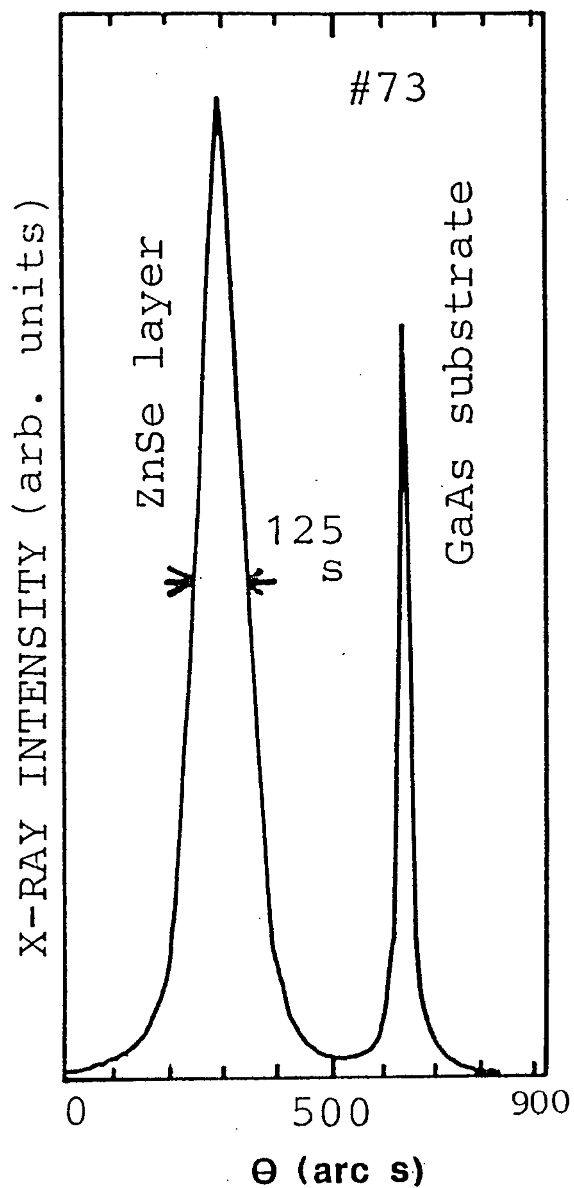

Fig.2.1.13. ZnSe(400) diffraction of a ZnSe heteroepilayer grown at an atmospheric pressure measured by a double crystal X-ray spectrometer.

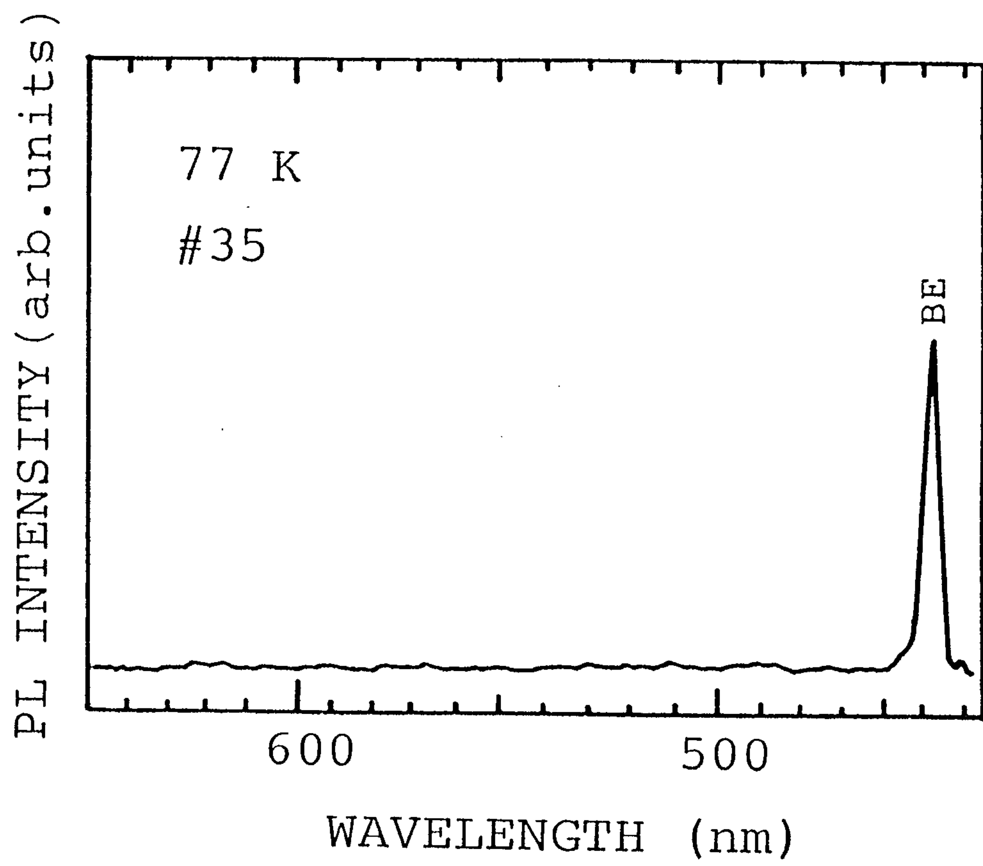

Fig.2.1.14. PL spectrum at 77 K of a ZnSe heteroepilayer grown by atmospheric pressure MOVPE.

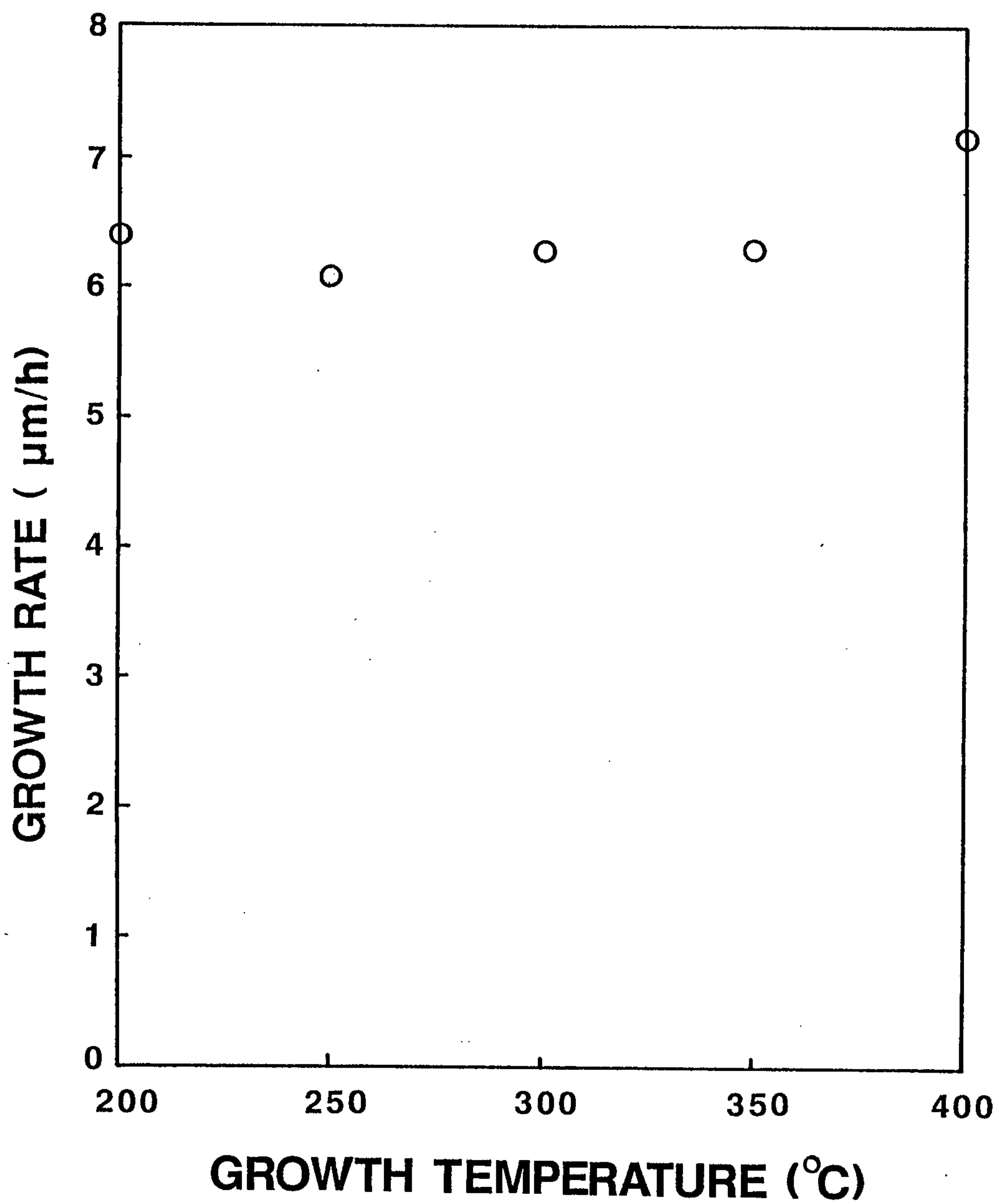

Fig.2.1.15. Dependence of growth temperature on the growth rate of the ZnSe heteroepilayers.

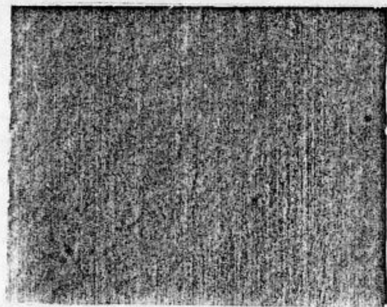

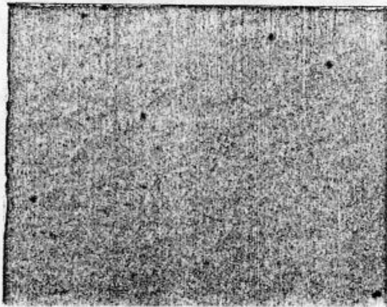

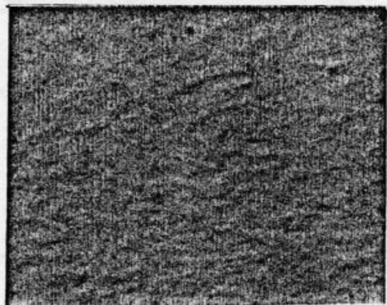

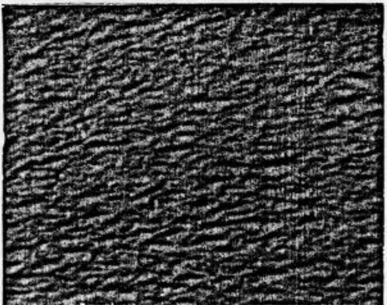

Fig.2.1.16. Surface morphologies of the epilayers grown at different temperatures.

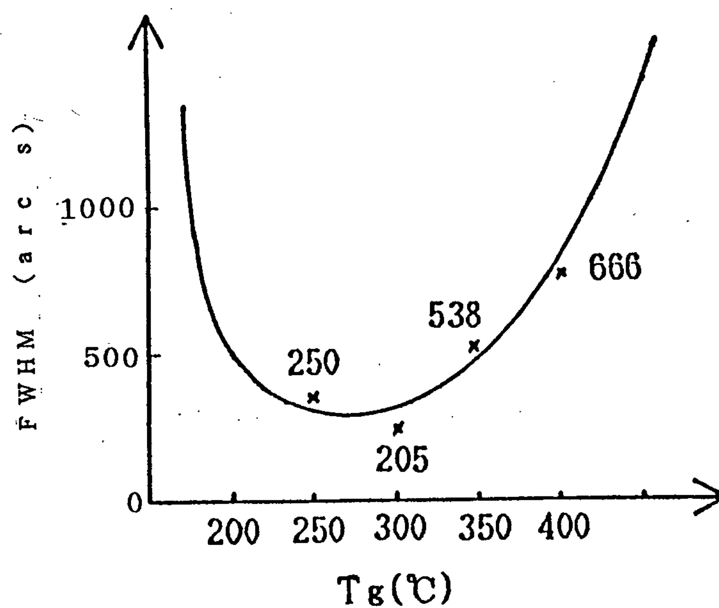

Fig.2.1.17. Dependence of growth temperature on the FWHM of ZnSe(400) diffraction patterns of ZnSe heteroepilayers.

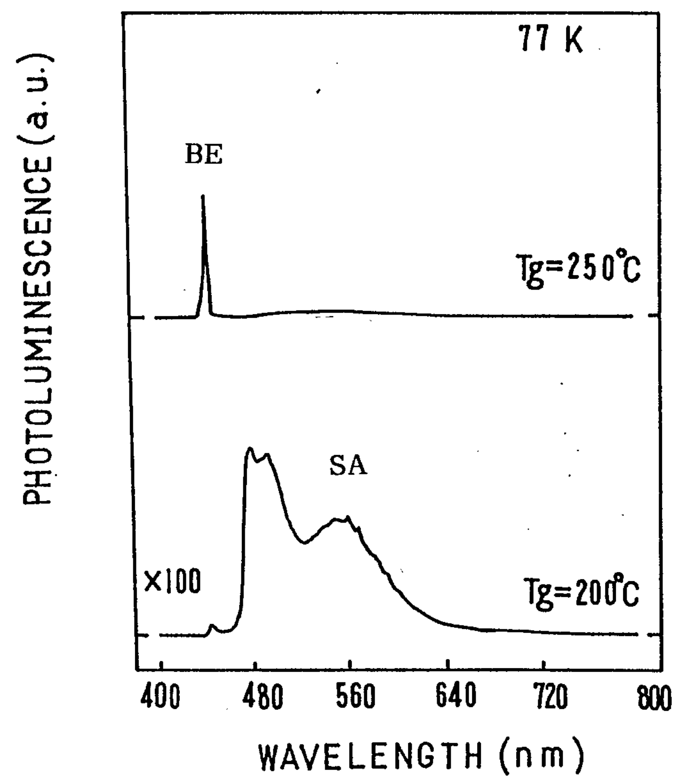

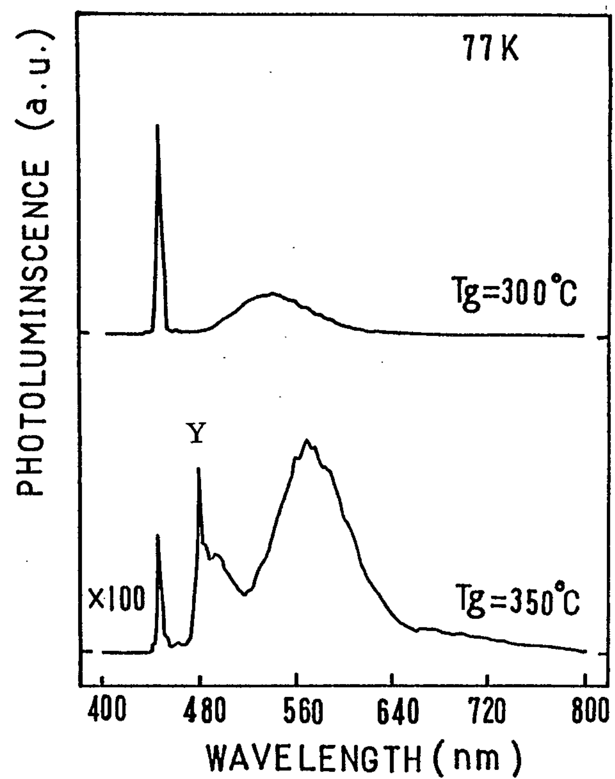

Figs.2.1.18. and 19. PL spectra at 77 K of ZnSe heteroepilayers grown at different temperatures.

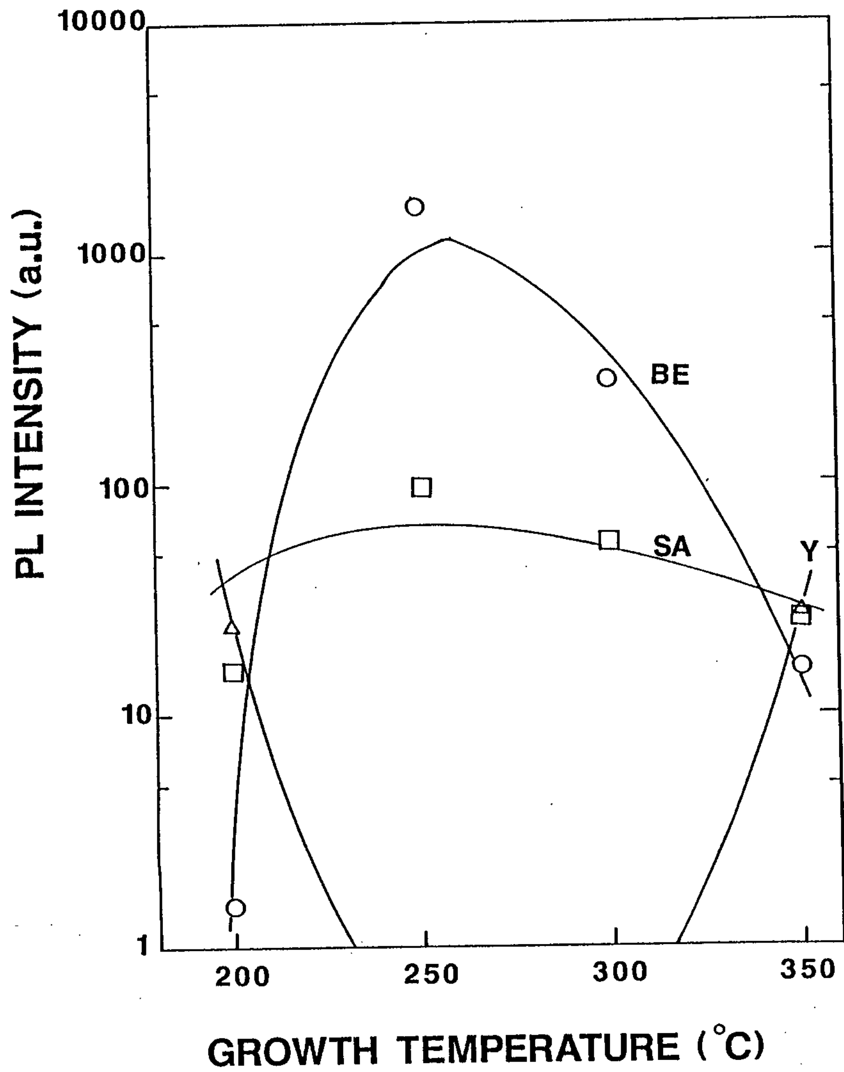

Fig.2.1.20. Growth temperature dependence of PL intensities of BE, Y and SA emissions and PL ratio (the ratio of BE-PL intensity to SA-PL intensity) at 77 K.

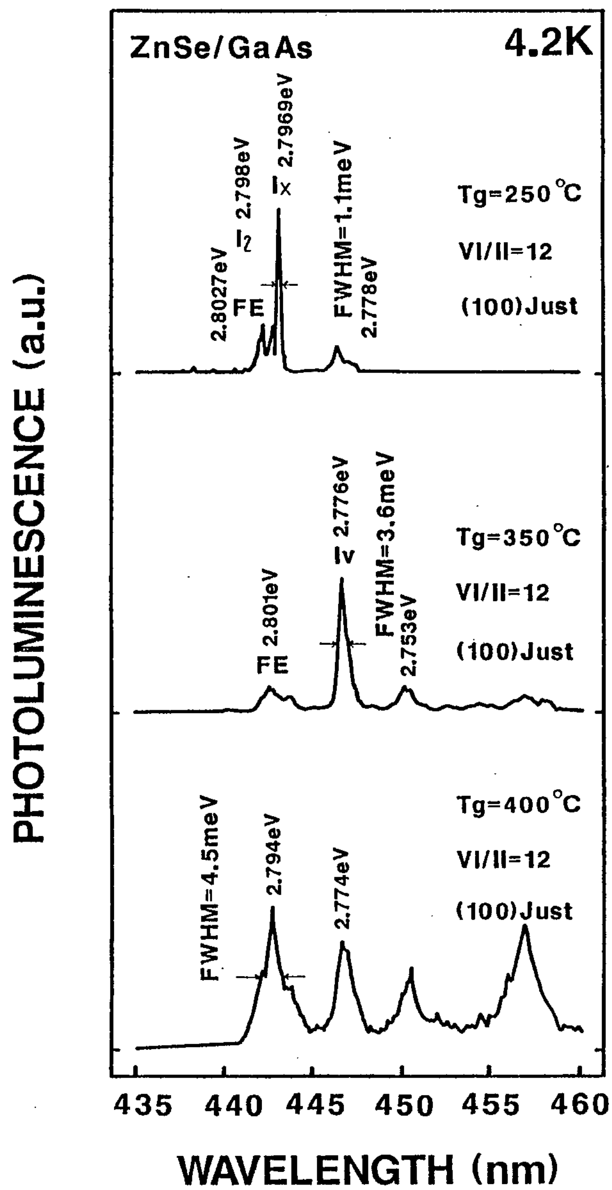

Fig.2.1.21. PL spectra at 4.2 K near the band-edge region (435-460 nm) of the ZnSe heteroepilayers grown at different temperatures.

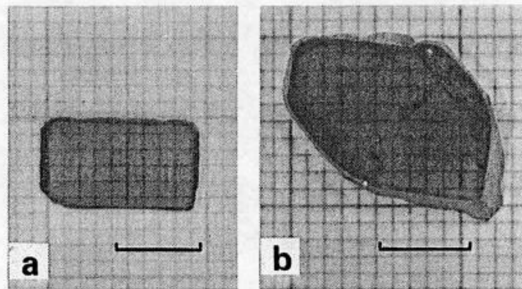

Fig.2.2.1. Photographs of typical ZnSe substrates.

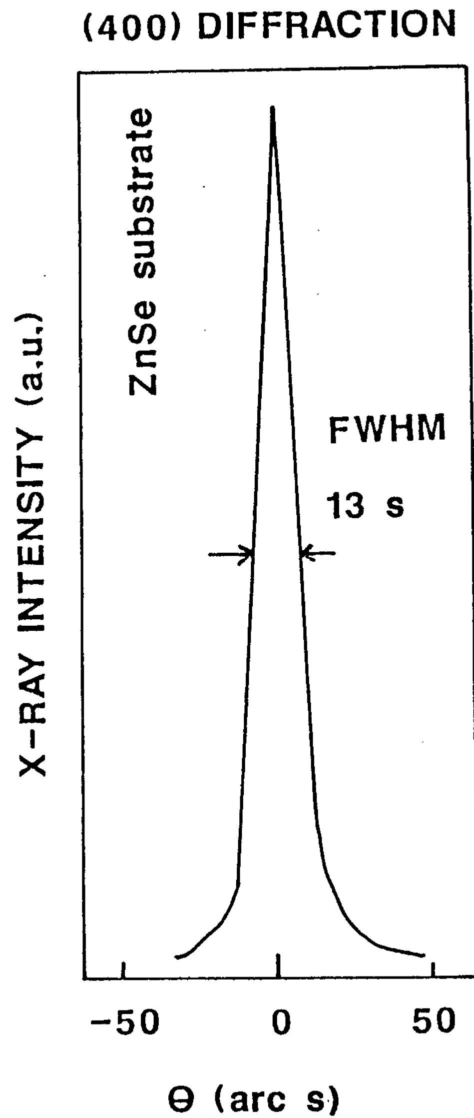

Fig.2.2.2. A typical ZnSe(400) x-ray diffraction spectrum of the ZnSe substrate measured by the double crystal x-ray diffraction spectrometer.

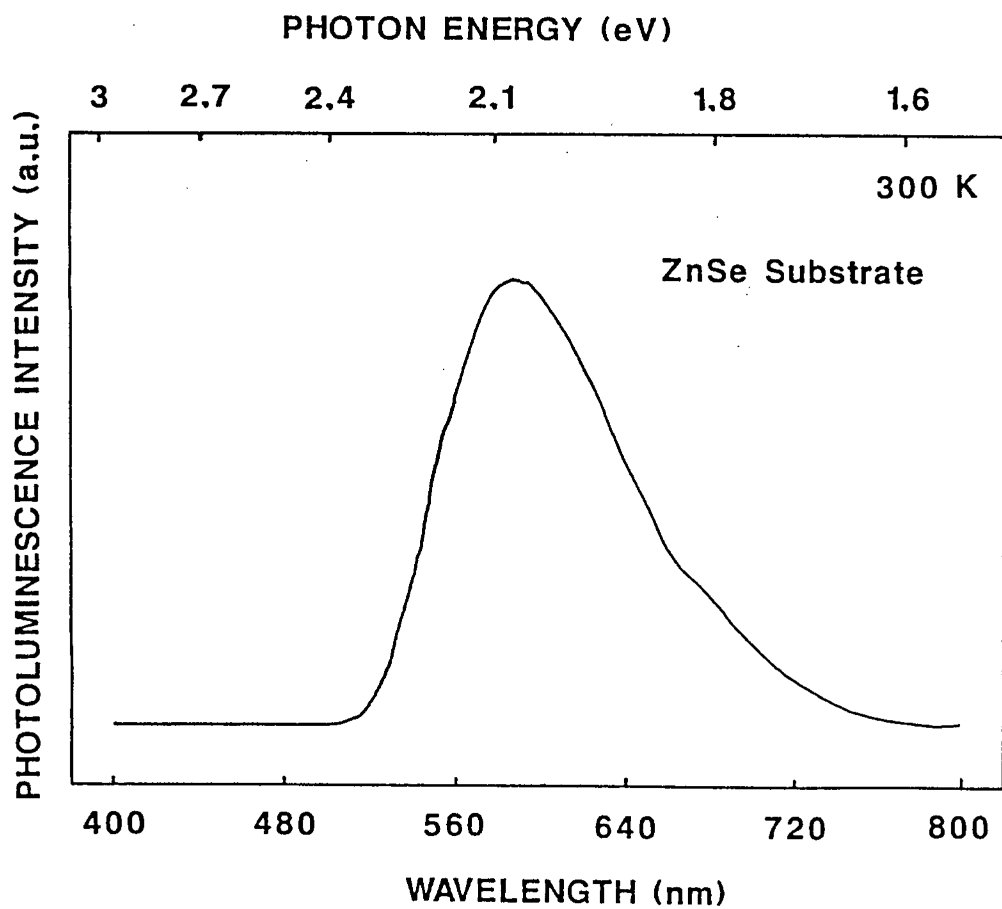

Fig.2.2.3. PL spectrum at 300 K of a ZnSe substrate.

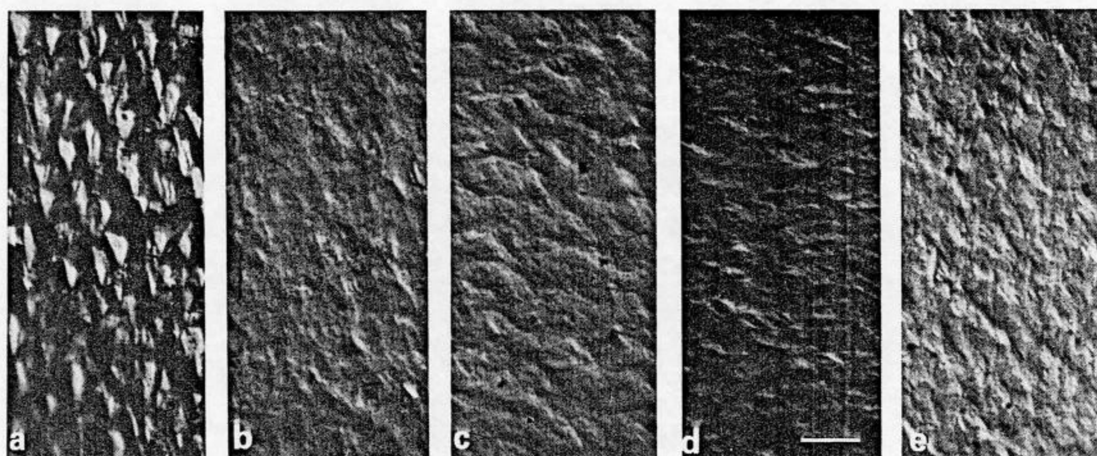

Fig.2.2.4. Surface morphologies of ZnSe epilayers grown on the ZnSe substrates pretreated at various temperatures and periods (the flow rate of H_2 is kept 4 l/min.).

(a) No heat treatment;#149.

(b) 400 ^{o}C and 30 min.; # 112.

(c) 600 ^{o}C and 20 min.; # 133.

(d) 650 ^{o}C and 10 min.; # 147.

(e) 650 ^{o}C and 20 min.; # 139.

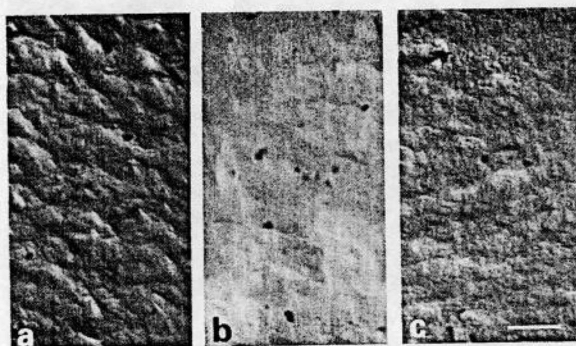

Fig.2.2.5. Surface morphologies of ZnSe epilayers grown on the ZnSe substrates preheated under various atmospheres at 600 ^{o}C for 20 min.

(a) H_2: 4 l/min.; # 133.

(b) H_2: 2 l/min. and H_2Se: $4.6x10^{-4}$ mol/min.; #131.

(c) H_2: 2 l/min. and DMZ: $3.2x10^{-5}$ mol/min.; #135.

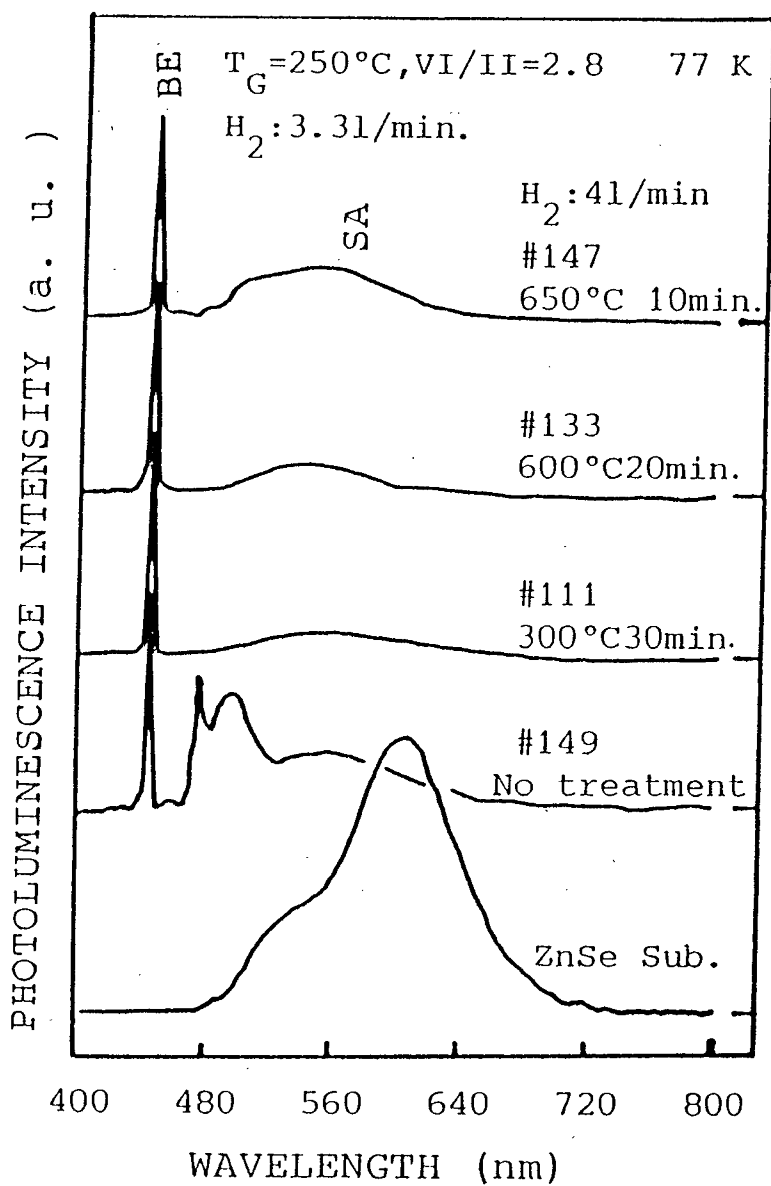

Fig.2.2.6. PL spectra of ZnSe homoepilayers measured at 77 K as a function of temperature of treatment and of the typical ZnSe substrate (the flow rate of H_2 is kept 4 l/min.).

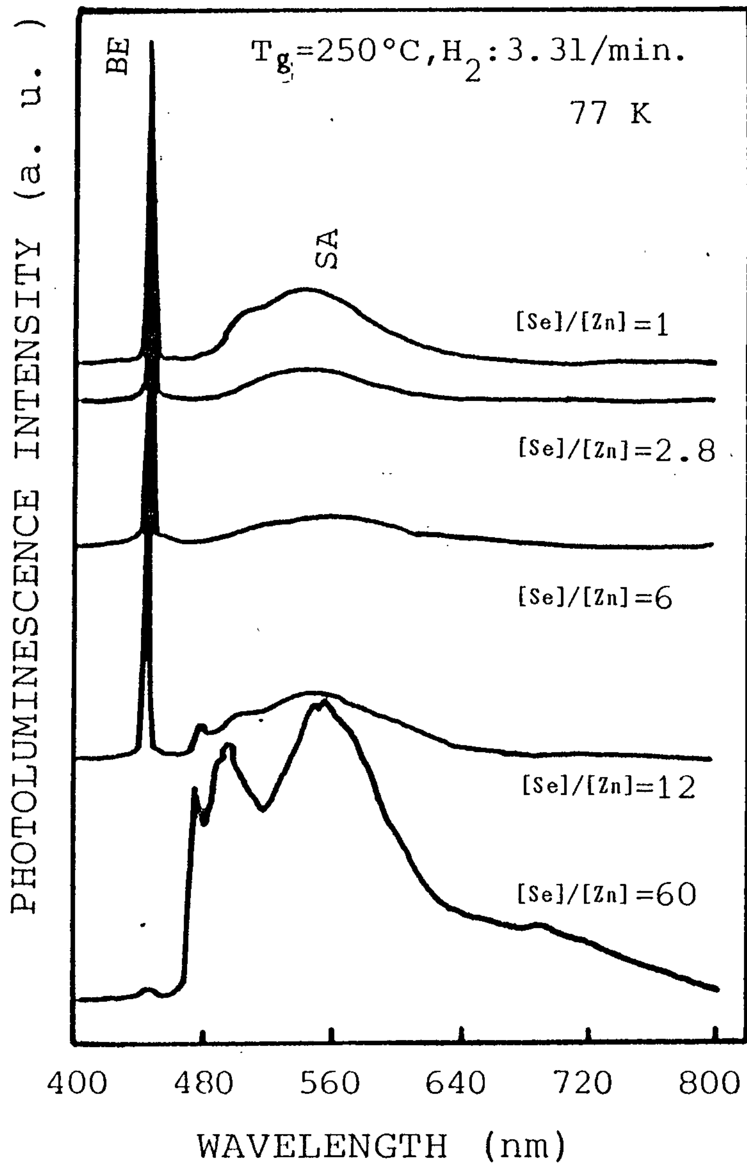

Fig.2.2.7. PL spectra (at 77 K) of ZnSe homoepilayers grown at various [Se]/[Zn] between 1 and 60.

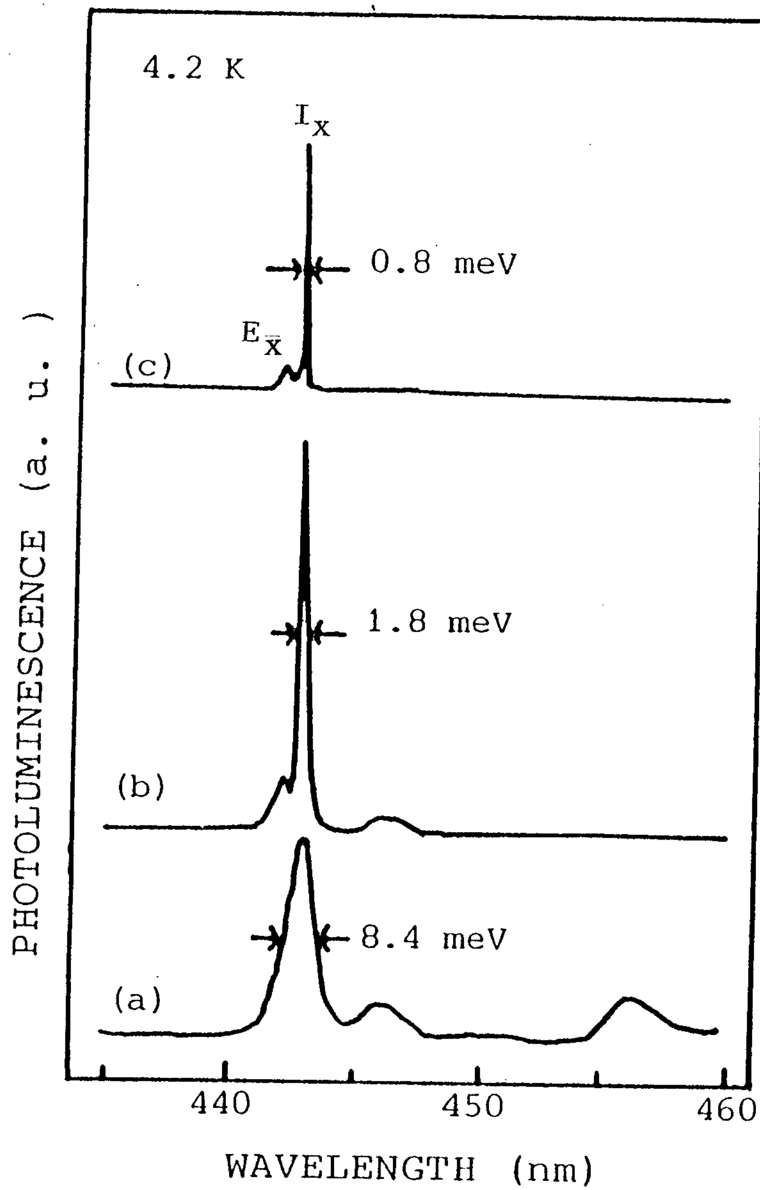

Fig.2.2.8. PL spectra of ZnSe homoepilayers measured at 4.2 K.

(a) No heat treatment.

(b) 400 ^{o}C and 30 min.; # 112.

(c) 600 ^{o}C and 20 min.; # 133.

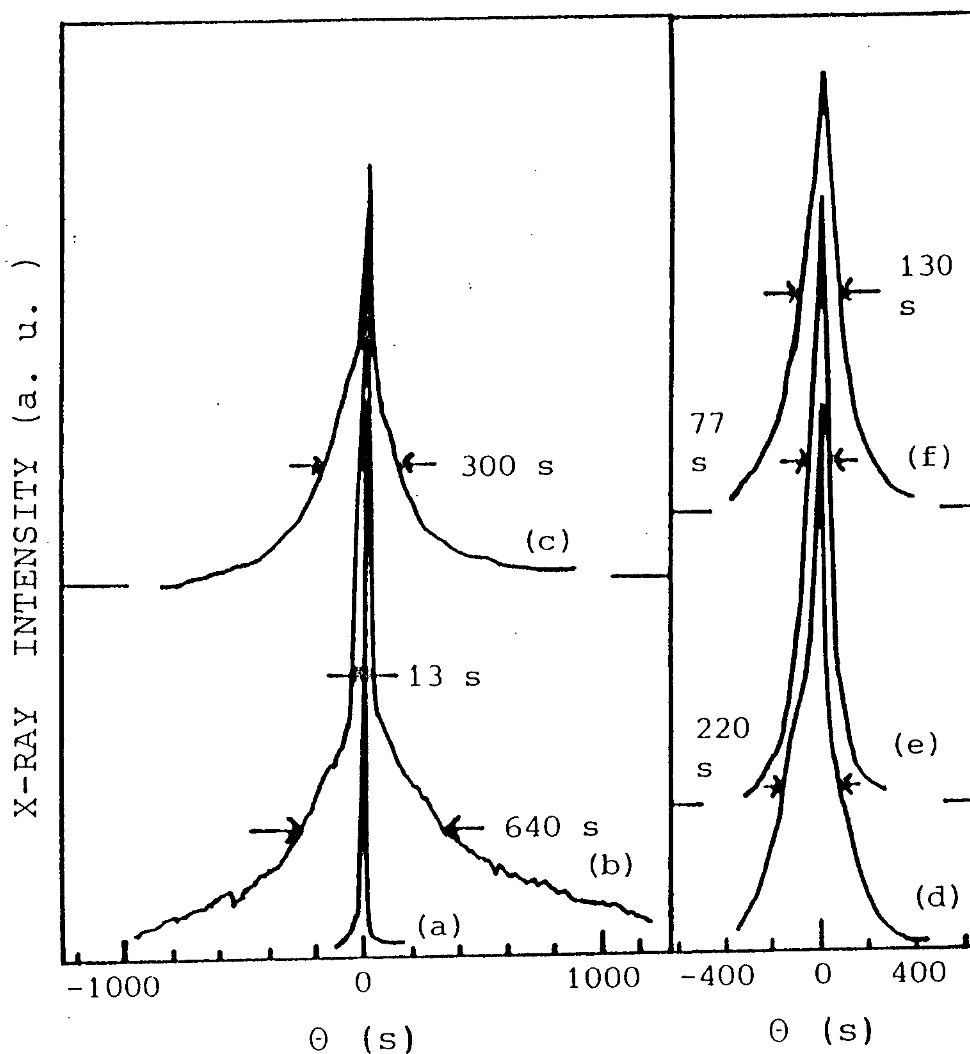

Fig.2.2.9. Double x-ray diffraction patterns of ZnSe(400) of homoepilayers and a typical substrate used in this work.

(a) ZnSe substrate.

(b) No heat treatment.

(c) 300 ^{o}C and 30 min.

(d) 400 ^{o}C and 30 min.

(e) 600 ^{o}C and 20 min.

(f) 650 ^{o}C and 10 min.

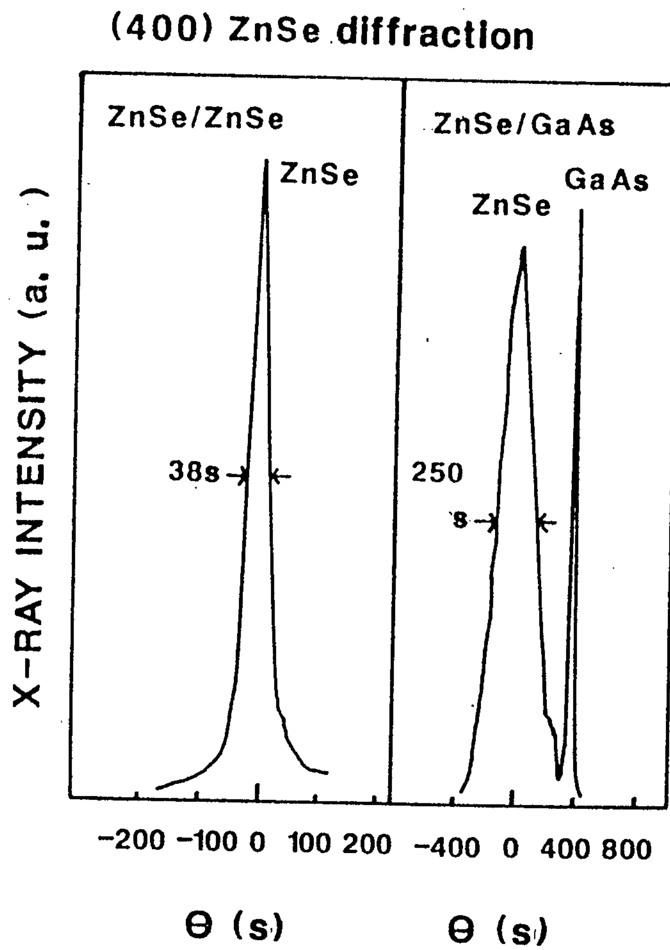

Fig.2.2.10. Double x-ray diffraction patterns of ZnSe (400), (a) a homoepilayer (HOMO-1) and (b) a heteroepilayer (HETERO-1) grown under the same conditions.

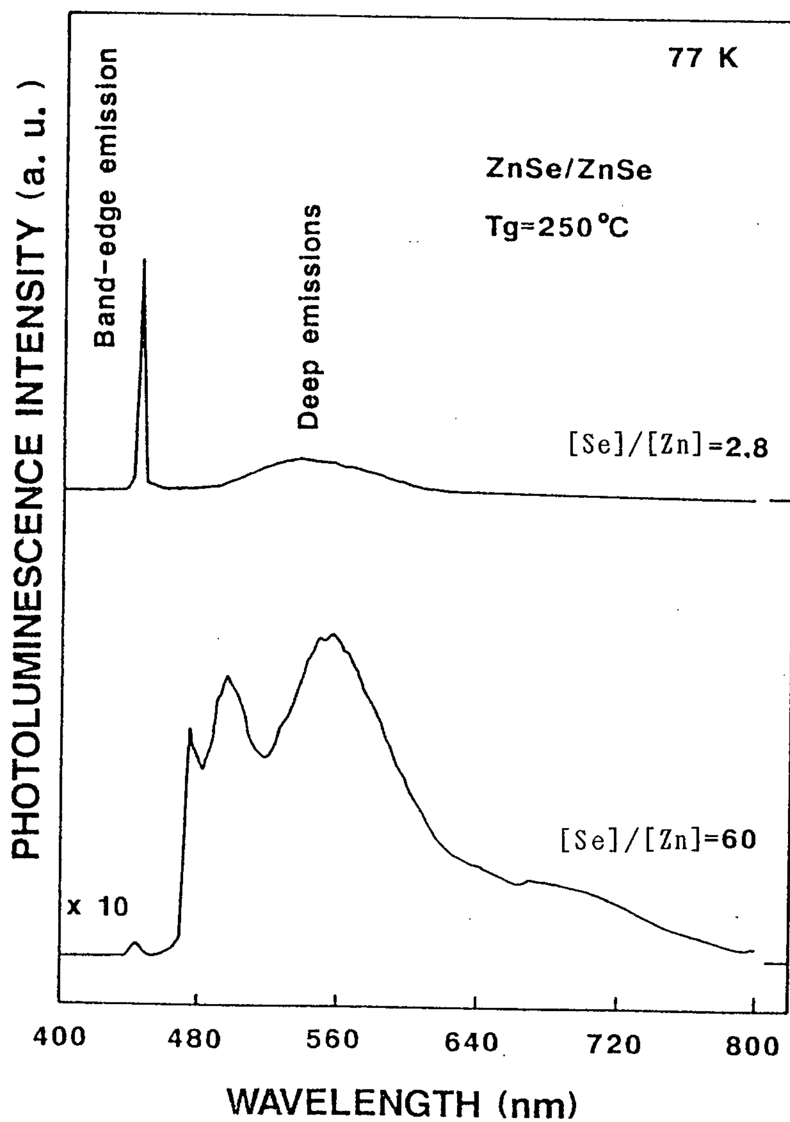

Fig.2.2.11. PL spectra of ZnSe homoepilayers measured at 77 K.

(a) [Se]/[Zn]=2.8; HOMO-2.

(b) [Se]/[Zn]=60 ; HOMO-5.

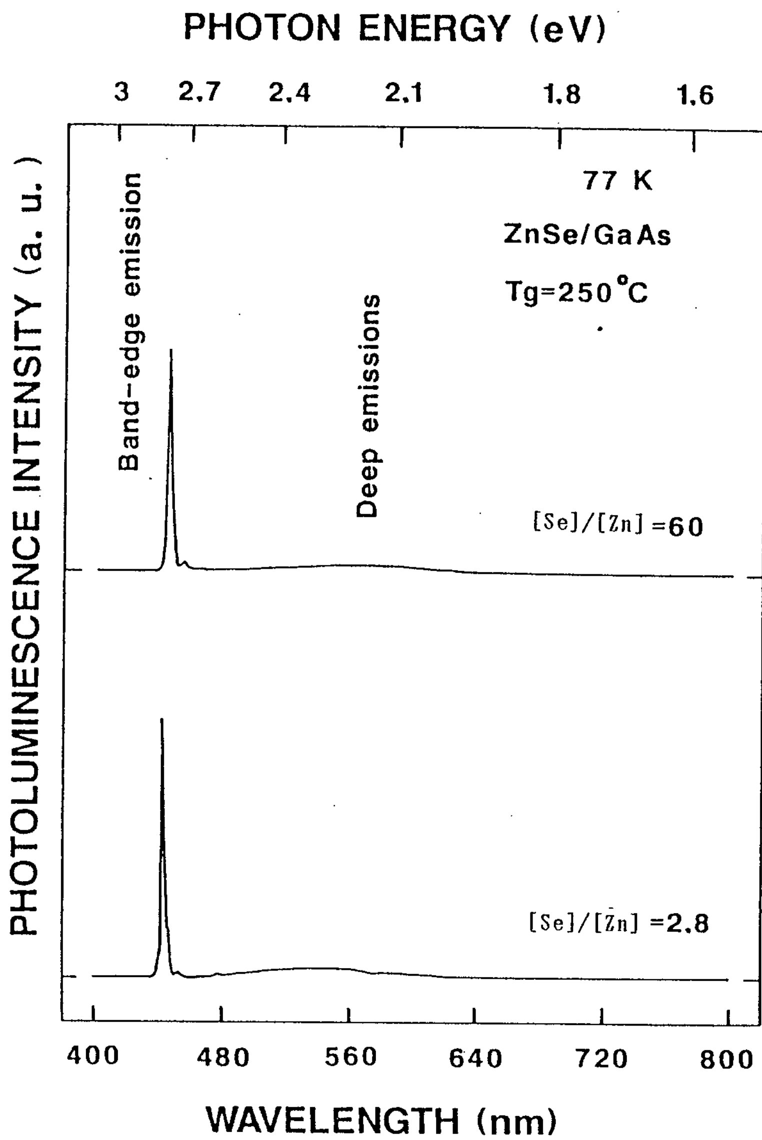

Fig.2.2.12. PL spectra of ZnSe heteroepilayers (HETERO-2 and-3) measured at 77 K.

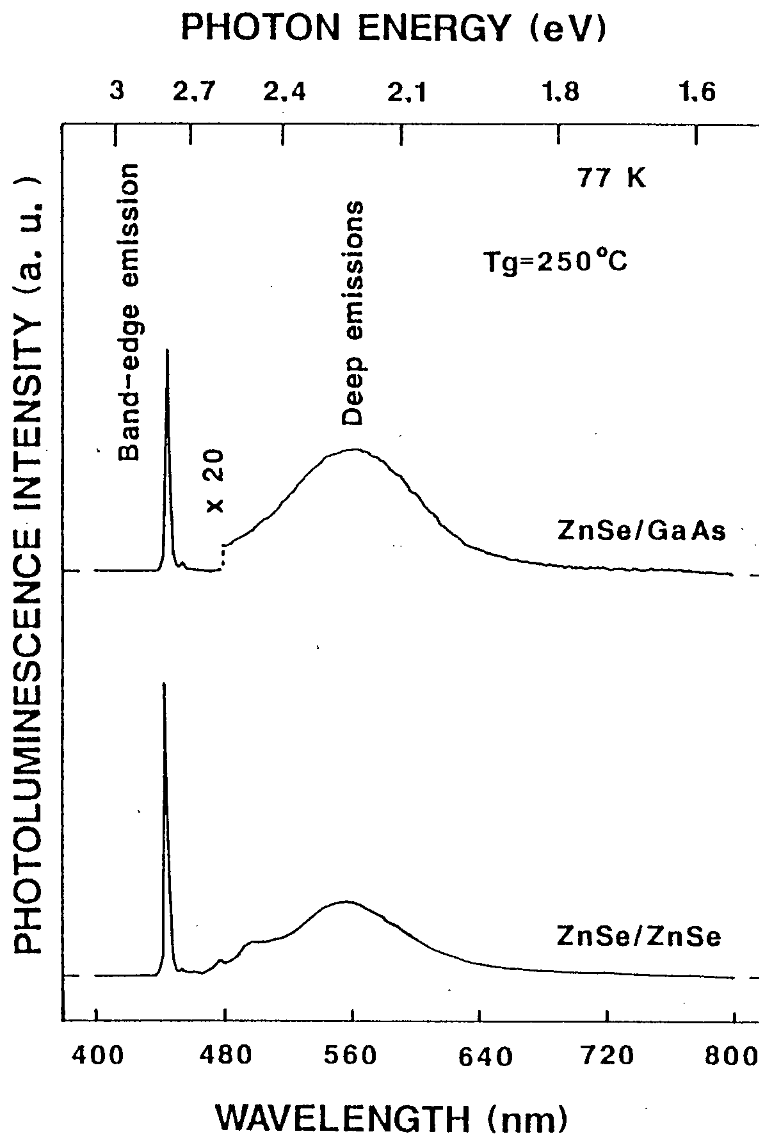

Fig.2.2.13. PL spectra of both homo (HOMO-2) and hetero (HETERO-3) epilayers measured at 77K. Deep emissions of the heteroepilayer are magnified by twenty times.

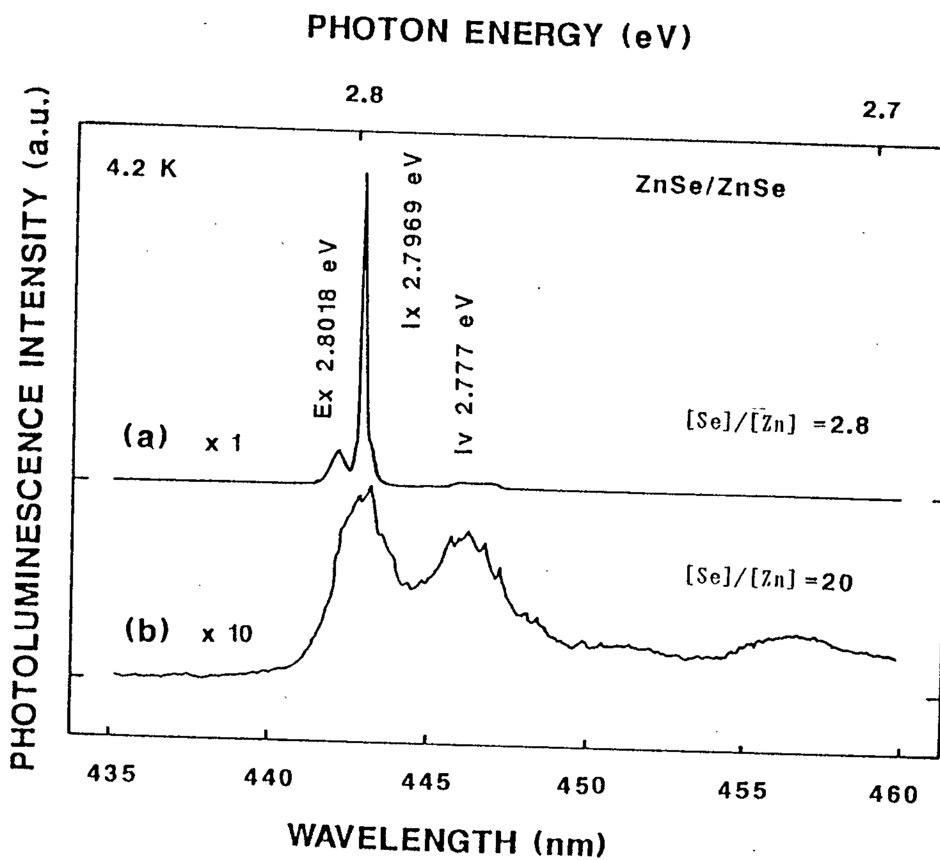

Fig.2.2.14. PL spectra of ZnSe homoepilayers (HOMO-1 and -2) near the band-edge region measured at 4.2 K.

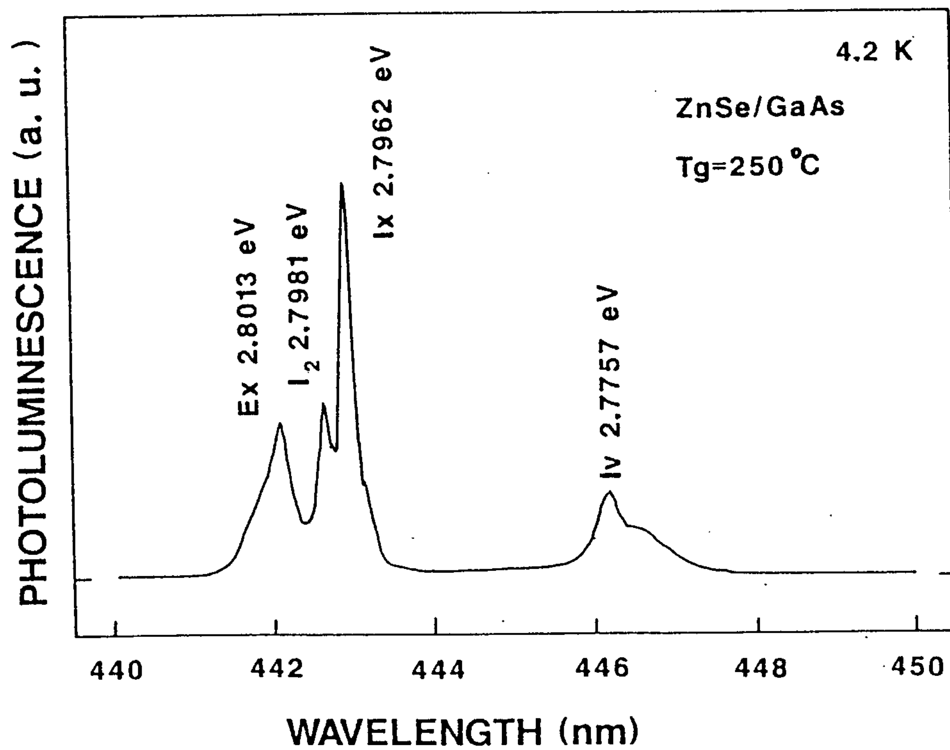

Fig.2.2.15. PL spectrum of a ZnSe heteroepilayer (HETERO-1) near the band-edge region measured at 4.2 K.

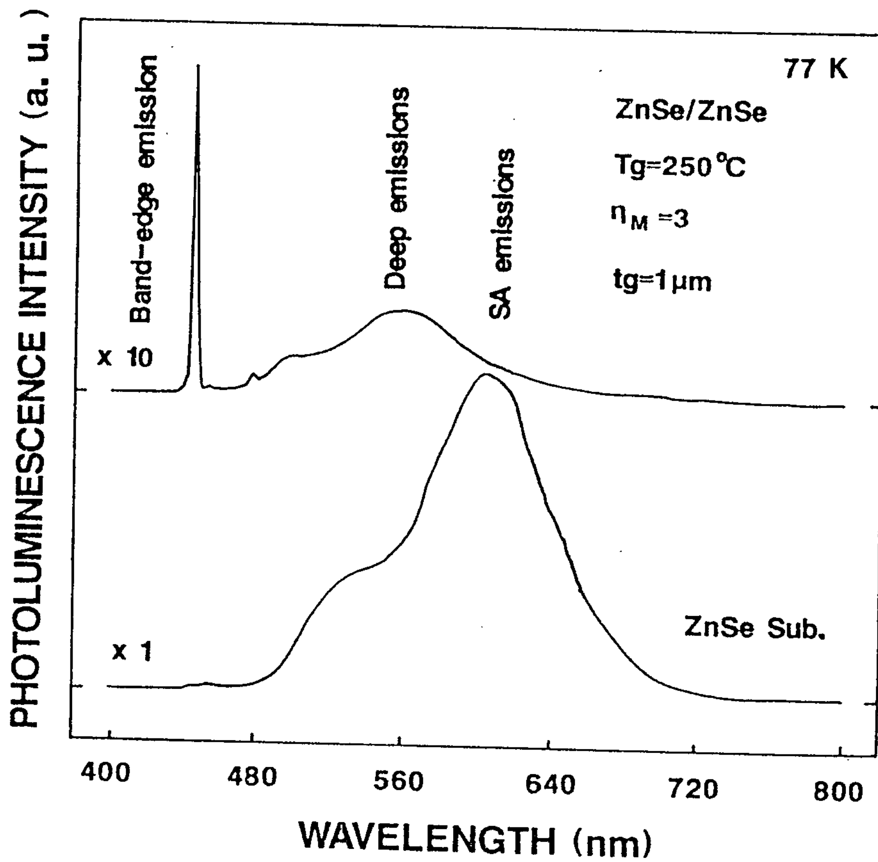

Fig.2.2.16. PL spectra of the homoepilayer (HOMO-3) and the ZnSe substrate measured at 77 K.

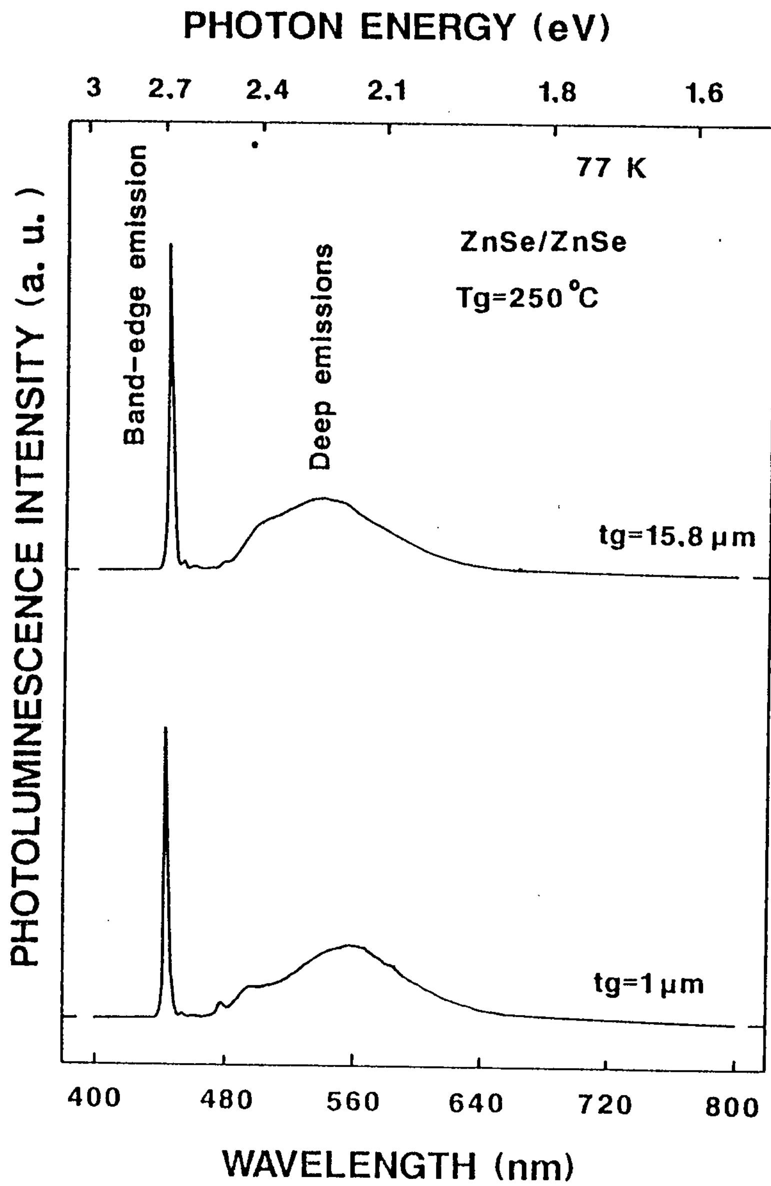

Fig.2.2.17. PL spectra of ZnSe homoepilayers (HOMO-3 and -4) with different thicknesses measured at 77 K.

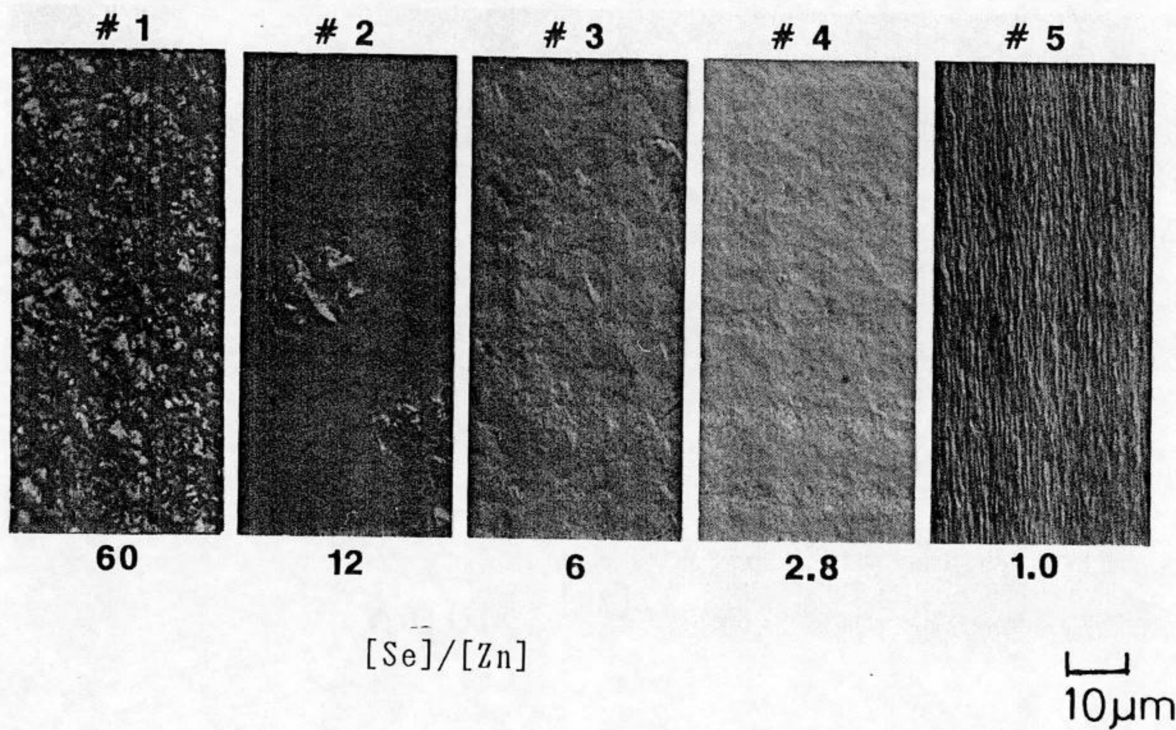

Fig.2.2.18. Surface morphologies of ZnSe homoepilayers at various source mole ratios ([Se]/[Zn]) observed by a Nomarski phase interference microscope.

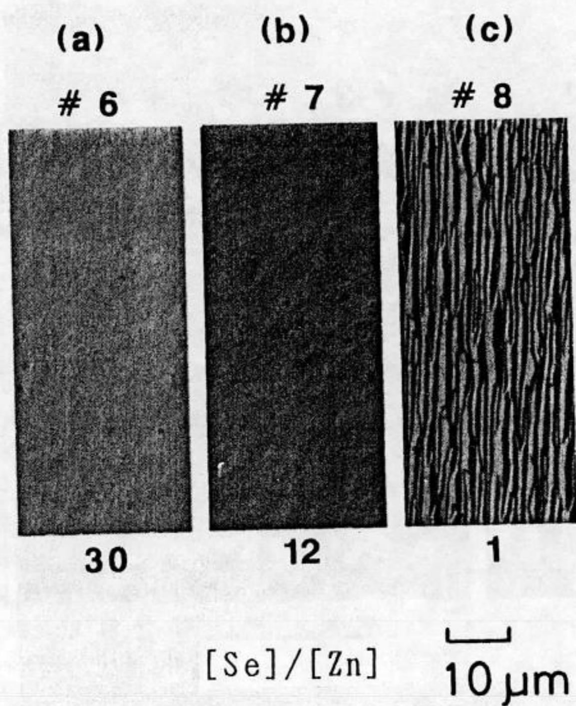

Fig.2.2.19. Surface morphologies of ZnSe heteroepilayers at various [Se]/[Zn] observed by a Nomarski phase interference microscope.

(a) [Se]/[Zn]=30, epilayer thickness(t_g) is 6.6 μm ; # 6.

(b) [Se]/[Zn]=12, t_g=4.3 μm; # 7.

(c) [Se]/[Zn]=1, t_g=5.1 μm; # 8.

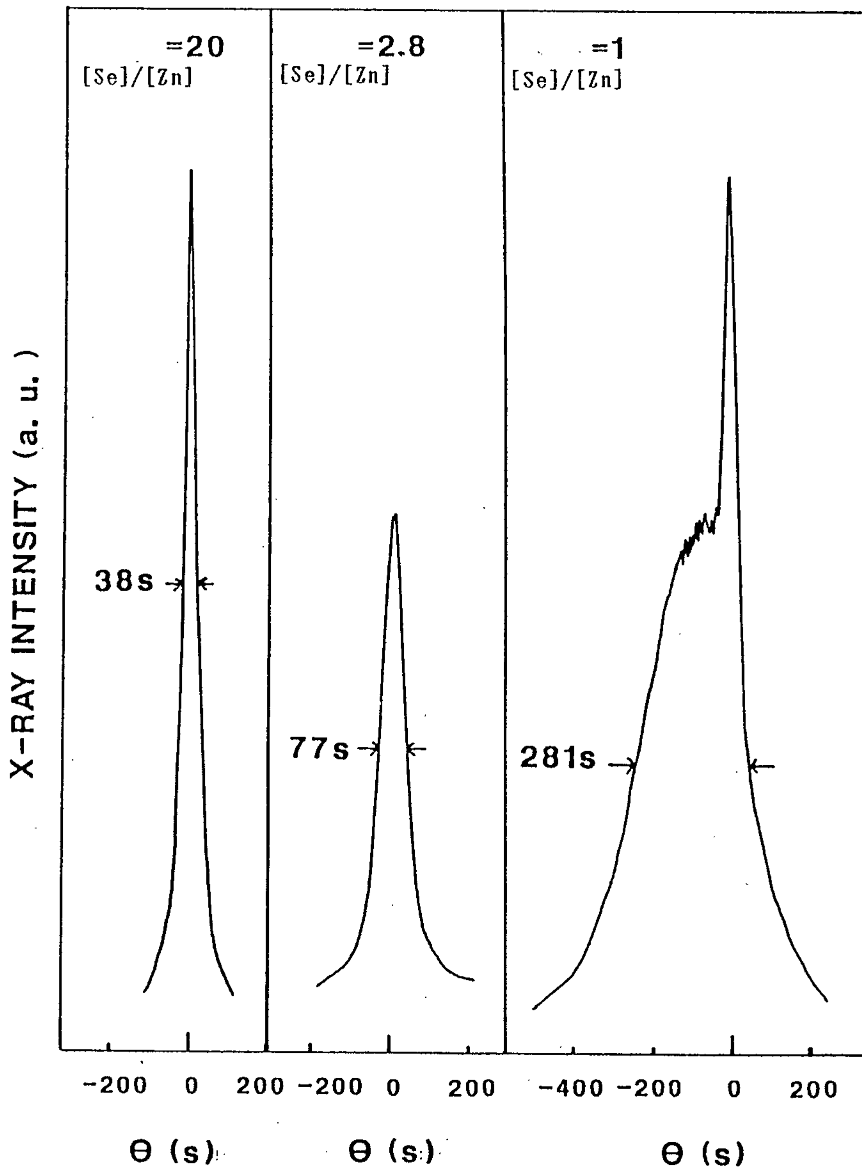

Fig.2.2.20. The ZnSe(400) diffraction spectra of ZnSe homoepilayers at various [Se]/[Zn] measured by double crystal x-ray diffraction spectrometer.

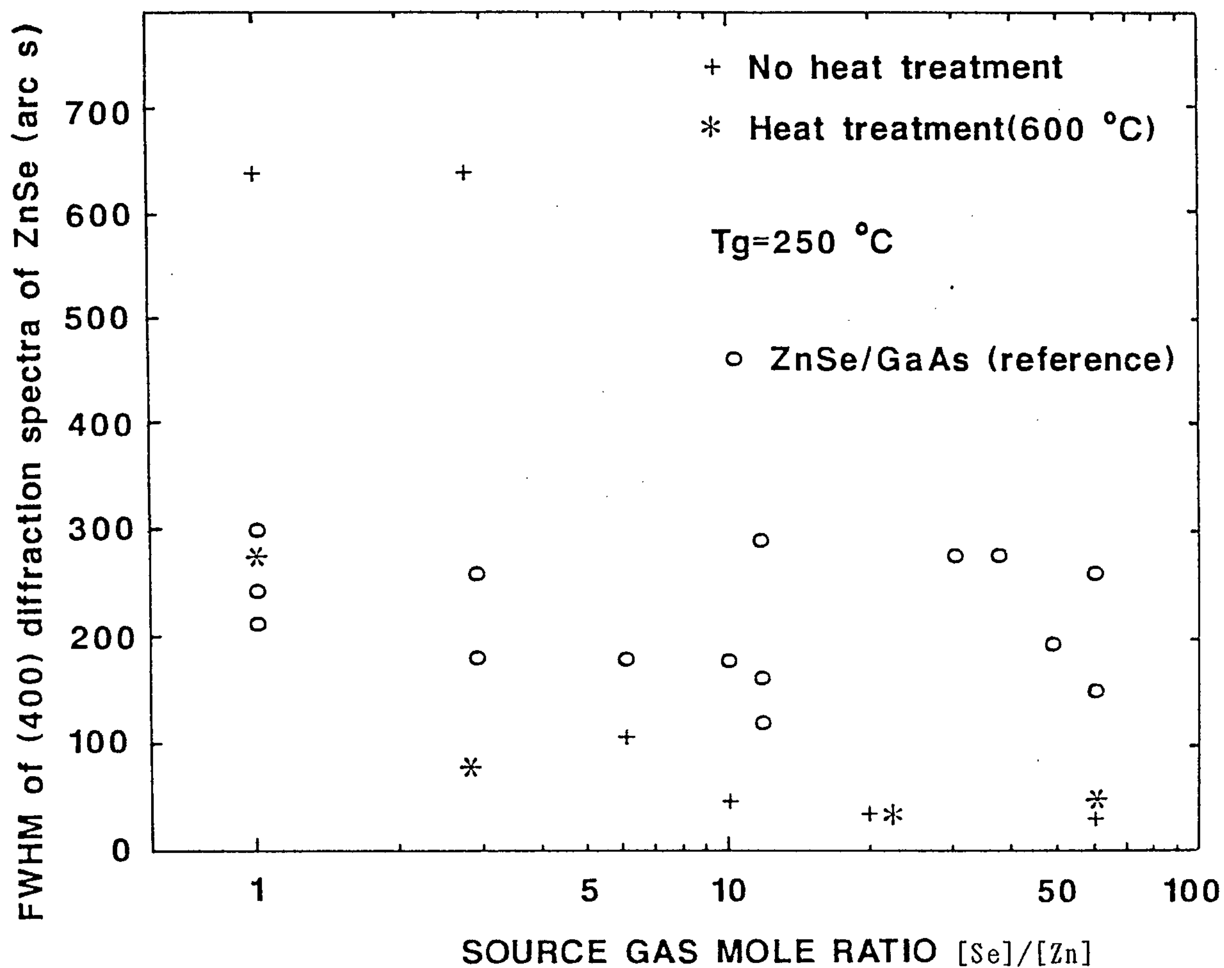

Fig.2.2.21. The dependence of [Se]/[Zn] on the crystalline quality (FWHM of (400) diffraction spectra) of homoepilayers.

+ Without heat treatment.

* With heat treatment (600 °C).

O ZnSe epilayers on GaAs substrates.

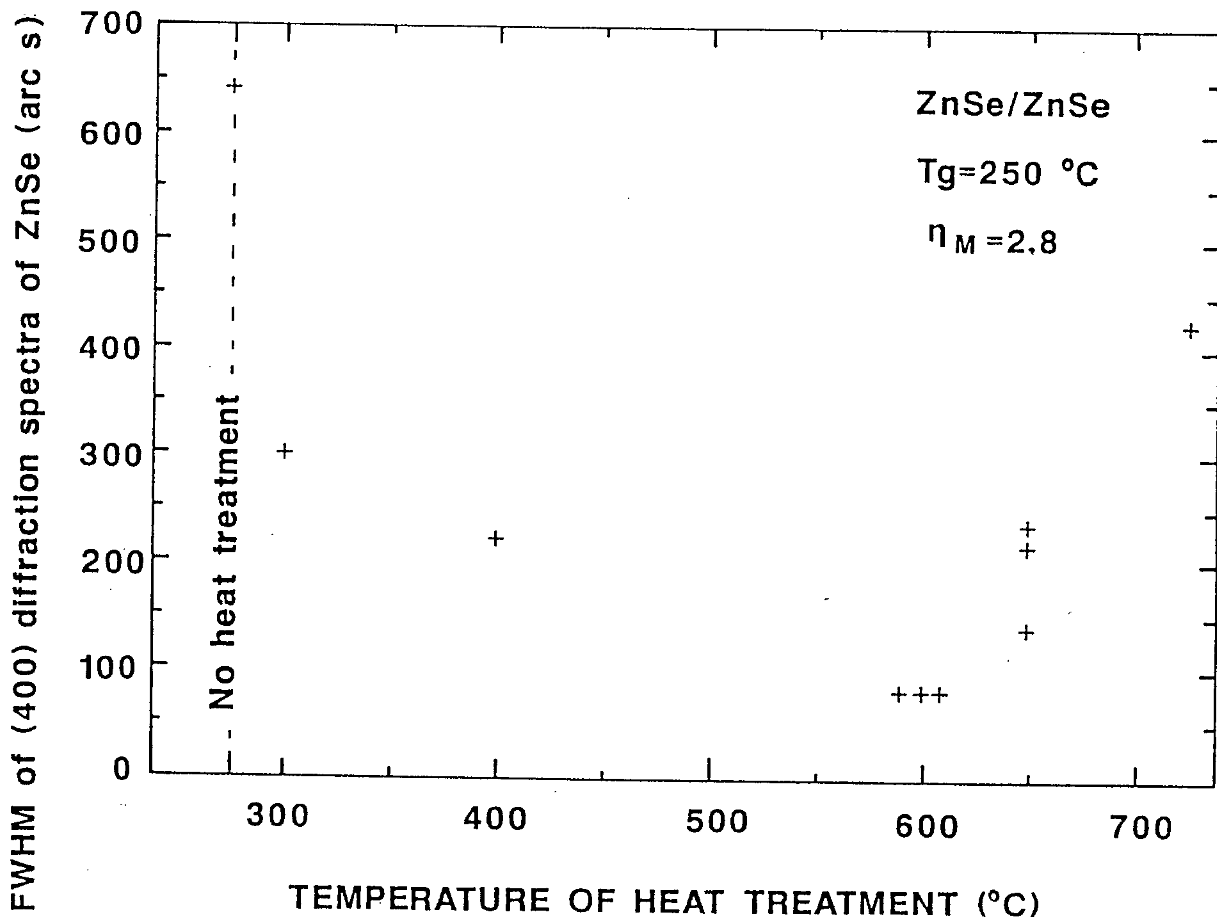

Fig.2.2.22. The dependence of temperatures of the heat treatment before the growth on the crystalline quality of homoepilayers at low [Se]/[Zn] (=2.8).

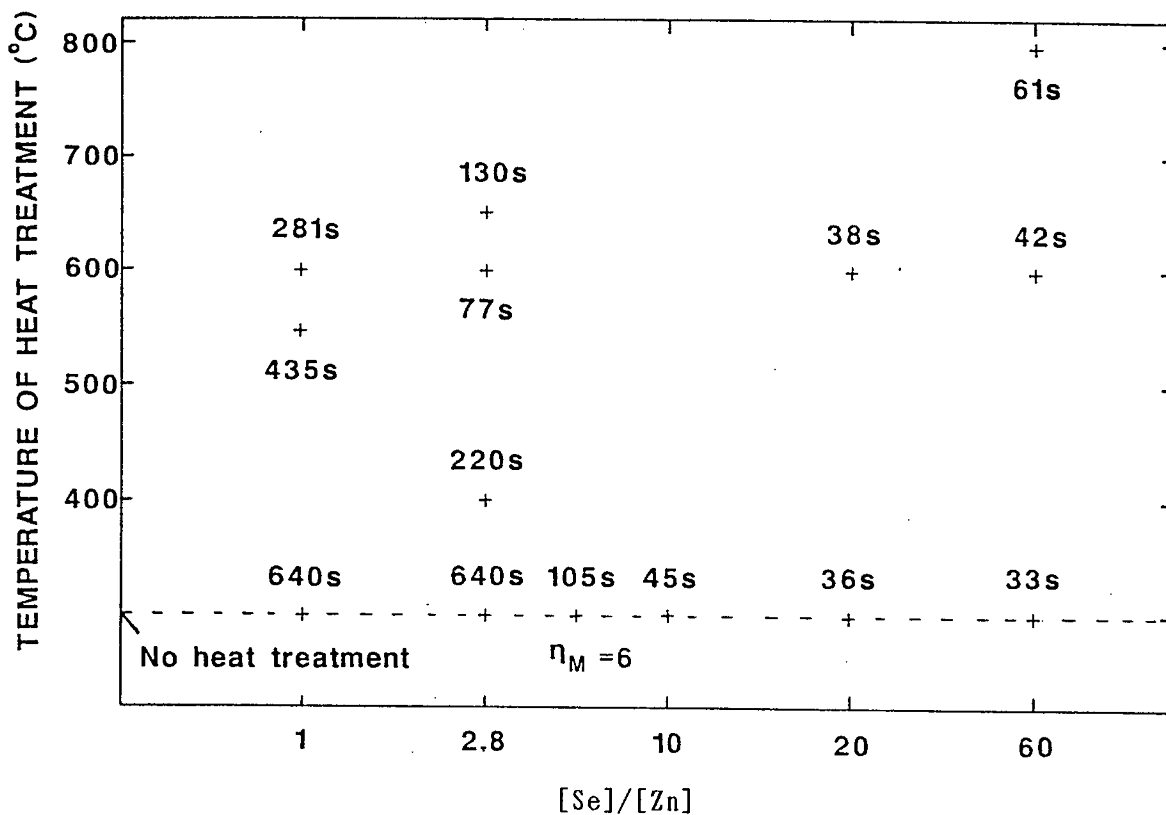

Fig.2.2.23. The map of FWHM of ZnSe(400) diffraction spectra of ZnSe homoepilayers. The abscissa and ordinate indicate [Se]/[Zn] and the temperature of the heat treatment before the growth, respectively.

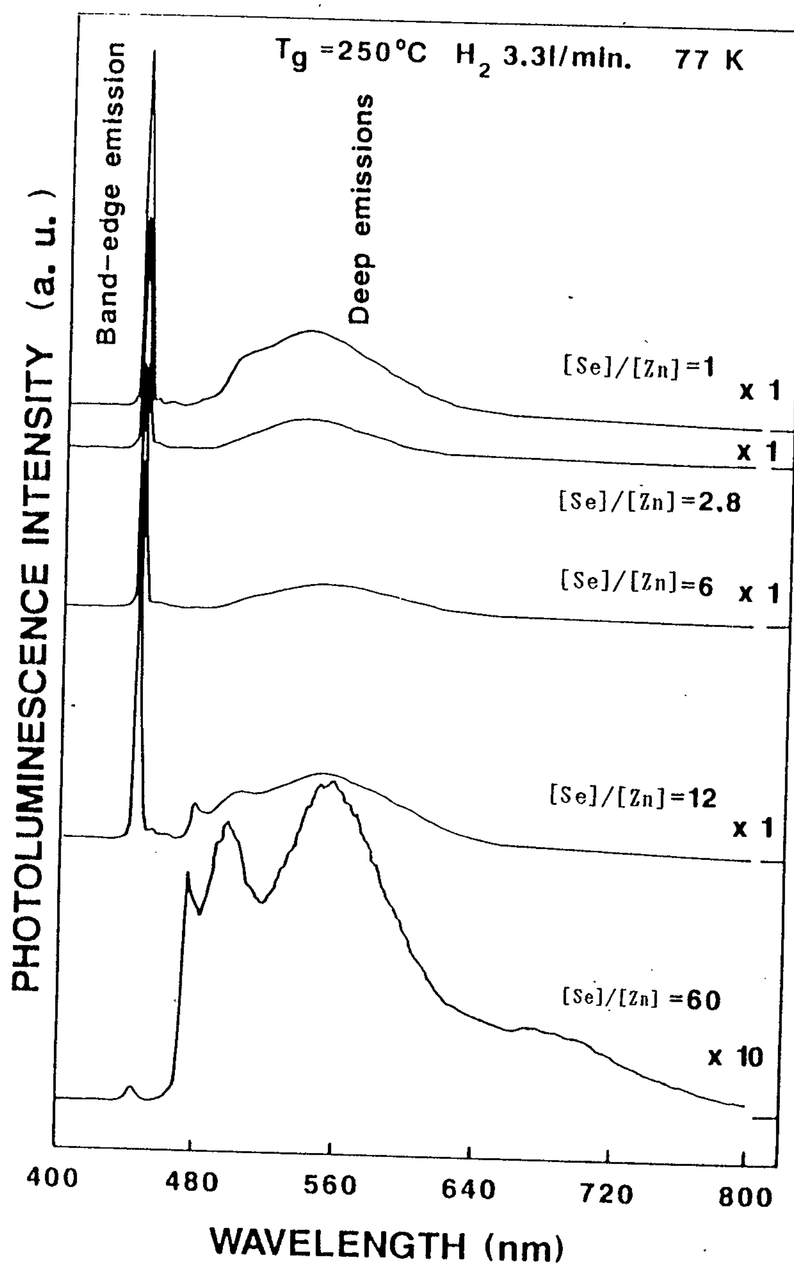

Fig.2.2.24. The typical PL spectra of homoepilayers under various [Se]/[Zn] measured at 77 K.

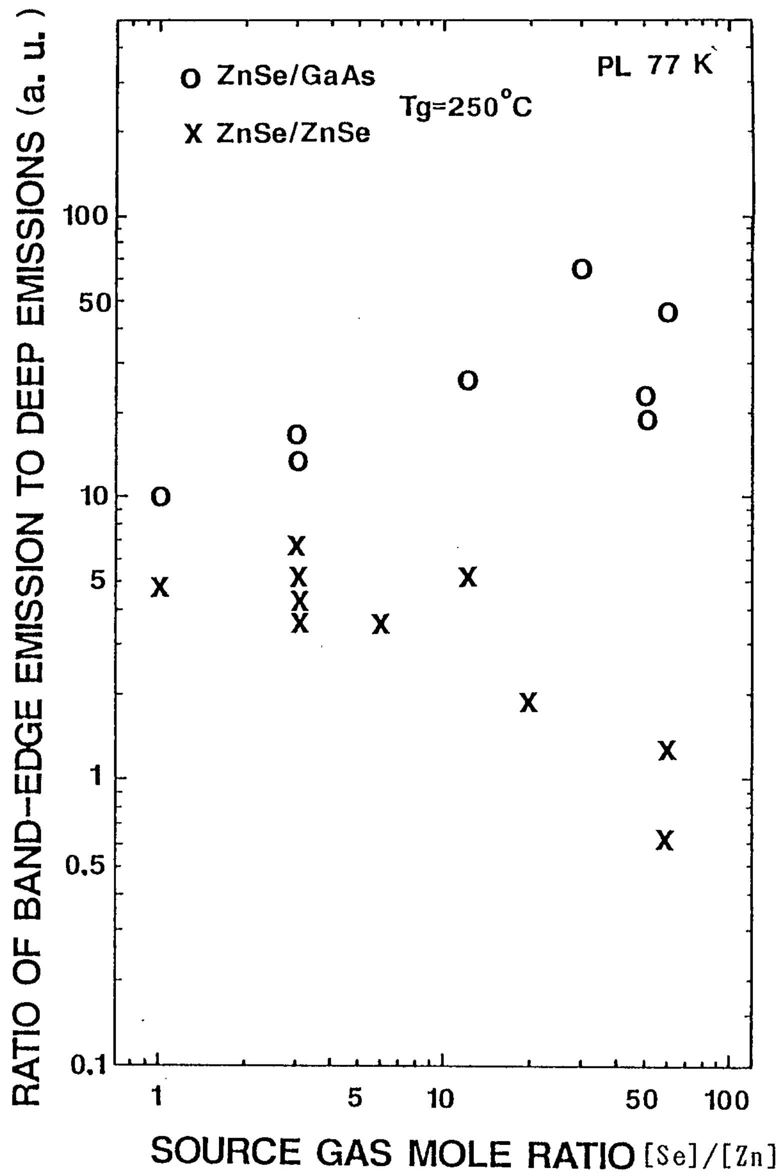

Fig.2.2.25. The dependence of [Se]/[Zn] on the PL ratio in both homo- and hetero-epilayers.

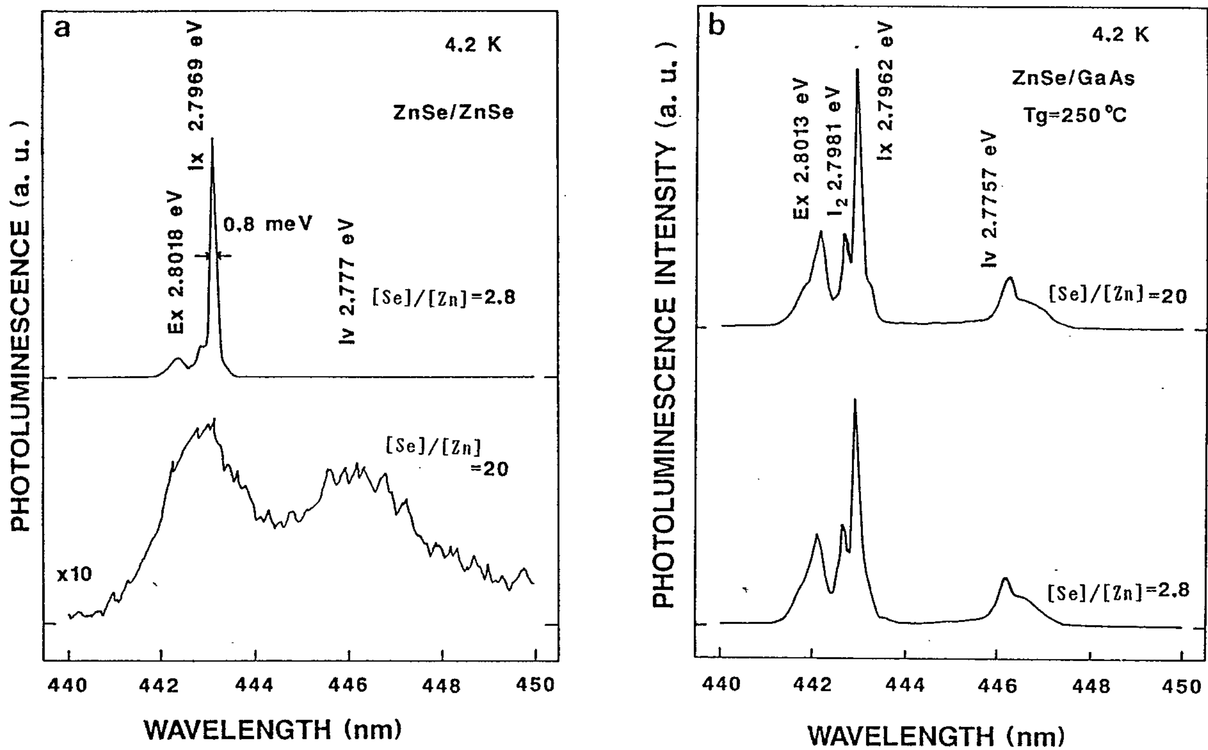

Fig.2.2.26. (a) The near band-edge PL spectra of homoepilayers under various [Se]/[Zn] measured at 4.2K.

(b) The near band-edge PL spectra of heteroepilayers under various [Se]/[Zn] measured at 4.2 K.

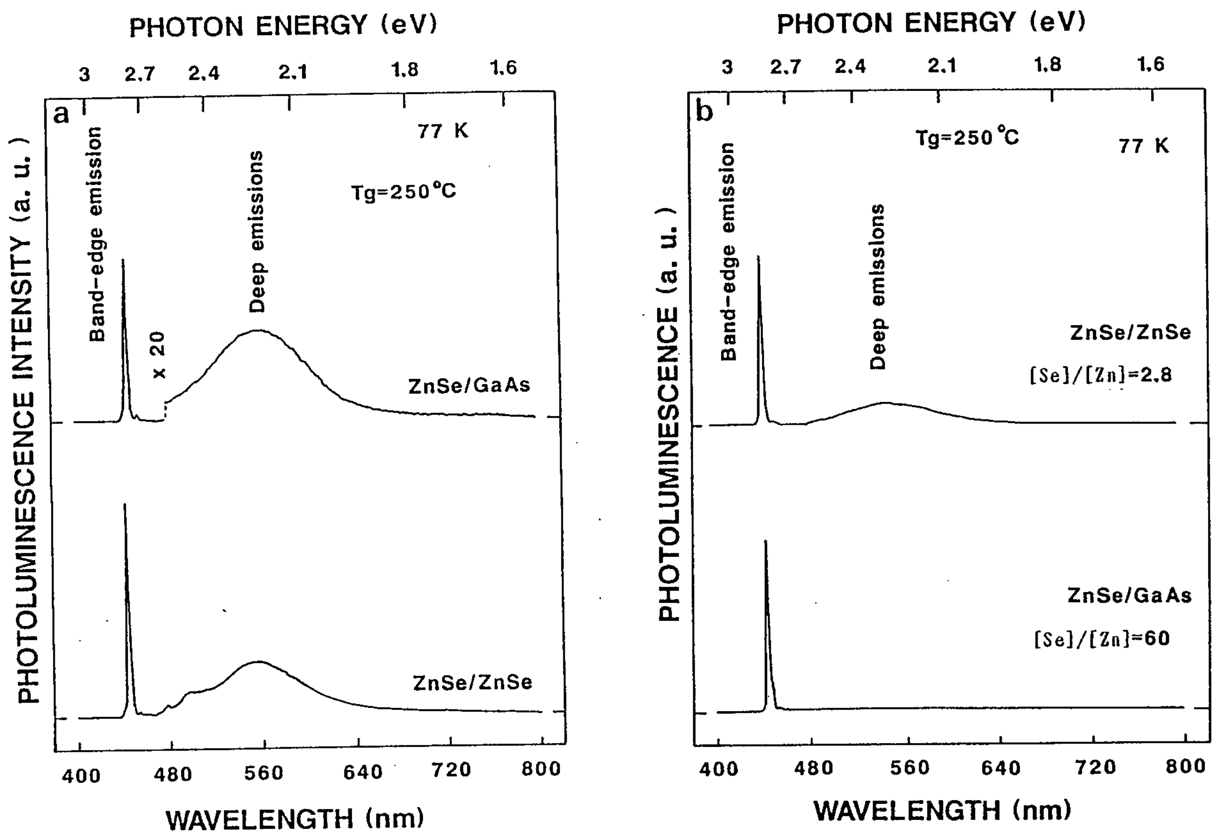

Fig.2.2.27. (a) PL spectrum of a heteroepilayer magnified only in the region of SA emissions by twenty times.
(b) The PL spectra of homoepilayer and heteroepilayer measured at 77 K.

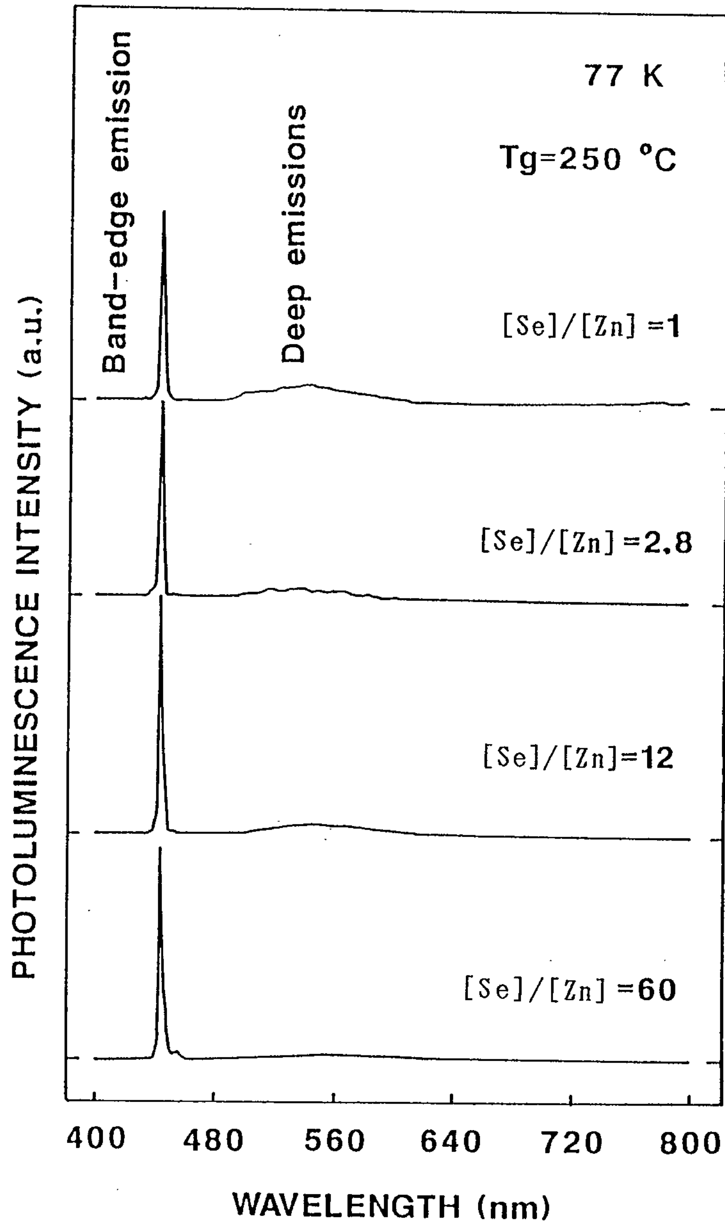

Fig.2.2.28. PL spectra of heteroepilayers under various [Se]/[Zn] measured at 77 K.

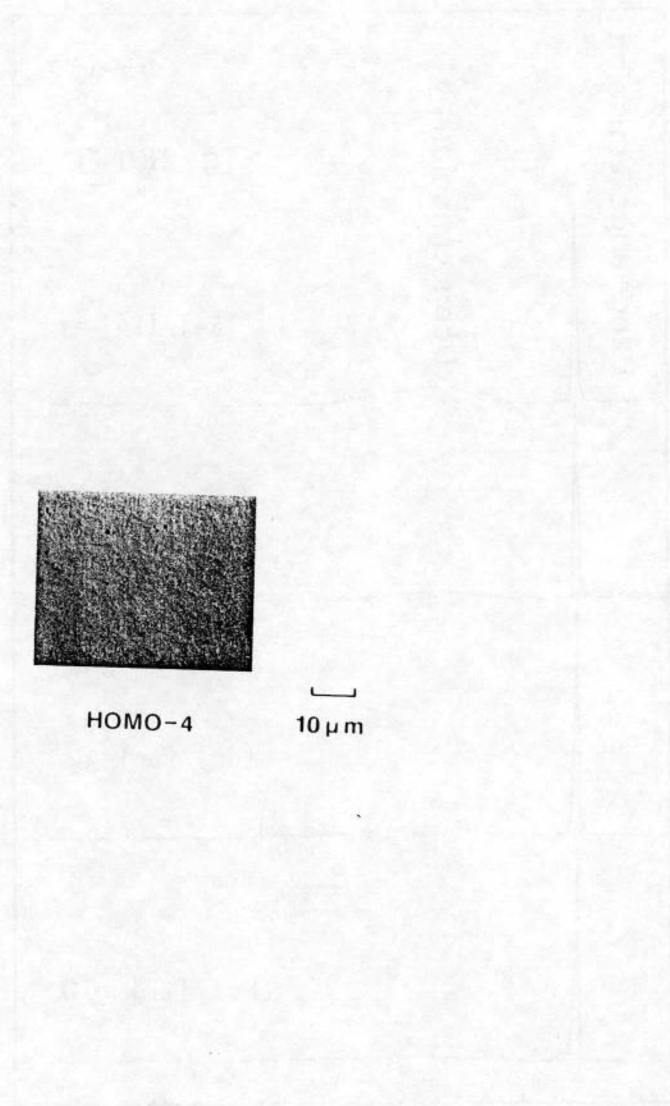

Fig.2.2.29. Typical surface morphology of a homoepilayer grown at 210 ^{o}C.

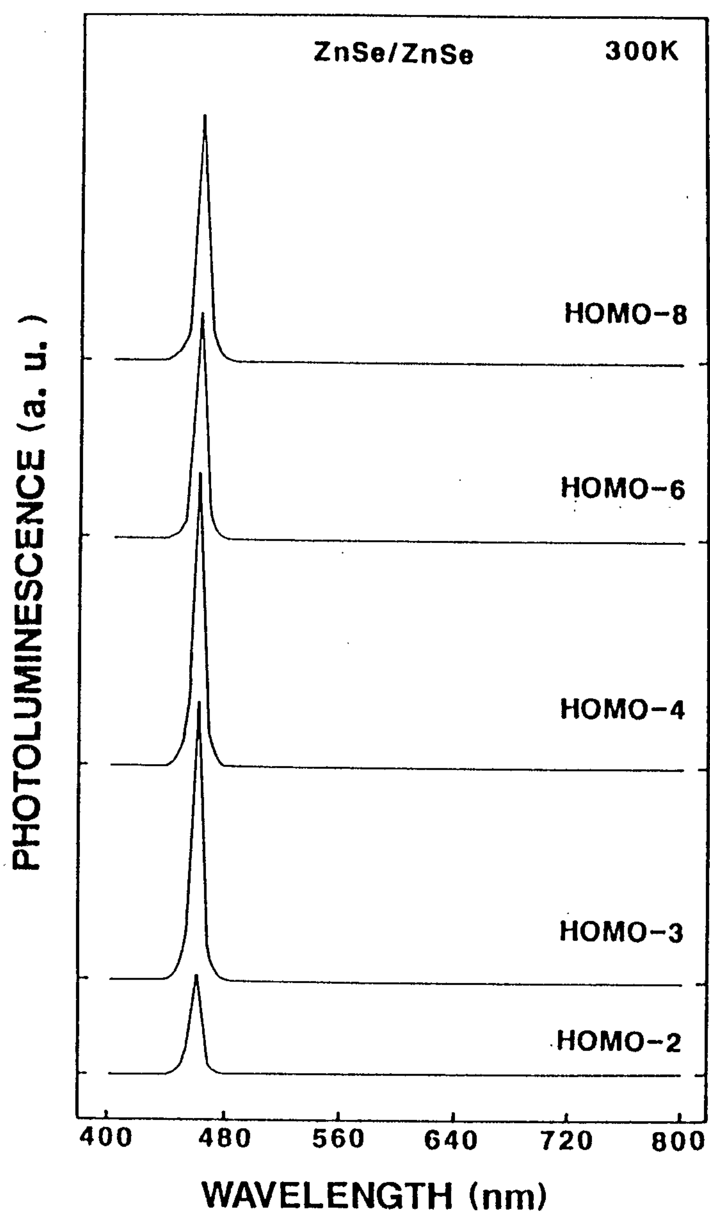

Fig.2.2.30. PL spectra (measured at 300 K) of the homoepilayers grown at various growth temperatures.

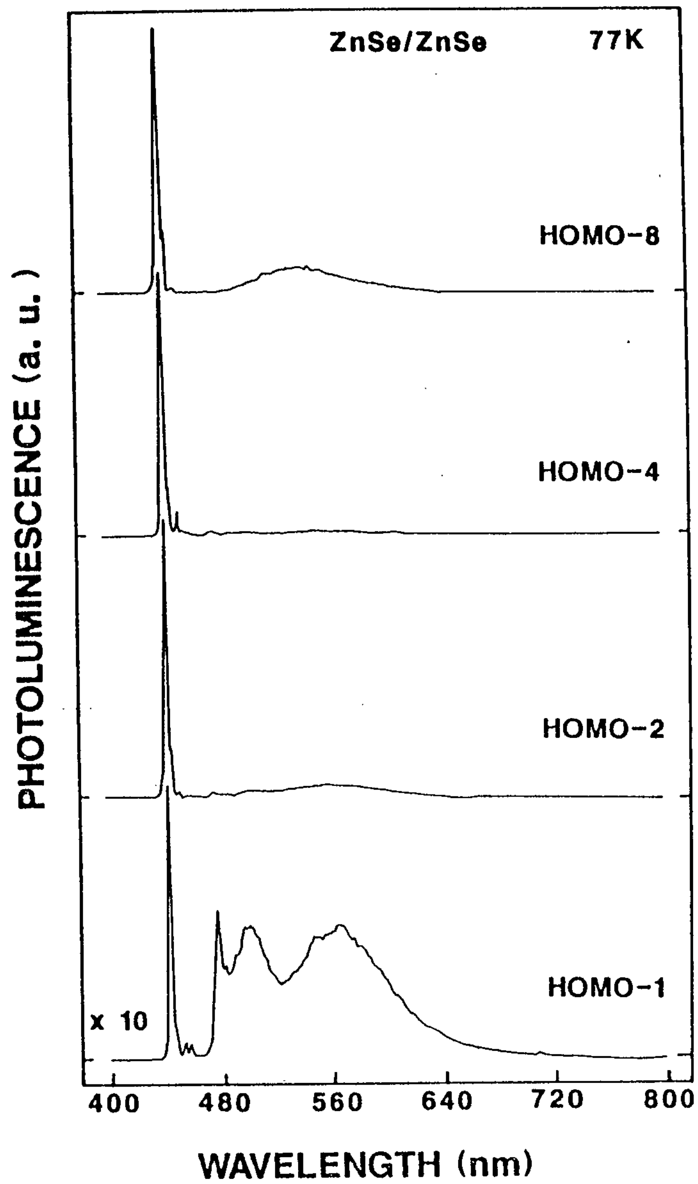

Fig.2.2.31. PL spectra (measured at 77 K) of the homoepilayers grown at various growth temperatures.

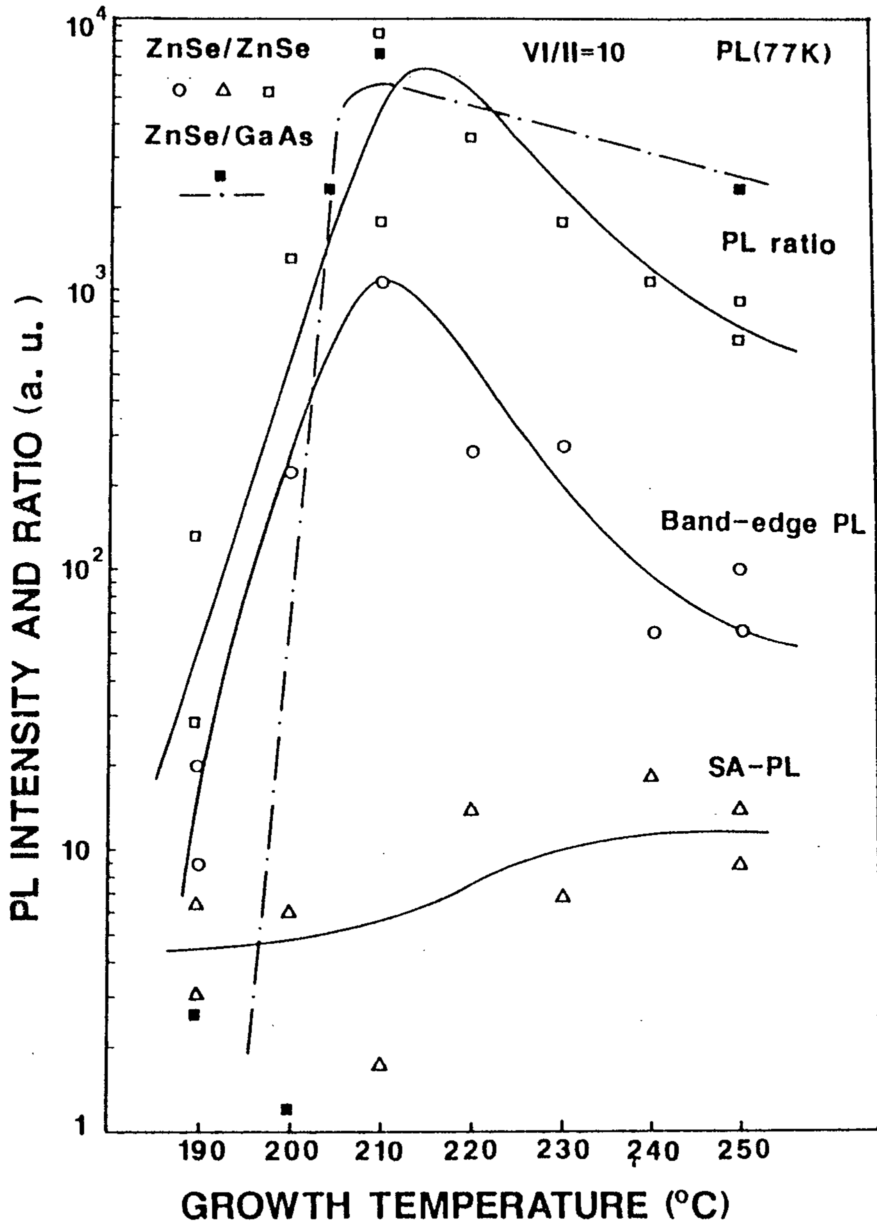

Fig.2.2.32. Dependence of the growth temperature on the relative ratio of the BE-PL intensity to the SA-PL intensity and the absolute PL intensities of both BE and SA emissions (ZnSe/ZnSe, Δ ○ —— ; ZnSe/GaAs, —·——·—).

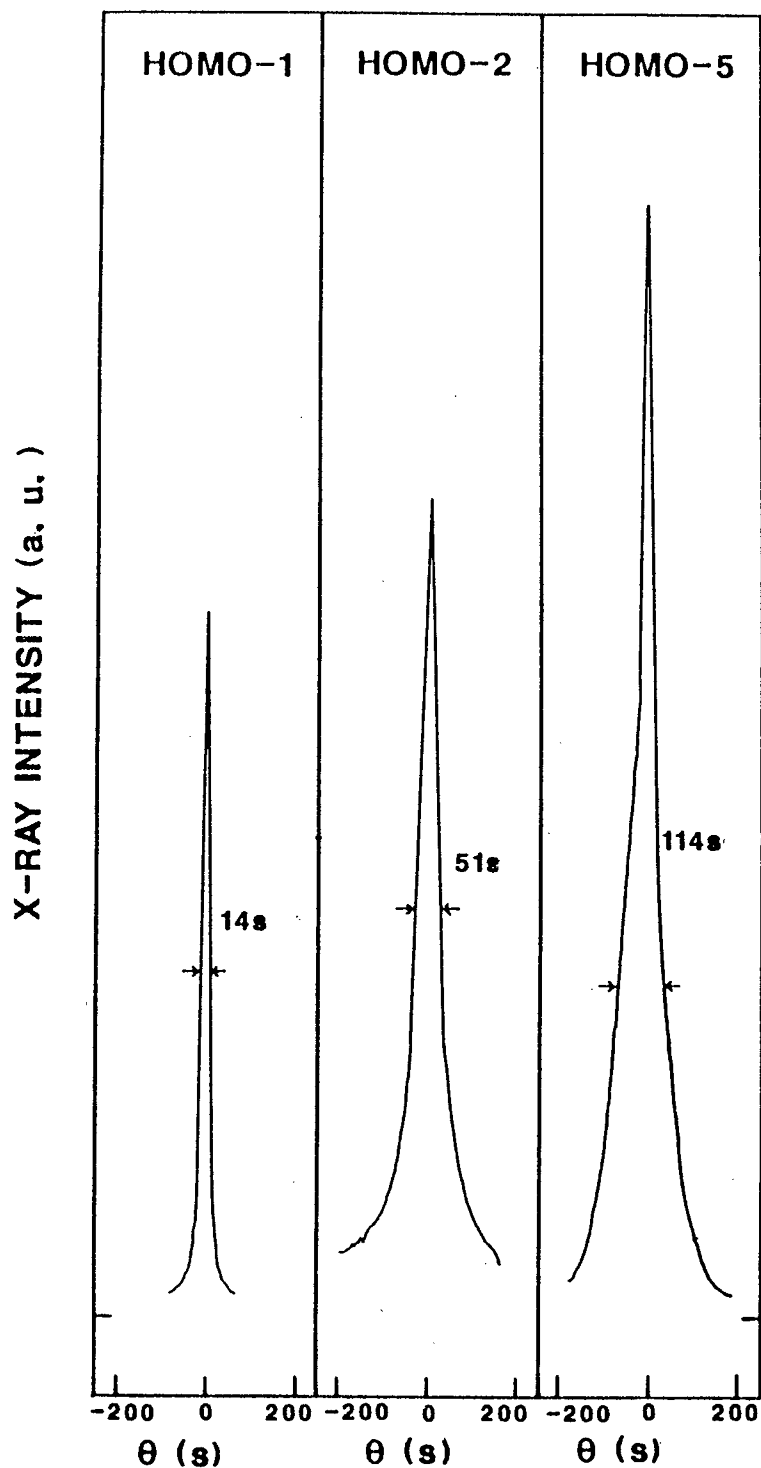

Fig.2.2.33. ZnSe(400) diffraction patterns of the homoepilayers grown at various growth temperatures, which are measured by double crystal x-ray spectrometer.

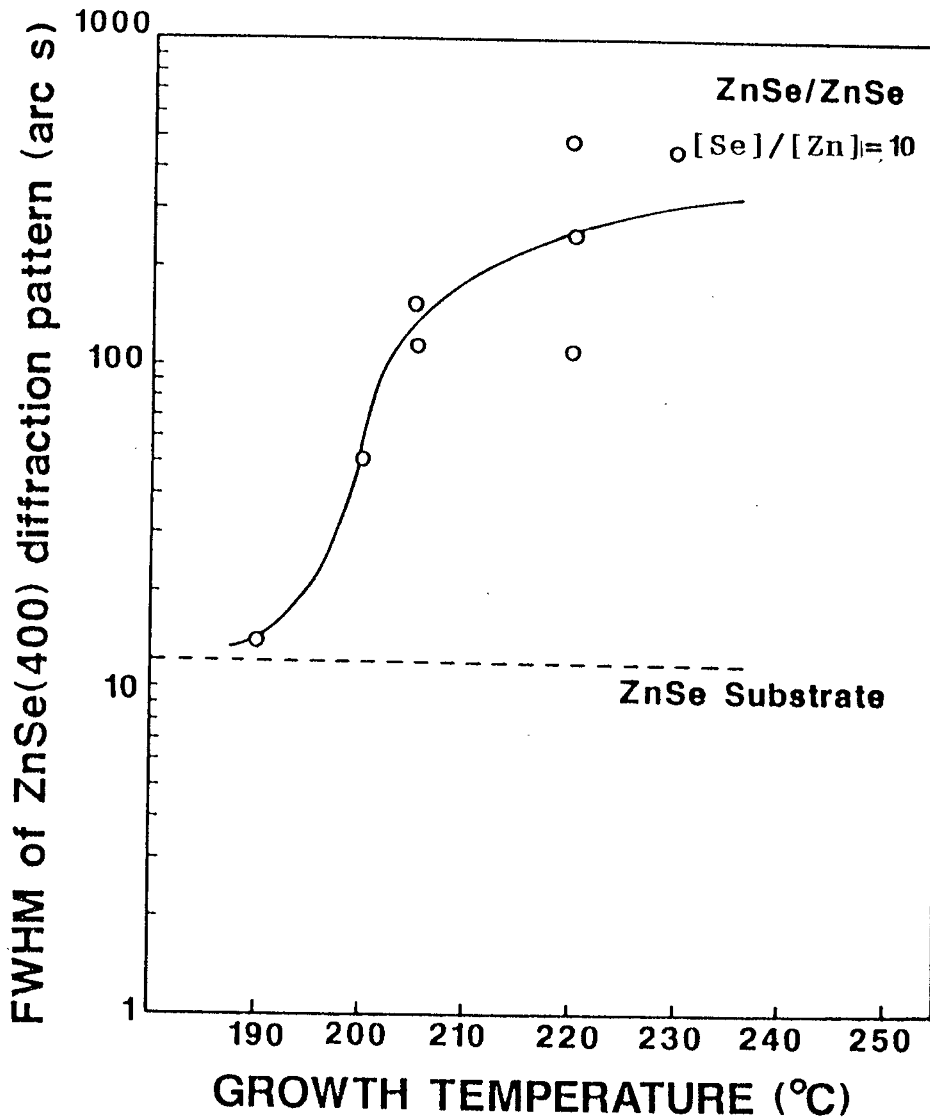

Fig.2.2.34. Dependence of the growth temperature on the FWHM of ZnSe(400) diffraction patters of the homoepilayers.

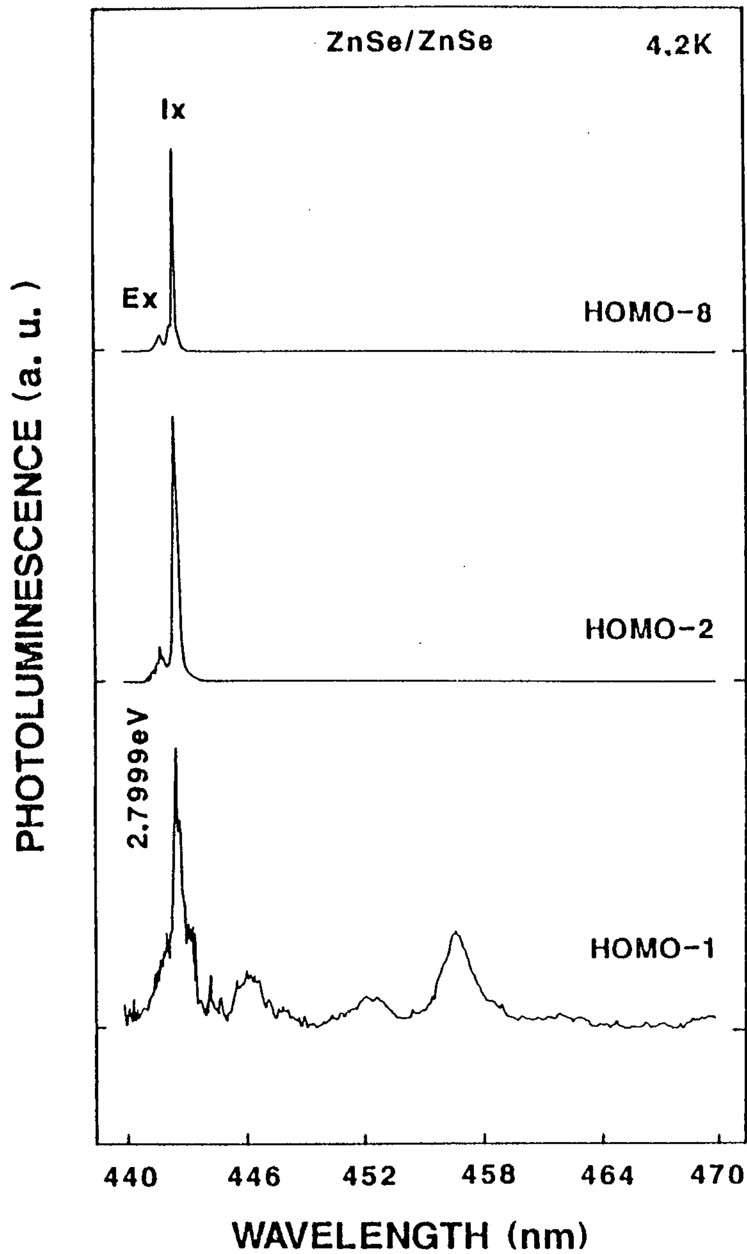

Fig.2.2.35. PL spectra of the homoepilayers grown at various growth temperatures, which are measured near band-edge region (440-470 nm) at 4.2 K.

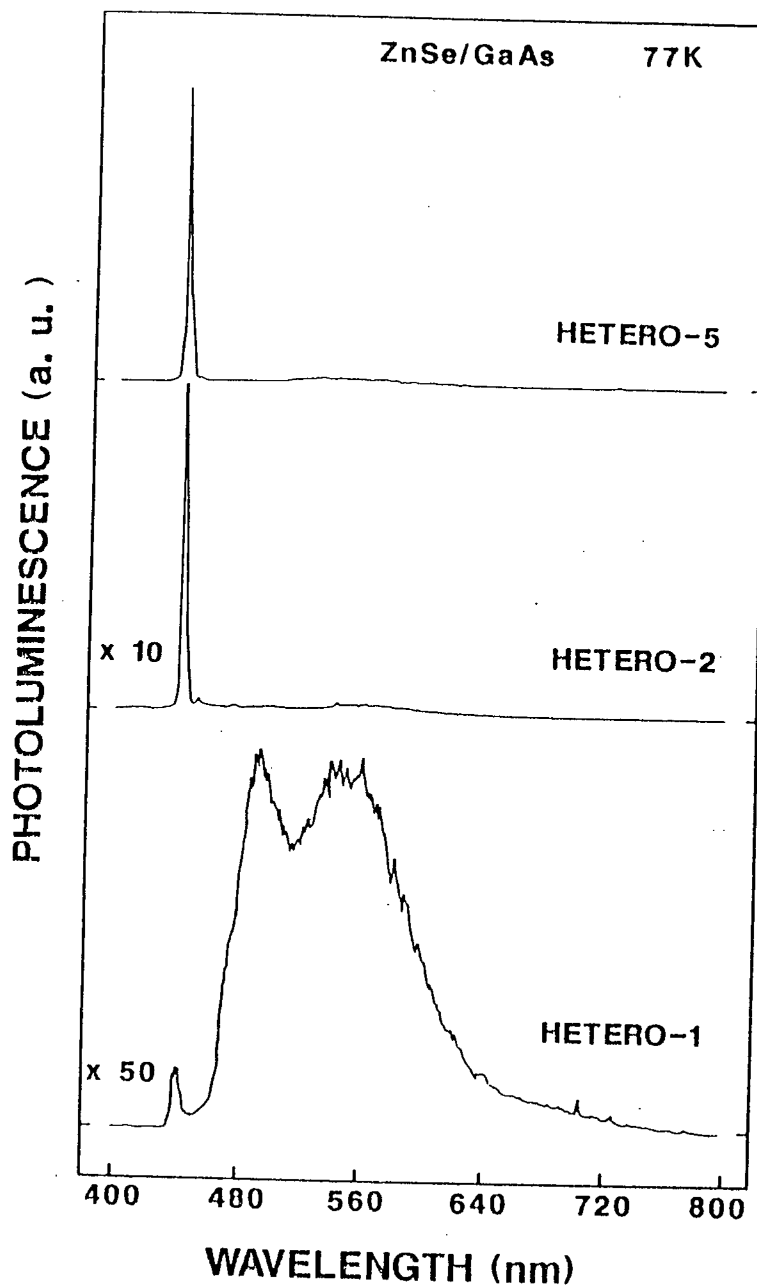

Fig.2.2.36. PL spectra (measured at 77 K) of the heteroepilayers grown at various growth temperatures.

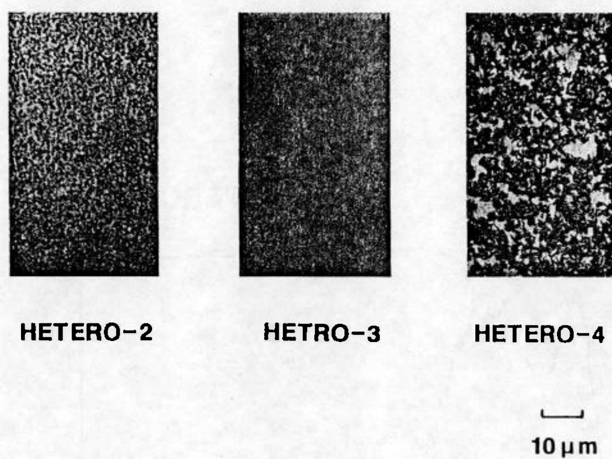

Fig.2.2.37. Surface morphologies of the heteroepilayers grown at respective growth conditions (205 ^{o}C, [Se]/[Zn]=20; 210 ^{o}C, [Se]/[Zn]=20; 210 ^{o}C, [Se]/[Zn]=40.).

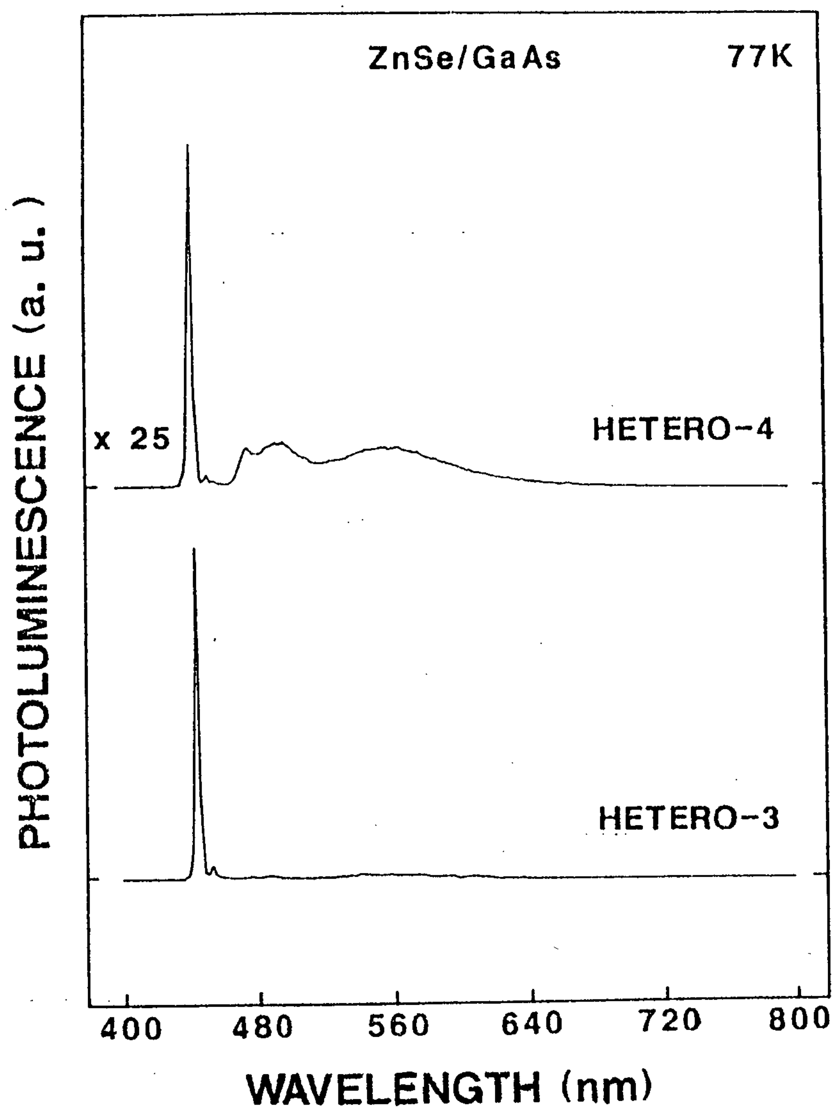

Fig.2.2.38. PL spectra of the heteroepilayers (measured at 77 K) grown at two different [Se]/[Zn] (the growth temperature is 210 ^{o}C.).

3. Thermal stability of epilayer

Epitaxial growth techniques like MBE, MOVPE etc. can produce ZnSe epilayers with high crystalline quality at low growth temperatures. However, there exists a serious problem inherent to II-VI compounds, since Zn and Se atoms in ZnSe have vapor pressure higher than As atom in GaAs. Also ZnSe itself has a high vapor pressure of about 10^{-5} Torr at 600 ^{o}C. If not only the epitaxial growth, but also thermal processes after the growth (for example, the post-annealing after ion implantation etc.) were done at high temperatures, it would be feared that the crystalline quality of epilayers were degraded due probably to the generation of many deep centers like SA centers or native defects. If the annealing at relatively low temperatures (about 200 ^{o}C) degrades the crystalline quality of the ZnSe epilayers, the thermal process itself would be fatal in the fabrication process of the B-LED. Details little have been reported on the thermal stability of ZnSe epilayers, however. Very recently, Ohmi et. al. [89] reported the effect of lattice mismatching on the out-diffusion of impurities. They investigated thermal stability of ZnSe and ZnS_xSe_{1-x} grown at 450 ^{o}C by MOVPE and emphasized that lattice matching is important for suppressing out-diffusion of impurities from the substrates. Yet nobody has ever reported on the thermal stability of ZnSe epilayers itself grown at low temperature (less than 300 ^{o}C). In section 3-1, we will discuss the thermal stability of the ZnSe heteroepilayers. Moreover, we will apply it to the post-annealing after ion implantation for

realizing the p-type conversion of ZnSe in chapter 4. Therefore, the optimum annealing conditions should be found so as not to degrade the crystalline quality even by annealing at temperature as high as possible, for example by controlling the annealing atmosphere. Furthermore, we discuss the thermal stability of the ZnSe homoepilayers with high crystalline quality, clarify the merits in section 3-2 and will dope p-type impurities into the homoepilayers by ion implantation in the next chapter.

3-1. Heteroepilayer

The purpose of the present section is twofold. Firstly, we discuss thermal instability in crystalline quality of epilayers grown at low temperatures (250-300 ^{o}C) by MOVPE and the relation between the thermal stability and growth conditions. Secondly, we investigate how the crystalline quality is changed by conditions of the heat treatments.

The MOVPE system and procedures employed here were given in section 2.1.4. ZnSe heteroepilayers were grown on GaAs substrates, using DMZ and H_2Se as source gases in two different growth conditions. The first growth conditions were that growth temperature (Tg_1) was 300 ^{o}C, flow rate of DMZ was $3.1x10^{-5}$ mol/min., [Se]/[Zn] was 3, P_g was 0.1 Torr and growth period was 1 hour. The t_g was 3 μm under the above conditions. The second growth conditions were that Tg_2 was 250 ^{o}C, [DMZ] was $1.15x10^{-5}$ mol/min., [Se]/[Zn] was 20, P_g was an atmospheric pressure and

the growth period was 1 hour. Under the growth conditions, t_g was 4 μm.

After the growth, each epilayer was treated thermally at various temperatures T_t (200-800 ^oC), for various periods t (1 and 5 minutes) and in various ambiences (H_2, DMZ, nitrogen (N_2) and H_2Se). The conditions of heat treatments are listed in Table 3.1.1.

3-1-1. Effect of growth conditions on thermal stability of ZnSe epilayer

Figure 3.1.1 shows PL spectra (measured at 300 K) of the first group of epilayers treated thermally under H_2 atmosphere for 1 minute after growth. As T_t is elevated, the PL intensity of SA emissions which appear at about 590 nm increases drastically. These SA centers are considered to be due to complexes between Zn vacancies and some impurities from source gases [83]. It clearly shows that SA centers are easily generated by heat treatments at temperatures higher than the growth temperature (Tg_1=300 ^oC). Even the treatment at such a low T_t as Tg_1 results in generating a low concentration of SA centers.

As described previously [49], the surface morphologies of ZnSe epilayers grown under the reduced pressure are hazy and uncountable hillocks are observed along the <0$\bar{1}\bar{1}$> direction. The appearance of the directional hillocks is due to deviation from stoichiometry, particularly lack of Se atoms [83]. It is strongly

suggested that the thermal stability of ZnSe epilayers grown at a low growth temperature greatly influences the stoichiometry in the epilayers.

Figure 3.1.2 shows PL spectra (measured at 300 K) of the second group of samples treated at various T_t (no treatment, T_t=550 and 700 ^oC) under H_2 atmosphere for 5 minutes. Differing from the case of heat treatment of the first group, even the treatment at 550 ^oC (the high temperature treatment; T_t>500 ^oC) does not generate SA centers in spite of Tg_2 lower than Tg_1. Since the surface morphologies of the second group of epilayers are mirror-like and it obviously shows that the stoichiometry in the epilayers is kept very well [49], One cannot but conclude that even epilayers grown at a low growth temperature can have high thermal stability by precisely controlling the stoichiometry.

3-1-2. Effect of annealing conditions on thermal stability of ZnSe epilayer

Figure 3.1.2 shows that treatments at temperatures higher than 600 ^oC degrade the crystalline quality abruptly. The intensity of BE emission, which appears at 461 nm, however, increases remarkably. Figure 3.1.3 (a) shows the PL spectrum measured at 77 K. The donor-acceptor (DA) pair emission is observed at 460.4 nm, which is generated by the high temperature treatment. Namely, the high temperature treatments easily increase both SA centers

and impurities (donors and acceptors) in the epilayers even if the stoichiometry of ZnSe epilayers is kept well before the treatments.

It is necessary to investigate where, how and when SA centers are generated from. It should be clarified by the step etching of the degraded epilayers. Figures 3.1.3 (c) and (d) show the PL spectra (measured at 300 K) of the epilayer before and after the etching by a boiled solution of NaOH, respectively. It is obviously shown that SA centers are generated from the surface, not from the interface. Also Figs. 3.1.3 (a) and (b) show the PL spectra at 77 K of the epilayers before and after the etching, respectively. It is shown that the intensities of BE and DA pair emissions after the etching are weaker than those before. Particularly, the BE-PL intensity (the origin is thought to be a donor.) in the region near the interface decreases to that of an as-grown one. The density of impurities is obviously decreasing near the interface rather than at the surface. Figures 3.1.4 (a) and (b) show the PL spectra of epilayers (treated thermally under H_2 atmosphere) before etching measured at 4.2 K. The strong E_x, I_2, and I_x are observed at 2.8025, 2.7998 and 2.7981 eV, respectively in an as-grown sample. Also, in the epilayer treated at 550 ^oC, the E_x, I_2 and I_x are observed to shift downward by the same amount of energy (about 1 meV) due to the yield of strain by the difference in thermal expansion between ZnSe and GaAs. This is consistent with the fact that the peak energy of the excitonic emission line was shifted downward with the increase of the growth temperature as reported in the MBE growth of ZnSe [39].

The heat treatment at 600 ^{o}C additionally generates a strong bound exciton emission line at 2.7919 eV (labeled I_1(As)). This is thought to be the bound exciton emission line (see Fig.3.1.4 (c).) due to As acceptor. It clearly indicates the out-diffusion of As impurities from the GaAs substrate. The I_1(As) emission line shows up at 550 ^{o}C. It means that the out-diffusion of As impurities becomes serious at the annealing temperature above 550 ^{o}C and it is also assumed to degrade the crystalline quality. Moreover, we will see the role of impurities diffused into the epilayers from the substrates or from the ambience during the treatment. Figure 3.1.4 (d) shows the PL spectra measured at 4.2 K of the epilayers after the etching. They show that the species and existence of impurities near the interface are almost unchanged with that near the surface except for the broadening of FWHM of bound exciton emission lines due to the degradation of the crystalline quality near the interface. It is not clear which line is the origin of the BE emission enhanced from the surface by the high temperature treatment among some bound exciton emission lines, though the total concentration of donors and acceptors is lower near the interface as determined by the PL measurements at 77 K. The bound exciton emission line (at 2.7813 eV) due to Zn vacancy itself [81] appears in the region near the interface. The Zn vacancies increased by the high temperature treatment would generate the high concentration of SA centers at the surface and the isolated Zn vacancies would simultaneously diffuse into the epilayer.

3-1-3. Effect of ambient gases on thermal stability

In order to see whether SA centers are increased prominently by some chemical reaction between H_2 and ZnSe, we will examine the effects of other ambient gases in the second group of epilayers on the crystalline quality. Figure 3.1.5 shows the PL spectra of the epilayers treated under N_2 atmosphere at various T_t. Even at T_t=657 ^{o}C, SA centers are not generated in the epilayers. Figure 3.1.6 shows the surface morphologies of epilayers treated under H_2 or N_2 atmosphere at high temperatures (700 and 757 ^{o}C). In the case of H_2, the surface of epilayer becomes hazy to the eye and a high concentration of hillocks along <0$\bar{1}\bar{1}$> direction are formed on the surface morphology by the treatment. These two phenomena strongly suggest that some chemical reaction between ZnSe and active H_2 molecule generates high concentration of SA centers even at 600 ^{o}C. Only the thermal energy, which corresponds to 600 ^{o}C without any chemical reaction, does not generate SA centers (i. e., does not cause a thermal instability.). Since we observe a drastic increase of both SA and BE emissions by the treatment at 757 ^{o}C under N_2 atmosphere, the thermal instability in ZnSe probably starts at about 700 ^{o}C. The crystalline quality of the ZnSe heteroepilayers is degraded under H_2 atmosphere more heavily than under N_2 atmosphere in the heat treatment at 700 ^{o}C. It indicates that the heavy out-diffusion of constituting atoms through the vapor phase from the GaAs substrate is more repressed in the N_2 atmosphere because of high viscosity.

The origin of SA centers is now discussed. Figures 3.1.7 (a),

(b) and (c) show the PL spectra of epilayers (measured at 300 K) treated at 700 ^{o}C under only H_2 atmosphere, under H_2 atmosphere including Zn vapor (the Zn source is supplied by DMZ, and the flow rate is same as that during the growth (1.15×10^{-5} mol/min.).) and under H_2 atmosphere including Se vapor (the Se source is H_2Se and the flow rate is 2.3×10^{-4} mol/min.), respectively. It is clearly shown that the generation rate of SA centers is prevented by the introduction of the Zn vapor, but it is enhanced in the ambient containing Se vapor. One of the origin of SA centers is accordingly thought to be Zn vacancy as described previously [83]. It is essential to suppress Zn vacancies generated at high temperature treatment to keep the crystalline quality high.

Thermal stability of ZnSe heteroepilayers grown at 250 ^{o}C by atmospheric pressure MOVPE is much better than that of ZnSe epilayers grown at 300 ^{o}C by the conventional reduced pressure (at 0.1 Torr) MOVPE. It shows that the thermal stability is related to the degree of stoichiometry in epilayers, which is controlled by the growth conditions. Heat treatment at temperatures higher than 600 ^{o}C, however, generates a high density of SA centers and takes impurities in the epilayer from the surface by some chemical reaction with H_2, irrespectively of the degree of the stoichiometry in the as-grown epilayer. It is because some reaction of H_2 molecule with ZnSe accelerates the degradation of the crystalline quality at 600 ^{o}C. Heat treatment in N_2 atmosphere does not generate SA centers and impurities even at 657 ^{o}C. At 757 ^{o}C, however, they are generated. It is consequently found

that ZnSe epilayers grown at 250 ^{o}C by the atmospheric pressure MOVPE are thermally stable at least up to about 700 ^{o}C. Also the introduction of Zn vapor into H_2 atmosphere has an effect of suppressing the multiplication of SA centers and of preventing impurities from flowing in the epilayers even at 700 ^{o}C. It is thus strongly suggested that one of the origin of SA centers is Zn vacancy. Controlling the concentration of Zn vacancy, accordingly, is a key factor in the high temperature treatment.

The crystalline quality of the ZnSe heteroepilayers is related to not only the presence of Zn vacancies but also the heavy out-diffusion of the constituting atoms from the GaAs substrates. Particularly, the ZnSe heteroepilayers are doped highly by heavy out-diffusion of As atoms with high vapor pressure. The crystalline quality is easily degraded and the high density of SA centers are generated in the ZnSe heteroepilayers. The out-diffusion causes an increase of residual impurities in the epilayers. It is expected that homoepilayers have thermal stability higher than the heteroepilayers. The idea is applied to post-annealing after the ion implantation for increasing the activation rate of acceptors. The thermal stability of the ZnSe homoepilayers now remains to be discussed.

3-2. Homoepilayer

ZnSe with low resistivity of p-type conduction is not obtained yet. One reason is thought to be the deterioration of

crystalline quality due to lattice mismatching between ZnSe and GaAs. So we have made the ZnSe homoepitaxial growth using (100)-oriented ZnSe substrate and investigated the effects of the growth conditions on the crystalline quality as seen in section 2-2. And as one of the p-type doping-techniques, possibility of the ion implantation in chapter 4 has been studied. The ion implantation needs a post-annealing. However, the thermal treatment itself would degrade the crystalline quality of the homoepilayers because of the very low growth temperature. As stated in section 3-1 [90,91], the crystalline quality of the heteroepilayers is not degraded by the thermal treatment at temperatures less than 600 ^{o}C. Above 600 ^{o}C, degradation of the crystalline quality starts to be observed from the edge of the sample by the heavy out-diffusion of the constituents of the GaAs substrate through the vapor phase during the heat treatment. Thus, though it is expected that the thermal stability of homoepilayers is higher than that of heteroepilayers, the thermal stability itself of homoepilayers grown at very low temperature (220 ^{o}C) has not been investigated yet.

The objective of this section is to report the thermal stability of the homoepilayers grown at 220 ^{o}C, which is lower than the growth temperature of the heteroepilayers [90-92] (250-300 ^{o}C), by atmospheric pressure MOVPE using DMZ and H_2Se as source gases and to investigate the effects of the atmospheres on the crystalline quality as the first stage before proceeding to the ion implantation.

The pretreatment of ZnSe substrates before growth has been

described in section 2-1 [69]. The ZnSe homoepilayers were grown at the following conditions. The growth temperature was 220 ^{o}C, the reactor pressure was an atmospheric pressure, the flow rate of DMZ was $11.5x10^{-5}$ mol/min., the [Se]/[Zn] was 10 and the growth period was one hour. Under the above growth conditions, the epilayer thickness was about 4 μm. After the growth, homoepilayers were treated under various T_t (600-757 ^{o}C) and atmospheres (H_2, N_2 and H_2 including DMZ) for 5 minutes. Also the homoepilayer was etched by 1% Br_2-CH_3OH solution in sequence to get the information on PL at 77 and 4.2 K of the inter-epilayer. Also for comparison, the heteroepilayers were grown at 250 ^{o}C. The thickness of the heteroepilayers was about 4 μm. After growth, both epilayers were left in the air for several days and were thermally treated under various conditions listed in Table 3.2.1.

Figure 3.2.1 shows the PL at 300 K of a homoepilayer treated at 700 ^{o}C for 5 min in H_2 atmosphere, compared with the PL of an as-grown homoepilayer. The homoepilayer with heat treatment has almost the same PL spectrum as the as-grown homoepilayer. That is to say, the SA centers, whose peak emission appears at about 600 nm, are not generated in homoepilayers, and the BE-PL intensity at 460 nm is unchanged even after the heat treatment. The surface morphologies do not change and remain mirror-like after that. These phenomena are very different from the situation in the heteroepitaxial growth [91]. Figure 3.2.2 shows the dependence of the absolute PL intensities of the BE and SA emissions in the epilayers on T_t. The PL intensities of both the BE and SA emis-

sions increase rapidly from the region near the edge of the sample in the heteroepilayers as T_t increases. On the other hand, the phenomenon is not observed in the homoepilayers and the PL spectra are uniform over the whole area. It indicates that the main mechanism of degrading the crystalline quality is related to GaAs substrates used in the heteroepitaxial growth. We have already assumed that the degradation is due to the heavy out-diffusion of As atoms in GaAs from PL at 4.2 K. It is expected that the homoepilayers have a thermal stability which is higher than that of the heteroepilayers. We will examine the PL properties at 77 and 4.2 K to see if the crystalline quality of the homoepilayers is well maintained even after thermal treatment.

Figure 3.2.3 shows the PL spectra at 77 K of homoepilayers treated at various T_t and in different atmospheres. In contrast with the result in Fig. 3.2.1., it is shown that the SA-PL intensity increases slightly even in the homoepilayers. Compared with the PL spectrum of the heteroepilayers, the generation rate of SA emissions is very low (see Figs. 3.2.3 and 3.2.4.). Thus the PL ratio (R) changes from 33.0 to 8.1 at 700 ^{o}C under H_2 atmosphere in the homoepilayers, while it goes from 33.5 to 0.4 in the heteroepilayers. Figure 3.2.4 shows the dependence of T_t on R in both epilayers. Even the PL properties of the homoepilayers start to degrade above 700 ^{o}C. This indicates that another degradation mechanism exists besides the heavy out-diffusion at high T_t. We saw that the PL spectra at 77 K of the heteroepilayers were influenced by the types of atmosphere in the heat treatment [90,91]. As seen in Fig. 3.2.4., the R value recovers to the

level of an as-grown homoepilayer by adding DMZ vapor, corresponding to about 0.1 % of the total flow rate in the H_2 atmosphere at 700 ^{o}C. It is suggested that the generation mechanism of SA centers is more closely related to the occurrence of Zn vacancies in homoepilayers, than the out-diffusion of a low concentration of unknown impurities (probably iodine impurities including in the substrate.) through the vapor phase. It is also shown that N_2 atmosphere is superior to H_2 atmosphere at the same flow rate in both homo- and hetero-epilayers. The out-diffusion of impurities through the vapor phase is suppressed with N_2 atmosphere. For this reason, the low thermal conductivity [93] or/and high viscosity of the N_2 atmosphere suppresses the scattering of the impurities diffused from the substrate through the vapor phase.

Figure 4.2.5 shows the PL spectra in near the band-edge region at 4.2 K of an as-grown homoepilayer (Fig. 3.2.5(a)) and a homoepilayer treated at 757 ^{o}C in N_2 atmosphere for 5 min (Fig. 3.2.5(b)). Figure 3.2.6 shows the PL of an as-grown heteroepilayer and one treated at 757 ^{o}C under N_2 atmosphere for 5 min. In homoepilayers, both E_x and I_x lines at 2.8059 and 2.8004 eV, respectively, are observed at higher energy (about 4 meV) than those of the heteroepilayers. Nevertheless, in homoepilayers, energy positions of all the peaks shift 4.5-5.3 meV upward compared with heteroepilayers. They are unchanged by T_t. It probably indicates that homoepilayers are strain free because of the complete coincidence of the thermal expansion coefficients of the epilayer and the substrate. It has been shown that the homoepilayers maintain the crystalline quality better than the

heteroepilayers at high T_t. An intense peak at 2.7864 eV appears after the heat treatment. The origin of this peak is identified with the emission related to the Zn vacancy (I_1^{deep} emission), by considering the above energy separation and the emission energies in the heteroepilayers [91]. The reason is ascertain that there is some concentration of Zn vacancies diffusing from the highly iodine-doped ZnSe substrates. It is hardly observed in the heteroepilayers. We have examined whether there is another possibility of the out-diffusion of impurities from the ZnSe substrates into the homoepilayers after the heat treatment or not. In the PL spectra at 4.2 K, emission peaks due to other impurities are not observed. One can thus see that the purity of the homoepilayers is well maintained even after heat treatment at 700 ^{o}C. In the heteroepilayers, on the other hand, the heavy doping of As atoms by the out-diffusion, and the onset of the degradation of the crystalline quality are seen. Indeed broad peaks composed of E_x, I_x and I_1(As) (appearing at 2.7904-2.7919 eV) are observed with weaker intensities [91]. This clearly indicates that one of the main causes of generating SA centers and of degrading the crystalline quality is the heavy out-diffusion coming through the vapor phase during the heat treatment at high temperatures. In homoepilayers, both the concentration of the residual impurities and the crystalline quality are well controlled in spite of the heavy out-diffusion of Zn vacancies. It is also confirmed that the inclusion of DMZ (11.5×10^{-6} mol/min.) in the ambient gas can have only a small effect in suppressing the concentration of Zn vacancies. One can thus see how difficult

it is to suppress the heavy out-diffusion of Zn vacancies from the highly iodine-doped ZnSe substrates.

In summary, the thermal stability of ZnSe homoepilayers is found superior to that of heteroepilayers despite the lower growth temperature. While an overall crystalline quality is maintained, the heavy out-diffusion of Zn vacancies from the highly iodine-doped ZnSe substrates is caused by the heat treatment at high temperatures. As a mechanism of degradation of the homoepilayers in the heat treatment at high temperatures, the out-diffusion of Zn vacancies, which is closely related to the occurrence of SA centers, is proposed. In fact, the inclusion of Zn vapor in the ambience has an effect in suppressing the concentrations of both SA centers and Zn vacancies. One has to admit, however, that it is difficult to suppress their concentrations completely at present.

As long as the impure ZnSe substrates are used in ZnSe homoepitaxial growth, the out-diffusion of Zn vacancies from the substrates cannot be prevented completely during the heat treatment at temperatures higher than 700 ^{o}C. Since the out-diffusion of impurities in the ZnSe homoepilayers is less than that in the ZnSe heteroepilayers, the heavy out-diffusion degrading the crystalline quality is largely removed in the homoepitaxial growth. The annealing temperature of keeping the crystalline quality in the ZnSe homoepilayer can be higher than that in the ZnSe heteroepilayer in post-annealing after the ion implantation for p-type doping.

Table 3.1.1. Heat treatment conditions.

Sample No.	Growth conditions		Conditions of heat treatment				
	T_g (°C)	P_g (Torr)	T_t (°C)	Atmosphere	Total flow rate (l/min.)	t (min.)	t_g (μm)
1	300	0.1	– [a]	–	–	–	3.0
2	300	0.1	300	H_2	4.0	1	3.0
3	300	0.1	350	H_2	4.0	1	3.0
4	300	0.1	400	H_2	4.0	1	3.0
5	250	760	– [a]	–	–	–	4.0
6	250	760	550	H_2	4.0	5	4.0
7 [b]	250	760	600	H_2	4.0	5	4.0
8 [b]	250	760	700	H_2	4.0	5	4.0
9	250	760	700	H_2 + DMZ	2.0 (DMZ: 11.5 μmol/min.)	5	4.0
10	250	760	700	H_2 + H_2Se	2.0 (H_2Se: 230 μmol/min.)	5	4.0
11	250	760	657	N_2	4.0	5	4.0
12	250	760	757	N_2	4.0	5	4.0

[a] No treatment
[b] The sample is also etched by chemical solution.

Table 3.2.1. Thermal treatment conditions.

Temperature (°C)	Atmosphere	Flow rate (l/min.)	Period (min.)	Substrate
– [a]	– [a]	– [a]	– [a]	ZnSe, GaAs
200–700	H_2	4.0	5	GaAs
600, 700	H_2	4.0	5	ZnSe, GaAs
700	H_2 + DMZ	2.0 [b]	5	ZnSe
757	N_2	4.0	5	ZnSe, GaAs

[a] No thermal treatment
[b] DMZ, 11.5 μmol/min.

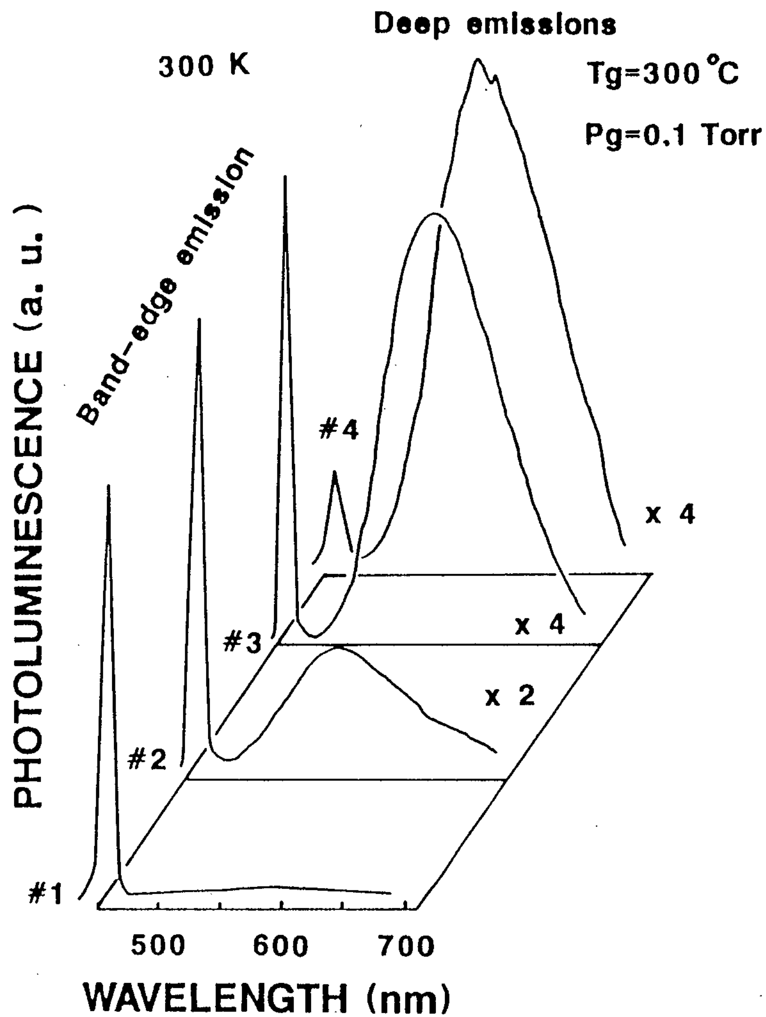

Fig.3.1.1. PL spectra (measured at 300 K) of ZnSe heteroepilayers (grown under the reduced pressure) treated at various temperatures under H_2 atmosphere (# 1-4).
(# 1, no treatment; # 2, T_t=300 ^oC, t=1 min. ; # 3, T_t=350 ^oC, t=1 min. ; # 4, T_t=400 ^oC, t=1 min.).

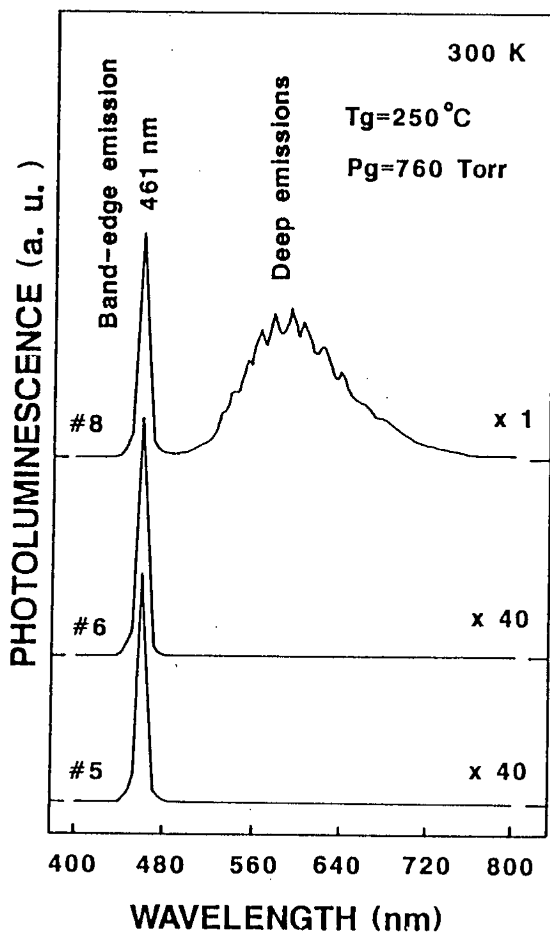

Fig.3.1.2. PL spectra (measured at 300 K) of ZnSe heteroepilayers (grown under the atmospheric pressure) treated at various temperatures under H_2 atmosphere (# 5, 6 and 8).
(# 5, no treatment; # 6, T_t=550 ^oC, t=5 min. ; # 8, T_t=700 ^oC, t=5 min.).

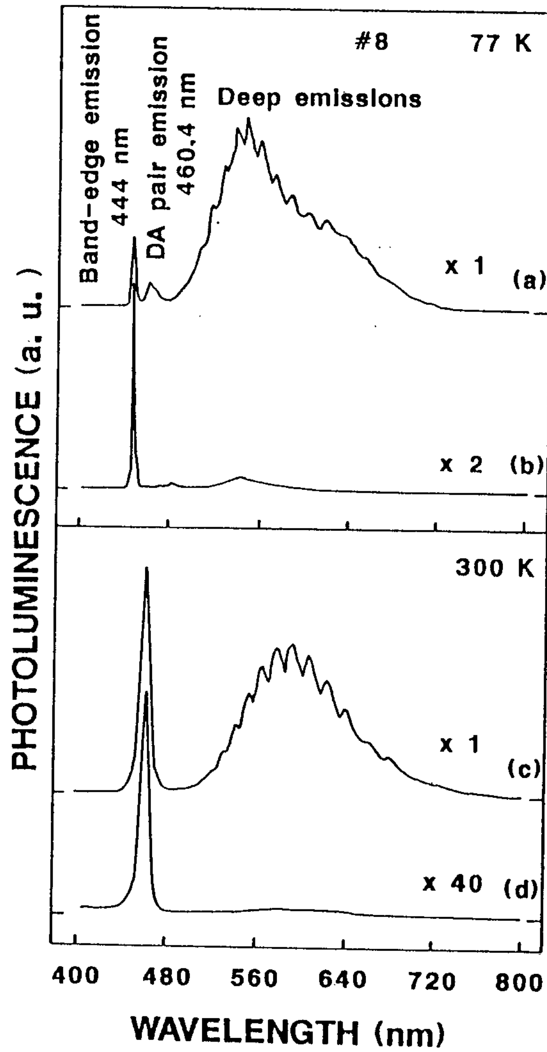

Fig.3.1.3. PL spectra (measured at 77 K and 300 K) of a ZnSe heteroepilayer (# 8) before and after the etching.

(a) Before the etching, measured at 77 K.

(b) After the etching, measured at 77 K.

(c) Before the etching, measured at 300 K.

(d) After the etching, measured at 300 K.

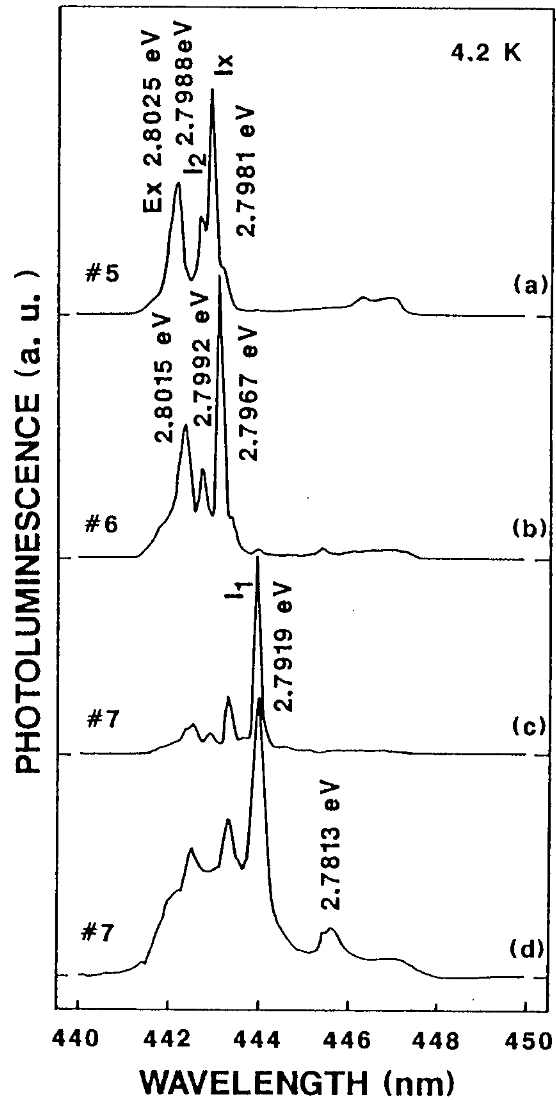

Fig.3.1.4. PL spectra at 4.2 K of ZnSe heteroepilayers in the near band-edge region.

(a) As-grown (# 5).

(b) Epilayer treated at 550 ^{o}C under H_2 atmosphere (# 6).

(c) Epilayer treated at 600 ^{o}C under H_2 atmosphere (# 7).

(d) Epilayer after the etching of # 7.

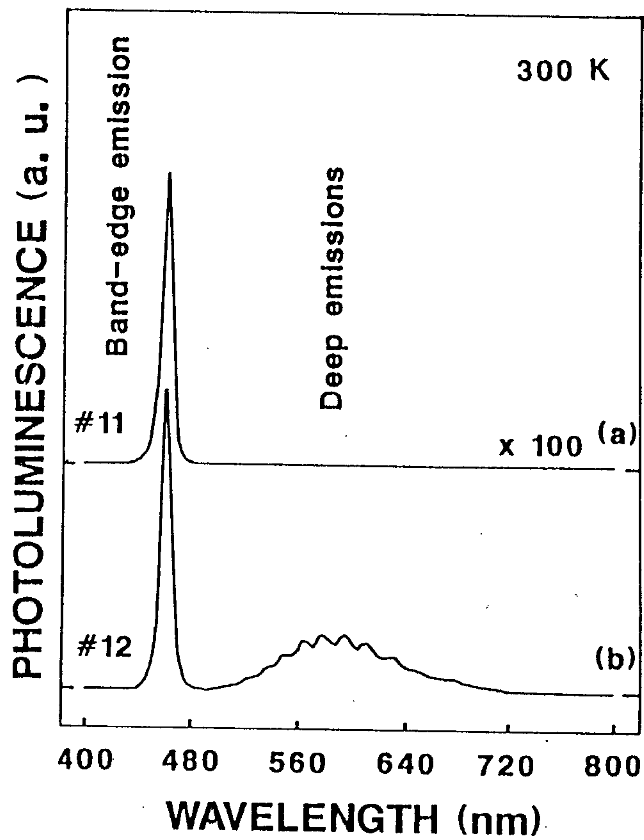

Fig.3.1.5. PL spectra at 300 K of heteroepilayers treated at various T_t under N_2 atmosphere.

(a) T_t=657 ^oC (# 11).

(b) T_t=757 ^oC (# 12).

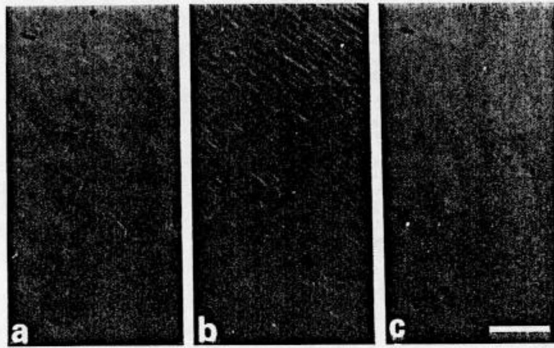

Fig. 3.1.6. Surface morphologies of ZnSe epilayers observed by a Nomarski phase contrast interference microscope.
(a) As-grown (# 5).
(b) Epilayer treated at 700 ^{o}C under H_2 atmosphere (# 8).
(c) Epilayer treated at 757 ^{o}C under N_2 atmosphere (# 12).

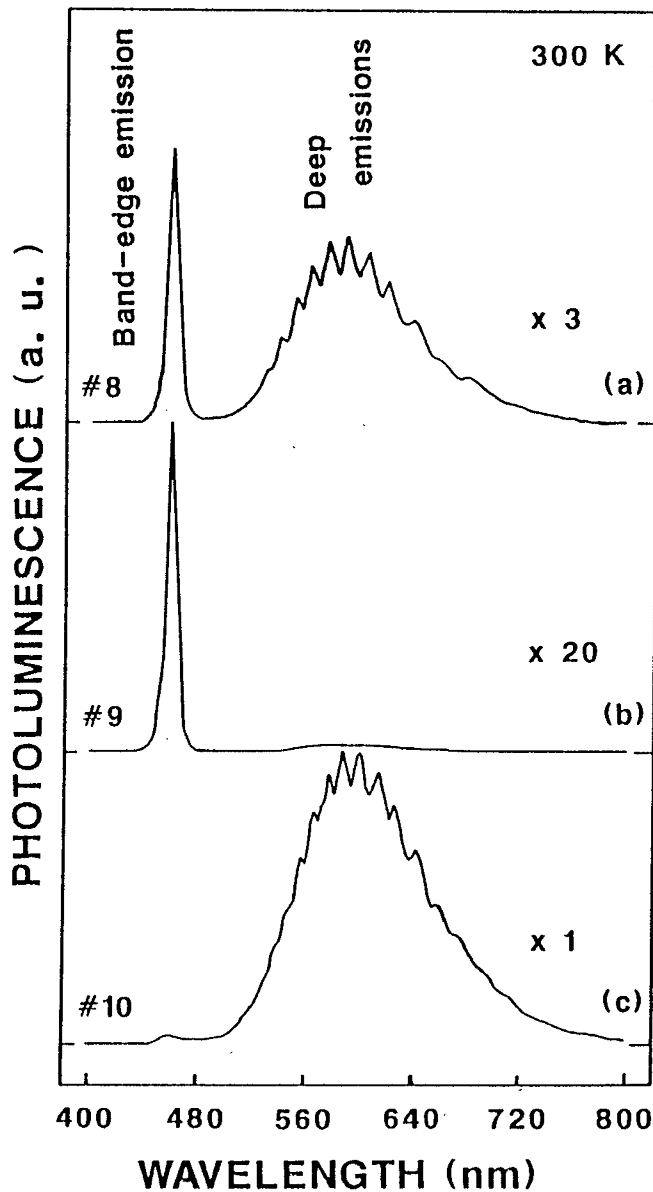

Fig.3.1.7. PL spectra (measured at 300 K) of ZnSe heteroepilayers treated at 700 ^{o}C under various atmospheres.

(a) Epilayer treated under H_2 atmosphere only (# 8).

(b) Epilayer treated under H2 atmosphere including Zn vapor (# 9).

(c) Epilayer treated under H_2 atmosphere including Se vapor (# 10).

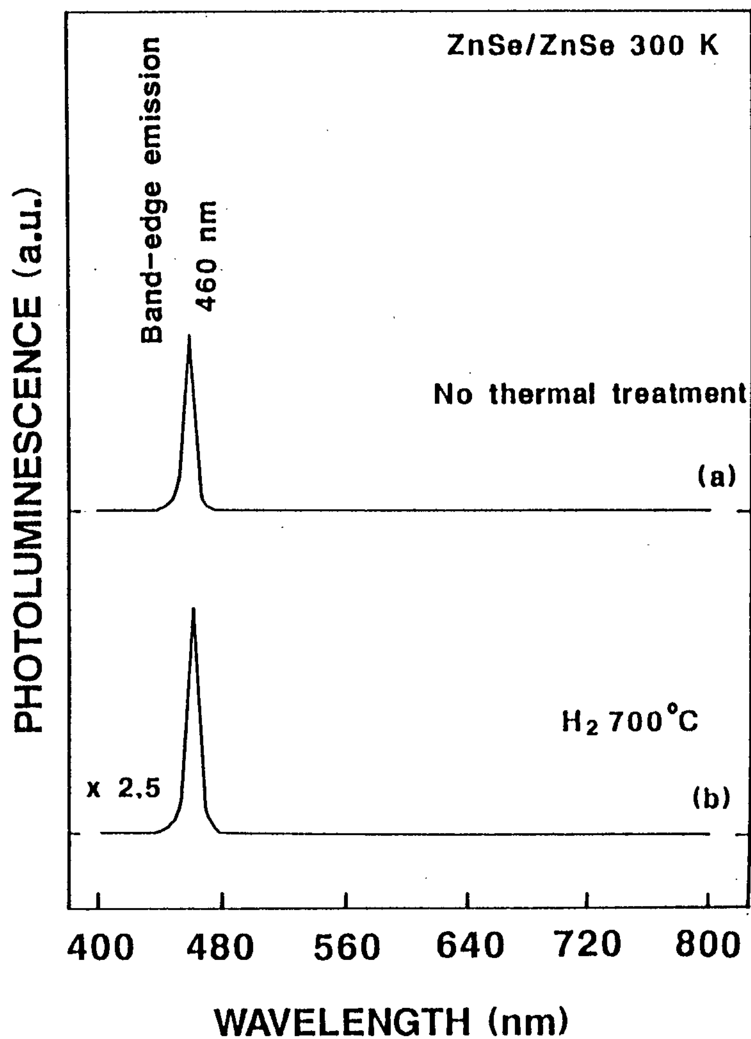

Fig. 3.2.1. PL spectra (measured at 300 K) of (a) an as-grown homoepilayer and (b) a homoepilayer treated at 700 ^{o}C under H_2 atmosphere for 5 min after growth.

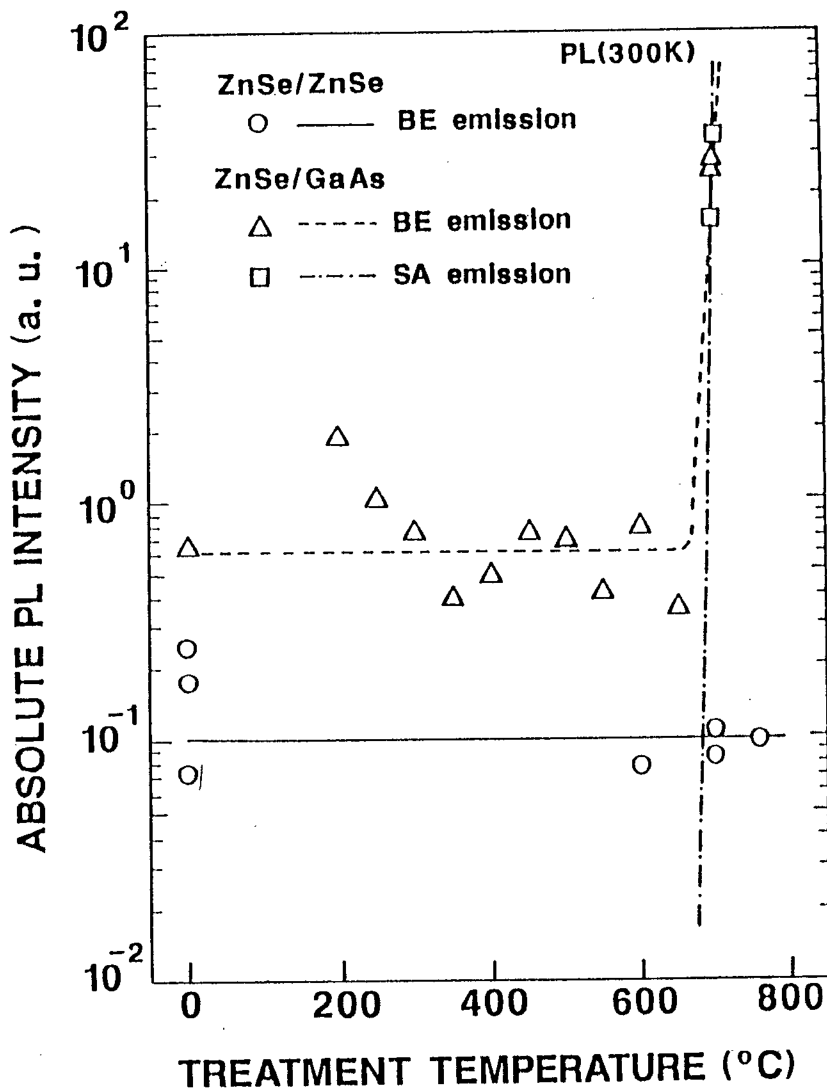

Fig. 3.2.2. The dependence of the absolute PL intensities at 300 K of the BE and SA emissions in the epilayers on the thermal treatment temperatures.

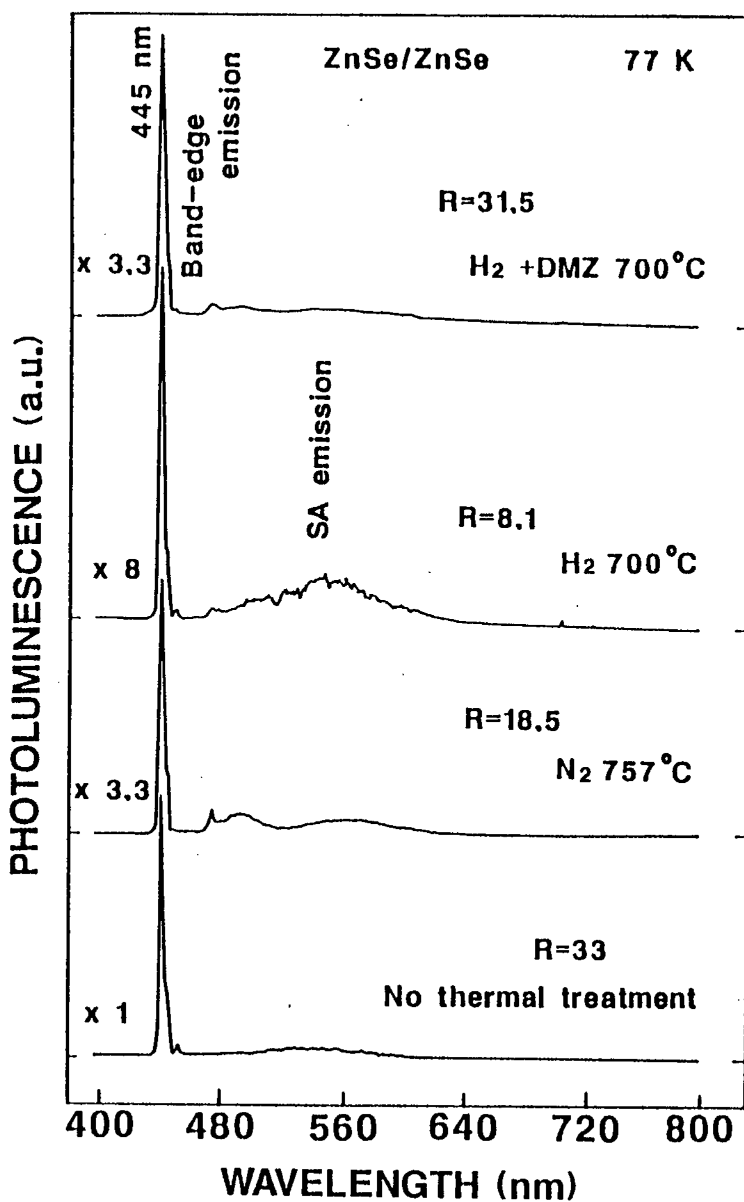

Fig. 3.2.3. PL spectra of the homoepilayers treated at various temperatures and atmospheres. The measurement temperature is 77 K.

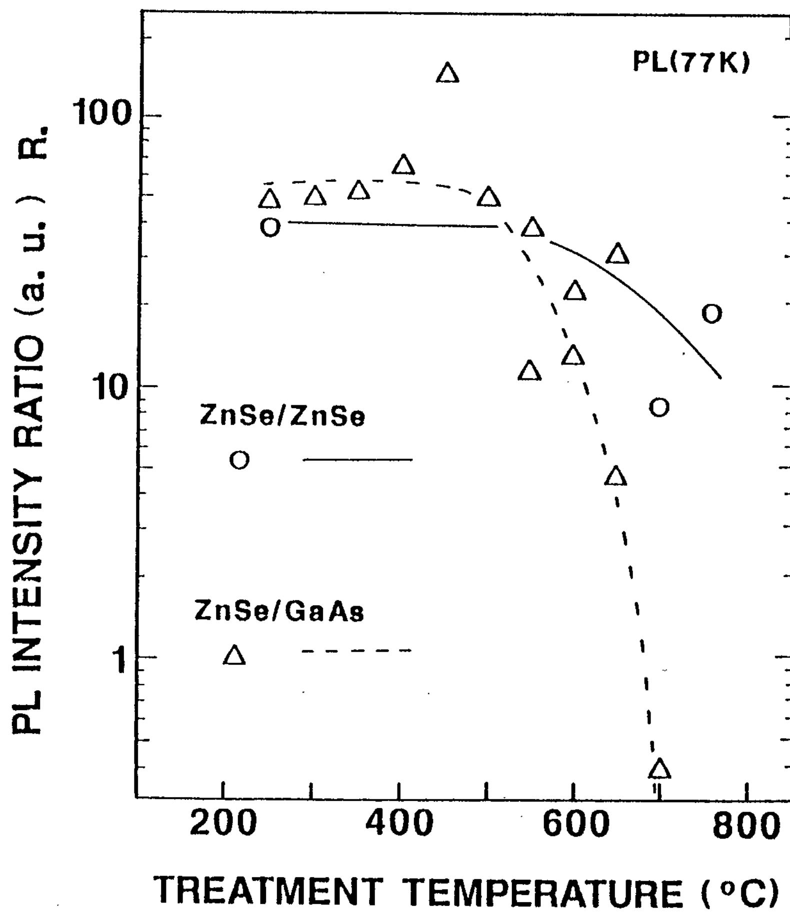

Fig.3.2.4. Dependence on T_t of R in both homo- and hetero-epilayers.

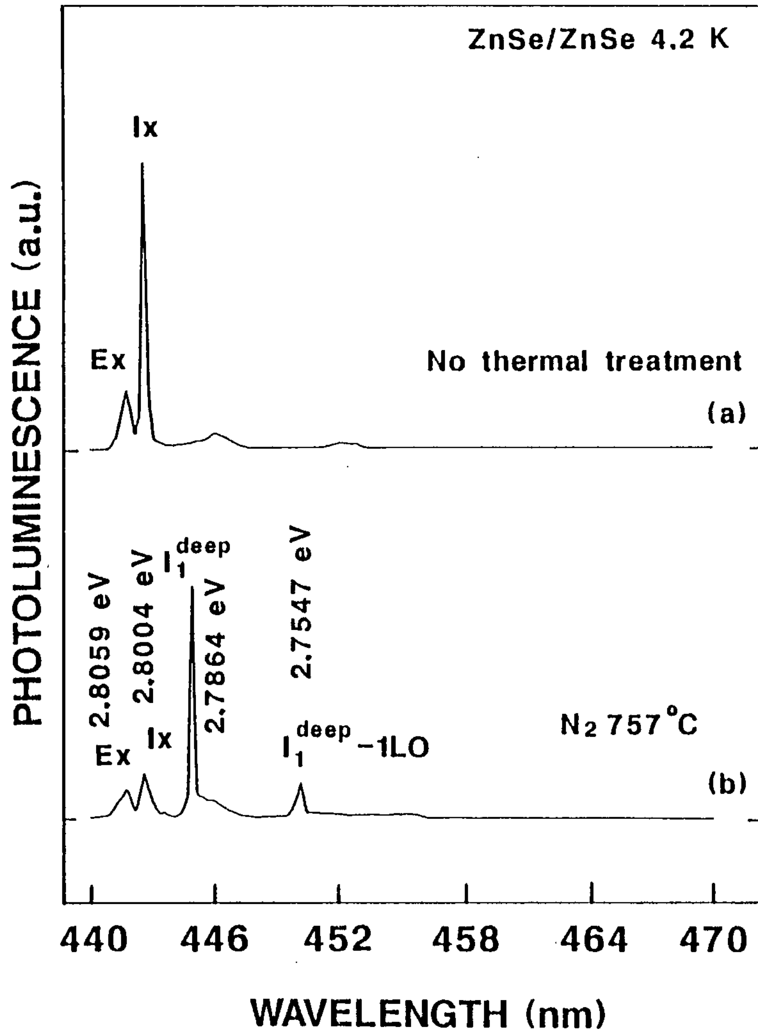

Fig. 3.2.5. PL spectra of (a) an as-grown homoepilayer and (b) a homoepilayer treated at 757 ^{o}C under N_2 atmosphere for 5 min. The treatment temperature and wavelength region are 4.2 K and near the band-edge region (440-470 nm).

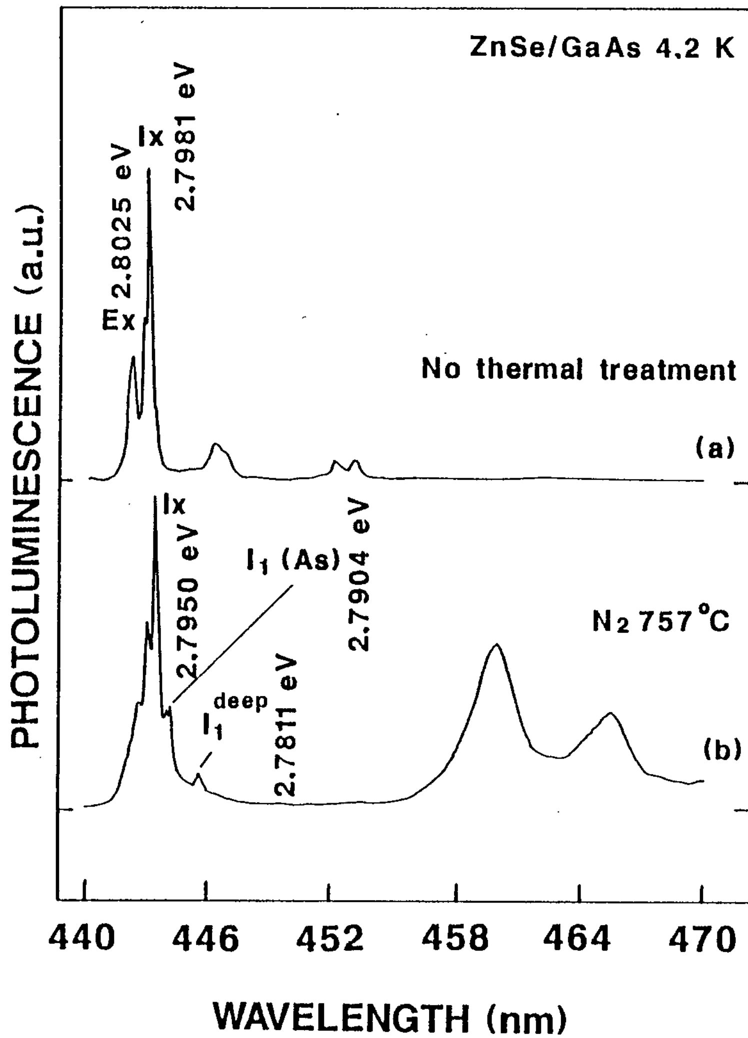

Fig.3.2.6. PL spectra at 4.2 K in near the band-edge region (440-470 nm) of (a) an as-grown heteroepilayer and (b) a heteroepilayer treated at 757 ^{o}C under N_2 atmosphere for 5 min.

4. p-type ZnSe by ion implantation

ZnSe presents a difficult problem of p-type crystal growth because of the so-called self-compensation [18] inherent in II-VI compounds. Accordingly, a low temperature epitaxial growth is required to control the incidence of native defects in the epilayer, which is generally thought to be the main cause of self-compensation. The epitaxial growth at low temperatures has been discussed in chapter 2. It is confirmed that ZnSe epilayers with high crystalline quality can be grown at 250 ^{o}C by MOVPE. Nevertheless, a p-type ZnSe with low resistivity could never be obtained so far. Recently, numerous attempts have been made to incorporate several p-type impurities including N [18,38 97,98] , P [19,38,102], As [101], Sb [99], and Li [94,95,96,100], using gas phase or solid phase impurity sources during growth. Stutius [38] reported p-type doping with group V impurities (N and P) by MOVPE and suggested that N was superior to P. Park et al. [98-100] tried p-type doping of ZnSe using N, Li and Sb, and Yao [19] also investigated P-doped ZnSe by MBE. Attempts to dope p-type impurities into ZnSe bulk crystals by ion implantation with Li [103], P [102] and N [104,105] have also been reported. However, ZnSe epilayers with good p-type conversion have not been obtained yet except for a few successful reports. Some photoluminescence spectra at low temperatures indicate that p-type impurities such as N, Li and As are actually substituted and formed acceptor levels into the ZnSe epilayers. Nishizawa [95] and Yasuda [96] reported that Li impurity forms a shallow acceptor level in

ZnSe, and confirmed p-type conduction with a hole carrier concentration from 10^{16} to 10^{17} cm^{-3}. Ohki et al. [97] obtained N-doped p-type ZnSe epilayers with a maximum hole carrier concentration of 10^{14} cm^{-3}, by introducing a large quantity of NH_3 during the MOVPE growth. The suggested reasons for this are that the doping source of Li used was impure while that of N required too high a deposition temperature. As a result, the concentration of residual impurity in the epilayers increased with Li doping [94] while the acceptor concentration of N [18] in MBE-grown epilayers was much limited to a low concentration despite of high density of N atoms in ZnSe (10^{19} cm^{-3}). The Li impurity can create a shallow acceptor level up to a relatively high hole concentration (10^{16}-10^{17} cm^{-3}), while the N impurity produces only a low hole concentration (10^{14}-10^{15} cm^{-3}) despite the very high impurity concentration (10^{19} cm^{-3}) in the epilayers. Thus the activation rate of N acceptors in ZnSe becomes very low.

In summary, a big problem of realizing p-type conversion is that there are no appropriate sources for p-type dopants with both high purity and thermal instability at low temperatures.

Ion implantation is very promising as a method of p-type doping in ZnSe because it can dope impurities to high concentration under non-equilibrium conditions with high purity. Meanwhile it gives radiation damage to the epilayer and would degrade the crystalline quality. The last demerit has never been discussed.

4-1. Li^+ ion implantation into ZnSe epilayer

4-1-1. Effects of annealing conditions on the crystalline quality of the ZnSe heteroepilayer

In this section, we report the result of Li^+ ion implanted ZnSe epilayers grown at a low temperature of 250 ^oC by MOVPE and show the optimum thermal annealing conditions, in which the radiation damage is removed and a high activation rate of Li atoms substituted on Zn sites can be accomplished without generating SA centers.

The growth conditions were as follows. The growth temperature was 250 ^oC, the flow rate of DMZ was $11.5x10^{-6}$ mol/min., the [Se]/[Zn] was kept at 20 , the total flow rate was 4 l/min and the growth period was 1 hour. Under these conditions, the surface morphologies were reproducibly mirror-like and the epilayer thickness was about 4 μm. After growth, the undoped ZnSe epilayers were removed from the chamber and implanted with Li^+ ions with a dose density of 10^{14} cm^{-2} at an acceleration energy of 50 keV and current density of 80 $\mu A/cm^2$. The thermal annealing conditions (after or before ion implantation) are listed in Table 4.1.1. The annealing conditions were chosen as stated in section 3-1 following our previous work [90,91] so that the thermal treatments would maintain the high crystalline quality of ZnSe heteroepilayers.

Firstly, we mention the crystalline quality of ZnSe heteroepilayers before ion implantation. Figure 4.1.1 shows the PL spec-

tra (measured at 77 and 300 K) of an undoped ZnSe epilayer without Li^+ ion implantation. Though BE emission is observed, there is little SA emission at the respective measurement temperatures. This indicates that an as-grown epilayer merely contains a very low concentration of impurities and native defects. Figure 4.1.2 shows the PL spectra at 77 K of the ZnSe epilayers annealed thermally as indicated in Table 4.1.1., without Li^+ ion implantation. Even at 557 ^{O}C, the crystal quality of the ZnSe heteroepilayers grown at 250 ^{O}C has not been degraded, and the concentration of SA centers has not increased. The crystalline quality is maintained even after the annealing at temperatures up to 557 ^{O}C. It is observed that an unknown emission begins to appear at 458.6 nm (2.703 eV) after the annealing at temperatures above 557 ^{O}C. Also the phenomenon commences from the fringe of the samples around 657 ^{O}C. It probably indicates that the annealed epilayer has a concentration of acceptors higher than an as-grown one. Figure 4.1.3 shows the PL spectra at 4.2 K of the heteroepilayers annealed thermally at various temperatures as indicated in Table 4.1.1. As expected, both I_1(As) and DA pair emissions are intensely observed at 2.7914 and 2.6940 eV respectively after the annealing at 657 ^{O}C. It is strongly suggested that a high concentration of impurities are taken into the epilayers during the annealing and that the origin of the impurity is thought to be As atom, which forms a shallow acceptor in ZnSe, diffusing from the GaAs substrates.

Next, we discuss the effects of Li^+ ion implantation on the crystalline quality of the ZnSe heteroepilayers. It is well-known

that a substitutional Li atom on a Zn site acts as a shallow acceptor, while an interstitial Li impurity as a donor [106]. Figure 4.1.4 shows the PL spectra at 77 K of the Li^{+} ion implanted epilayers including the thermal annealing. The implanted epilayer without thermal annealing emits little light at 300 K because of the radiation damage. Furthermore, PL spectrum at 77 K shows no emission except for weak SA and Y emissions. The total PL intensity is three orders of magnitude less than that of an as-grown one. As the annealing temperature was increased, however, the total PL intensity composed of both BE and free to acceptor (FA) emissions (appearing at 459.8 nm (2.695 eV)) increased abruptly. Compared with the results of Fig. 4.1.2., the energy position of the transition emission is almost the same as the peak emission (probably related to As impurity) appearing in the annealed sample at 657 ^{o}C without ion implantation. The origin of the peak emission is obviously different from that observed in Fig. 4.1.2 and is assumed to be the FA transition emission related to Li acceptor because the PL intensity becomes one hundred times stronger than that of the epilayer without ion implantation. It was necessary to measure the PL spectra of the epilayers at 4.2 K in more detail in order to discuss the origin of the impurities. Before doing that, we should prove that the radiation damage due to Li^{+} ions can be recovered by thermal annealing and, at the same time, the activation rate of substituted Li impurities on Zn sites increases dramatically. At 757 ^{o}C, only the FA emission was seen and the PL intensity was twenty times stronger than that from the epilayer treated at 657 ^{o}C. Nevertheless, the

SA-PL intensity did not increase. One can thus strongly support the conclusion that the implanted Li impurity acts as an acceptor rather than a donor following the thermal annealing. The crystalline quality was completely recovered at relatively low temperatures below 557 ^{o}C, as indicated by the saturation of the BE-PL intensity. On the other hand, the activation rate of the Li acceptors was still increasing even at 757 ^{o}C. Figure 4.1.5 shows the PL spectra at 4.2 K of Li^{+} ion implanted epilayer after post-annealing. The I_1(Li) (acceptor bound exciton emission line due to Li acceptor) and DA pair emissions were observed with intense intensities in the epilayer annealed at 657 ^{o}C. The energy position of the I_1(Li) peak is 2.7905 eV. Since the same thermal strain was imposed on both implanted and unimplanted epilayers at 657 ^{o}C, the energy position of the I_1(Li) peak is clearly different from that of the I_1(As) peak in Fig. 4.1.3., which is thought to be the acceptor bound exciton emission line due to the As acceptor. It has not been reported yet, except for reference 4, that ZnSe doped by p-type impurity exhibits such a main and simple I_1(Li) emission peak. This indicates that the epilayers maintained their crystalline quality very well even after the high Li-doping. This also clearly supports the suggestion that the implanted Li impurity forms a shallow acceptor level in ZnSe, especially after the high temperature annealing, in contrast with the abrupt increase of the interstitial Li donor impurities following the low temperature treatment (below 557 ^{o}C). At 757 ^{o}C, the I_1(Li) peak completely disappears and only DA pair emission is seen.

In summary, we confirm that the Li-doped ZnSe epilayers (annealed thermally at temperatures above 657 ^{o}C) exhibit a possibility of p-type conversion. We have not measured their electrical properties because of the difficulty of distinguishing them from those of p-type conduction of the GaAs substrate due to Zn atoms diffused from the ZnSe epilayers. We will discuss whether p-type conduction in ZnSe is confirmed by implanting Li^+ ions on ZnSe homoepilayers. Before proceeding to the Li^+ ion implantation, in the next section, we discuss the optimum conditions to realize the p-type conversion of ZnSe by investigating the implantation and annealing conditions in Li^+ ion implantation systematically.

4-1-2. Dependence of ion implantation and annealing conditions on the crystalline quality, radiation damage and activation rate of acceptor level in Li^+-implanted ZnSe heteroepilayer

After reporting the Li^+ ion implantation into ZnSe epilayers and suggesting a possible route to p-type conversion of ZnSe, we will find, in this session, the optimum conditions to realize the p-type conversion by systematically investigating the implantation and annealing conditions.

The purpose of this section is to see the effects of ion implantation conditions (dose density N_d and acceleration energy E_a) on the activation rates of the shallow acceptors as well as

SA center levels, radiation damage and crystalline quality in ZnSe epilayers grown at low temperatures.

ZnSe heteroepilayers were grown on (100)-oriented GaAs substrates at 250 ^{o}C, with a [Se]/[Zn] of 40 and flow rate of DMZ of 11.5×10^{-6} mol/min. The growth period was 1 hour and the resultant epilayer thickness was about 4 μm under these conditions. After the growth, Li^{+} ions were implanted into the epilayers under the conditions listed in Table 4.1.2. The post implant capless-annealing conditions are also described. These were the optimum annealing conditions for E_a and N_d of 50 keV and 10^{14} cm^{-2}, respectively, for Li doping as described in section 4.1.1.

We now discuss the PL property at 300 K. Implanted ions are distributed in the epilayer and the implanted region is damaged. Though the annealing at high temperature could remove the radiation damage efficiently, it ought for a proper understanding to be discussed in detail by characterizing epilayers implanted under various conditions. Figure 4.1.6 shows PL spectra at 300 K of Li-doped heteroepilayers implanted at an E_a of 200 keV with various dose densities. From all epilayers, a strong BE emission (at 460 nm) was observed with little SA emission. A similar result was observed for an as-grown epilayer. The PL spectrum at 300 K in the implanted ZnSe epilayer is suitable to directly estimate the extent of the radiation damage, because the BE-PL intensity reflects the degree of degradation of the crystalline quality (see Fig.4.1.7.; it shows the relation between the BE-PL intensity and FWHM of ZnSe(400) diffraction pattern measured by the double crystal x-ray spectrometer.). It is of primary impor-

tance to examine the relationship between the excitation depth in ZnSe at 300 K of the exciting light with a wavelength of 325 nm and the depth profile of the implanted Li^+ ions.

Figure 4.1.8 shows the calculated depth profiles of Li^+ ions in ZnSe after implantation at a dose density of 10^{14} cm^{-2} for E_a of 10, 50 and 200 keV according to the Lindhard-Scharff-Schiott (LSS) theory. The position of the peak Li concentration is 0.94 μm below the surface at an E_a of 200 keV. It is generally supposed that the heaviest radiation damage by ion implantation occurs around a similar depth in the epilayer.

The photo-excitation depths in PL at 300 K were deduced by investigating the PL spectra from as-implanted epilayers at various acceleration energies. For instance, the PL emission at 300 K in an as-implanted epilayer at an E_a of 50 keV with an N_d of 10^{14} cm^{-2} was not observed at all because of the radiation damage. But it was observed at an E_a of 200 keV. The PL spectrum was similar to that from an as-grown epilayer despite the heavier radiation damage, which was seen in the region of some 0.94 μm below the surface. It is therefore thought that the excitation depth of 325 nm u.v. radiation at 300 K corresponds approximately to the depth of the peak concentration of Li^+ ions implanted at an E_a of 50 keV and the depth is estimated to be about 0.2 μm. Though it was feared that high temperature annealing at 757 ^{o}C might bring radiation damage to propagate deeply into the epilayer, it was confirmed not to occur, since the PL spectrum and the intensity at 300 K of an annealed epilayer were almost the same as those of an as-implanted epilayer.

Figure 4.1.9 shows the PL spectra at 300 K of Li^+-implanted ZnSe heteroepilayers at an E_a of 50 keV with various N_d. The BE-PL intensity from an epilayer annealed at 757 ^oC after being implanted with an N_d of 10^{15} cm^{-2} is very weak. In other words, annealing at 757 ^oC for 1 minute does not completely restores the crystalline quality degraded by radiation damage. On decreasing the dose density, the BE-PL intensity is increased abruptly. It shows that the radiation damage can be removed efficiently by thermal annealing, and the crystalline quality can be fully recovered when the dose density is lower than 10^{15} cm^{-2}. The SA-PL intensity increases dramatically at an N_d of 10^{11} cm^{-2} and becomes stronger than that of an as-grown epilayer. In addition, the PL spectrum coincides with that of an as-grown epilayer treated thermally in the N_2 atmosphere without ion implantation. This suggests that the effect of degradation is due rather to high temperature annealing than to high doping by ion implantation as described in a previous paper [91]. Figure 4.1.10 shows the PL spectra at 300 K of epilayers implanted at an E_a of 10 keV with dose densities of 10^{12} and 10^{14} cm^{-2}. The SA emissions are observed at an N_d of 10^{14} cm^{-2} and the intensity decreases at an N_d of 10^{12} cm^{-2}.

Figure 4.1.11 shows the dependence of the absolute PL intensities of both BE and SA emissions on the dose density. The value of the BE-PL intensity of an as-grown epilayer corresponds to values between 0.5 and 2 in Fig. 4.1.11.

Let us then discuss the PL properties of the epilayers implanted at each acceleration energy. At an E_a of 200 keV, the

crystalline quality of the ZnSe epilayer implanted with an N_d of 10^{15} cm^{-2} is worse than that of an as-grown ZnSe epilayer. This demonstrates that the radiation damage occurs even near the surface (about 0.2 μm) and cannot be fully recovered, though the depth of the heaviest damaged region is about 0.94 μm below the surface and the radiation damage should be substantially smaller at the region near the surface. At an N_d of 10^{12} cm^{-2}, the BE-PL intensity tends to be stronger than that of an as-grown ZnSe epilayer. This is attributed to the degradation of the crystalline quality due to the annealing at high temperature in ion implantation at light dose densities discussed in the case of an N_d of 10^{11} cm^{-2} with an E_a of 50 keV. The overall dependence on N_d at E_a of 200 and 50 keV is reflecting the complex relationship among doping, annealing and crystalline quality. The annealing is effective in the epilayer implanted at an E_a of 50 keV with an N_d of 10^{15} cm^{-2}, and the BE emission begins to be observed, but the PL intensity is still weaker than that in an as-grown epilayer. The degree of recovery of the crystalline quality at an E_a of 50 keV is more directly affected than that at other E_a because the most damaged region at an E_a of 50 keV completely coincides with the region estimated by PL at 300 K as described above. Thus the optimum implanting and annealing conditions, which have been already determined for ZnSe epilayers implanted at an E_a of 50 keV with an N_d of 10^{14} cm^{-2}, are no longer optimum ones for epilayers implanted at an E_a of 50 keV with an N_d of 10^{15} cm^{-2}. Also when the dose density is decreased below 10^{14} cm^{-2} at an E_a of 50 keV, the dependence of

the BE-PL intensity on N_d is almost the same as that of the epilayer implanted at an E_a of 200 keV. This indicates that the annealing removes the radiation damage at E_a of 200 and 50 keV.

At an ion energy of 10 keV, a very different dependence is observed. The BE-PL intensity does not simply depend on the dose density. Two reasons can be considered. Firstly, since the ion implantation depth (45 nm) is much smaller than the PL excitation depth, the degree of removal of the radiation damage through the annealing is not reflected on the estimation by PL measurement. Secondly, it is thought that most of the Li impurities diffuse out of the ZnSe epilayer during the capless-annealing. On this point, it is confirmed from SIMS that about 99 % of the implanted Li impurities (E_a=50 keV, N_d=10^{14} cm^{-2}) diffuse out during the capless-annealing [1]. Moreover, it is supposed that the out-diffusion similarly occurs even when changing the acceleration energy from 10 through 50 to 200 keV. The strong BE-PL intensity shows that the radiation damage does not propagate deeply at an E_a of 10 keV. At the same time, the radiation damage is removed effectively. The fact that the SA emissions are observed slightly at an N_d of 10^{14} cm^{-2} suggests that the region near the surface includes some concentration of SA centers. This can be understood because the peak concentration at 10 KeV is 9 times higher than that at 200 keV with the same dose density (see for example, Fig. 4.1.8.; the Li peak concentration is 1×10^{19} cm^{-3} at 200 keV, while that amounts to 9×10^{19} cm^{-3} at 10 keV under the same 10^{15} cm^{-2}.). The radiation damage caused by an E_a of 10 keV is thus estimated to be about 10 times heavier than that caused by the

bombardment at 200 keV at the same dose density. It is thought that the optimum annealing conditions for an E_a of 200 keV are different from those at 10 keV. One can conclude that the radiation damage does not propagate so deeply into the epilayer by this annealing procedure, though the increase in concentration of the SA centers is slight.

Figures 4.1.12, 13 and 14 show the PL spectra at 77 K of Li-doped ZnSe heteroepilayers implanted at various E_a and N_d. In all Li-doped ZnSe epilayers, the BE and FA emissions are seen at 445 and 460 nm, respectively, with strong intensities. Figure 4.1.15 shows the dependence on the N_d at E_a of 10, 50 and 200 keV for Li^+ ion implantation of the absolute PL intensities of BE, FA and SA emissions. A similar dependence on the dose density for implanted Na^+ ions is also plotted in Fig. 4.1.15. Compared with Fig. 4.1.11., the dependence on N_d is not so pronounced. The reason is probably that the excitation depth for PL at 77 K is deeper than that at 300 K. It is suggested by the fact that PL emission from an as-implanted ZnSe epilayer even at an E_a of 50 keV with an N_d of 10^{15} cm^{-2} is observed at 77 K, but not at 300 K. The excitation depth in PL at 77 K thus seems to be deeper than that at 300 K, and the PL information about the degradation of the implanted region is extended over a wider region including the undamaged region in the epilayer. The PL intensity of Li^+-implanted ZnSe at an N_d of 10^{15} cm^{-2} is definitely lower than that of an as-grown ZnSe. This clearly shows that the effects of radiation damage are also observed by PL at 77 K.

Figures 4.1.16, 17 and 18 show the PL spectra at 4.2 K in the

near band-edge region of Li-doped ZnSe heteroepilayers implanted at various E_a and N_d. At an N_d of 10^{14} and 10^{15} cm^{-2} with an E_a of 200 keV, the $I_1(Li)$ emission is intensely observed at 2.7896 eV and the E_x, I_x and DA(Li) pair emissions are also resolved at 2.7992, 2.7958 and 2.700 eV, respectively. This clearly demonstrates that the epilayers have a high crystalline quality, though the radiation damage in the narrow region of the epilayers is not completely removed as discussed above. Also the I_1^d emission associated with the Zn vacancy is observed at 2.7808 eV. It has been reported [4] that the high temperature annealing generates Zn vacancies. The I_1^d-PL intensity of the epilayer implanted at an N_d of 10^{13} cm^{-2}, however, is stronger than that of an as-grown epilayer annealed at 757 ^{o}C. It shows that the process including both ion implantation and annealing generates more Zn vacancies than annealing alone. The mechanism of forming the acceptor levels is thought to be that the Li impurities introduced by ion implantation are trapped by Zn vacancies generated by the annealing and substitute for Zn sites. This suggestion is reasonably explained by the fact that the I_1^d-PL intensity in the epilayer implanted at an N_d of 10^{13} cm^{-2} is almost the same as that in the epilayer implanted at an N_d of 10^{14} cm^{-2}, while the PL intensity of the $I_1(Li)$ emission in the epilayer implanted at an N_d of 10^{13} cm^{-2} is ten times as weak as that of the epilayer implanted at an N_d of 10^{14} cm^{-2}. The concentration of Zn vacancies generated by annealing alone is not always equal to that of Li^+ ions implanted at the N_d below 10^{13} cm^{-2}. So it is difficult to accept the simple hypothesis stated

above. The effect of the radiation damage must also be considered in discussing the activation rate of the acceptor levels. The PL results suggest that the simple idea is probably all right for the region of N_d between 10^{13} and 10^{14} cm^{-2}. . For N_d greater than 10^{14} cm^{-2}, the absolute PL intensities begin to saturate, indicating that the activation rate of the acceptor levels decreases drastically despite the increase in N_d. It means that the radiation damage decreases the activation of the acceptor levels. Since sharp E_x and I_x emissions are seen even at an N_d of 10^{15} cm^{-2}, it seems that the crystalline quality of the epilayer is maintained very well in spite of the heavy radiation damage. This phenomenon is easily explained from the above discussion of the excitation depth in PL at low temperature.

The sharp emissions (E_x, I_x, I_1(Li)) are broadened and the PL intensity of the DA(Li) pair emission increases abruptly at an N_d of 10^{12} cm^{-2}. This is thought to be the effect of high temperature annealing rather than that of Li doping. It shows that the thermal stability of the Li^+-implanted ZnSe epilayer is a little lower than that of the undoped ZnSe epilayer in spite of the light radiation damage. The annealing conditions (757 ^oC, 1 min.) are not suitable for activating the acceptor levels in the epilayer implanted at an N_d of 10^{12} cm^{-2} and the high temperature annealing degrades the crystalline quality. The optimum annealing temperature would have to be reduced below 757 ^oC for an N_d of 10^{12} cm^{-2}. It is feared that the crystalline quality would be degraded if the same optimum annealing conditions for high N_d are chosen for low N_d.

The peak concentration of Li^+ ions at an E_a of 50 keV is higher than that at 200 keV for the same N_d and the radiation damage is also heavier near the surface. As seen from the structure of the PL spectra of the epilayer implanted with an N_d of $10^{15}cm^{-2}$, the PL intensity of the DA(Li) pair emission is strong. It means that the radiation damage is not removed, or the annealing conditions are no longer optimum conditions. The unknown broad emission appearing at 2.765 eV is frequently observed in epilayers with heavy radiation damage. As N_d is decreased, the I_1(Li) emission disappears and the excitonic emission lines are broadened. It is thought that both ion implantation and annealing process degrade the crystalline quality at a low N_d. In the annealed epilayers implanted at an E_a of 10 keV, the PL intensity of the I_1(Li) emission is weak and those of the E_x and I_x emissions are strong for an N_d of 10^{14} cm^{-2}. From the LSS theory, the peak concentration of Li^+ ions is highest (9x10^{19} cm^{-3} at an N_d of 10^{14} cm^{-2}) and the peak depth is shallowest (45nm) for E_a of 10, 50 and 200KeV. Most of the Li impurities diffuse out of the epilayers during the capless-annealing. At the same time, since the excitation depth in PL is thought to be deep at 4.2 K, the damaged region may not apparently be observed. It also indicates that the radiation damage does not propagate into the epilayer.

In summary, the optimum annealing conditions, which are needed to remove the radiation damage and to activate the acceptor levels without generating SA centers, are dependent on the ion implantation conditions. The effects of the ion implantation

conditions on the crystalline quality of heteroepilayers are examined and subjected to the optimum annealing conditions. The PL emission of the epilayers annealed under the same conditions is affected by changing the ion implantation conditions (E_a and N_d). It is concluded that the crystalline quality of the epilayers is dependent on the combination of their overall treatments, which determine the complex interrelations between the radiation damage by the ion implantation and the activation rate of the acceptor levels, between the radiation damage and the dose density, and between the removal of the radiation damage and the annealing conditions. As N_d changes, the optimum annealing condition for heightening the activation rate and the degree of recovery of radiation damage also change. The depth profile of the implanted ions and the radiation damage is greatly affected by E_a. As a result, it is difficult to define the degree of the radiation damage with a nonuniform depth profile in the epilayer. Moreover, the high-temperature annealing does not lead to the propagation of the radiation damage deep into the epilayers.

It is concluded that Li^+ ion implantation in ZnSe epilayers is hopeful as p-type doping technique. In what follows, we will see the Na^+ ion implantation in the ZnSe epilayers as other p-type doping species. It is known that Na atom has a diffusion coefficient lower than Li atom in ZnSe. It would degrade the characteristics of the ZnSe B-LED because the pn interface is destroyed by the diffusion of Li atoms into n-type ZnSe. In chapter 5, we will also discuss the diffusion of Li atoms into the ZnSe epilayers by actually fabricating the device structure

of a B-LED.

4-2. Na^+ ion implantation into ZnSe epilayer

The Li impurity can form a shallow acceptor levels up to a relatively high concentration of holes (10^{16}-10^{17} cm^{-3}). It is a useful p-type doping species as stated in section 4-1. It is known that Li impurity atoms can diffuse easily even at 280 ^{o}C in ZnSe [107]. Cheng et al. [107] investigated the p-type doping with Na impurity instead of Li impurity by MBE, and confirmed by SIMS that the Na impurity does not diffuse in ZnSe. The high diffusion rate of Li would degrade the electrical properties of the epilayers in forming pn junction in B-LED. If p-type conversion is achieved by Na impurity, it might be expected accordingly, that the Na impurity would have more advantage than the Li impurity. The p-type ZnSe epilayers, however, have not been obtained so far by doping Na impurities and the PL spectra show the presence of a high concentration of SA center levels.

4-2-1. Effect of annealing conditions on crystalline quality of ZnSe heteroepilayer

The purpose of this section is to report the successful Na^+ ion implantation into ZnSe epilayers grown by the atmospheric pressure MOVPE. Furthermore, the optimum annealing conditions after ion implantation have been investigated in order to remove the radiation damage and to form shallow Na acceptor levels efficiently.

ZnSe epilayers were grown on (100) oriented GaAs substrates at 250 ^{o}C. The flow rate of DMZ was 11.5×10^{-6} mol/min., the [Se]/[Zn] was 20, and the growth period was 1 hour. The epilayer thickness was 4 μm under these conditions. After the growth of undoped ZnSe epilayers, Na^{+} ions were implanted at an E_a of 50 keV and with an N_d of 10^{14} cm^{-2}. Then the implanted ZnSe epilayers were annealed at various T_t (451-757 ^{o}C) and t (5 and 30 minutes) in N_2 atmosphere as listed in Table 4.2.1. The effect of the annealing on the crystalline quality of the epilayers grown at 250 ^{o}C has already been discussed in the previous section.

Implanted epilayers were annealed at various T_t for 5 minutes. Figure 4.2.1 shows the dependence on T_t of their PL spectra at 300 K. Almost no PL emissions were observed from the implanted epilayers without post-annealing. BE emission at 300 K began to be observed after annealing at 557 ^{o}C (T_t=557 ^{o}C) for 5 min. This indicates that the radiation damage caused by the ion implantation is gradually removed and the crystalline quality begins to recover at about 550 ^{o}C. As T_t increases, intensities of both BE and SA emissions increase rapidly. In particular, with T_t> 657 ^{o}C, the SA-PL intensity, with its peak at about 600 nm, increases more rapidly than the BE-PL intensity. It is evident that the Na impurity generates SA center levels easily. Figure 4.2.2 shows the dependence of t on the PL property at two different T_t (557 and 657 ^{o}C). At 451 ^{o}C, no emissions are observed at 300 K in spite of increasing t. At 557 ^{o}C, however, with lengthening t, the BE-PL intensity increases without generating SA

center levels. In contrast, at 657 ^{o}C, the SA-PL intensity becomes stronger than the BE-PL intensity with increasing t. These results show that thermal treatments at 557 ^{o}C for 30 minutes, or at 657 ^{o}C for 5 minutes, are suitable conditions for removing the radiation damage generated by the Na^{+} ion implantation. Figure 4.2.3 shows the dependence on T_t of the PL spectra of the implanted epilayers measured at 77 K. With T_t=451 ^{o}C, the BE-PL intensity is very weak, while both FA and SA emissions are observed with strong intensity. As T_t increases from 451 ^{o}C to 557 ^{o}C, the BE- and FA-PL intensities increase abruptly while the SA-PL intensity remains almost constant. After annealing at 657 ^{o}C, the BE-PL intensity becomes stronger than the FA-PL intensity, which indicates that the crystalline quality of the implanted epilayers is restored. That is consistent with the PL results measured at 300 K. The FA-PL intensity saturates after annealing at temperatures higher than 557 ^{o}C, though the BE-PL intensity is still increasing. Figure 4.2.4 shows the dependence on T_t of the absolute intensities of various PL peaks (BE, FA, and SA emissions) measured at 77 K. It clearly shows that the crystalline quality recovers completely at about 650 ^{o}C while the activation rate of Na acceptor levels (the ratio of the concentration of the activated acceptor levels to the implanted Na^{+} ions) saturates at around 550°C. Figure 4.2.5 shows the dependence on t of the PL spectra at 77 K of epilayers annealed at 451 and 557 ^{o}C. After annealing at 451 ^{o}C, the FA-PL intensity increases in the same manner as the BE-PL intensity, which shows that the crystalline quality is recovering and the activation rate of Na acceptor

levels is also increasing at this annealing temperature. However, SA-PL intensity decreases dramatically with increasing t. It is suggested that the remnants of the implanted Na impurities are taken into Zn sites to form the acceptor levels with increasing t, particularly at low T_t (=451 ^{o}C). On the other hand, after annealing at 557 ^{o}C, only the BE-PL intensity increases while the other FA- and SA-PL intensities remain constant. It implies that the activation rate of Na acceptor levels is unchanged with increasing t. From these results, one can conclude that the necessary T_t (557 ^{o}C) of forming Na acceptor levels is lower than that (657 ^{o}C) for recovering the crystalline quality. Figure 4.2.6 shows the PL spectra of Na^+-implanted ZnSe epilayers annealed at 451 and 557 ^{o}C, which are measured near the band-edge region at 4.2 K. Though no PL emissions are observed at 300 K for epilayers annealed at 451 ^{o}C, the PL spectra at 4.2 K show that the dominant peak is the acceptor bound exciton emission line (I_1(Na)) related to the Na acceptor. The I_1(Na) emission is seen at 2.7917-2.7928 eV. This is in good agreement with the value (2.7931 eV) reported by Dean et. al [112]. The reason for the increase of the BE emission observed at 300 K would also be explained by the phenomenon that the I_x-PL intensity becomes stronger as the radiation damage is removed, or the donors inadvertently included in the epilayers are activated.

In summary, the Na doping by ion implantation into MOVPE-grown ZnSe heteroepilayers has been demonstrated and the optimum annealing temperature for forming Na shallow acceptors without generating SA centers has been established to be about 550 ^{o}C. It

is suggested that recovering the crystalline quality from the radiation damage is still continuing at this annealing temperature.

Thus Na^+ ion implantation in ZnSe is more difficult than Li^+ ion implantation because of generating the heavy radiation damage, though Na also forms an shallow acceptor level. SA centers are easily formed by the post-annealing after Na^+ ion implantation and the activation rate of Na acceptor levels is too low compared with that of Li acceptor. The next step is to find the optimum conditions of realizing the p-type conversion by systematically investigating the implantation and annealing conditions in Na^+ ion implantation systematically.

4-2-2. Dependence of ion implantation and annealing conditions on crystalline quality, radiation damage and activation rate of acceptor levels in Na^+-implanted ZnSe

The purpose of this section is to report the effects of Na^+ ion implantation conditions (N_d and N_a) on the activation rates of the shallow acceptors and SA center levels, radiation damage and the crystalline quality in ZnSe epilayers grown at low temperatures. Comparison will also be made with the case of Li^+ ion implantation.

After the growth, Na^+ ions were implanted into the epilayers under the conditions listed in Table 4.2.2. The post implant capless-annealing conditions are given in Table 4.2.2. These are

the optimum annealing conditions for an E_a and N_d of 50 keV and 10^{14} cm^{-2} for Li and Na doping as described in previous sections 4.1 and 4.2. The diffusion rates of Li and Na impurities in ZnSe will also be discussed, as these consist a most important factor in developing the ZnSe B-LED.

Figure 4.2.7 shows the PL spectra at 300 K of Na-doped ZnSe epilayers implanted with N_d of 10^{12} and 10^{14} cm^{-2} at an E_a of 50 keV. The BE emission is not seen at an N_d of 10^{14} cm^{-2}, but unknown broad deep emissions swamping BE and SA emissions are observed with a maximum around 493 nm. Compared with the case of Li^+ ion implantation, SA center levels are very easily generated in Na^+-implanted ZnSe. It is because the radiation damage caused by Na^+ ions degrades the crystalline quality heavily, and it is not recovered even after post-annealing. With Na^+-implanted ions, the annealing temperature of 557 ^oC is insufficient to remove the whole radiation damage. Since the atomic mass of the Na^+ ion (23 a.m.u.) is much heavier than that of Li^+ ion (7 a.m.u.), it is suggested that the radiation damage due to Na^+ ions is heavier than that due to Li^+ ions under the same implantation conditions. The higher generation rate of SA center levels in Na^+ ion implantation is probably related in a complex way to the heavier radiation damage, degradation due to annealing at high temperature and the high concentration of Na impurities. The BE emission is observed in the absence of SA emissions at 10^{12} cm^{-2}. Thus the radiation damage due to Na^+ ions is entirely removed by the annealing at low N_d. The absolute BE-PL intensity is also plotted in Fig. 4.1.11. Figure 4.2.8 shows the depth profile of

Na impurities in Na^+-implanted (E_a=50 keV, $N_d=10^{12}$ cm^{-2} and E_a=50 keV, $N_d=10^{14}$ cm^{-2}) ZnSe calculated using LSS theory. Compared with Li, the implantation depth (65 nm) at the peak concentration ($8.5x10^{18}$ cm^{-3} at an N_d of 10^{14} cm^{-2}) of Na^+ ions is shallower than that (256 nm) in Li.

Figure 4.2.9 shows the PL spectra at 77 K of Na-doped ZnSe epilayers implanted at an E_a of 50 keV with N_d of 10^{12} and 10^{14} cm^{-2}. Though the FA-PL intensity of Na^+-implanted ZnSe at 10^{14} cm^{-2} is seemingly stronger than that at 10^{12} cm^{-2}, the absolute FA-PL intensity is lower because of the heavy damage left in the epilayer. Thus the activation rate of Na acceptor levels at high N_d is much lower than that at low N_d. This strongly suggests that the activation rate of acceptor levels is related to the degree of radiation damage left in the epilayer. Compared with the PL spectra at 300 K (see Fig. 4.2.7.), the concentration of SA centers seems to decrease at 77 K. Considering that the depth of peak concentration of Na impurities is only 65 nm from the surface and the radiation damage by Na^+ ions is heavier than that by Li^+ ions, one can expect that the excitation depth in PL is connected with the degree of radiation damage. Indeed most of the carriers generated by the excitation light recombine in the heavily damaged region before diffusing into the undamaged region.

Figure 4.2.10 shows the PL spectra at 4.2 K of Na-doped epilayers implanted at an E_a of 50 keV with two N_d (10^{12} cm^{-2} and 10^{14} cm^{-2}). Though the total PL intensity of the epilayer implanted with an N_d of 10^{14} cm^{-2} is very weak, the I_x, I_1(Na) and

DA(Na) pair emissions are observed at 2.7962, 2.7919 and 2.681 eV, respectively. The weak PL intensity implies that the effect of radiation damage is still present in the epilayer ever after annealing. On the other hand, at an N_d of 10^{12} cm^{-2}, sharp and intense emissions of E_x at 2.8016 eV, the other donor bound exciton emission lines (I_2) at 2.7993 eV, I_x and I_1(Na) are seen with little DA(Na) pair emission. This indicates that the Na^+-implanted epilayer dose not have much radiation damage and the annealing at 557 ^oC for 5 min is the optimum conditions for Na^+ ion implantation at an E_a of 50 keV with an N_d of 10^{12} cm^{-2}. The next subject will be the diffusion rates of Li and Na impurities in ZnSe. These will be a central problem to develop the ZnSe B-LED.

Figure 4.2.11 shows depth profile (after annealing) of Li^+-implanted (T_t=757 ^oC) and Na^+-implanted (T_t=557 ^oC) (at 50 keV) epilayers measured by SIMS, and PL spectra at 77 K of Li-doped inter-epilayer (10^{14} cm^{-2}, 200 keV; T_t=757 ^oC) at etching depth x. The epilayer thickness is 3.8 μm. It is confirmed that Li diffuses at 757 ^oC and Na at 557 ^oC almost uniformly in ZnSe (each optimum annealing condition). As expected from the SIMS analysis, the FA-PL intensity of Li-doped epilayer is independent of the etching depth except at the surface and interface. Moreover, the FWHM of the FA emission observed in these regions is broader than that observed in other cases. This indicates that diffusing Li impurities would tend to piling themselves up near the surface and interface. Thus, as long as the ion implantation is utilized in ZnSe, it is concluded that the diffusion rate of

Li is not much different from that of Na. It is not certain yet, however, whether it is possible to fabricate B-LED using Li as a p-type dopant, which is well-known to diffuse easily only from the result. The diffusion rate of Li atoms in ZnSe from the viewpoint of device structure will be discussed in detail in chapter 5.

The Na^+ ion implantation degrades the crystalline quality of the ZnSe epilayers heavily by the radiation damage. The radiation damage is much related to N_d. The degradation of the crystalline quality proceeds still more by the annealing, rather than recovery. Though the Na atom forms a shallow acceptor, it also seems to form a concentration of SA centers higher than that of Li. It shows that Li is superior to Na as p-type doping species. Moreover, it is suggested that Li and Na diffuse into the epilayers uniformly after each optimum annealing condition, and as long as ion implantation is utilized in ZnSe, the diffusion rate of Li is not much different from that of Na.

4-3. Li^+ ion implantation into ZnSe homoepilayer

The thermal stability of the ZnSe homoepilayers with high crystalline quality has been discussed and it is found that the annealing temperature of keeping the crystalline quality in the ZnSe homoepilayer should be higher than that in the ZnSe heteroepilayer. It is expected that the ion implantation into the ZnSe homoepilayer is effective of heightening the activation rate

of Li acceptors and the crystalline quality. It is because the annealing temperature of the homoepilayer can be held higher than that of the heteroepilayer.

The objective of this section is to report the ion implantation into the homoepilayers and to try to confirm the p-type conduction of ZnSe. The ZnSe homoepilayers were grown at the following conditions. The growth temperature was 220 ^{o}C, the reactor pressure was an atmospheric pressure, the flow rate of DMZ was 11.5x10^{-6} mol/min., the [Se]/[Zn] was 10 and the growth period was one hour. Under these growth conditions, the epilayer thickness was about 4 μm. After the growth, the homoepilayers were annealed at 700 ^{o}C under H_2 atmosphere for 1 min.

Figure 4.3.1 shows PL spectrum at 300 K of Li-doped ZnSe homoepilayers implanted at an E_a of 50 keV with an N_d of 10^{14} cm^{-2}, which were subjected to post-implant thermal annealing. It shows that BE emission is observed with almost the same intensity as the undoped ZnSe homoepilayer and SA emissions are not seen. The PL property of the Li-doped ZnSe homoepilayer is the same as that of Li-doped ZnSe heteroepilayer. As discussed in section 4-1, the emission related to Li acceptor level is scarcely observed at 300 K. Thus the improvement of the crystallographic quality by the homoepitaxial growth does not always increase activation rate of the acceptor level.

Figure 4.3.2 shows PL spectra at 77 K of Li-doped ZnSe homo- and heteroepilayers implanted at an E_a of 50 keV with an N_d of 10^{14} cm^{-2}, which were subjected to post-implant thermal

annealing. It shows that the concentration of SA centers in the ZnSe homoepilayer is slightly higher than that in the ZnSe heteroepilayer. On the other hand, the FA-PL intensity of the ZnSe homoepilayer is slightly weaker than that of the ZnSe heteroepilayer. It indicates that the concentration of Li acceptor levels is lower than that in the ZnSe heteroepilayer. Namely, the activation rate of acceptor levels is low and the generation rate of SA centers is a little high in the ZnSe homoepilayer despite the improved crystallographic property due to lattice matching. We have seen in section 3-2 that the ZnSe homoepilayer was not degraded by the annealing at 700 ^{o}C for 5 min., so that the SA centers were not generated only by the annealing. It is feared that some native defects (probably, Zn vacancies) would be generated by ion implantation and they produce SA centers. It is suggested as a reason why native defects are created by ion implantation that the crystalline quality is too excellent in homoepilayers. Be what as it may, the heteroepilayer seems to be superior to the homoepilayer, so long as the ion implantation is taken as p-type doping technique. Figure 4.3.3 shows PL spectra at 4.2 K near the band-edge region of Li-doped ZnSe homoepilayers implanted at an E_a of 50 keV with an N_d of 10^{14} cm^{-2}, which were subjected to post-implant thermal annealing. The sharp E_x and I_1(Li) emission lines are observed with strong intensities. It seems that the crystalline quality is highly maintained and Li shallow acceptors are formed. Moreover, I_1^{deep} is also observed. It is understood that Zn vacancies are generated by the thermal annealing as described in section 3-2,

not by the ion implantation. It will be difficult to repress the generation of Zn vacancies in the process including thermal annealing in the homoepitaxial growth. It is suggested that the high generation rate of Zn vacancies is much related to that of SA centers as discussed above.

Also we also try to confirm the p-type conversion by measuring the Hall effect of the Li^+-implanted homoepilayers, as expected in section 4-1. The p-type conversion, however, is not confirmed at present because the electric current does not flow between the Au electrodes deposited by evaporation. Since it is doubtful whether the Li-implanted epilayer really has p-type conductivity or whether Au is truly suitable as an electrode material for p-type ZnSe, the eventual accreditation of the p-type ZnSe is still very difficult.

We shall compare the vapor phase with the ion implantation in iodine-doped ZnSe epilayers from the doping technique in the next section. The I (iodine) impurity is indeed convenient to control the n-type conduction, easily by both doping techniques.

4-4. Comparison of doping technique between vapor phase and ion implantation into ZnSe epilayer

Ion implantation generates the radiation damage and the nonuniformity of the implanted impurities in the epilayer as described in sections 4-1, 2 an 3. The distributions of radiation damage and the implanted impurities cause the depth profile of

crystalline quality in the epilayer. It is difficult to estimate the crystalline quality in the epilayer. Also, since it is very difficult to estimate the activation rate of the acceptor levels in p-type ZnSe independently of the doping techniques, we will dope I (iodine) donor species as monitoring the activation rate of donor levels into ZnSe epilayers by two kind of techniques (the vapor phase and ion implantation). The vapor phase will be compared with the ion implantation for doping technique, and the close relations between activation rate of the I impurity, crystalline quality and radiation damage in the ZnSe epilayer will be discussed in this section. Moreover, by investigating n-type doping, we will try to find a clue to the control of the electrical properties by ion implantation as a p-type doping technique in ZnSe.

ZnSe epilayers were grown on the (100) oriented GaAs substrates at 250 ^{o}C and 20 of [Se]/[Zn]. The I^{+} ions are implanted at 50 keV and 10^{12}-10^{13} cm^{-2}. The epilayer thickness was 4μm. The post-annealing conditions were that T_t was 400-600 ^{o}C and the t was 5-30 min. The n-type ZnSe epilayers were made by mixing n-buthyliodine (n-BuI;C_4H_9I) in H_2Se flow gas during the epitaxial growth. The n-type carrier concentration was 10^{18} cm^{-3} in an I-doped ZnSe grown by the vapor phase.

Figure 4.4.1 shows the depth profile of I atoms of the I^{+}-implanted (50 keV, 10^{13} cm^{-2}) ZnSe calculated by LSS theory before the annealing. The I-doped ZnSe epilayer implanted under the above conditions has a peak concentration of 4.1×10^{18} cm^{-3} at the depth of 18 nm from the surface. If the I^{+}-implanted ZnSe epilay-

er is annealed, the I impurities would be redistributed uniformly in the epilayer. It is so expected from the uniform depth profile of Li and Na impurities in the implanted ZnSe epilayers after post-annealing. Presuming that the I impurities are uniform in the epilayer, the concentration of I atoms is estimated to be 5×10^{17} cm^{-3}.

Figure 4.4.2 shows the PL spectrum at 77 K of the I^+-implanted (50 keV, 10^{13} cm^{-2}) ZnSe heteroepilayer after the post-annealing (600 ^{O}C, 5 min.). The SA emissions except BE emission are observed, indicating that the epilayer is damaged by I^+ ion implantation.

Figure 4.4.3 shows the PL spectra at 300 K of the I^+-implanted (50 keV, 10^{12} cm^{-2}) ZnSe heteroepilayer after various post-annealing (400-600 ^{O}C, 30 min.). Both PL spectra and intensities of I-doped ZnSe epilayers are unchanged by T_t. The BE-PL intensity is about 40 times as strong as that of an undoped ZnSe epilayer. The I impurity forms an excellent donor level in ZnSe without generating SA center levels. The radiation damage is much lighter in the implantation and annealing conditions (N_d (10^{12} cm^{-2}), E_a (50 keV), T_t (400-600 ^{O}C) and t (30 min.)). The crystalline quality of I^+-implanted ZnSe epilayers is not degraded even at the annealing temperature of 600 ^{O}C

Figure 4.4.4 shows the PL spectra at 77 K of the I^+-implanted (50 keV, 10^{12} cm^{-2}) ZnSe epilayer after various post-annealing (400-600 ^{O}C, 30 min.). For low N_d, the BE emission is observed with strong intensity while the SA-PL intensity is weaker than that of the ZnSe epilayers implanted with I^+ ions at

a high N_d (10^{13} cm^{-2}; Fig.4.4.2.). It is showing that the concentration of the generated SA centers is related to the radiation damage. As T_t increases, the PL intensity of the emission appearing at 2.699 eV increases. The origin of the emission is probably related to As impurity diffusing from the GaAs substrate in the annealing process.

Figure 4.4.5 shows the PL spectra at 4.2 K near the band-edge region of the I^+-implanted (50 keV, 10^{12} cm^{-2}) ZnSe epilayer after various post-annealing (400-600 ^{o}C, 30 min.). All the epilayers have sharp and strong excitonic emission lines (E_x and I_2 at 2.797 eV). One can thus see that a high crystalline quality is maintained. The I_2 emission is thought to be donor bound exciton emission line due to iodine donor level. As T_t increases, the PL intensity of the emission at 2.791 eV increases. It is probably thought to be I_1(As) due to As acceptor diffusing from the GaAs substrate as shown in Fig.4.4.4. The $I_1{}^d$ emission with strong intensity is observed after annealing at a T_t of 500 ^{o}C. Zn vacancies are probably generated by the annealing.

Figure 4.4.6 shows the PL spectra at 300 K of the I^+-implanted (50 keV, 10^{12} cm^{-2}) ZnSe epilayer after a post-annealing (500 ^{o}C, 30 min.) and of a ZnSe epilayer doped through the vapor phase. The BE-PL intensity of the ZnSe epilayer doped by ion implantation is about ten times as weak as that of the ZnSe epilayer doped through the vapor phase (n=1x10^{18} cm^{-3}). The carrier concentration of the ZnSe epilayer doped by ion implantation is estimated to be about 10^{17} cm^{-3}. This concentration coincides well with the values (the peak concentration of I atoms

is 4.1×10^{17} cm^{-3} and the average concentration is about 5×10^{16} cm^{-3}.) expected from the depth profile of I atoms in ZnSe.

Figure 4.4.7 shows the PL spectra at 4.2 K near the band-edge region of the I^+-implanted (50 KeV, 10^{12} cm^{-2}) ZnSe epilayer after a post-annealing (500 ^oC, 30 min.) and of a ZnSe epilayer doped through the vapor phase. In the ZnSe epilayer doped through the vapor phase, the I_2 emission is broad. It is therefore showing that the epilayer is highly doped by I impurities. On the other hand, the crystalline quality of the ZnSe epilayer doped by ion implantation seems to be maintained high, since the generation rate of SA centers is suppressed and the doping level is low as expected. By taking care of the radiation damage, it is thus concluded that the activation rate of I donors in ZnSe doped by ion implantation is as high as that in ZnSe doped through the vapor phase.

It is strongly suggested, accordingly, that the ion implantation as p-type doping technique in ZnSe will be hopeful if the radiation damage is removed.

Table 4.1.1. Thermal annealing conditions.

Type	Temperature (°C)	Atmosphere	Flow rate (ℓ/min.)	Period (min.)
A		No annealing		
B	451	N_2	4.0	5
C	557	N_2	4.0	5
D	657	N_2	4.0	5
E	757	N_2	4.0	5

Table 4.1.2. Ion implantation and annealing conditions.

	Ion implantation conditions			Annealing conditions		
No.	Species	Acceleration energy E_a (keV)	Dose density N_d (cm^{-2})	Atmosphere	Temperature (°C)	Period (min.)
1	Li	200	10^{12}	N_2	757	1
2	Li	200	10^{13}	N_2	757	1
3	Li	200	10^{14}	N_2	757	1
4	Li	200	10^{15}	N_2	757	1
5	Li	50	10^{11}	N_2	757	1
6	Li	50	10^{12}	N_2	757	1
7	Li	50	10^{13}	N_2	757	1
8	Li	50	10^{14}	N_2	757	1
9	Li	50	10^{15}	N_2	757	1
10	Li	10	10^{12}	N_2	757	1
11	Li	10	10^{14}	N_2	757	1

Table 4.2.1. Thermal annealing conditions.

Temperature (°C)	Atmosphere	Flow rate (ℓ/min.)	Period (min.)
451	N_2	4.0	5
451	N_2	4.0	30
557	N_2	4.0	5
557	N_2	4.0	30
657	N_2	4.0	5
657	N_2	4.0	30
757	N_2	4.0	5

Table 4.2.2. Ion implantation and annealing conditions.

Ion implantation conditions				Annealing conditions		
No.	Species	Acceleration energy E_a (keV)	Dose density N_d (cm^{-2})	Atmosphere	Temperature (°C)	Period (min.)
12	Na	50	10^{12}	N_2	557	5
13	Na	50	10^{14}	N_2	557	5

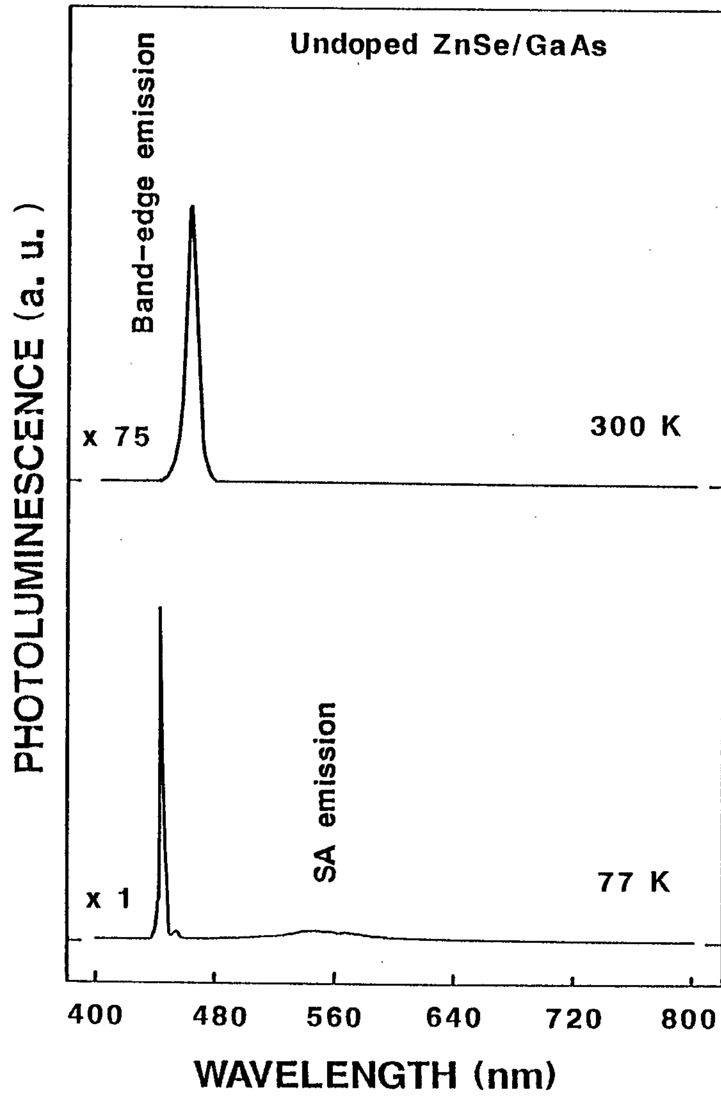

Fig.4.1.1. PL spectra of an as-grown ZnSe heteroepilayer without ion implantation measured at 300 and 77 K.

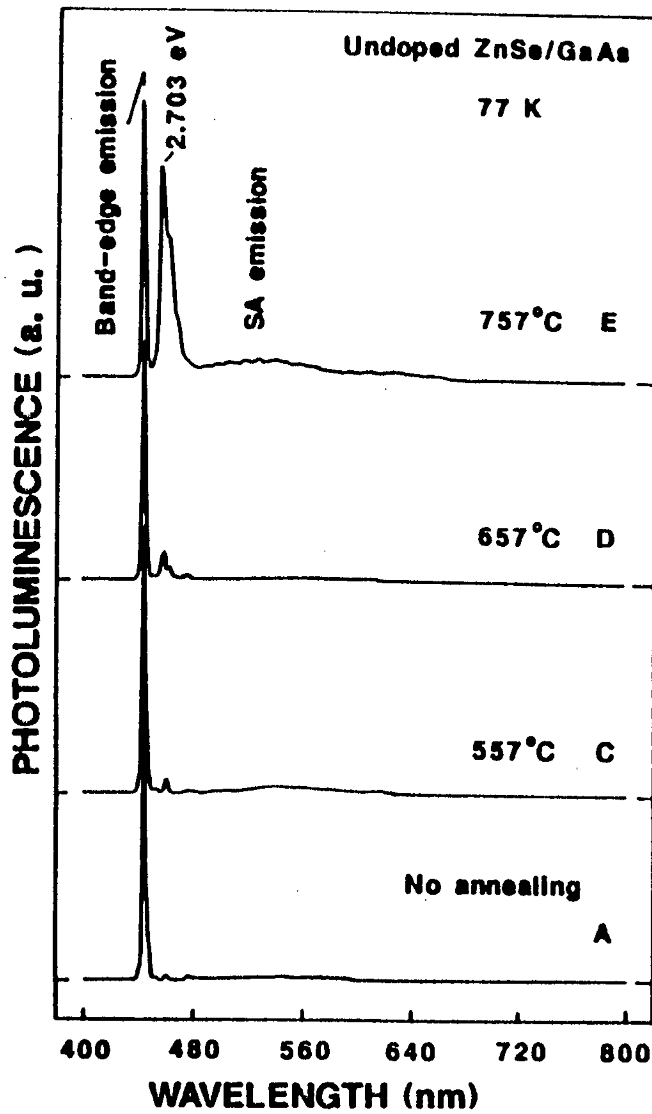

Fig.4.1.2. PL spectra at 77 K of ZnSe heteroepilayers annealed at various temperatures without ion implantation.

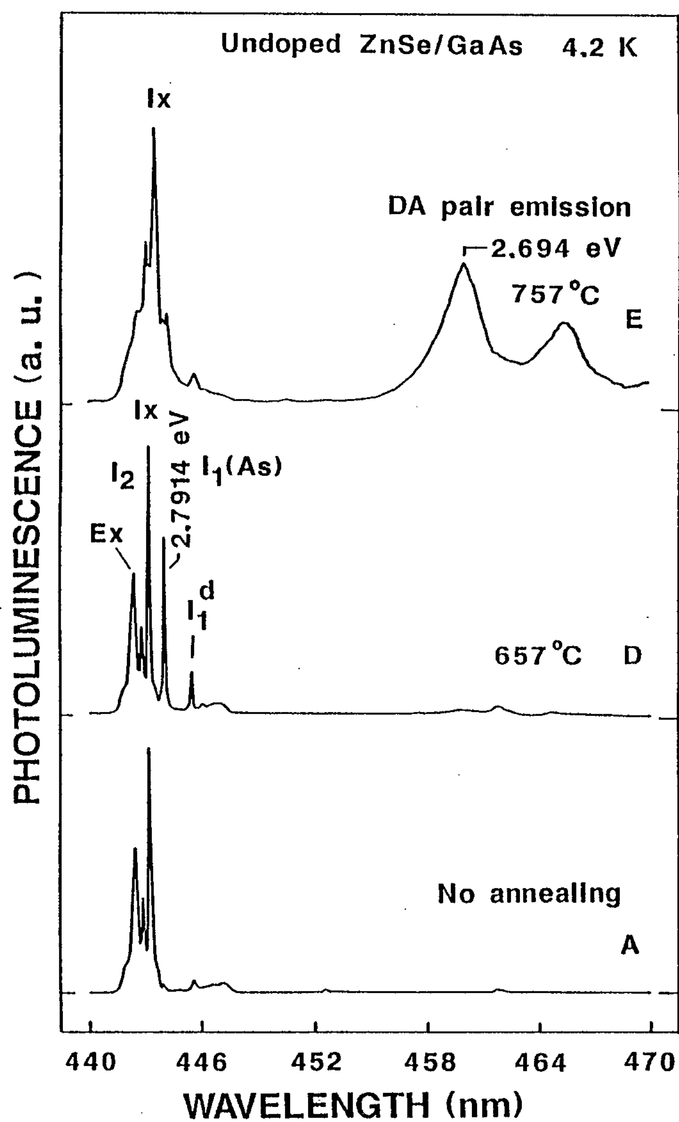

Fig.4.1.3. PL spectra (near the band-edge region) at 4.2 K of ZnSe heteroepilayers annealed at various temperatures without ion implantation.

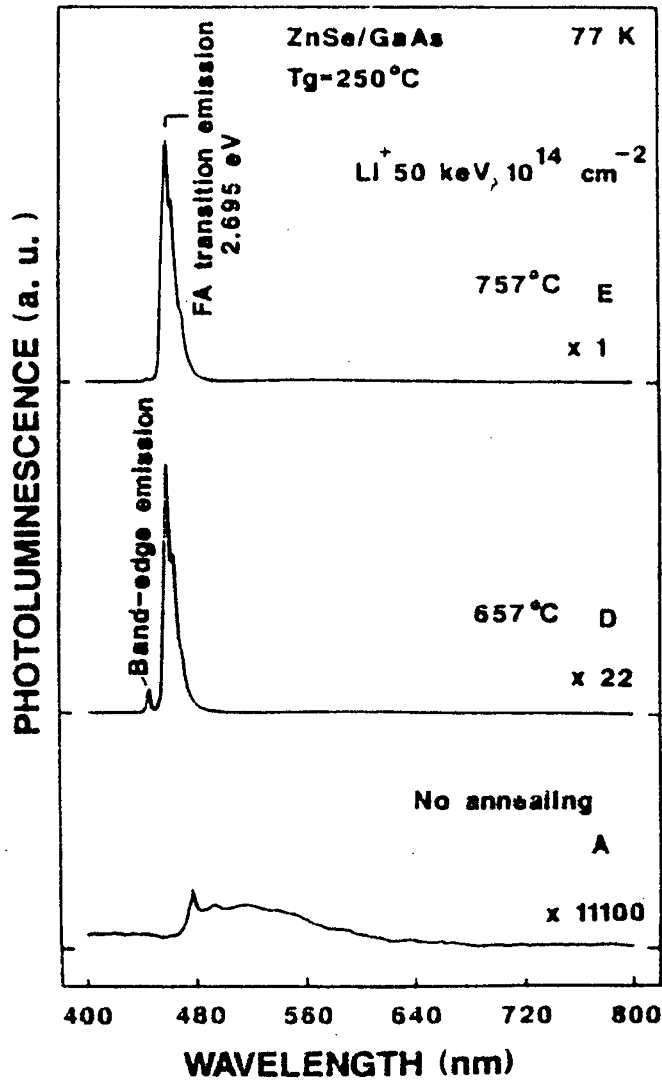

Fig. 4.1.4. PL spectra at 77 K of ZnSe epilayers annealed at various temperatures after ion implantation.

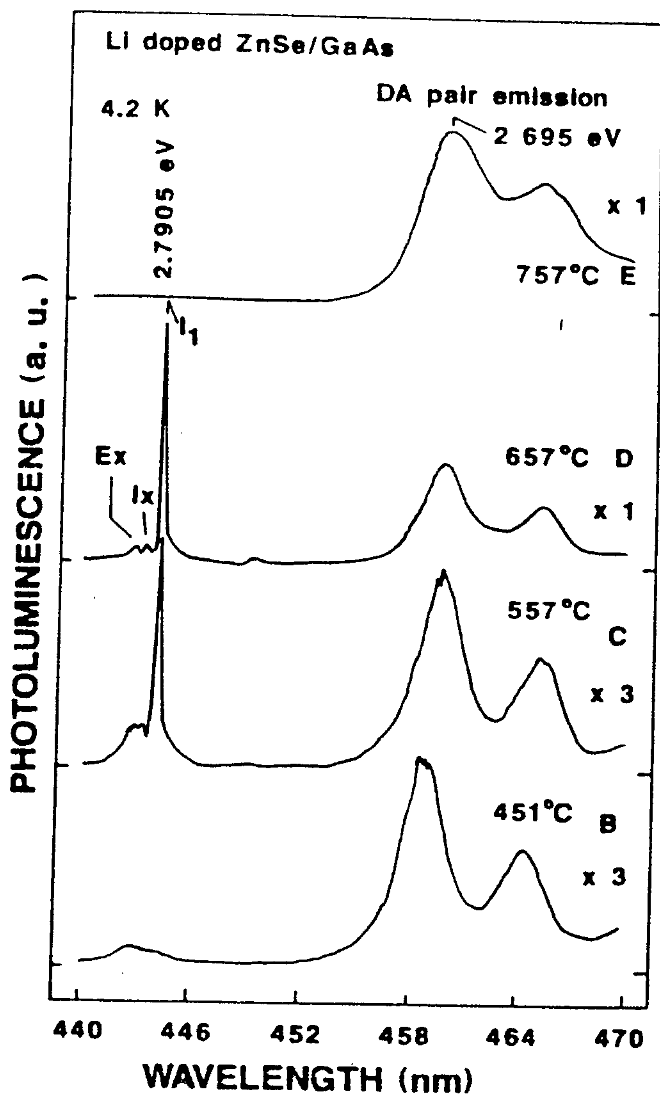

Fig.4.1.5. PL spectra at 4.2 K of ZnSe heteroepilayers annealed at various temperatures after ion implantation.

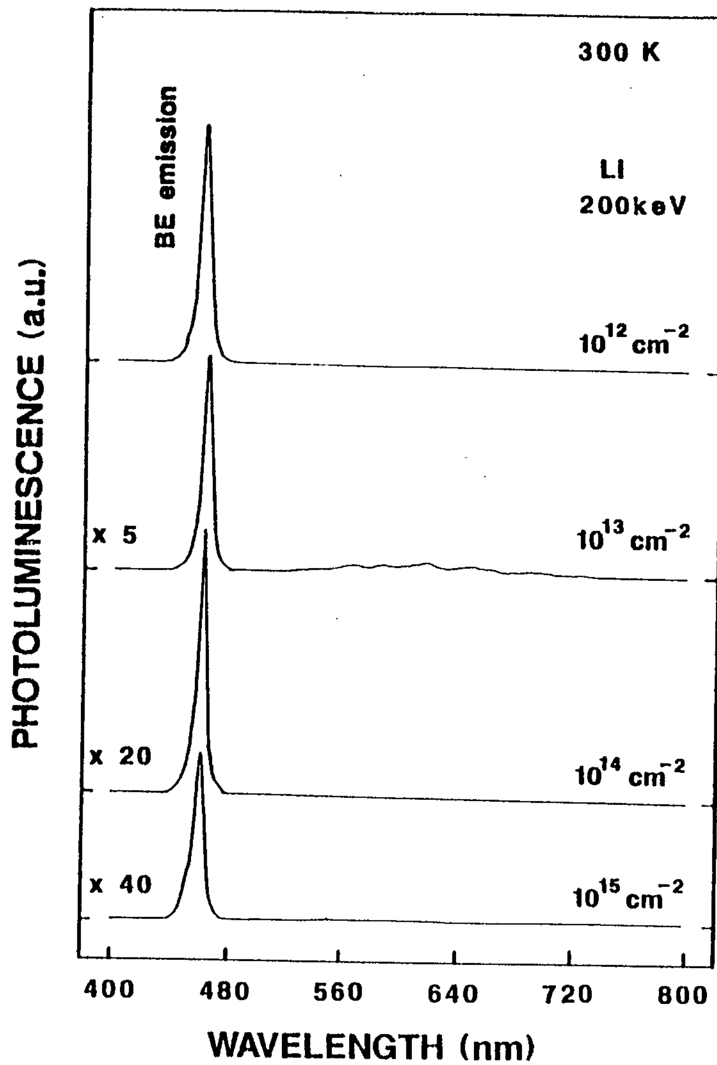

Fig.4.1.6. PL spectra at 300 K of Li-doped ZnSe heteroepilayers implanted at an E_a of 200 keV with various N_d (10^{12}-10^{15} cm^{-2}), which were subjected to post-implant thermal annealing.

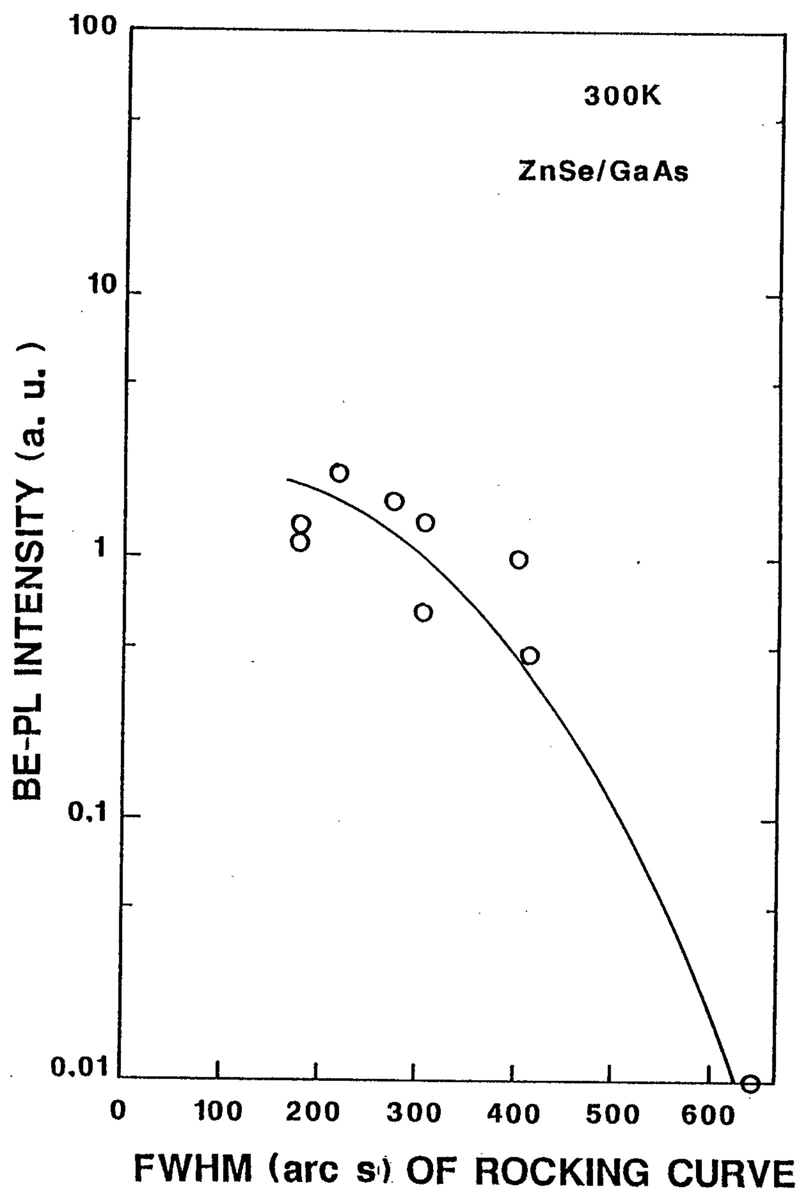

Fig.4.1.7. Relation between the BE-PL intensity and FWHM of ZnSe(400) diffraction pattern measured by the double crystal x-ray spectrometer.

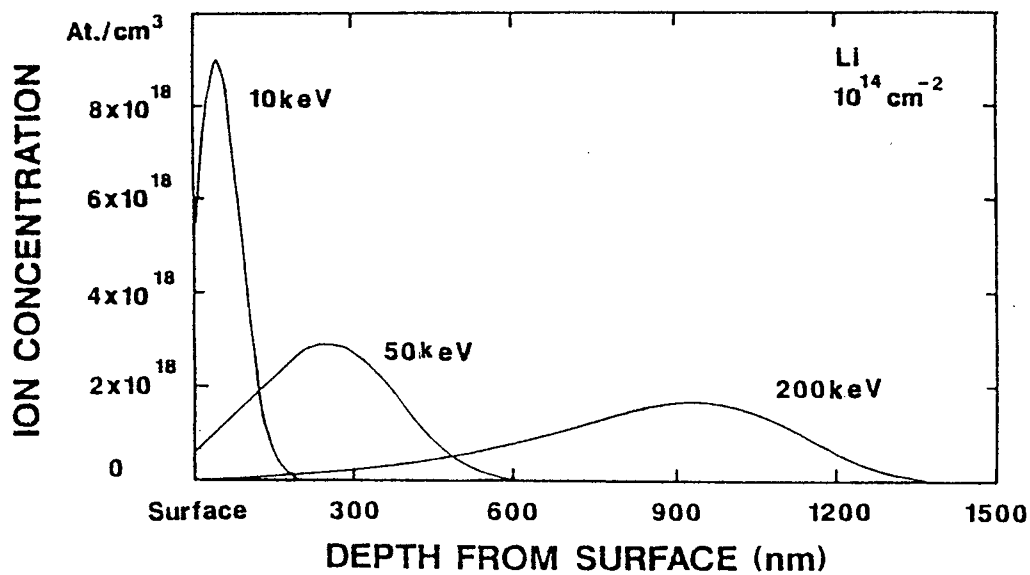

Fig.4.1.8. Calculation result of depth profile of Li impurities in ZnSe epilayers without annealing after Li^+ ion implantation with an N_d of 10^{14} cm^{-2} at E_a of 10, 50 and 200 keV according to LSS theory.

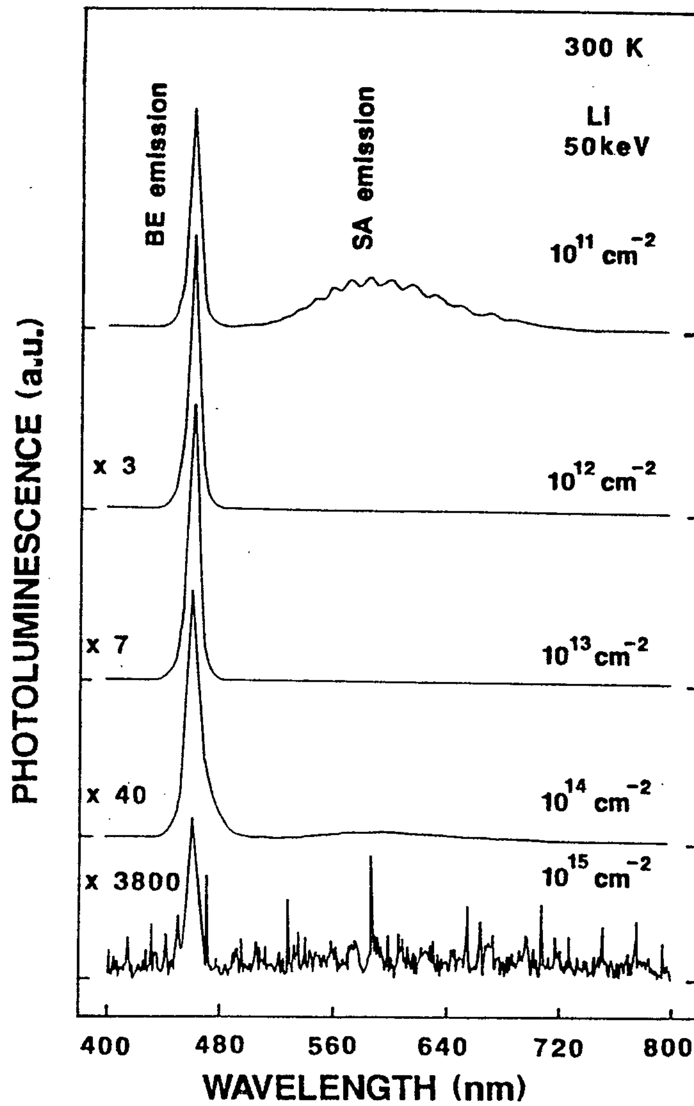

Fig.4.1.9. PL spectra at 300 K of Li-doped ZnSe heteroepilayers implanted at an E_a of 50 keV with various N_d (10^{11}-10^{15} cm^{-2}), which were subjected to post-implant annealing.

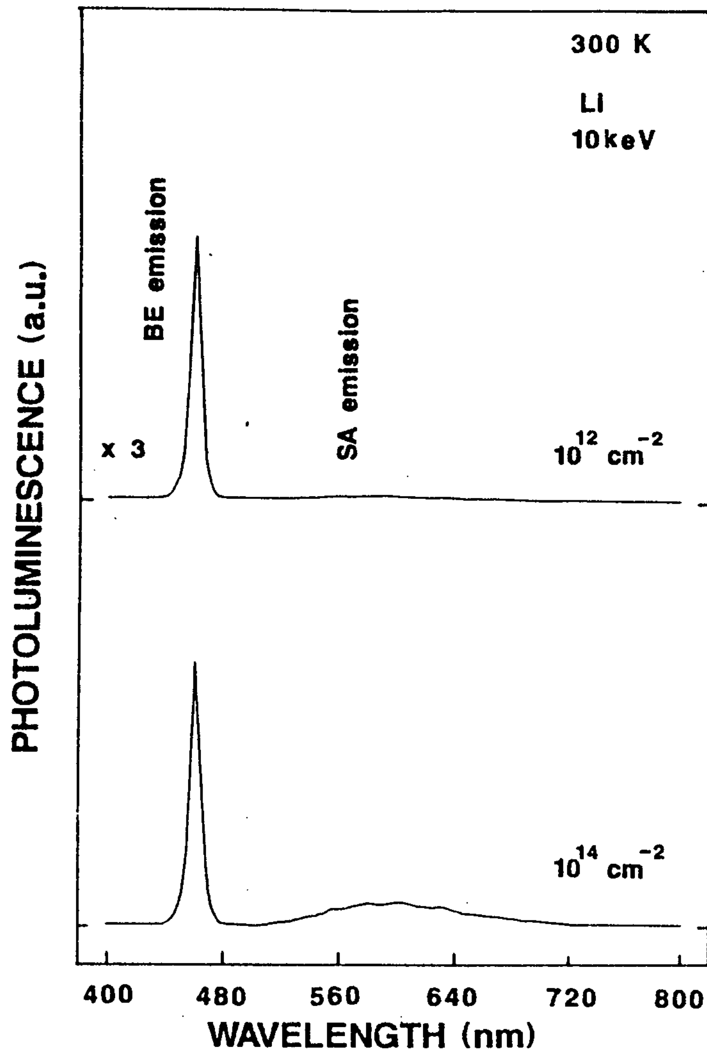

Fig.4.1.10. PL spectra at 300 K of Li-doped ZnSe heteroepilayers implanted at an E_a of 10 keV with various N_d (10^{12}, 10^{14} cm^{-2}), which were subjected to post-implant annealing.

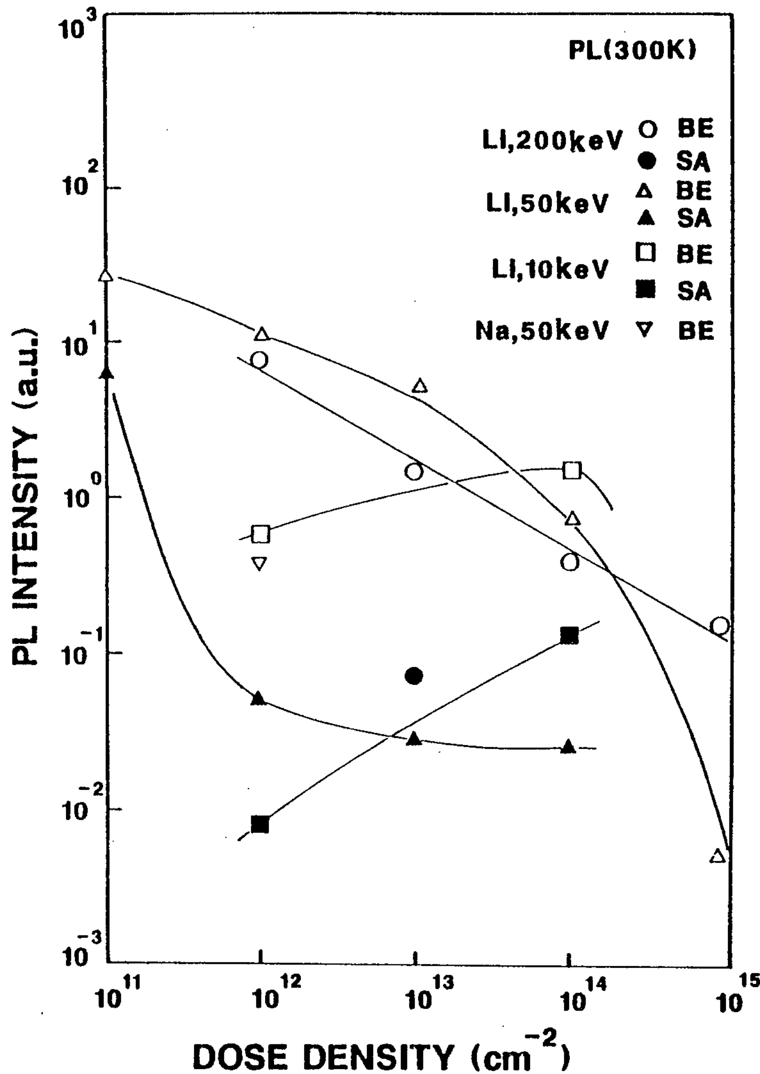

Fig.4.1.11. Dependence of N_d on the absolute PL intensities at 300 K of both BE and SA emissions in Li^+- and Na^+-implanted epilayers, which were subjected to post-implant thermal annealing.

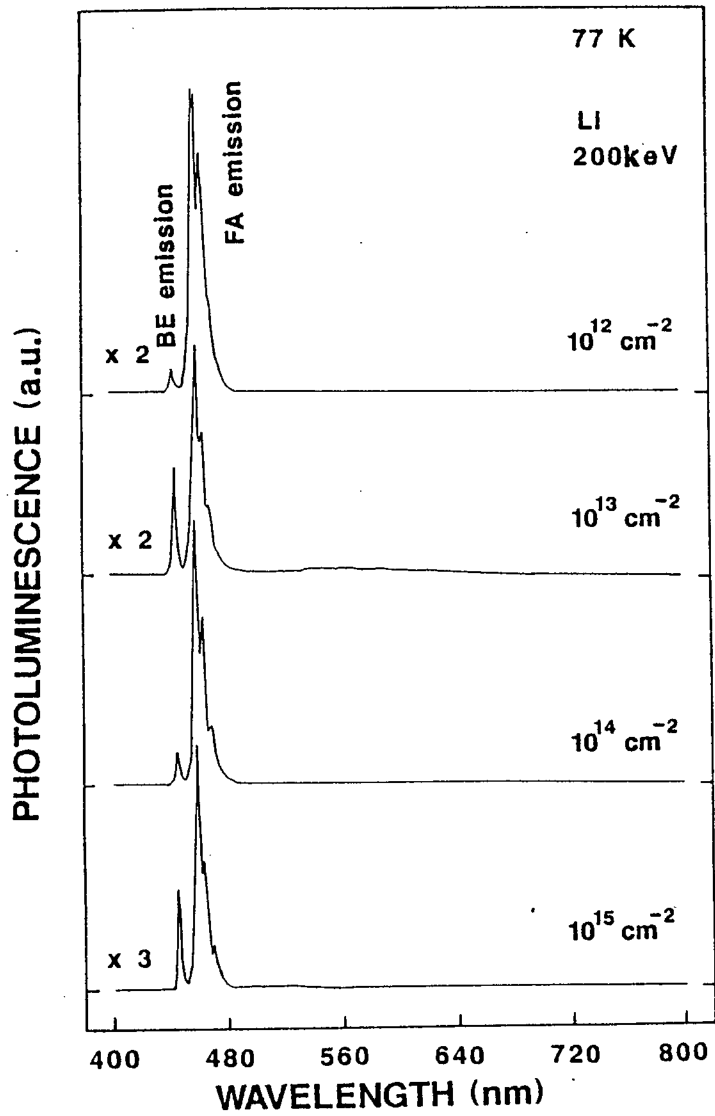

Fig.4.1.12. PL spectra at 77 K of Li-doped ZnSe heteroepilayers implanted at an E_a of 200 keV with various N_d (10^{12}-10^{15} cm^{-2}), which were subjected to post-implant thermal annealing.

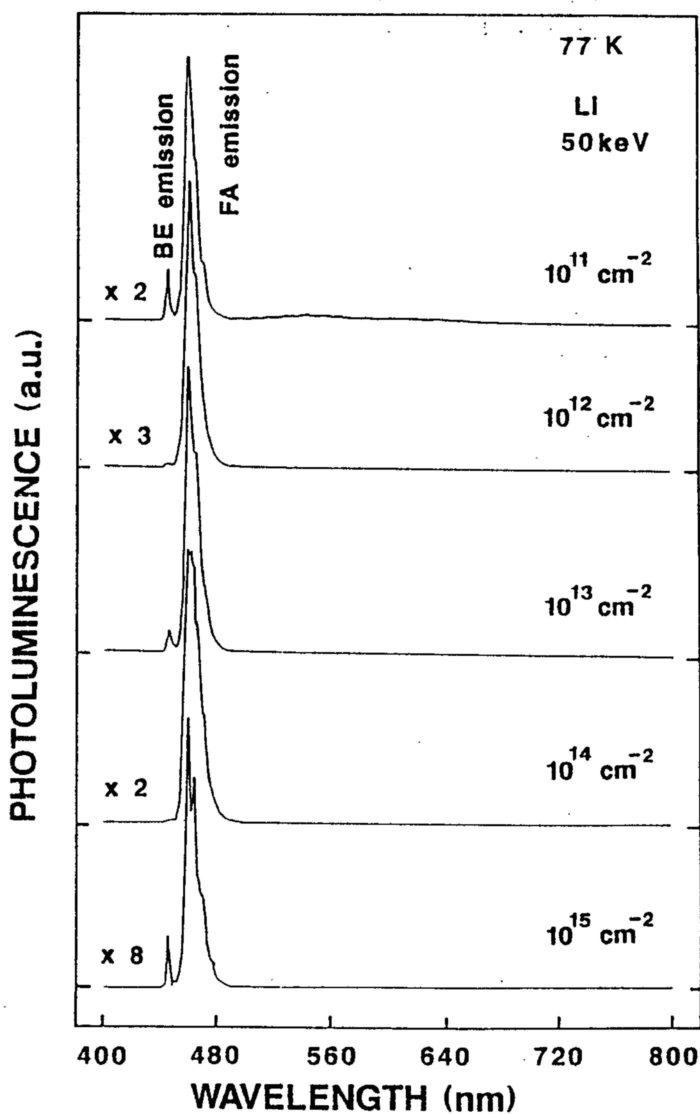

Fig.4.1.13. PL spectra at 77 K of Li-doped ZnSe heteroepilayers implanted at an E_a of 50 keV with various N_d (10^{11}-10^{15} cm^{-2}), which were subjected to post-implant annealing.

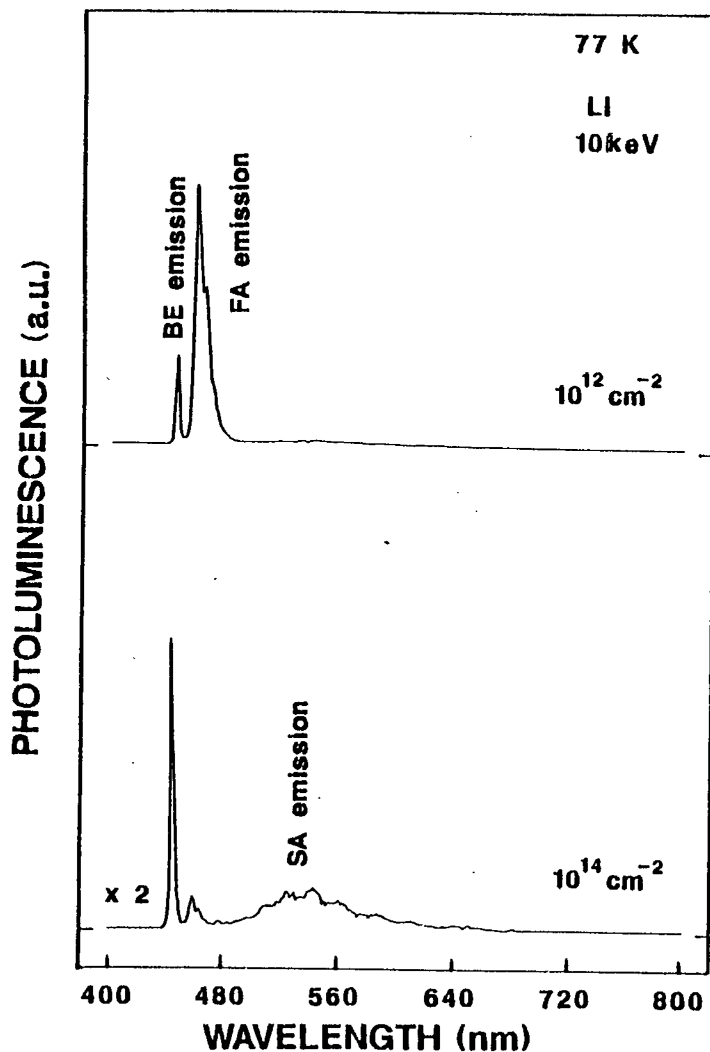

Fig.4.1.14. PL spectra at 77 K of Li-doped ZnSe heteroepilayers implanted at an E_a of 10 keV with various N_d (10^{12}, 10^{14} cm^{-2}), which were subjected to post-implant annealing.

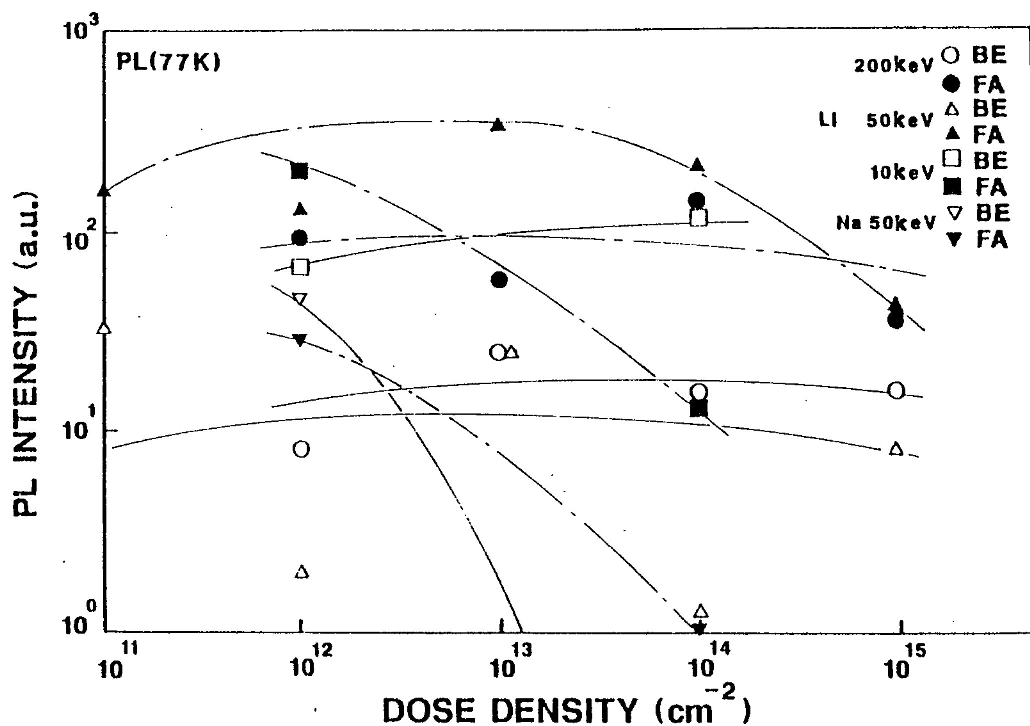

Fig.4.1.15. Dependence of N_d at E_a of 10, 50 and 200 keV on the absolute PL intensities of BE, FA and SA emissions in Li^+-implanted epilayers, which were subjected to post-implant thermal annealing. Also the dependence of N_d in Na^+ ion implantation is shown in the figure.

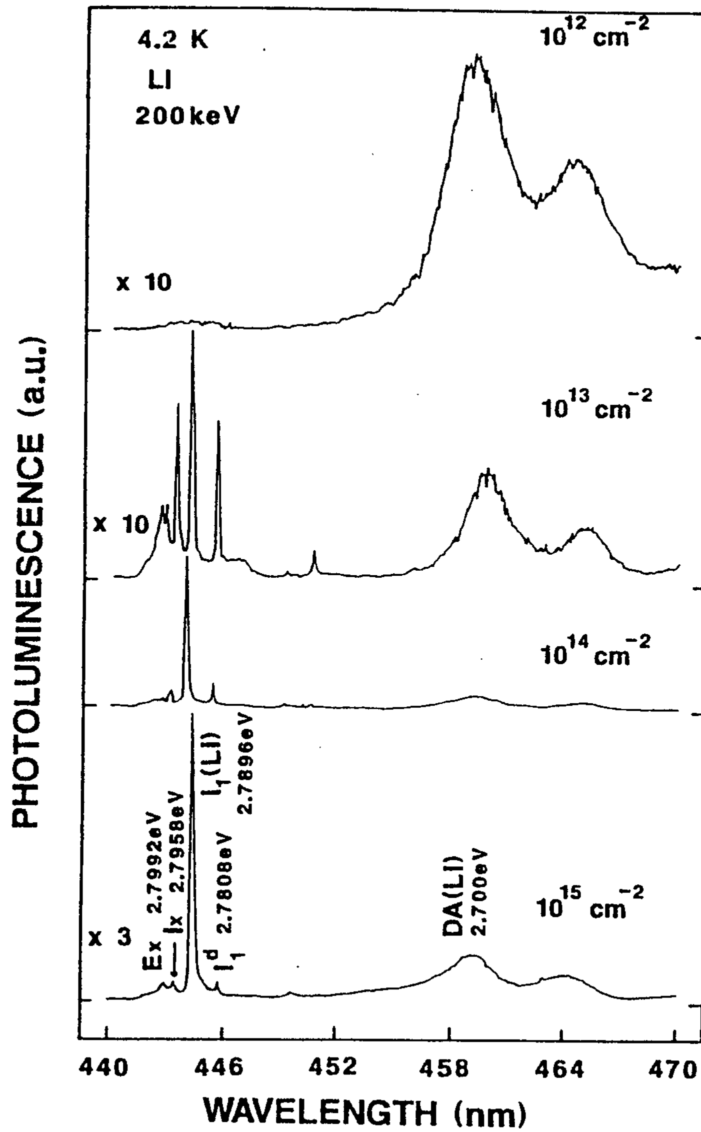

Fig.4.1.16. PL spectra at 4.2 K of Li-doped ZnSe heteroepilayers implanted at an E_a of 200 keV with various N_d (10^{12}-10^{15} cm^{-2}), which were subjected to post-implant thermal annealing.

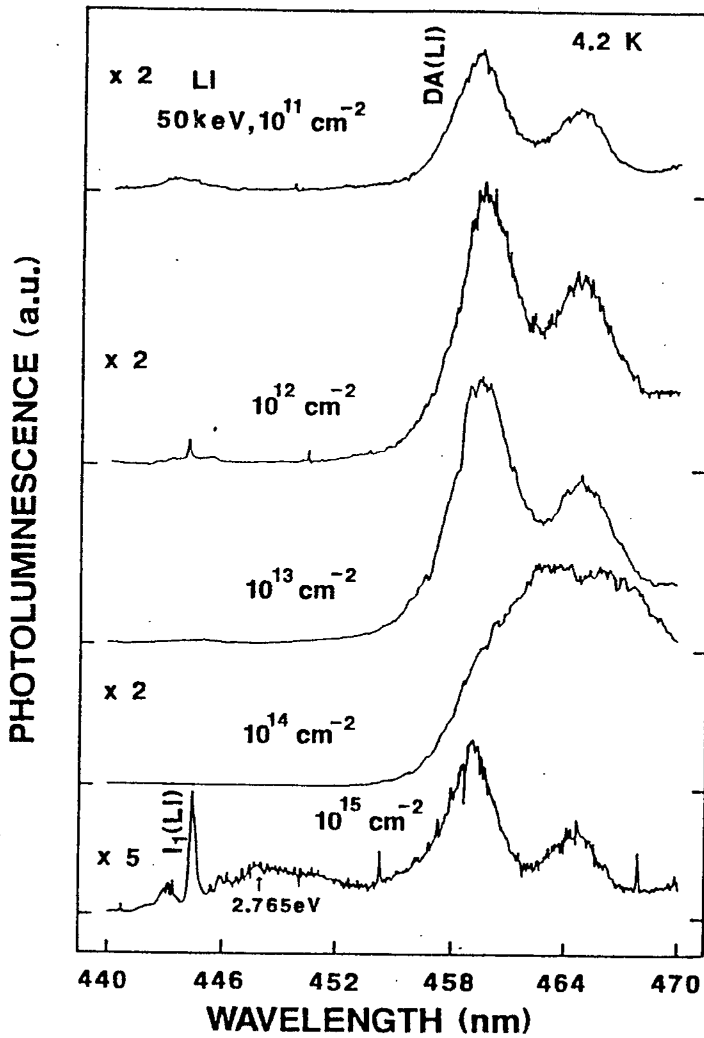

Fig.4.1.17. PL spectra at 4.2 K of Li-doped ZnSe heteroepilayers implanted at an E_a of 50 keV with various N_d (10^{11}-10^{15} cm^{-2}), which were subjected to post-implant annealing.

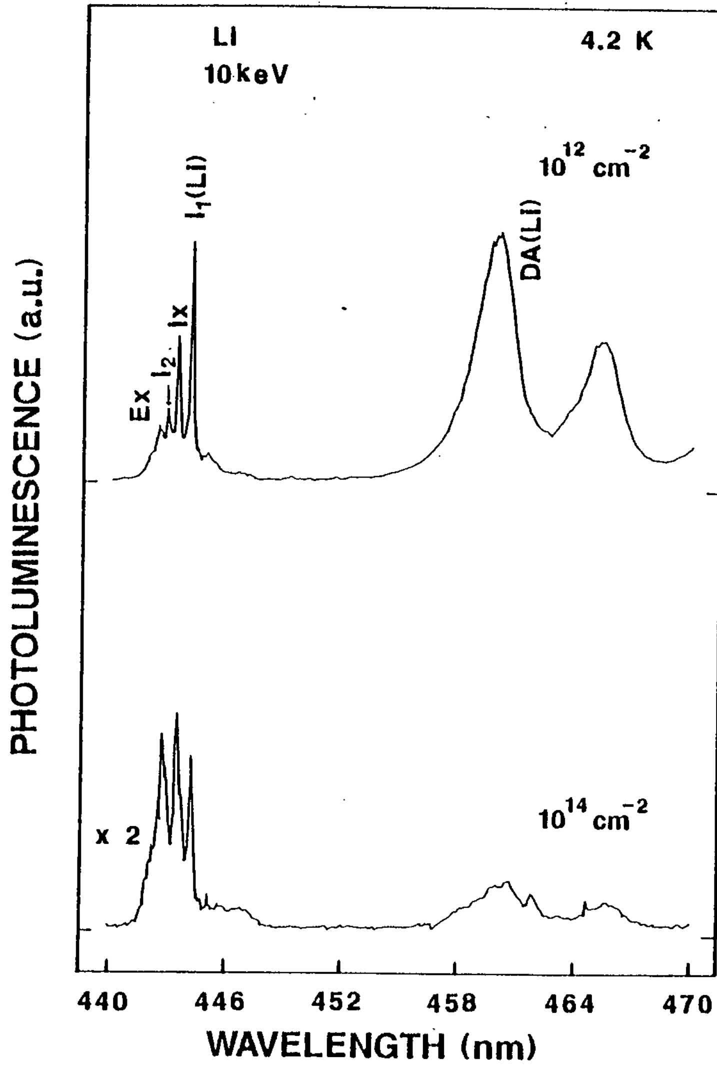

Fig.4.1.18. PL spectra at 4.2 K of Li-doped ZnSe heteroepilayers implanted at an E_a of 10 keV with various N_d (10^{12}, 10^{14} cm^{-2}), which were subjected to post-implant annealing.

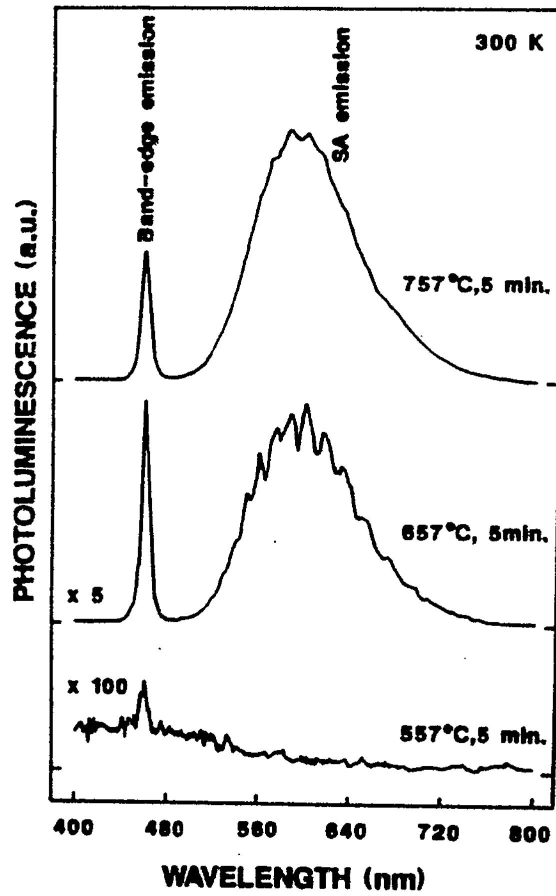

Fig.4.2.1. Dependence on T_t of the PL spectra at 300 K.

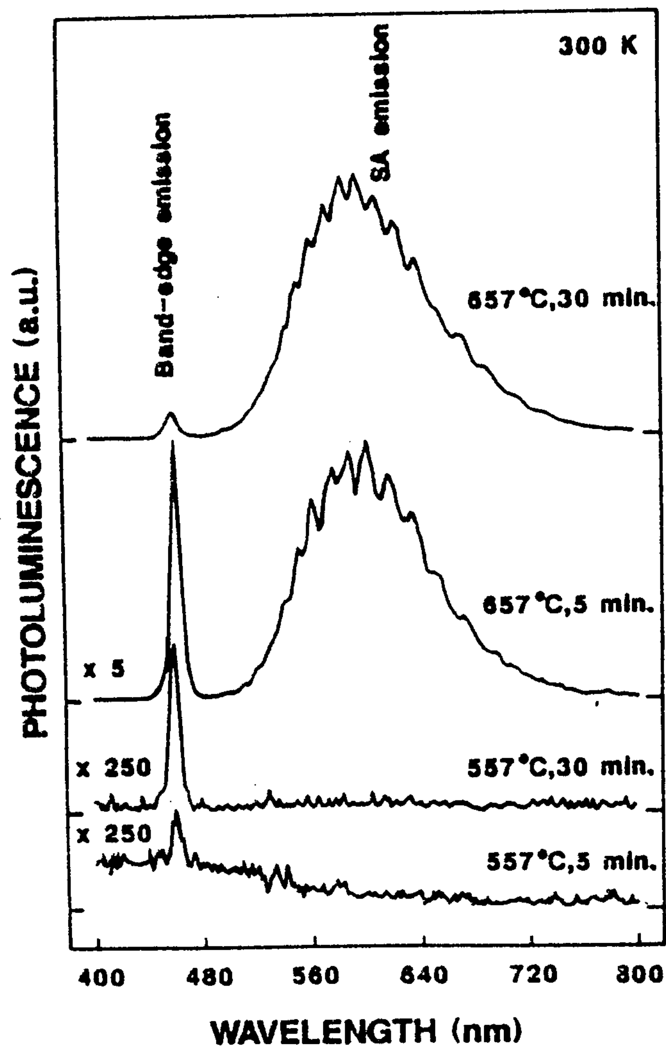

Fig.4.2.2. Dependence of the PL spectra at 300 K on t of the annealed at two different T_t (557 and 657 ^{o}C).

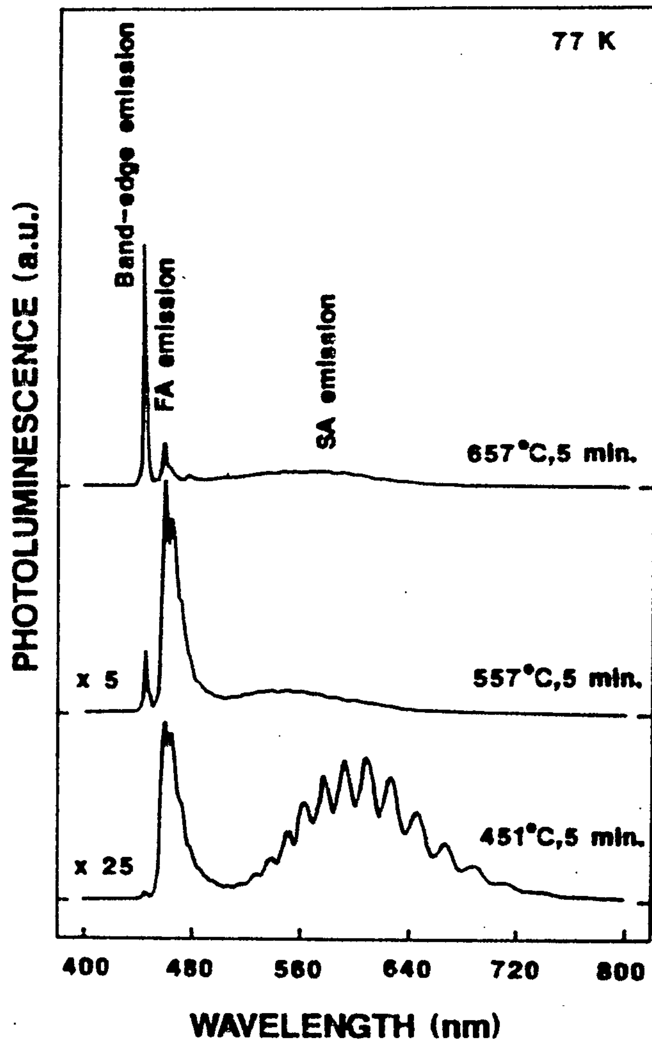

Fig.4.2.3. Dependence on T_t of the PL spectra of Na^+-implanted epilayers measured at 77 K.

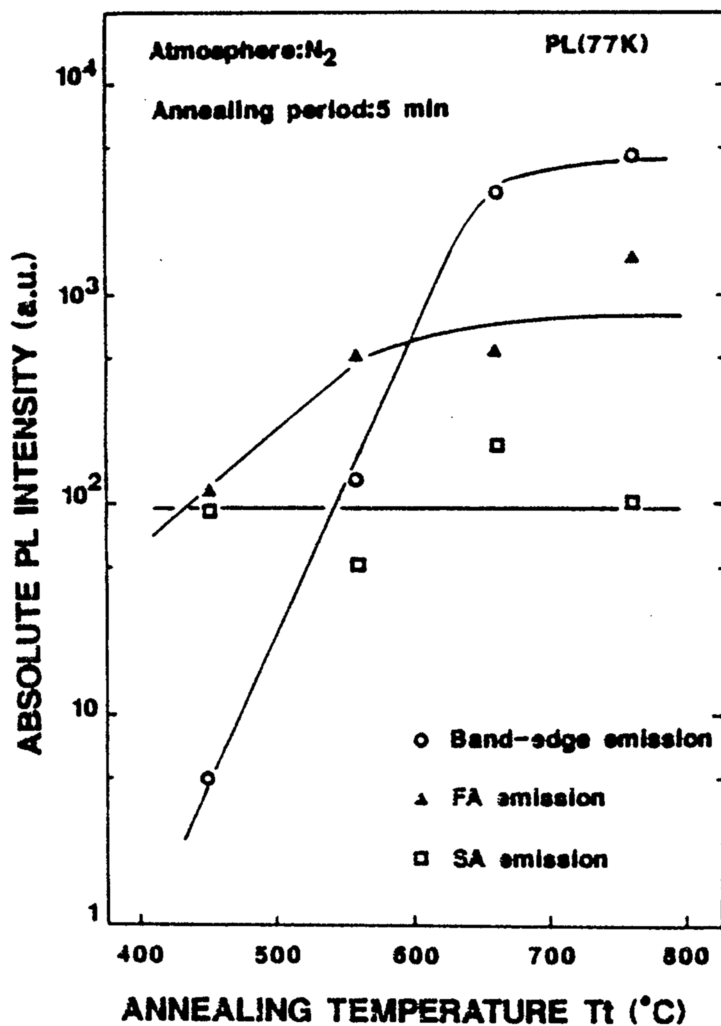

Fig.4.2.4. Dependence on T_t of the absolute intensities of various PL peak emissions (BE, FA, and SA emissions).

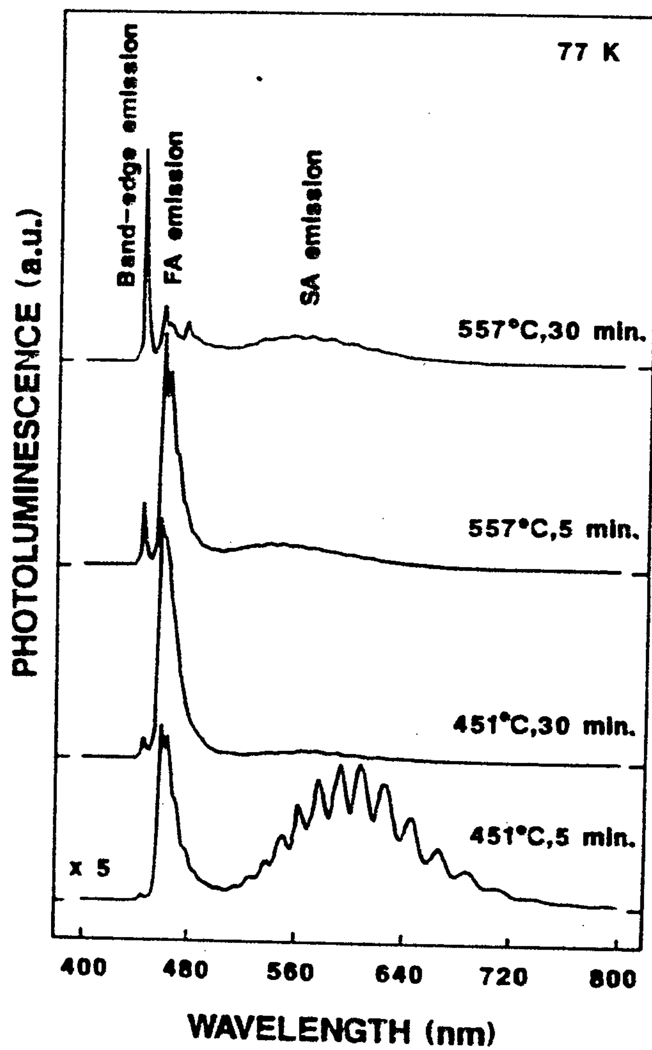

Fig.4.2.5. Dependence on t of the PL spectra at 77 K of epilayers annealed at 451 and 557 °C.

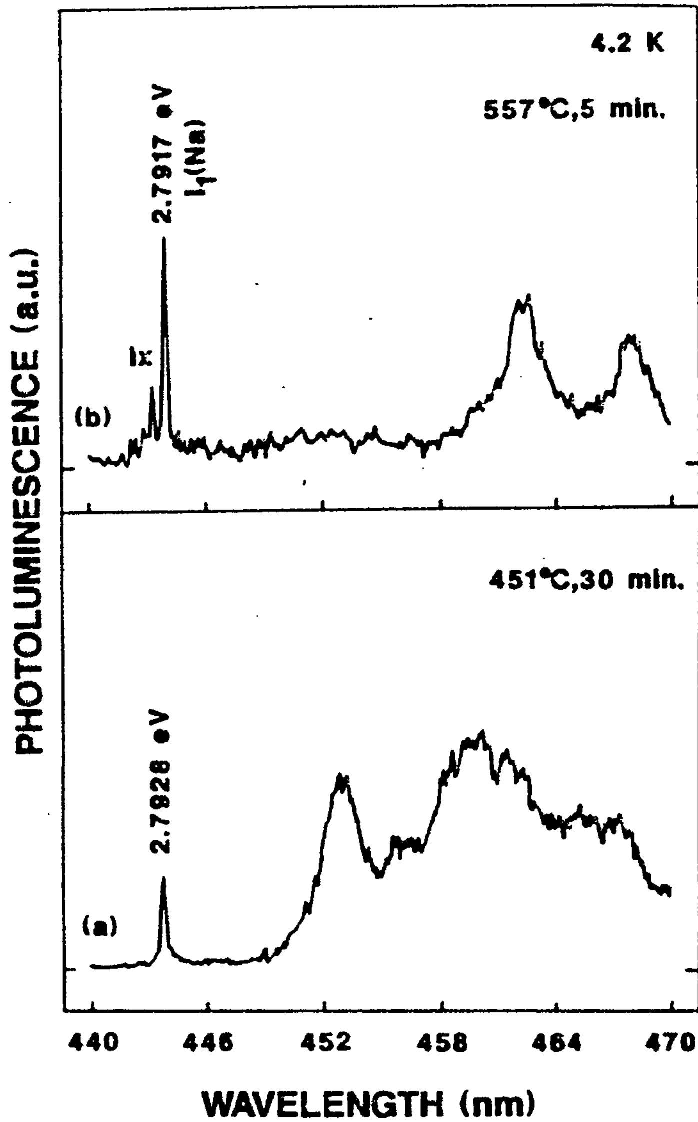

Fig.4.2.6. PL spectra at 4.2 K near the band-edge region of Na^{+}-implanted ZnSe epilayers in near band-edge region (440-470 nm).

(a) T_t=451 ^{o}C, t=30 min.

(b) T_t=557 ^{o}C, t=5 min.

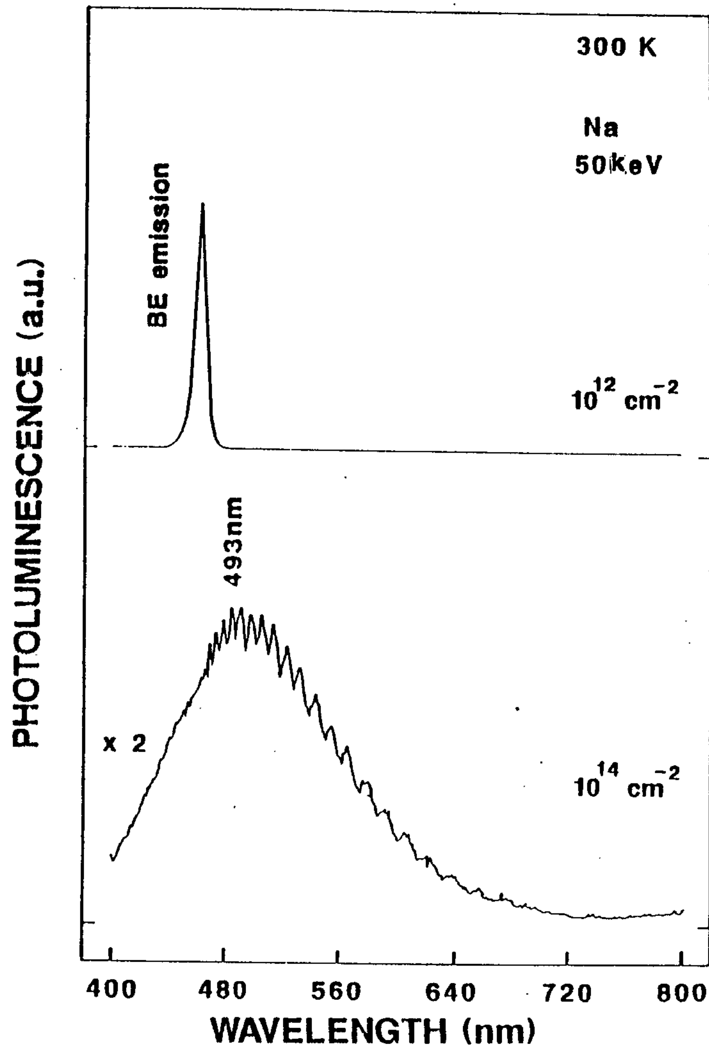

Fig.4.2.7. PL spectra at 300 K of Na-doped ZnSe heteroepilayers implanted at an E_a of 50 keV with various N_d (10^{12}, 10^{14} cm^{-2}), which were subjected to post-implant thermal annealing.

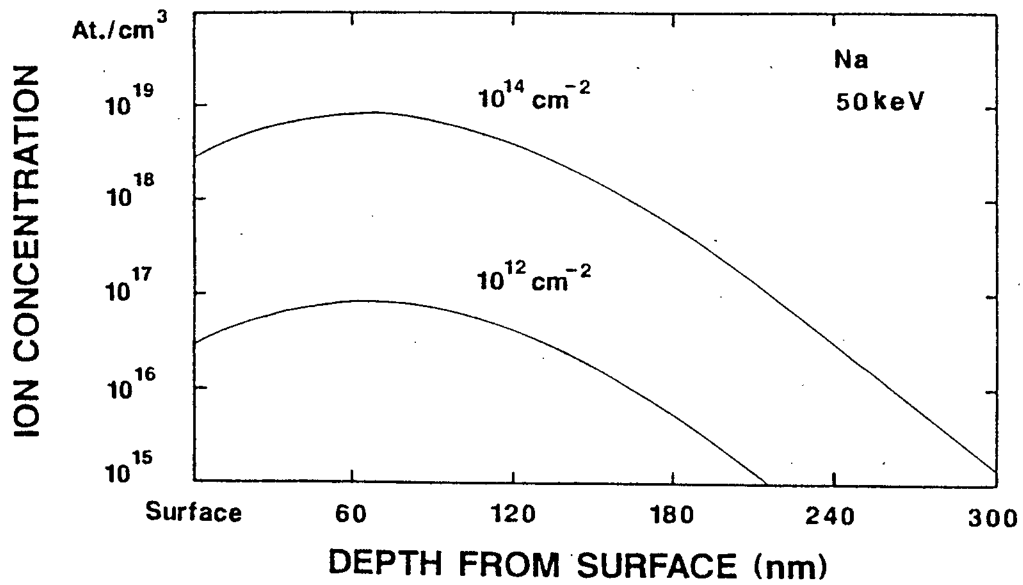

Fig.4.2.8. Depth profile of Na impurities in ZnSe after as implantation (Na^+ ion, 50 keV and 10^{12}, 10^{14} cm^{-2}) calculated according to LSS theory.

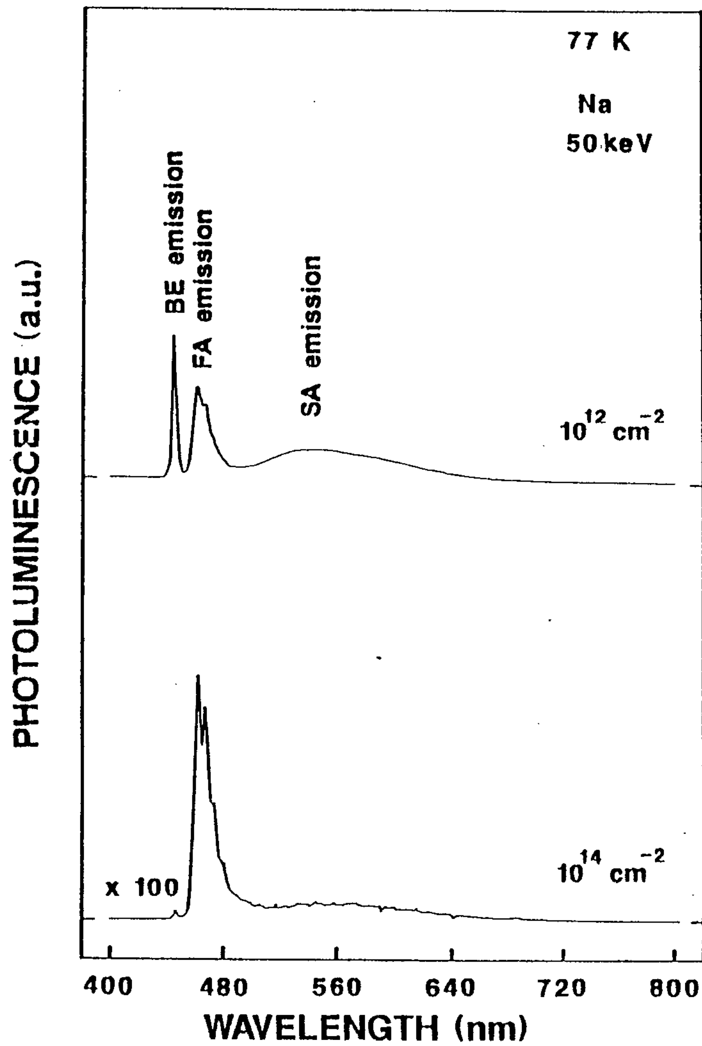

Fig.4.2.9. PL spectra at 77 K of Na-doped ZnSe heteroepilayers implanted at an E_a of 50 keV with various N_d (10^{12}, 10^{14} cm^{-2}), which were subjected to post-implant thermal annealing.

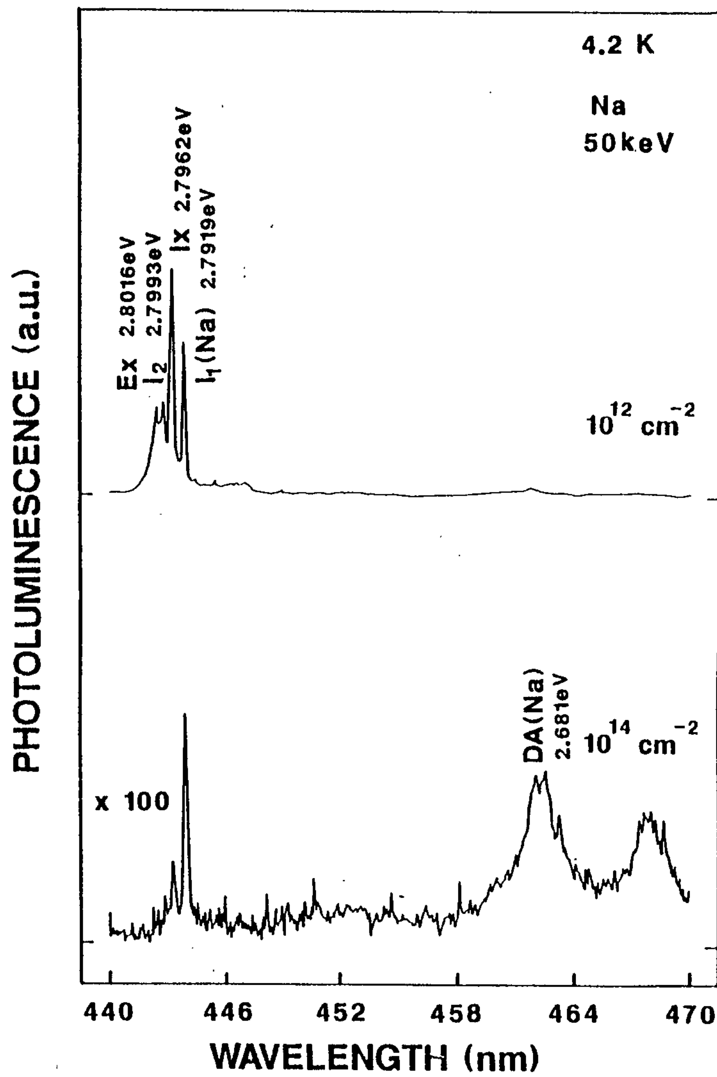

Fig.4.2.10. PL spectra at 4.2 K of Na-doped ZnSe heteroepilayers implanted at an E_a of 50 keV with various N_d (10^{12}, 10^{14} cm^{-2}), which were subjected to post-implant thermal annealing.

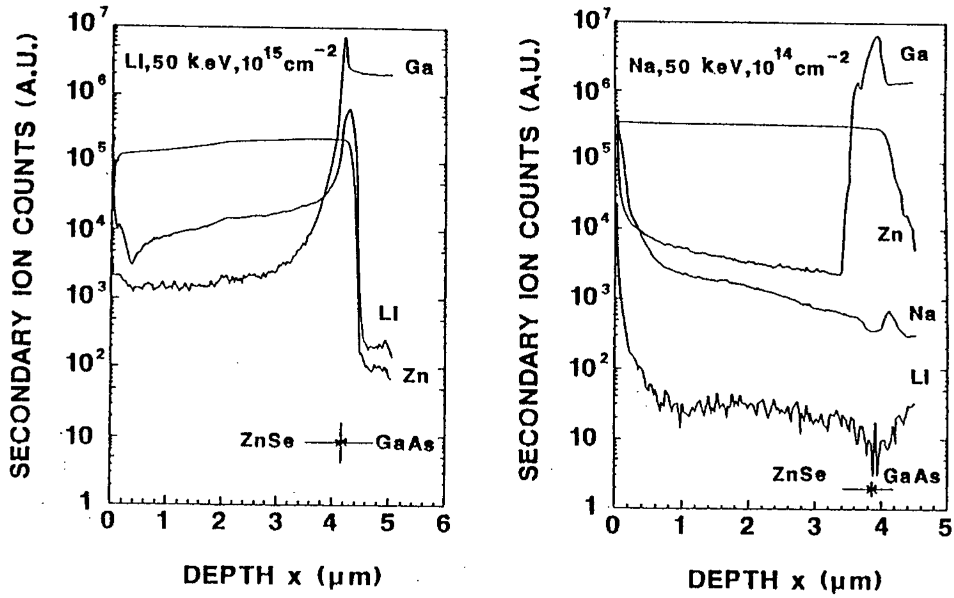

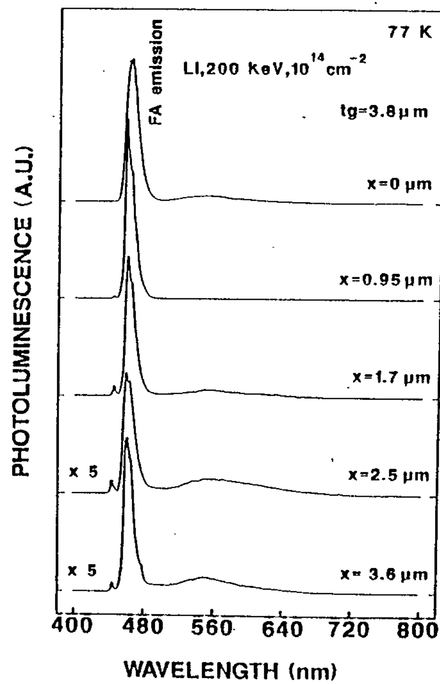

Fig.4.2.11. Depth profile (after annealing) of Li^+-implanted (T_t=757 ^oC) and Na^+-implanted (T_t=557 ^oC) (at 50 keV) epilayers measured by SIMS. And PL spectra at 77 K of Li-doped inter-epilayer (10^{14} cm^{-2}, 200 keV, T_t=757 ^oC) at etching depth x. The epilayer thickness is 3.8 μm.

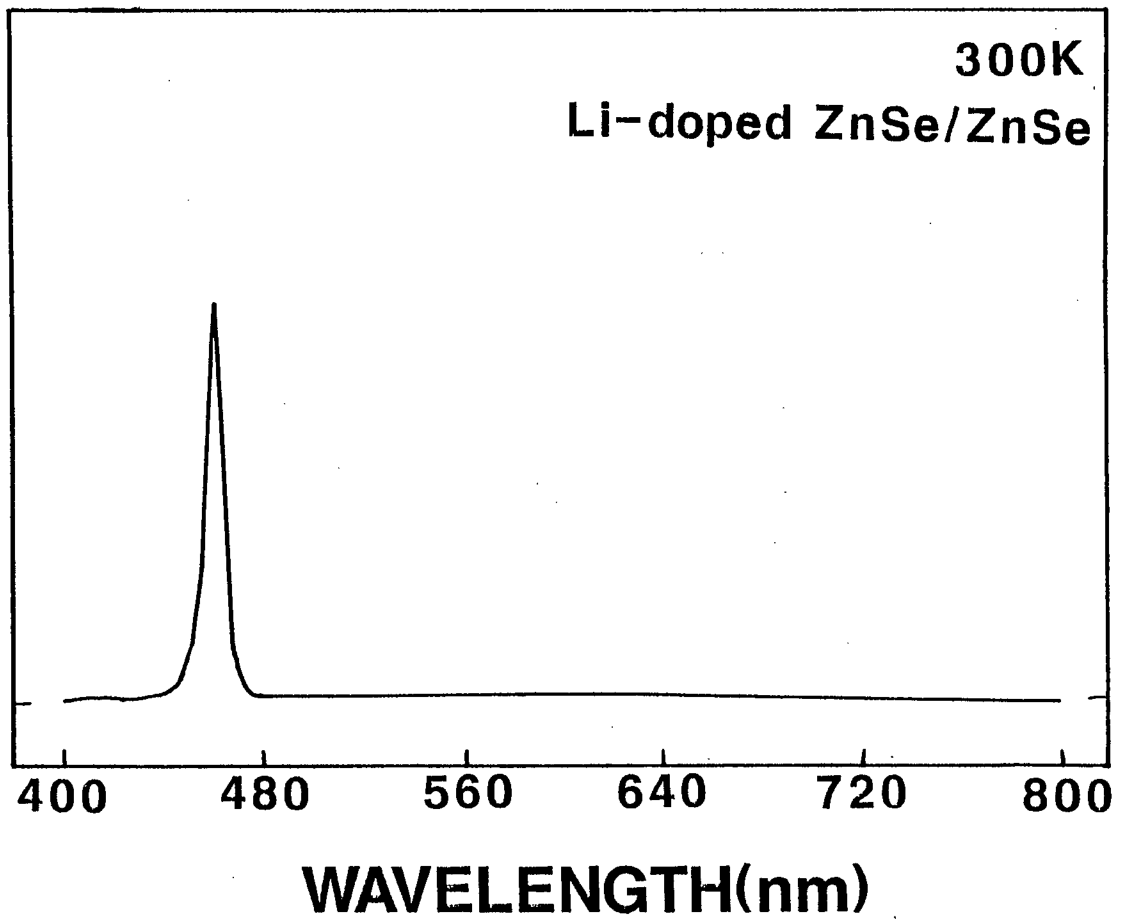

Fig.4.3.1. PL spectrum at 300 K of Li-doped ZnSe homoepilayers implanted at an E_a of 50 keV with an N_d of 10^{14} cm^{-2}, which were subjected to post-implant thermal annealing.

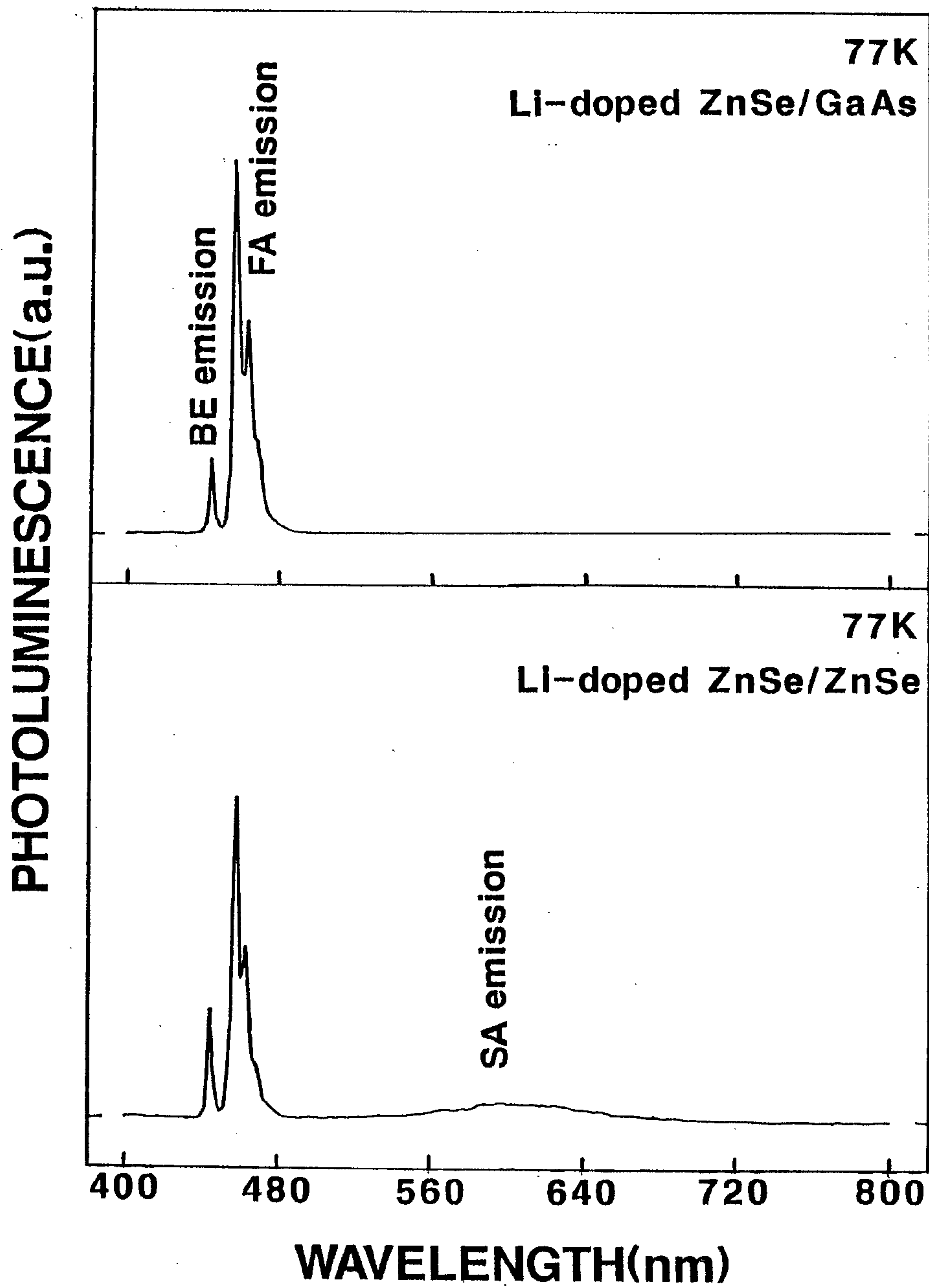

Fig.4.3.2. PL spectra at 77 K of Li-doped ZnSe homo- and heteroepilayers implanted at an E_a of 50 keV with an N_d of 10^{14} cm^{-2}, which were subjected to post-implant thermal annealing.

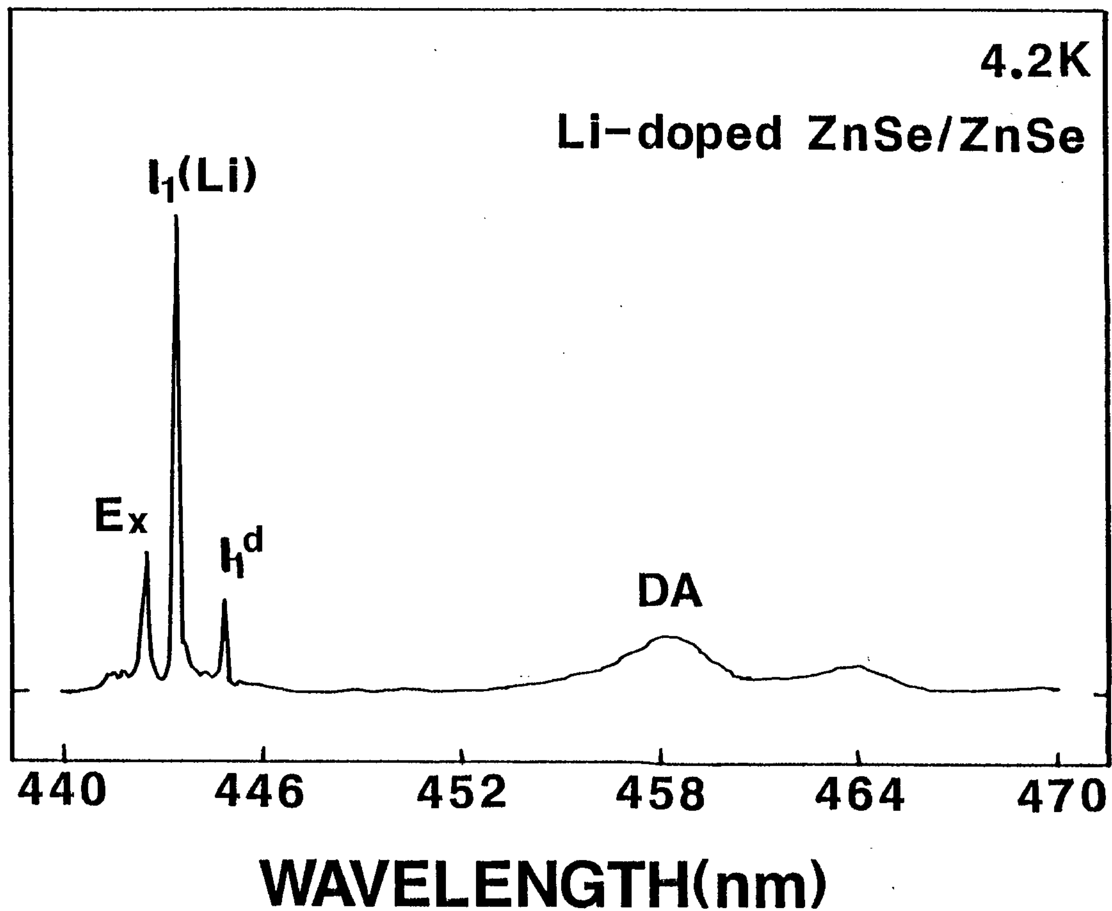

Fig.4.3.3. PL spectrum at 4.2 K near the band-edge region of Li-doped ZnSe homoepilayers implanted at an E_a of 50 keV with an N_d of 10^{14} cm^{-2}, which were subjected to post-implant thermal annealing.

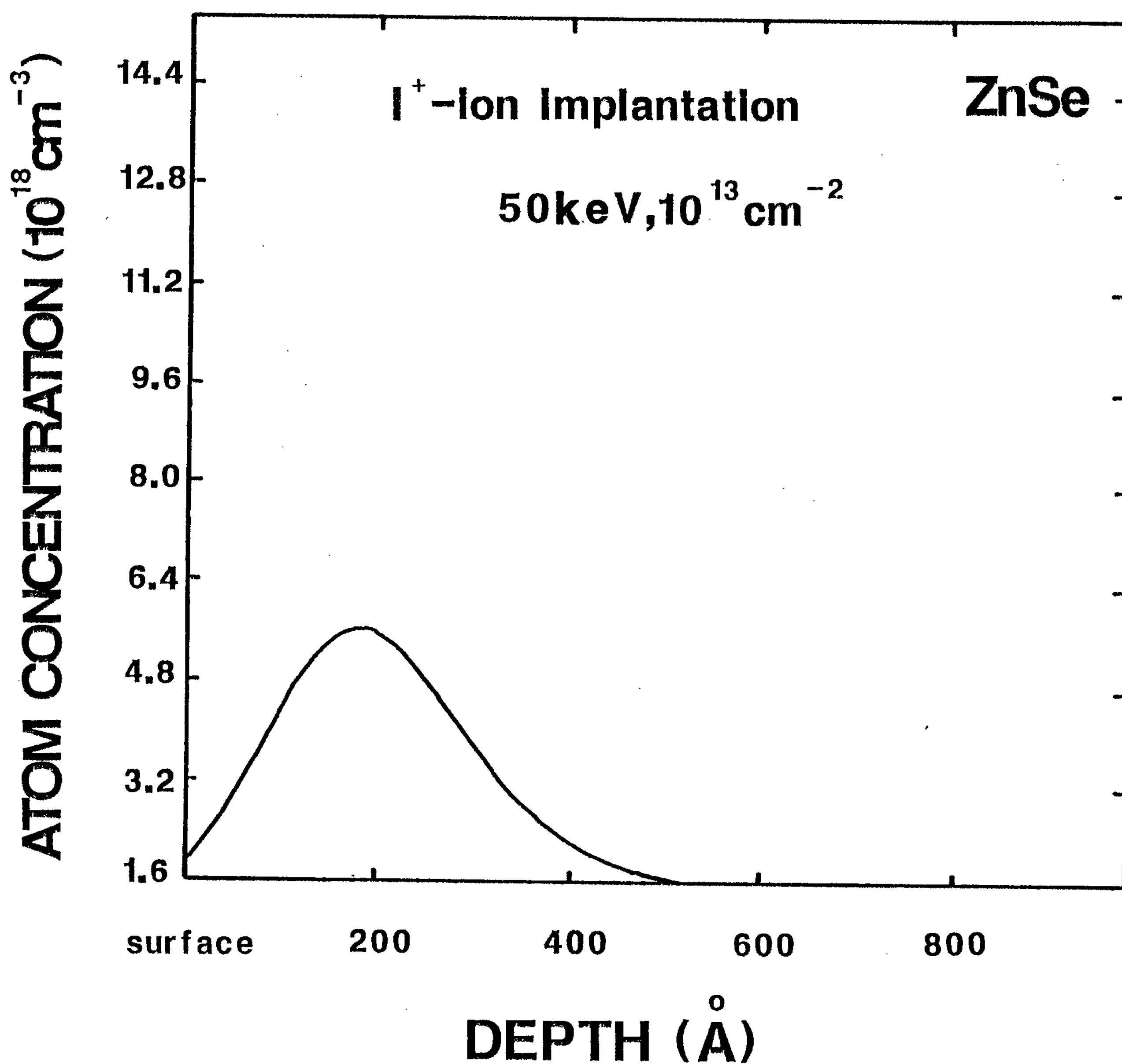

Fig.4.4.1. Depth profile of the I^{+}-implanted (50 keV, 10^{13} cm^{-2}) ZnSe calculated by LSS theory before the annealing.

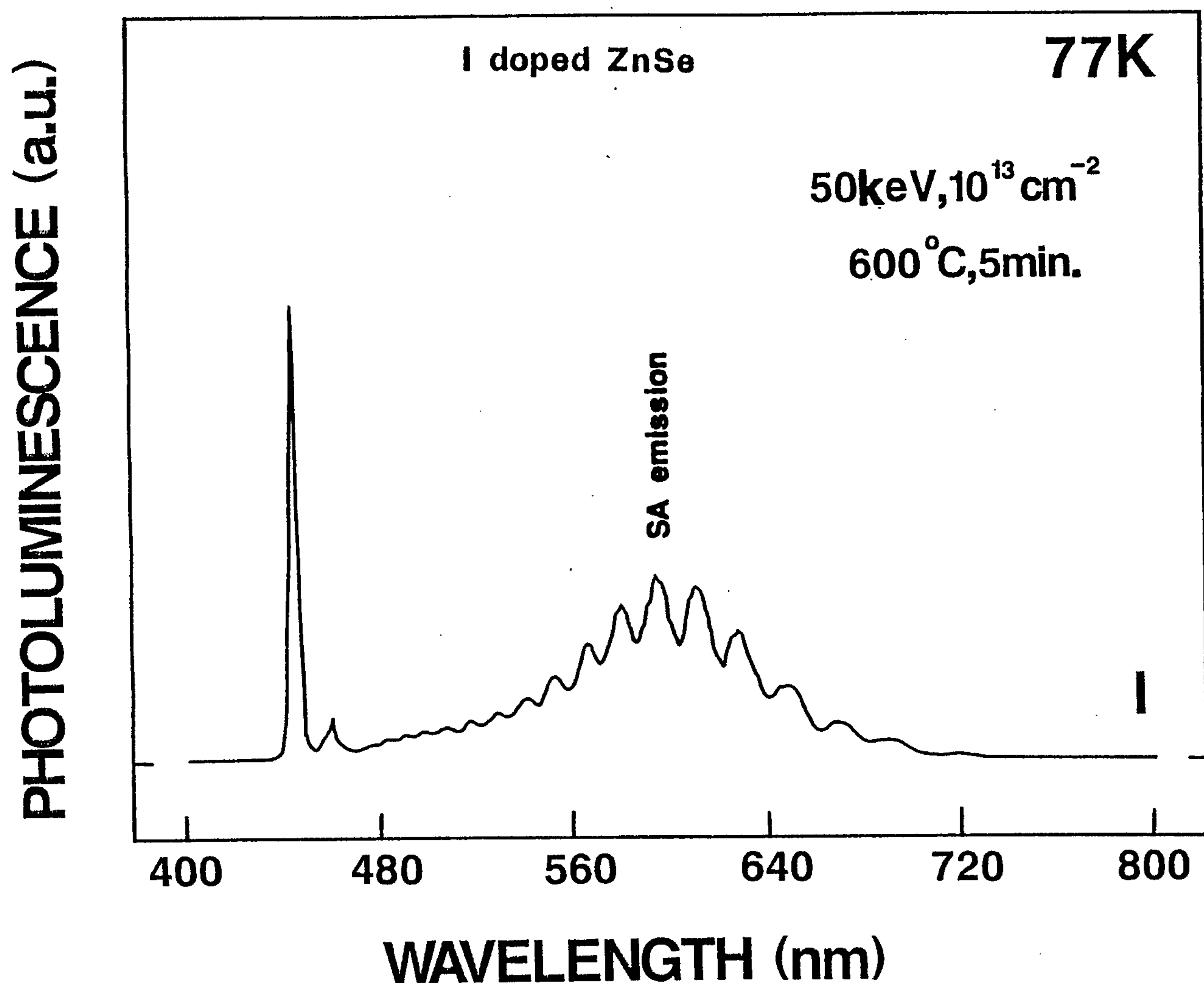

Fig.4.4.2. PL spectrum at 77 K of the I^{+}-implanted (50 keV, 10^{13} cm^{-2}) ZnSe epilayer after the post-annealing (600 ^{o}C, 5 min.). Also oscillations of SA emissions are explained by multi-scattering of the PL emission in the epilayer.

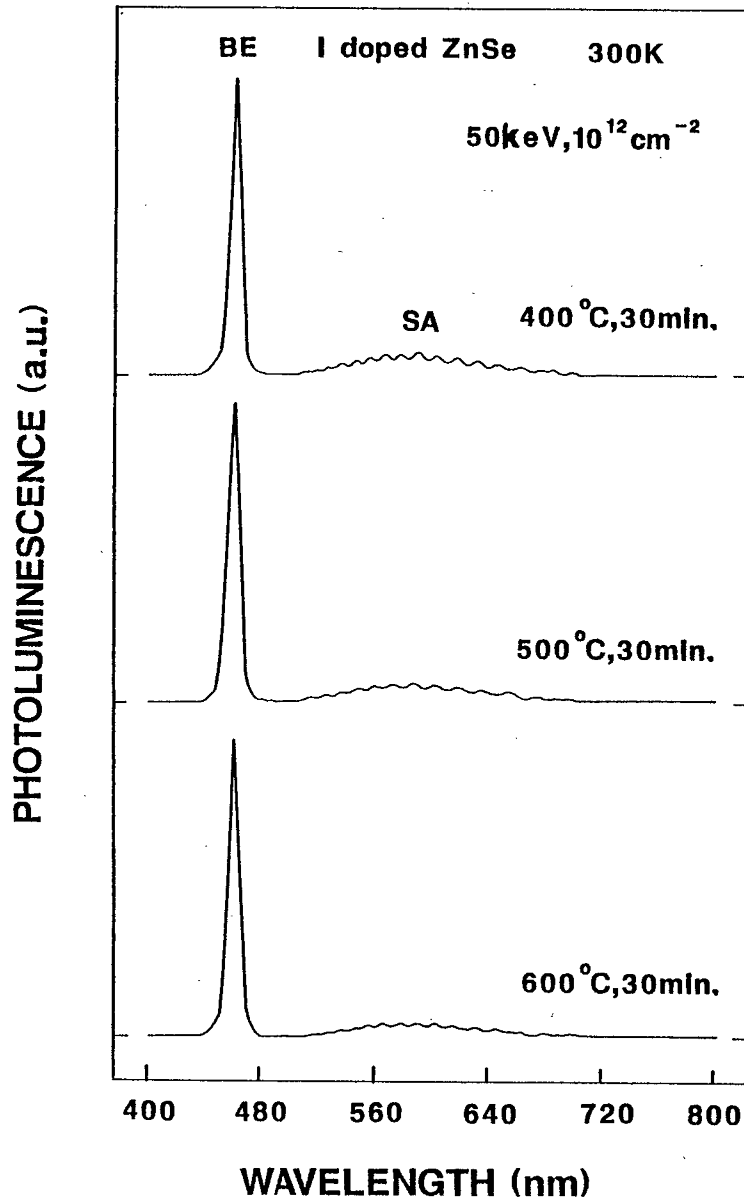

Fig.4.4.3. PL spectra at 300 K of the I^+-implanted (50 keV, 10^{12} cm^{-2}) ZnSe epilayer after various post-annealing (400-600 ^oC, 30 min.).

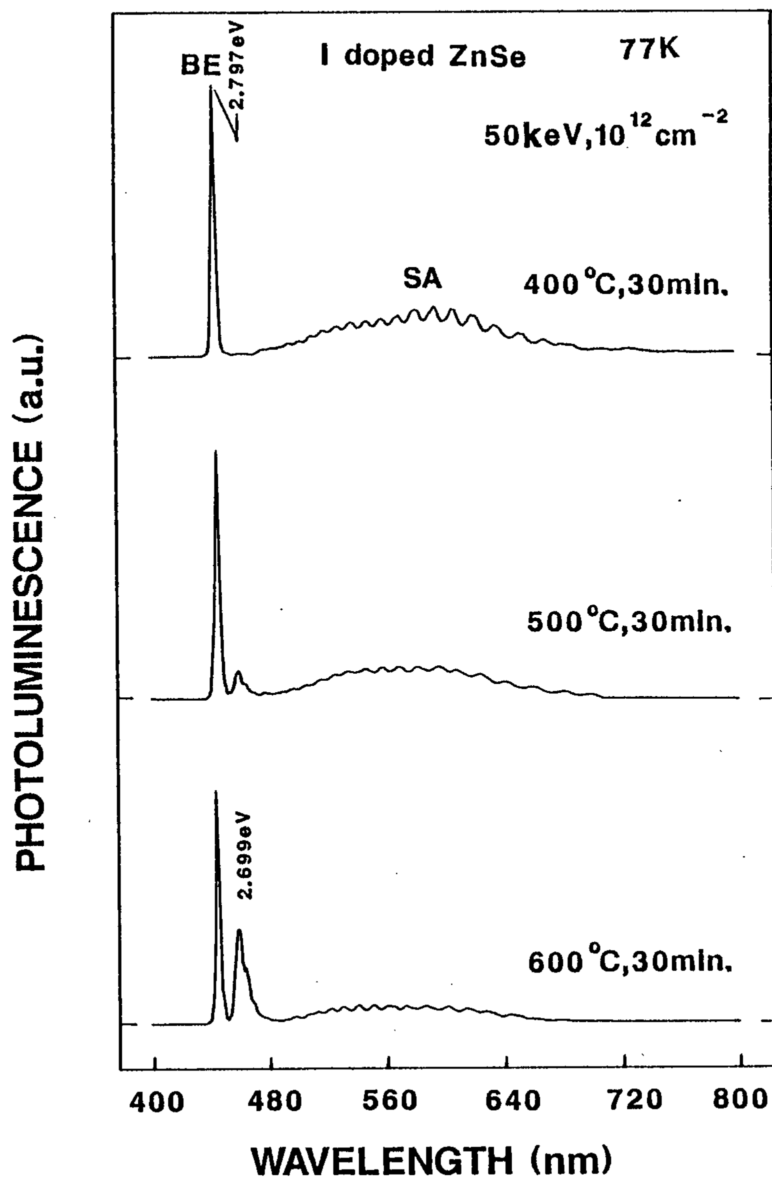

Fig.4.4.4. PL spectra at 77 K of the I^+-implanted (50 keV, 10^{12} cm^{-2}) ZnSe epilayer after various post-annealing (400-600 ^oC, 30 min.).

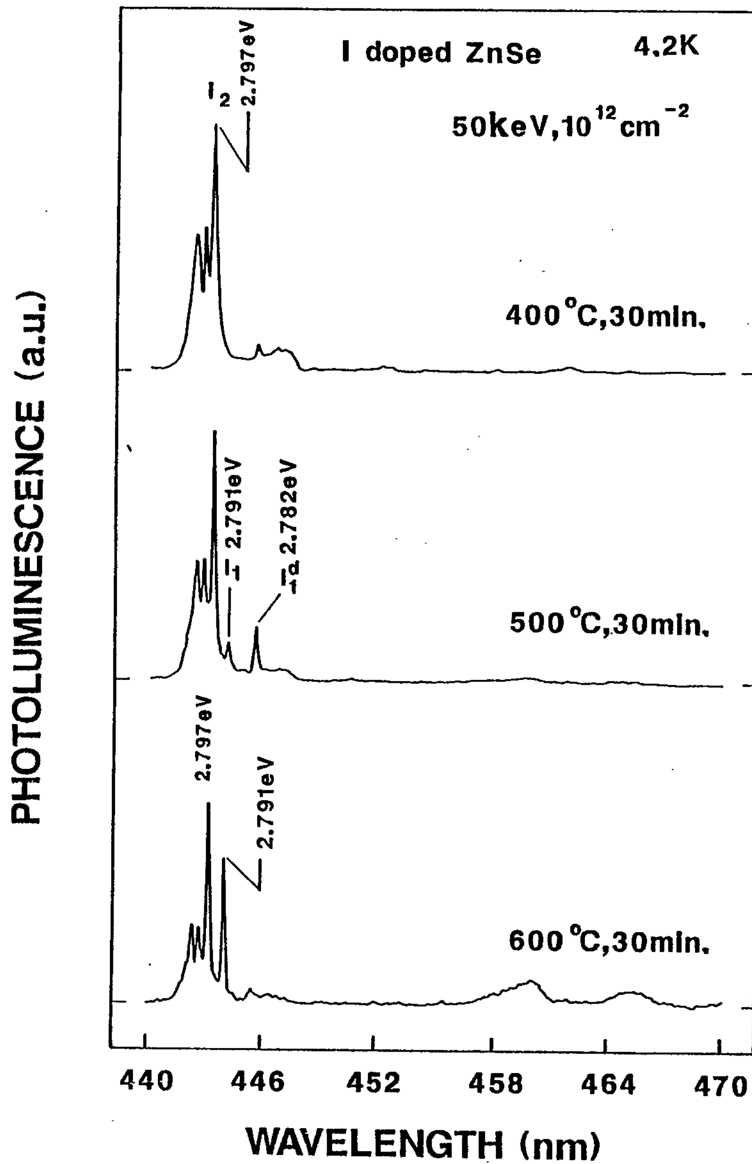

Fig.4.4.5. PL spectra at 4.2 K near the band-edge region of the I^+-implanted (50 keV, 10^{12} cm^{-2}) ZnSe epilayer after various post-annealing (400-600 ^oC, 30 min.).

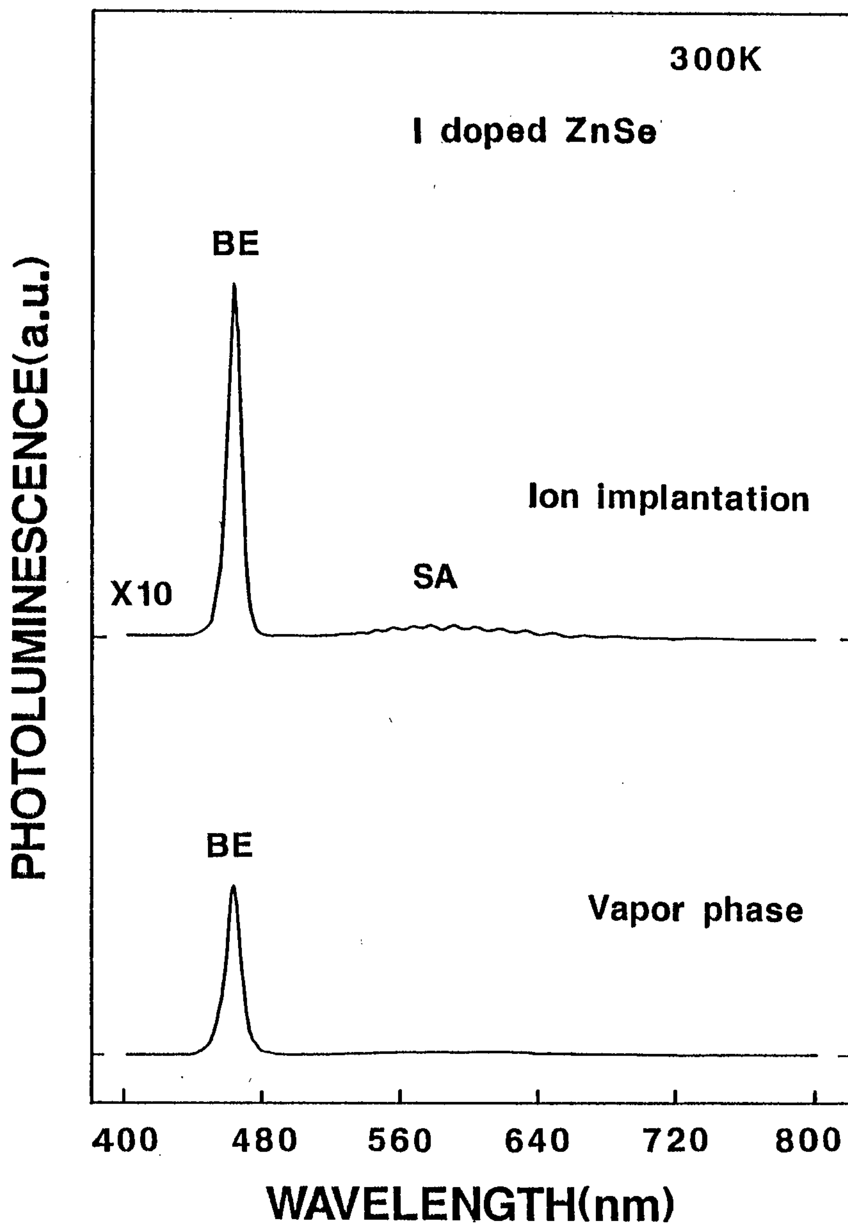

Fig.4.4.6. PL spectra at 300 K of the I^{+}-implanted (50 keV, 10^{12} cm^{-2}) ZnSe epilayer after a post-annealing (500 ^{o}C, 30 min.) and of a ZnSe epilayer doped through the vapor phase.

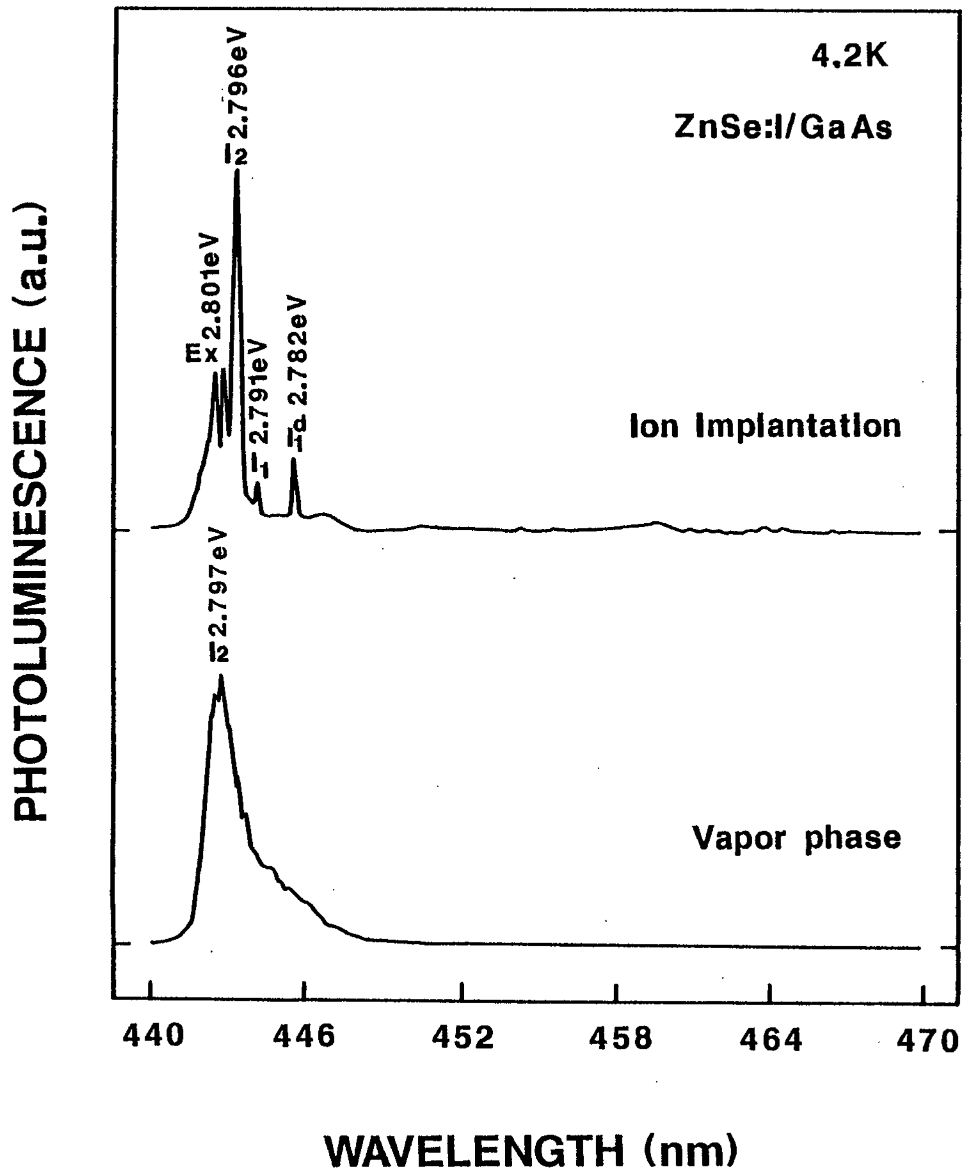

Fig.4.4.7. PL spectra at 4.2 K near the band-edge region of the I^{+}-implanted (50 keV, 10^{12} cm^{-2}) ZnSe epilayer after a post-annealing (500 ^{o}C, 30 min.) and of a ZnSe epilayer doped through the vapor phase.

5. Crystalline quality of ZnSe epilayers grown on Li^+-implanted ZnSe heteroepilayers

In order to fabricate the B-LED, pn junction should be formed. When ion implantation is applied as p-type doping technique, therefore, n-type ZnSe epilayers should be grown on the Li^+-implanted epilayers again. The property of B-LED will be much dependent on the crystalline quality of these p- and n-type ZnSe epilayers.

The crystalline quality of ZnSe epilayers (over-epilayers) on top of Li^+-implanted ZnSe epilayers grown by atmospheric pressure MOVPE is mainly governed by the radiation and annealing damage. The same of the over-epilayers will also be much related to the property of the B-LED. Usually the over-epilayer is n-type ZnSe epilayer for the B-LED, but it will be held by undoped ZnSe epilayer to investigate the crystalline quality in detail. Only in the next section, we will discuss the crystalline quality of n-type ZnSe epilayer.

The PL intensity of the BE emission (461 nm) at 300 K is affected by the radiation damage remaining in the implanted epilayers. The radiation damage affects the PL properties of the over-epilayers. It is suggested that the non-radiative centers propagate into the over-epilayers. The radiation damage cannot be removed completely by annealing under H_2 or N_2 atmosphere alone, and the crystalline quality is worsened still by annealing at high temperature. Since the annealing in an atmosphere containing Zn or Se vapor restores the PL properties at 300 K, of an over-

epilayer substantially to that of an as-grown epilayer, it is suggested that the non-radiative centers are related to native defects, particularly Zn vacancies.

5-1. Crystalline quality of undoped ZnSe epilayers grown on Li^+-implanted ZnSe heteroepilayers

The preparation of p-type ZnSe, which is expected to be one of the most suitable materials for the B-LED, has frequently been reported [18,96,108-110]. There remain, however, still a lot of difficulties before p-type ZnSe with both high reliability [109] and high hole concentration [110] is achieved. It was stated in chapter 3 that ZnSe epilayers grown at 250°C had a high thermal stability and the crystalline quality was not thermally degraded up to 700°C [91]. There arose a strong possibility of increasing the doping rate of acceptors in ZnSe (for example, by annealing at high temperature after ion implantation, etc.) while maintaining the high reliability of the devices. Li or Na impurity was doped into ZnSe epilayers by ion implantation [83,111] and the possibility of achieving p-type ZnSe by annealing in H_2 or N_2 atmosphere at high temperature was investigated. Moreover, we observed strong I_1(Li) and DA pair emissions in PL at 4.2 K, the FA and BE emissions at 77 K, and the BE and unknown emissions (probably FA emission) at 300 K. For the next stage, it became important to grow ZnSe over-epilayers with high crystalline quality on the Li^+-implanted ZnSe in order to fabricate a B-LED.

The purpose of the present paper is to investigate the effects of damage left in the Li^+-implanted epilayers on the crystalline quality of the over-epilayers and to find an effective annealing method of removing the radiation damage completely.

Firstly, ZnSe epilayers were grown at 250°C at an atmospheric pressure for 1 h on (100)-oriented GaAs substrates, using DMZ and H_2Se as source gases. The [Se]/[Zn] was 20. With these growth conditions, the epilayer thickness was about 4 μm. Thereafter, Li^+ ions were implanted into the ZnSe epilayers with N_d of 10^{13} or 10^{14} cm^{-2} at an acceleration energy of 200 keV. Moreover, the implanted epilayers were annealed at 550-757°C in various atmospheres (H_2(4 l/min.), N_2(4 l/min.), H_2(2 l/min.)+H_2Se (4.6x 10^{-4}mol/min.) or H_2(2 l/min.)+DMZ(11.5x10^{-6}mol/min.).) for 5-180 min. Finally, undoped ZnSe over-epilayers were grown on top of the annealed epilayers for 10 min. The thickness of the over-epilayers was about 0.5 μm.

Figure 5.1.1 shows the PL spectra at 300 K of the Li^+-implanted (200 keV, 10^{14} cm^{-2}) epilayers after annealing at various T_t in N_2 atmosphere. From an epilayer annealed at 451 °C, very weak BE and SA emissions are observed at 2.689 and 2.15 eV, respectively. As T_t is increased, the BE-PL intensity increases abruptly while the SA-PL intensity remains unchanged. This is indicative of the recovery by annealing the crystal whose quality has been degraded by radiation damage. Figure 5.1.2 shows the PL spectra at 300 K of Li^+-implanted (200 keV, 10^{13}-10^{14} cm^{-2}) epilayers after annealing at 657°C in N_2 atmosphere and of undoped over-epilayers on such Li^+-implanted ZnSe. The BE-PL inten-

sity of the annealed Li^+-implanted ZnSe is almost the same as that of an as-grown epilayer irrespective of N_d. It is concluded that most of the radiation damage is eliminated. Nevertheless, the PL property of an over-epilayer is much affected by N_d, since no PL emissions are observed from over-epilayers on implanted epilayers with an N_d of 10^{14} cm^{-2}. Thus the PL intensity of the over-epilayer decreases drastically as N_d increases. It appears that the radiation damage is not recovered completely even at 10^{13} cm^{-2}. The non-radiative centers are related to the radiation damage near the surface of the Li^+-implanted epilayers and propagate into the over-epilayers.

Figure 5.1.3 shows the PL spectra at 300 K of the over-epilayers grown after annealing under various atmospheres for an N_d of 10^{14} cm^{-2}. The period of annealing is one of the important parameters for recovering the radiation damage. Also when T_t is increased to 700°C in H_2 atmosphere, the PL intensity decreases and the emission finally disappears. The crystalline quality of the Li^+-implanted epilayer is degraded not only by the radiation damage, but also by the annealing in H_2 atmosphere. As a result, the crystalline quality of the over-epilayers is also degraded. The annealing in an atmosphere containing Zn vapor maintains a very high crystalline quality of the over-epilayers. It is true that annealing in an atmosphere with Se vapor is more effective than that in H_2 atmosphere without Se vapor, but it is not as effective as that with Zn vapor (see Fig.5.1.3.). Thus it is essential to anneal the Li^+-implanted epilayers in an atmosphere containing Zn vapor for full recovery of the radiation damage.

The non-radiative centers generated by the ion implantation must be closely related to native defects, particularly Zn vacancies. Figure 5.1.4 shows the surface morphologies of the over-epilayers after the various annealing treatments (T_t=700°C, t=3 h, only H_2 or H_2+DMZ.). The surface morphology of the over-epilayer after annealing in H_2 atmosphere only becomes very hazy, which is quite different from the effects of annealing in H_2 atmosphere including Zn vapor. The H_2 atmosphere degrades the crystalline quality by generating the native defects.

Next we now discuss the PL property at 77 K in order to examine the degraded crystalline quality and the species of the impurities in the epilayers. Figure 5.1.5 shows the PL spectra at 77 K of the over-epilayers following the various annealing conditions. The total PL intensity is about 10-20 times as weak as that of an as-grown ZnSe epilayer. The BE, Y (it is assigned to be associated with an exciton bound to some dislocations.) and SA emissions are observed at 2.785, 2.597 and 2.27 eV, respectively. As T_t is increased from 550 to 700°C, the BE-PL intensity decreases and Y emission line is broadened. Figure 5.1.5 also shows that the crystalline quality is degraded by the annealing at 700°C. The crystalline quality is indeed damaged by the annealing in N_2 atmosphere at 757 ^{o}C rather than by the radiation damage. But the radiation damage after annealing in N_2 atmosphere at 757°C is less than that in H_2 atmosphere. On the other hand, the over-epilayer after annealing in the atmosphere containing Zn vapor has almost the same PL spectrum as an as-grown epilayer with a low density of defects. As suggested by the PL results at

300 K, the non-radiative centers generated by the ion implantation can be effectively prevented by controlling the annealing atmosphere. Figure 5.1.6 shows the PL spectra at 4.2 K in the near band-edge region of the over-epilayers after various annealing conditions. After annealing at 550°C, E_x and I_x are hardly observed but an unknown emission appears at 2.7165 eV. In the over-epilayer annealed at 600°C in an atmosphere containing Zn vapor, sharp E_x, I_x and I_1(Li) lines are observed at 2.8013, 2.7966, and 2.7915 eV, respectively, similar to the PL spectrum of an as-grown epilayer with a low density of defects and impurities. When T_t is increased from 600 to 700°C, E_x disappears and only I_x is seen. When the atmosphere containing Se vapor is used for the annealing, however, both E_x and I_x are observed with a broad line shape. These results indicate that the crystalline quality starts to be degraded by the annealing at 700°C. The unknown emission at 2.7165 eV is also seen in the over-epilayers annealed at 700 ^{o}C.

The crystalline quality of the over-epilayer grown again is well maintained by controlling the atmosphere during the annealing and it is confirmed that Li impurity is not diffusing into the over-epilayer at a growth temperature of 250 ^{o}C from the highly Li^+-implanted ZnSe epilayer. It is concluded that the high diffusion rate of Li atoms in ZnSe causes little problem to grow the over-epilayer with high crystalline quality at 250 ^{o}C when fabricating the ZnSe B-LED.

In summary, the crystalline quality of the over-epilayer is related to that of the underlying Li^+-implanted epilayer, and

would be determined by the radiation as well as annealing damage. The non-radiative centers introduced by the damage propagate from the Li^+-implanted epilayer into the over-epilayer. The radiation damage cannot be removed completely by annealing in H_2 or N_2 atmosphere alone, and the degraded crystalline quality is worsened by annealing at high temperatures. Annealing in an atmosphere containing Zn vapor restores the crystalline quality of Li-doped epilayers effectively and prevents the propagation of the damage into the over-epilayer. The non-radiative centers induced by the damage are related to native defects, particularly Zn vacancies.

It thus becomes possible to grow ZnSe over-epilayers at 250 ^oC with high crystalline quality on the Li^+-implanted ZnSe in order to fabricate a B-LED, since the Li impurity has been found not to diffuse into the over-epilayer from the Li^+-implanted epilayer.

5-2. Crystalline quality of n-type ZnSe epilayer on implanted epilayer

In this section, we discuss the relation between the crystalline quality of the n-type over-epilayer and the property of the B-LED. The crystalline quality of n-type ZnSe over-epilayers on the top of Li^+-implanted ZnSe epilayers is mainly governed by the radiation and annealing damage. The crystalline quality of the over-epilayers is thus much related to the property of the B-LED.

Conversely, it is expected that the property of the B-LED is monitored by the crystalline quality of the n-type over-epilayer and improved.

5-2-1. Structure and characteristics of ZnSe B-LED

In order to fabricate the ZnSe B-LED, a device structure with pn junction should be grown at first. The device structure with pn junction is twofold. Both npp and pnn types of ZnSe B-LED are considered. Here the notation "npp" or "pnn" shows the type of electrical property in the order from the side of the top of the epilayer to the substrate.

When the ion implantation as p-type doping technique is utilized, the n-type ZnSe epilayer is grown on Li^+-implanted ZnSe epilayer again and the device structure with pn junction is formed.

Figure 5.2.1 shows the illustration of npp type of device structure. The special merits of the structure are that the activation rate of acceptors is heightened because it is possible to anneal the Li^+-implanted epilayer at high temperatures, and that it has a good ohmic electrode to n-type ZnSe (Au/Cr or In). On the other hand, the demerits are the contamination at pn interface by exposing Li^+-implanted epilayer to the air and the deterioration of the crystalline quality of n-type ZnSe epilayer generated from the radiation damage in the Li^+-implanted epilayer. Also when the thickness of the Li^+-implanted ZnSe epilayer is

large, the concentration of the diffused Li atoms is low in the epilayer, particularly near the interface between the epilayer and the substrate. Let us discuss merits and demerits of pnn type device structure.

Figure 5.2.2 shows the illustration of pnn type of device structure. After the n-type and undoped ZnSe epilayers are sequentially grown on n-type GaAs substrate in the order of the epitaxial growth. Thereafter, Li^+ ions are implanted into the epilayer with multi structure (inn type of device structure (the notation "i" shows a insulating (undoped) epilayer.).), annealed and pnn type of device structure is formed. The special merits are such that pn interface is clean and a high crystalline quality is maintained at pn interface, particularly when the n-type ZnSe epilayer is thick. The demerits are that the activation rate of acceptors cannot be raised, since it is impossible to anneal the Li^+-implanted epilayer at high temperatures because of the high diffusion rate of Li impurities, and that it is hard to have a good ohmic electrode to p-type ZnSe (Au?). Since the activation rate of acceptors is a key factor, we focus our attention to the npp type of device structure and discuss the characteristics of ZnSe B-LED with npp junction.

In npp type of device structure, the undoped ZnSe epilayers are grown at 250 ^{O}C at an atmospheric pressure for 0.5 h on (100)-oriented p-type GaAs substrates, using DMZ and H_2Se as source gases and [Se]/[Zn] of 20. Li^+ ions are implanted at the acceleration energies of 50 and 200 keV and the dose densities of 10^{13}-10^{15} cm^{-2}. Subsequently, the Li^+-implanted ZnSe epilayers

are annealed at various T_t (600-800 ^oC), t (0.5-10 min.) and atmospheres of (H_2(4 l/min.), N_2(4 l/min.), H_2(2 l/min.)+DMZ (11.5x10^{-6}mol/min.).). With these growth conditions, the epilayer thickness was about 2 μm. Moreover, the Li^+-implanted ZnSe epilayers with the post-annealing were treated thermally at 600 ^oC for 10 minutes under H_2 atmosphere including Zn vapor in order to remove the oxide layer and contaminants on them. Finally, n-type ZnSe over-epilayers (1x10^{18} cm^{-3}) were grown on the top of the annealed epilayers for 5-10 min. The thickness of the n-type over-epilayers was about 0.5 μm. The n^+-type ZnSe epilayer (1x10^{19} cm^{-3}, 0.05 μm) is grown on n-type ZnSe epilayer in sequence in order to improve the ohmic contact with the electrode. Au/Cr and Au/Zn electrodes are formed for n-type ZnSe and p-type GaAs, respectively. The annealing for ohmic contact is done at 250 ^oC for 1 min.

Figure 5.2.3 shows the PL spectra at 300 K of the n-type over-epilayers on the Li^+-implanted (200 keV, 10^{15} cm^{-2} and 50 keV, 10^{15} cm^{-2}) epilayers after annealing at a T_t of 800 ^oC for 0.5 min in N_2 atmosphere. The BE-PL intensity of the over-epilayers with the ion implantation is very weak and the crystalline quality is not so good. The degradation of the crystalline quality of Li^+-implanted epilayers propagates into the over-epilayer. Since it is shown at 77 K that FA emission with strong intensity is dominant and SA emissions are not seen from Li^+-implanted ZnSe epilayers, the crystalline quality of the Li^+-implanted ZnSe is not degraded seemingly. As seen in Fig.5.2.3., the crystalline quality of over-epilayers is very sensitive to that of the Li^+-

implanted ZnSe epilayers. Next we discuss the effects of crystalline quality of the n-type over-epilayer on properties (I-V and EL properties) of the B-LED.

Figure 5.2.4 shows PL spectra at 300 K, 14 K and EL spectrum at 16 K of the B-LED (n-type ZnSe/Li^+-implanted ZnSe; 50 keV and 10^{15} cm^{-2}; 800 ^oC, 0.5min.). The EL spectrum is measured at 40 V and 2 mA. The PL and EL spectra show the dominant SA emissions and the EL property almost coincides with the PL property. The EL emission is weak yellow light at 300 K. Thus, the EL property is monitored by the PL property. It is shown that the crystalline quality of the over-epilayer is much related to the EL property. As discussed already, the crystalline quality of the implanted epilayer succeeds to the crystalline quality of the over-epilayer. It is strongly suggested that the crystalline quality of the implanted epilayers, rather than the crystalline quality of the over-epilayer, determines the final EL property. Actually, the BE emission is observed with weak intensity in the PL spectra, while not in the EL spectrum. The EL intensity is about ten times as weak as the PL intensity. The PL spectrum of the B-LED is emission only from the n-type ZnSe epilayer. On the other hand, the EL spectrum of the B-LED is thought to be emission from the region near the pn junction, mainly implanted epilayer, considering the relation between the carrier concentration and the diffusion length of carriers. The PL property does not always coincide with the EL property. It is suggested that the crystalline quality of n- and p-type ZnSe epilayers near the pn junction is much related to the EL property. Also it is supported from the fact

that the EL property is worse than the PL property because the EL property is determined by the crystalline quality of the implanted epilayer, that degrades the crystalline quality of the over-epilayer so much.

Figure 5.2.5 shows I-V property of the B-LED (n-type ZnSe/Li^+-implanted ZnSe; 50 keV and 10^{15} cm^{-2}; 800 ^oC, 0.5 min.). The threshold voltage of an ideal B-LED is about 2 V. However, the threshold voltage of the fabricated B-LED is about 30 V. The break down voltage in the reverse bias is 80 V.

Figure 5.2.6 shows the relation between the breakdown voltage and hole carrier concentration. Considering the epilayer thickness, the hole carrier concentration is about 10^{15} cm^{-3}. The hole carrier concentrations of the implanted epilayers of the other B-LED are about 10^{15}-10^{16} cm^{-3}. These values are also confirmed by C-V measurement.

Figure 5.2.7 shows the dependence of N_d on the threshold voltage toward the forward of the B-LED. As N_d increases, the threshold voltage increases. Particularly, when N_d is 10^{15} cm^{-2}, it increases abruptly. The crystalline quality degraded by the radiation damage probably worsens the crystalline quality near the pn interface and increases the threshold voltage.

We finally discuss the improvement of the properties of the B-LED by optimizing the annealing conditions as discussed in section 5-1. We have seen that the crystalline quality of the over-epilayers is drastically improved by annealing the implanted epilayers under the H_2 atmosphere including DMZ (11.5×10^{-6} mol/min.). Figure 5.2.8 shows the PL spectra at 300 K of the n-

type ZnSe over-epilayers on the Li^+-implanted (200 keV, 10^{13} cm^{-2}; 200 keV, 10^{14} cm^{-2}) epilayers after annealing at various T_t 600-700 ^oC for 5-10 minutes in H_2 atmosphere including DMZ ($11.5x10^{-6}$ mol/min.). The total PL intensity of the over-epilayer (200 keV, 10^{14} cm^{-2}; 700 ^oC, 1 min.) is about 10 times as weak as those of others. The SA-PL intensity is intense. It indicates the degradation of the crystalline quality by the radiation damage. However, by introducing Zn vapor in the atmosphere, the crystalline quality of the over-epilayers is maintained as high as that of n-type ZnSe epilayer doped through the vapor phase. T_t is held 600-650 ^oC so as not to degrade the crystalline quality by the annealing. The threshold forward voltage is 15-18 V and the breakdown voltage is still higher (32-44 V). It is shown that T_t is not high enough to activate the acceptors for maintaining the crystalline quality. However, the B-LED emits blue light at 77 K (Fig.5.2.9.), but does not emit at 300 K. Because the crystalline quality of both over-epilayer and implanted epilayers at pn interface is improved by optimizing the annealing conditions, though the problem of the low activation rate of the acceptors in the implanted epilayer is left. The fact that no EL emissions were observed at 300 K indicates that the activation rate of the acceptors in the implanted epilayer is too low. It is therefore suggested that the activation rate of the acceptors should be raised in order to emit the blue light at 300 K. Also, it is suggested that the crystalline quality of the Li^+-implanted and n-type epilayers near the pn interface is not yet maintained high by the annealing condition.

5-2-2. Contrivance on device structure of ZnSe B-LED

Let us see now how the device structure is devised to emit the blue light at 300 K from the B-LED. The important points are to heighten the activation rate of the acceptors and to maintain the crystalline quality of the epilayer high at pn interface. As discussed in section 5-2-1, the npp type of the device structure has demerit of pn junction being exposed to the air. It would obviously degrade the crystalline quality at pn interface and the EL property. When the ion implantation is utilized as p-type doping technique in the npp type of device structure, the contamination at pn junction by the exposure to air is not necessary inevitable. Therefore, a new device structure should be proposed to emit the blue light at 300 K if the npp type of device structure is adopted to increase the activation rate of acceptors.

We now propose the B-LED with a new device structure here (see Fig.5.2.10.). The characteristics are such that an undoped ZnSe buffer epilayer is inserted between Li^+-implanted epilayer and n-type ZnSe epilayer. Namely, the undoped ZnSe buffer epilayer is grown on the Li^+-implanted epilayer again and annealed at high temperature for a long period (600 ^{o}C, 3h) in the reactor sequentially. By the annealing, Li impurities diffuse into an undoped ZnSe epilayer and the Li-diffused epilayer is considered as new interface of p-type ZnSe. Thereafter the n-type ZnSe epilayer is grown again on the Li-diffused epilayer in the epitaxial growth. The process has three special merits that a new pn junction is formed in the reactor, the crystalline quality is

maintained high by inserting the Li-diffused ZnSe epilayer with high crystalline quality, and the damaged region is much far away from the new pn junction together with the special merits of pnn-type of device structure. One should be aware of the two possible demerits: it is feared that 1) the activation rate of Li acceptors would become too low because of the high diffusion rate of Li atoms in an undoped ZnSe epilayer and 2) the annealing for a long time may degrade the crystalline quality of both the diffused- and over-epilayers. We call the new device structure the "nipp-type" here (the notation "i" shows a insulating (undoped) epilayer diffused by Li atoms.).

Figure 5.2.10 shows the illustration of nipp-type of device structure. The fabrication process of the new nipp-type of device used in this experiment will be stated. An undoped ZnSe epilayer is grown at 250 ^{o}C and a [Se]/[Zn] of 20 on the p-type GaAs substrate with an epilayer thickness of 2 μm. The Li^{+} ion implantation in 3 steps (200, 50 and 10 keV; 3.3×10^{13} cm^{-2}) or 2 steps (200 keV, 10^{14} cm^{-2} and 50 keV, 6×10^{13} cm^{-2}) is performed into the undoped ZnSe epilayer to make the depth profile of Li atoms uniform in the epilayer. An undoped ZnSe epilayer is grown at 250 ^{o}C on Li^{+}-implanted epilayer again with an epilayer thickness of 1 μm, following the procedure of the pretreatment for re-growth as discussed in section 5-2-1. After growth, the epilayer is annealed at 600 ^{o}C for 3 h under the H_2 atmosphere including DMZ (11.5×10^{-6} mol/min.) in order to diffuse Li impurity into the undoped ZnSe epilayer and to increase the activation rate of Li acceptors in the reactor. Thus the Li-diffused epilayer is formed

and, moreover, the n-type ZnSe epilayer is grown on the diffused epilayer again. The materials and procedures for electrodes are the same as those of the npp-type of device structure.

Figure 5.2.11 shows the PL spectra at 300 K of the B-LED with the nipp-type of device structure. Only ion implantation conditions are different; 3 steps and 2 steps as stated above. It shows that the BE emission is dominant while the SA-PL intensity is very weak. The crystalline quality of the over-epilayers is maintained well even by introducing the buffer epilayers despite the high temperature annealing for a long time. The long time annealing degrades the crystalline quality of neither the diffused- nor over-epilayers. The visible white light is observed at 300 K from the B-LED. Figure 5.2.12 shows an EL spectrum at 300 K of the B-LED (at 2 mA and 10 V). The threshold voltage is 1.3-2 V and the breakdown voltage is about 20 V. The activation rate of the acceptor is effectively increased by the long time annealing. The dominant peak is the blue spectrum observed at 471 nm and SA emission is also seen with weak intensity. Thus the EL emission with blue spectrum is achieved at 300 K. It is concluded that controlling the crystalline quality of the epilayers (both the Li-diffused epilayer and n-type over-epilayer) near the pn interface is an important factor for emitting the blue light at 300 K. The threshold voltage of the emission, however, is still too high. The crystalline quality should be improved near pn interface between the diffused epilayer and n-type epilayer, though it is reported that the threshold voltage of the emission of the npp-type of device structure is essentially high. Now we discuss

the crystalline quality and the activation rate of the Li acceptor level of the Li-diffused epilayer to some detail, which is the most important point of being related to the EL properties of the B-LED.

Figure 5.2.13 shows the PL spectrum at 77 K of the Li-diffused epilayer itself before fabricating the B-LED with nipp-type of device structure. The BE, FA, SA and Y emissions are observed. And the PL intensities of Y and SA emissions are relatively intense. And the FA-PL intensity is more than ten times as weak as that of the Li^+-implanted epilayer at post-annealing conditions (700 ^{o}C, 5 min.) treated previously in chapter 4. It is clearly shown that the crystalline quality of the Li-diffused epilayer is not so good, since some concentration of dislocations are included and the activation rate of the Li acceptors is unexpectedly low. Since the Li-diffused epilayer has dislocations and other faults, it is suggested that the crystalline quality of the Li^+-implanted epilayers after annealing is much worse than that of the Li-diffused epilayer.

Thus the B-LED emits the white light with a strong blue spectrum at 300 K despite the poor crystalline quality of the epilayer near the pn junction. It is hopeful to develop the B-LED with high efficiency, if the crystalline quality is improved still more.

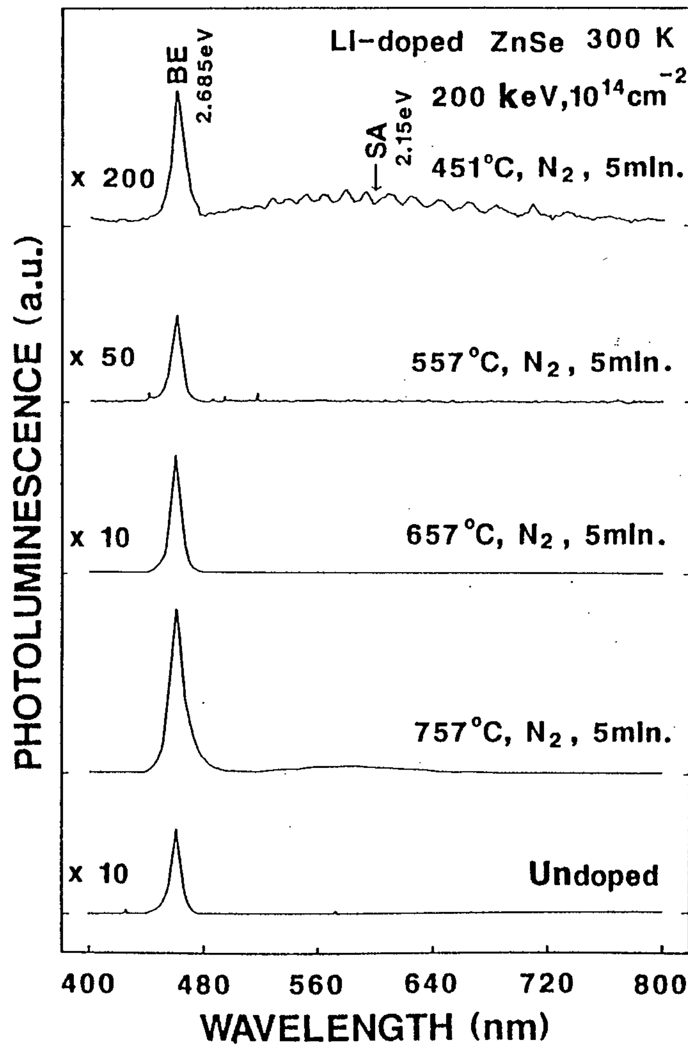

Fig.5.1.1. PL spectra at 300 K of the Li^{+}-implanted (200 keV, 10^{14} cm^{-2}) epilayers annealed at various temperatures in N_2 atmosphere.

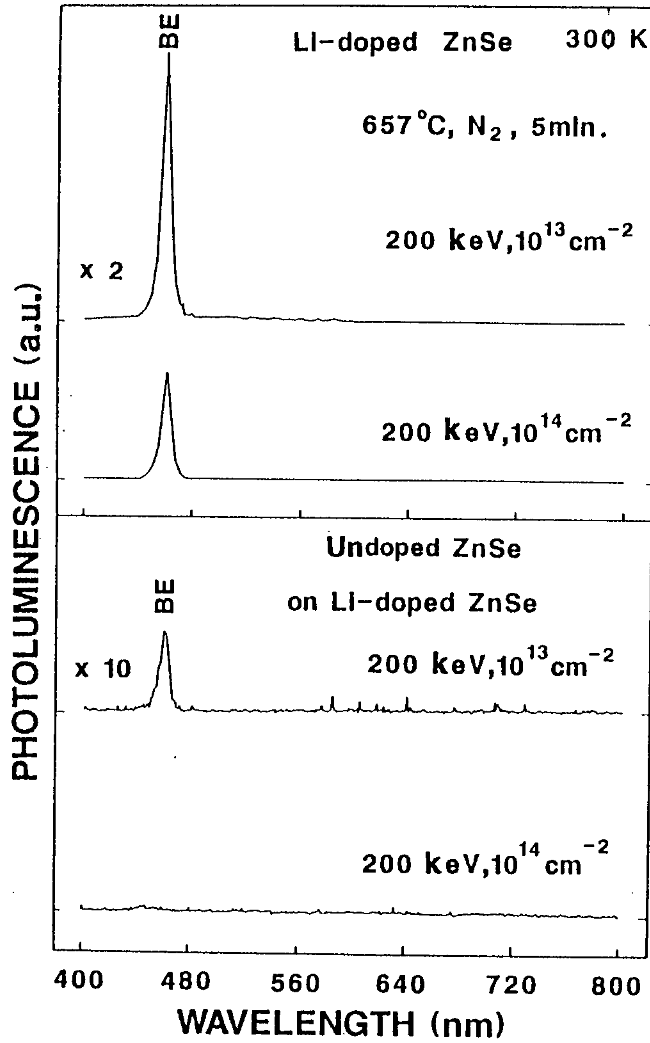

Fig.5.1.2. PL spectra at 300 K of the Li^+-implanted (200 keV, 10^{13}-$10^{14}cm^{-2}$) epilayers and the undoped epilayers on the top of the implanted epilayers.

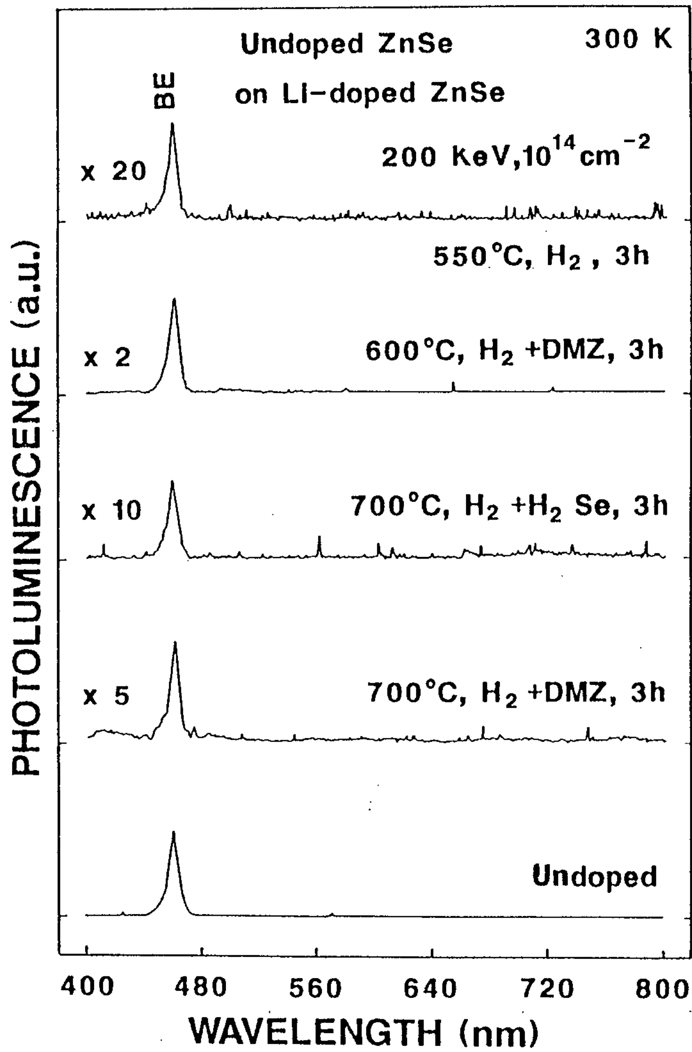

Fig.5.1.3. PL spectra at 300 K of the over-epilayers grown after the annealing in various atmospheres following a Li^+ ion implantation (10^{14} cm^{-2}).

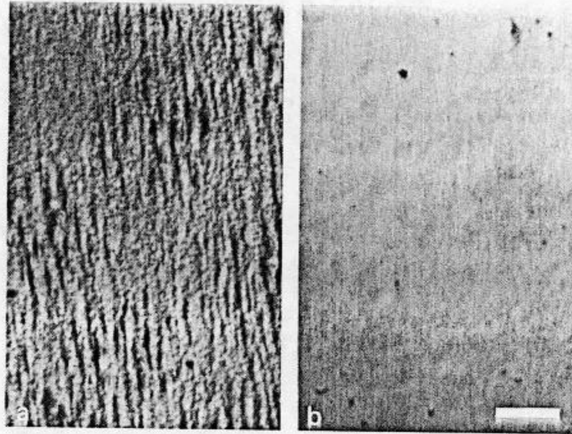

Fig.5.1.4. Surface morphologies of the over-epilayers after annealing at 700°C for 3 h in (a) H_2 or (b) H_2 atmosphere containing Zn vapor.

Undoped ZnSe on Li^+-implanted ZnSe.

200 keV, 10^{14} cm^{-2}.

(a) 700°C, H_2, 3 h.

(b) 700°C, H_2+DMZ, 3 h.

Marker represents 10 μm.

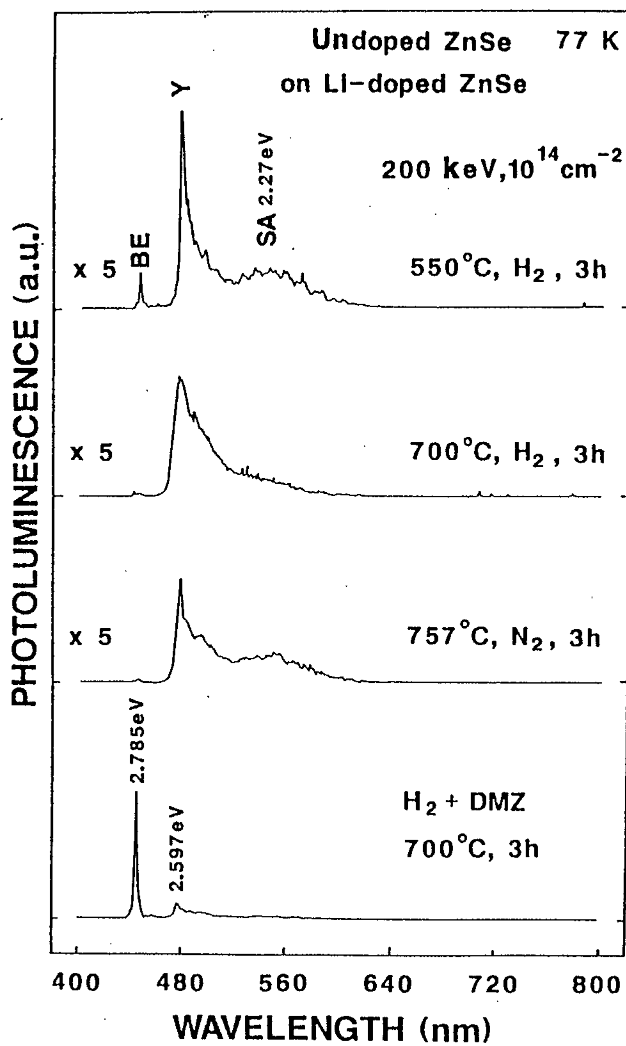

Fig.5.1.5. PL spectra at 77 K of the over-epilayers after annealing at various conditions.

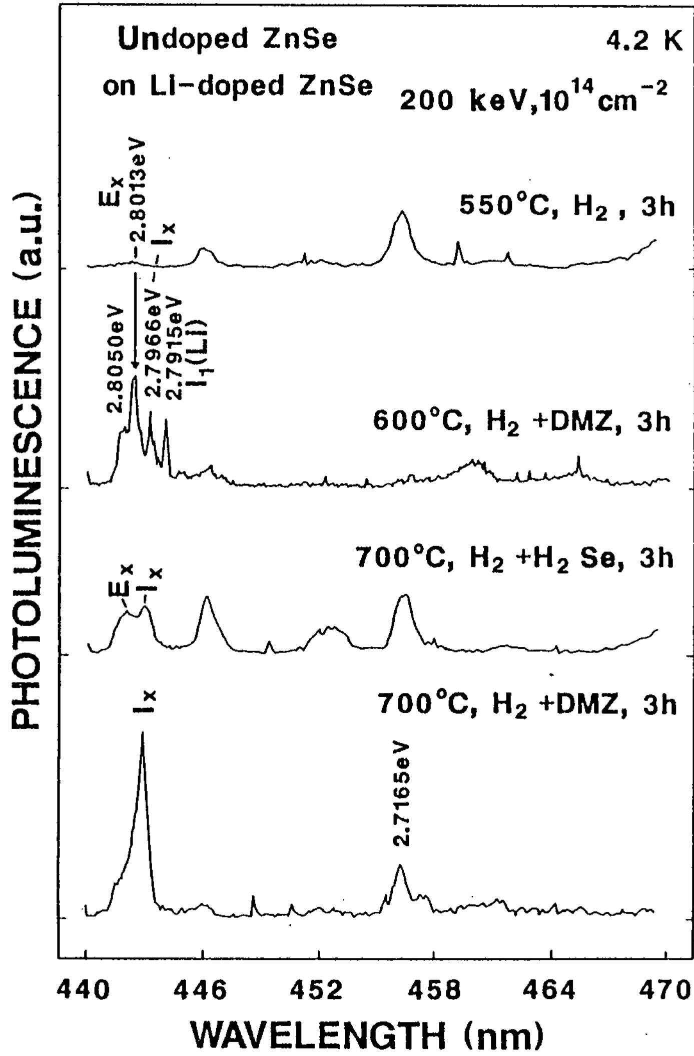

Fig.5.1.6. PL spectra at 4.2 K in the near band-edge region for over-epilayers after annealing at various conditions.

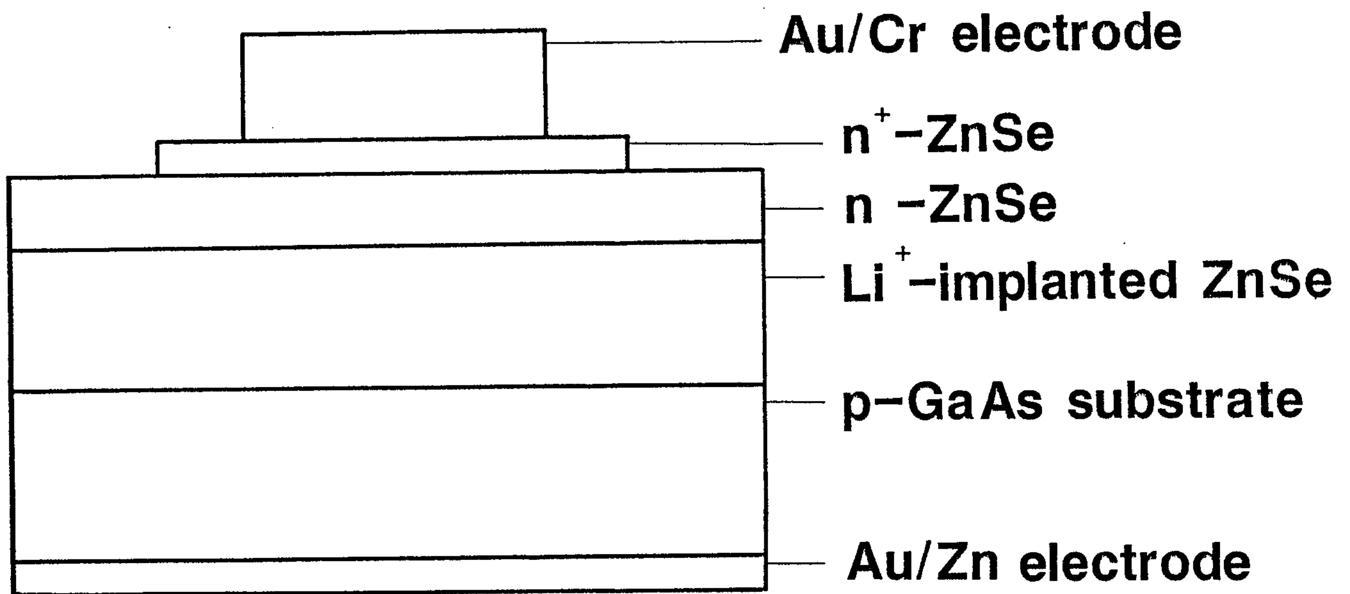

Fig.5.2.1. Illustration of npp type of device structure.

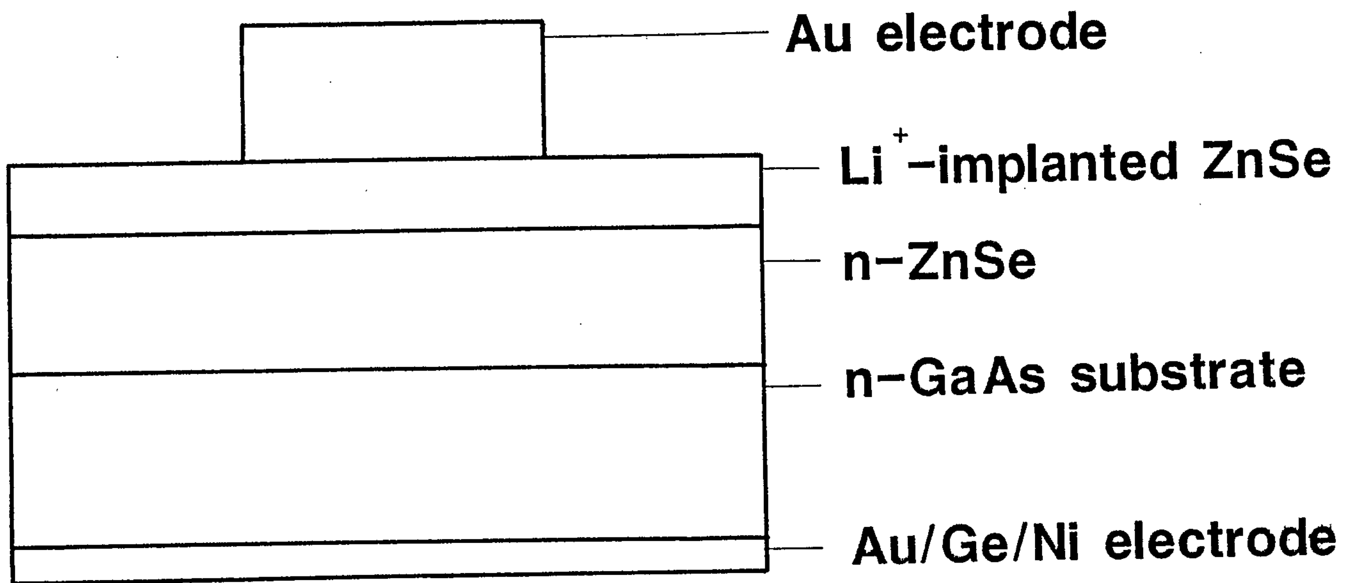

Fig.5.2.2. Illustration of pnn type of device structure.

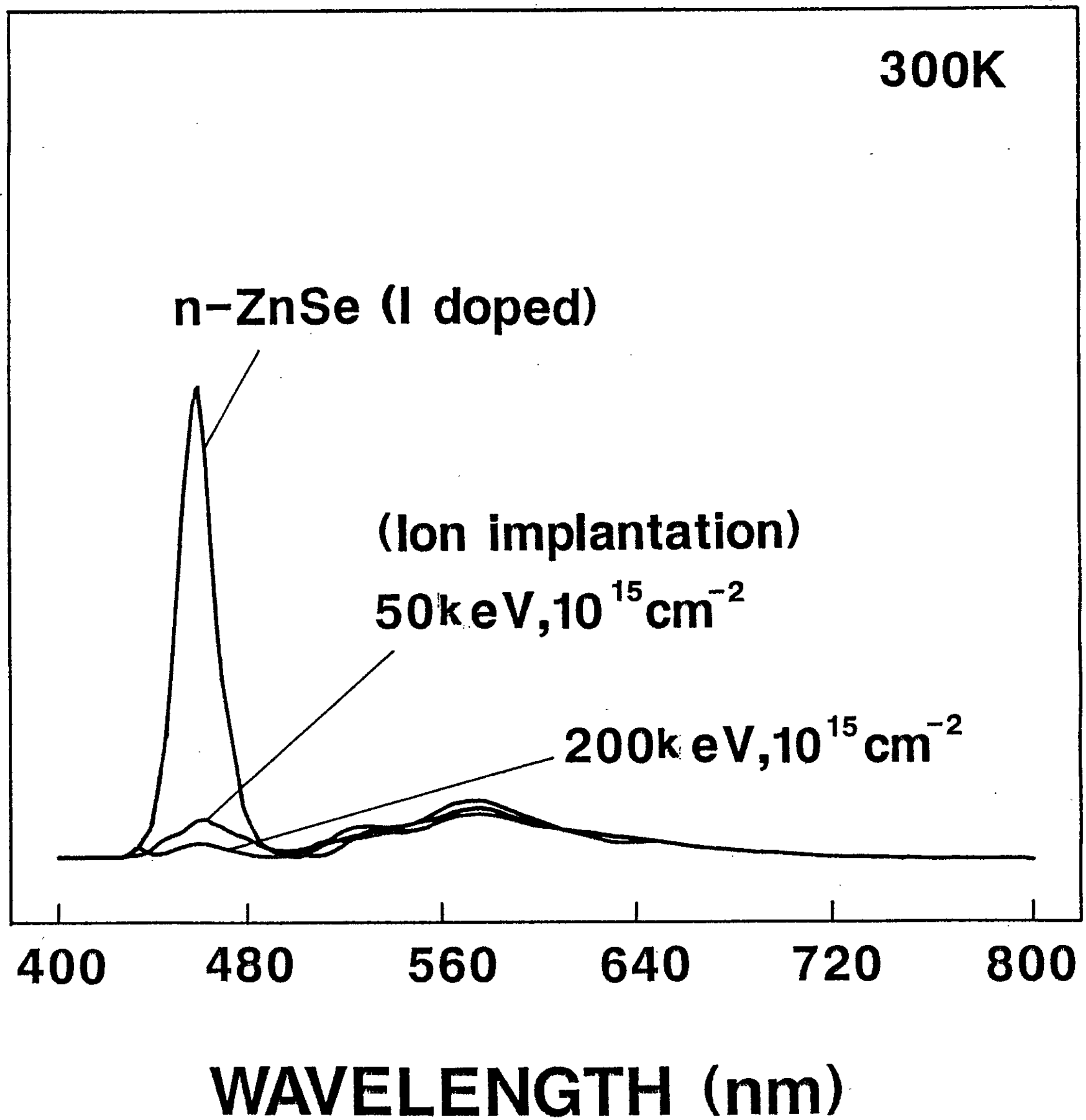

Fig.5.2.3. PL spectra at 300 K of the n-type over-epilayer on the Li^+-implanted (200 keV, 10^{15} cm^{-2} and 50 keV, 10^{15} cm^{-2}) epilayers after annealing at a T_t of 800 ^{o}C for 0.5 min in N_2 atmosphere.

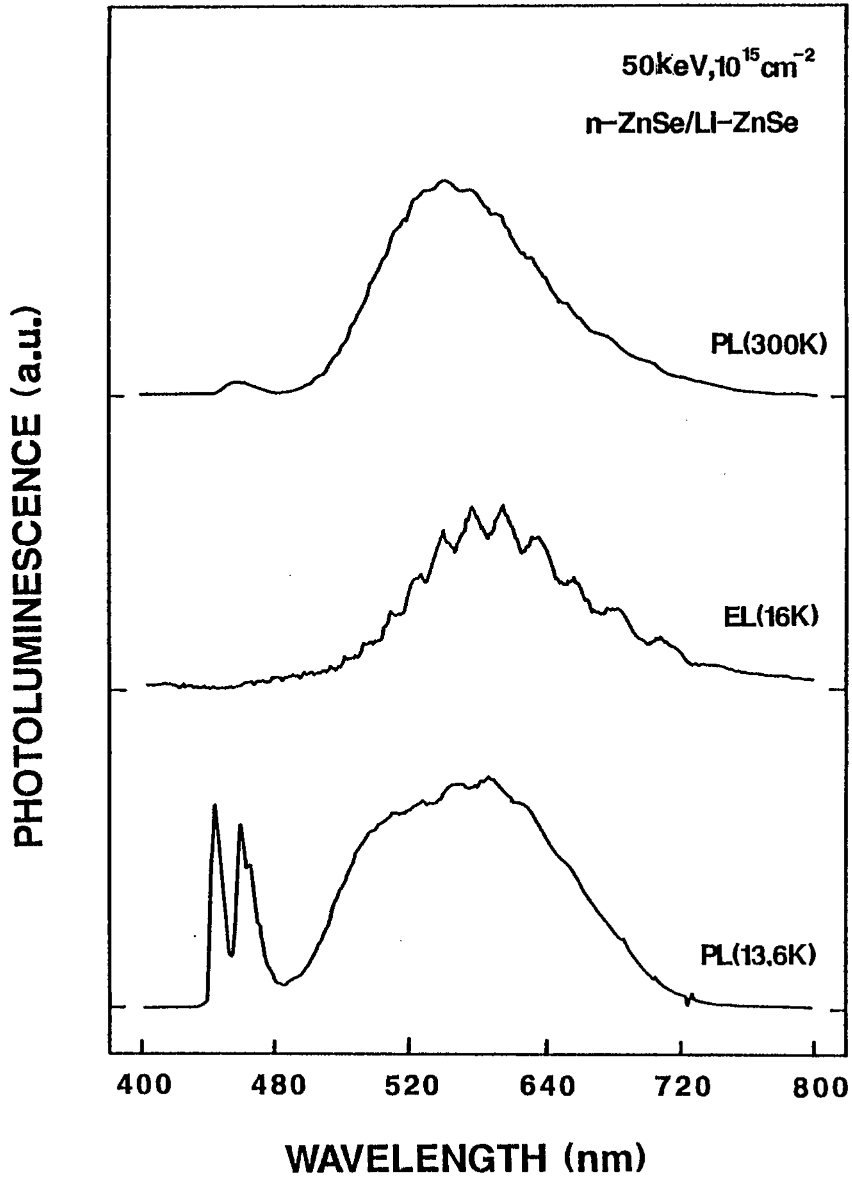

Fig.5.2.4. PL spectra at 300 K, 14 K and EL spectrum at 16 K of the B-LED (n-ZnSe/Li-ZnSe; 50 keV and 10^{15} cm^{-2}). The EL spectrum is measured at 40 V and 2 mA.

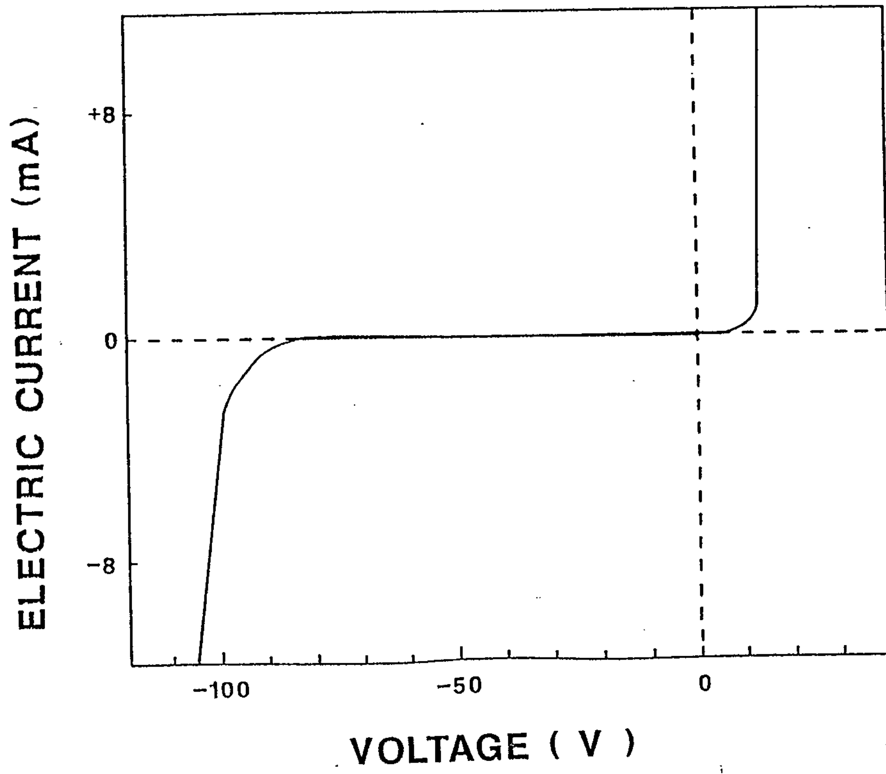

Fig.5.2.5. I-V property of the B-LED (n-ZnSe/Li-ZnSe; 50 keV and 10^{15} cm^{-2}).

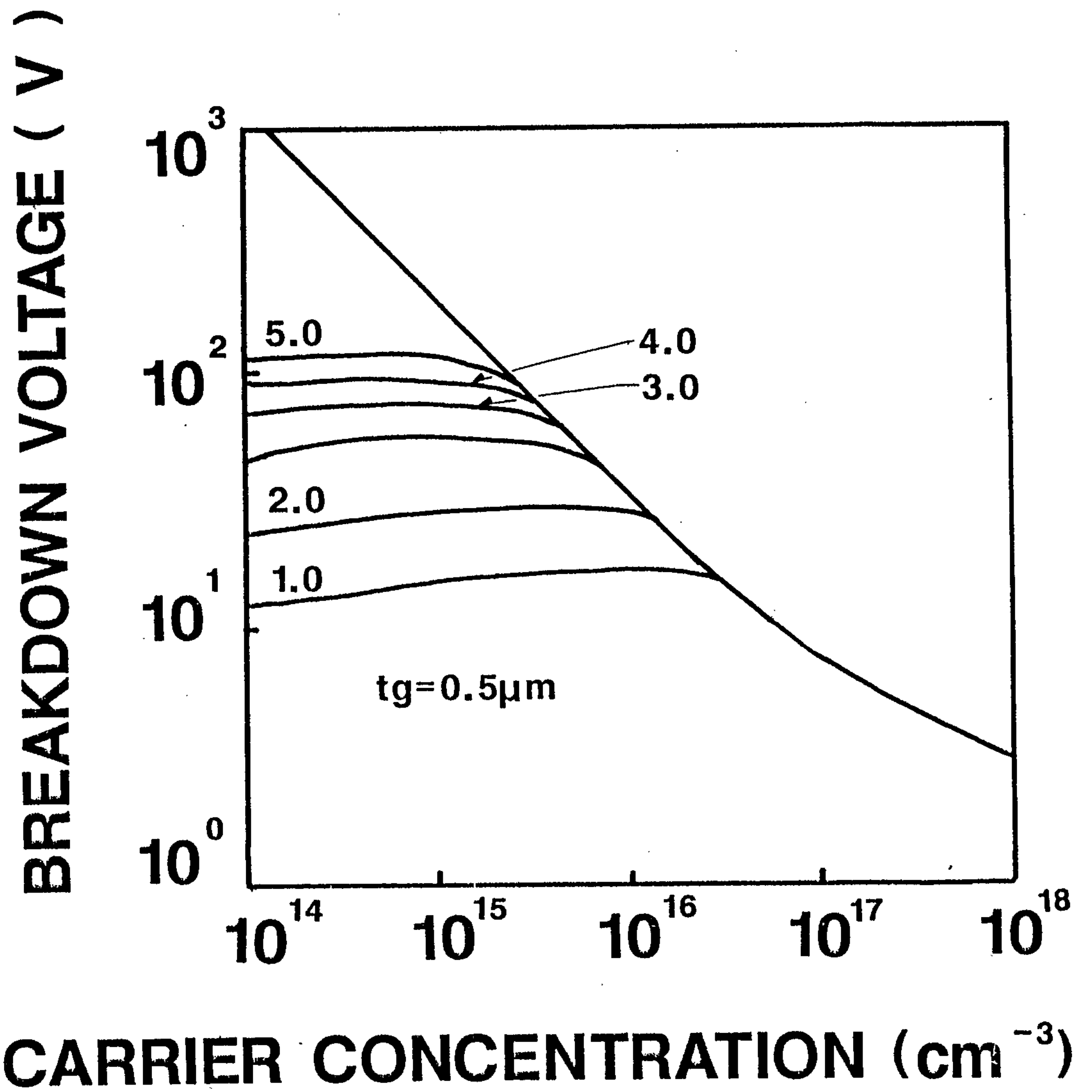

Fig.5.2.6. Relation between the breakdown voltage and hole carrier concentration. Considering the epilayer thickness, the hole carrier concentration of Li-doped ZnSe epilayer in the B-LED is about 10^{15} cm^{-3}.

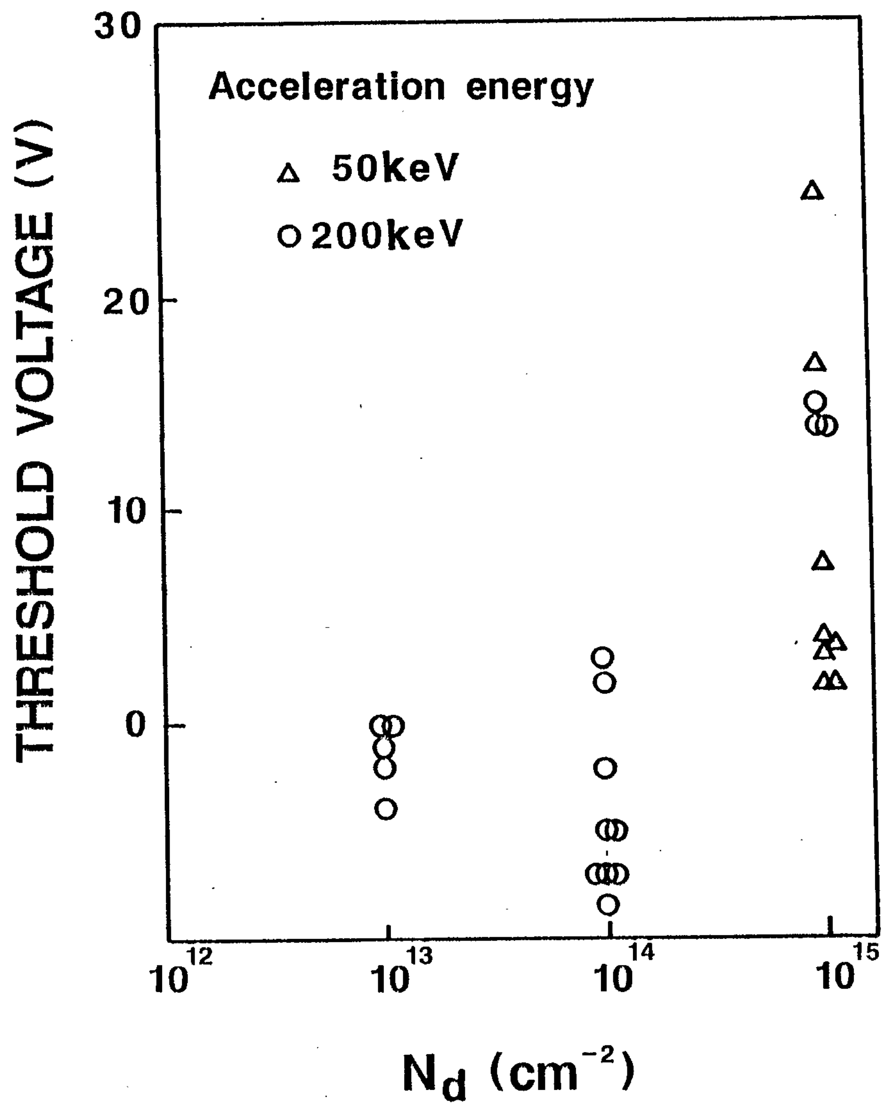

Fig.5.2.7. Dependence of N_d on the forward threshold voltage of the B-LED.

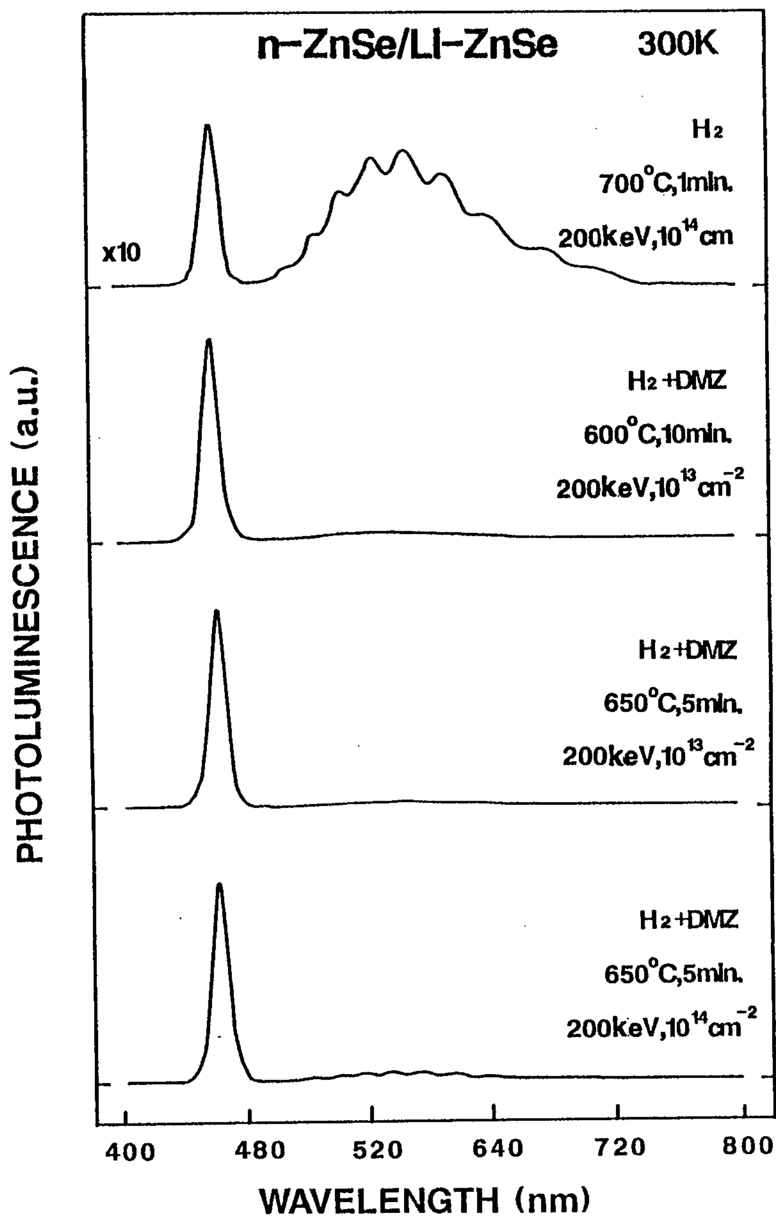

Fig.5.2.8. PL spectra at 300 K of the n-type ZnSe over-epilayers on the Li^{+}-implanted (200 keV, 10^{13} cm^{-2}; 200 keV, 10^{14} cm^{-2}) epilayers after annealing at various T_t (600-700 ^{o}C) for 1-10 min. in H_2 atmosphere including DMZ ($11.5x10^{-6}$ mol/min.) or only in H_2 atmosphere.

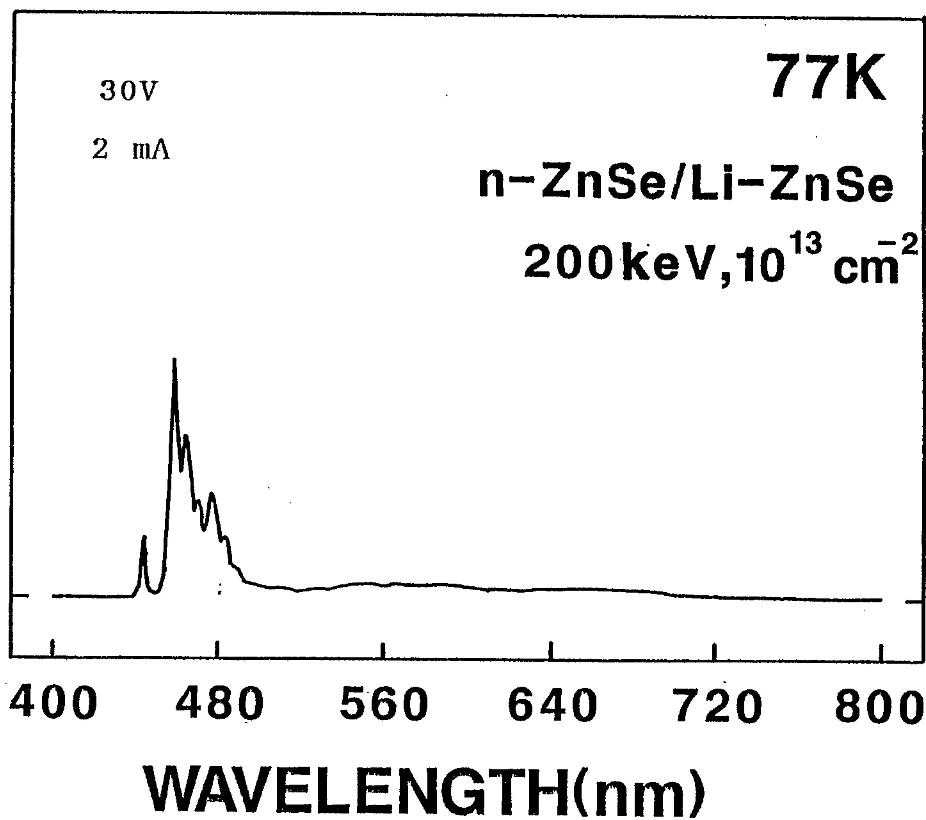

Fig.5.2.9. EL spectrum at 77 K of the B-LED with npp-type of device structure.

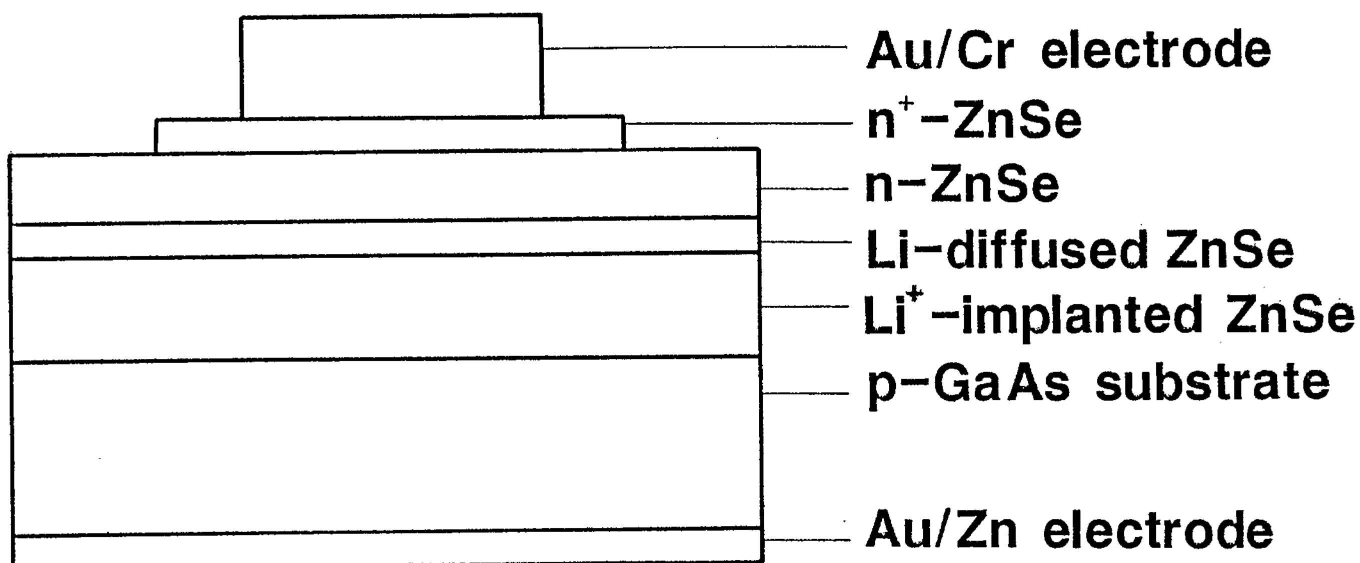

Fig.5.2.10. Illustration of nipp-type of device structure.

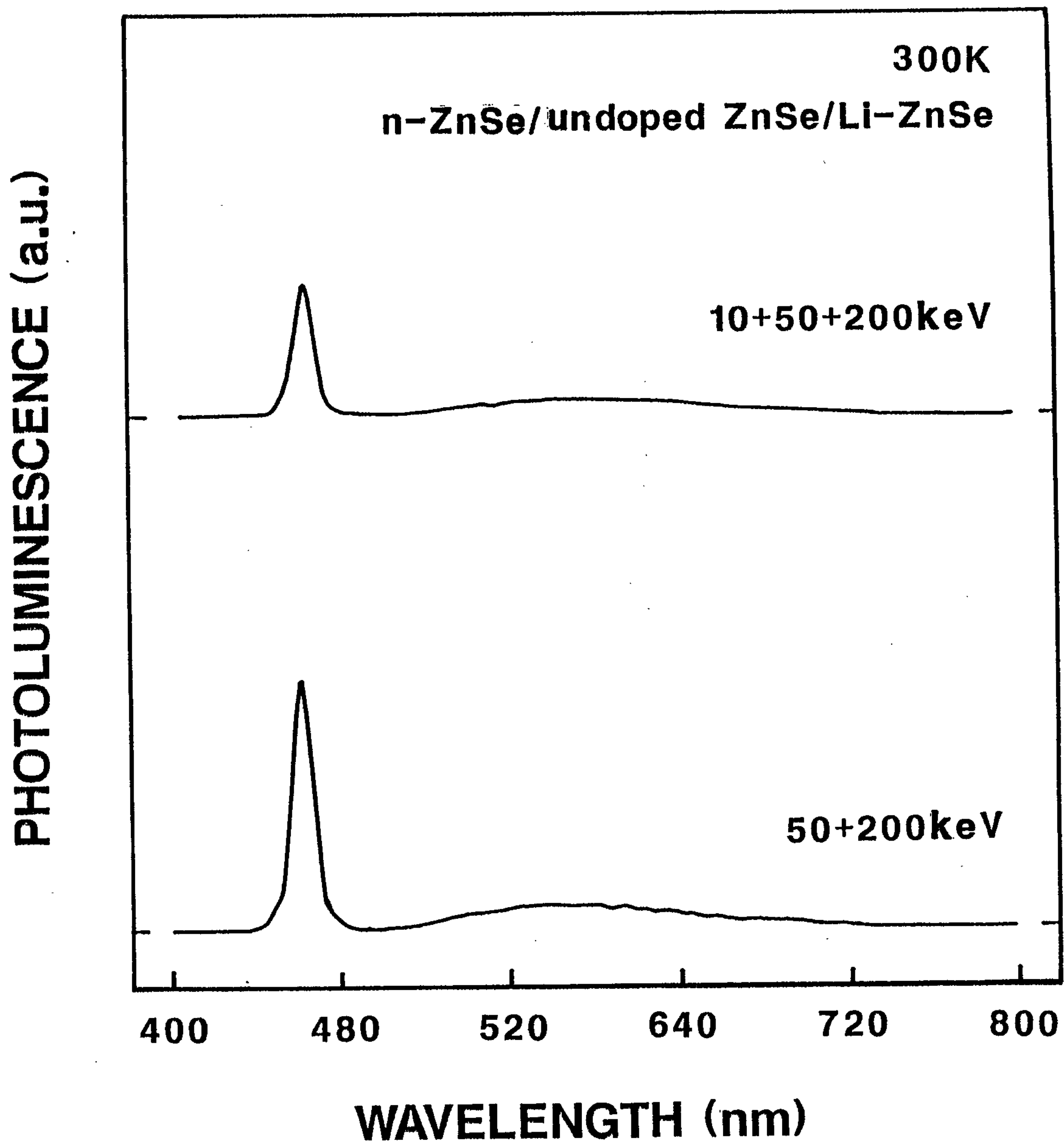

Fig.5.2.11. PL spectra at 300 K of the B-LED with the nipp-type of device structure (only ion implantation conditions are different; 3 steps and 2 steps as stated above.).

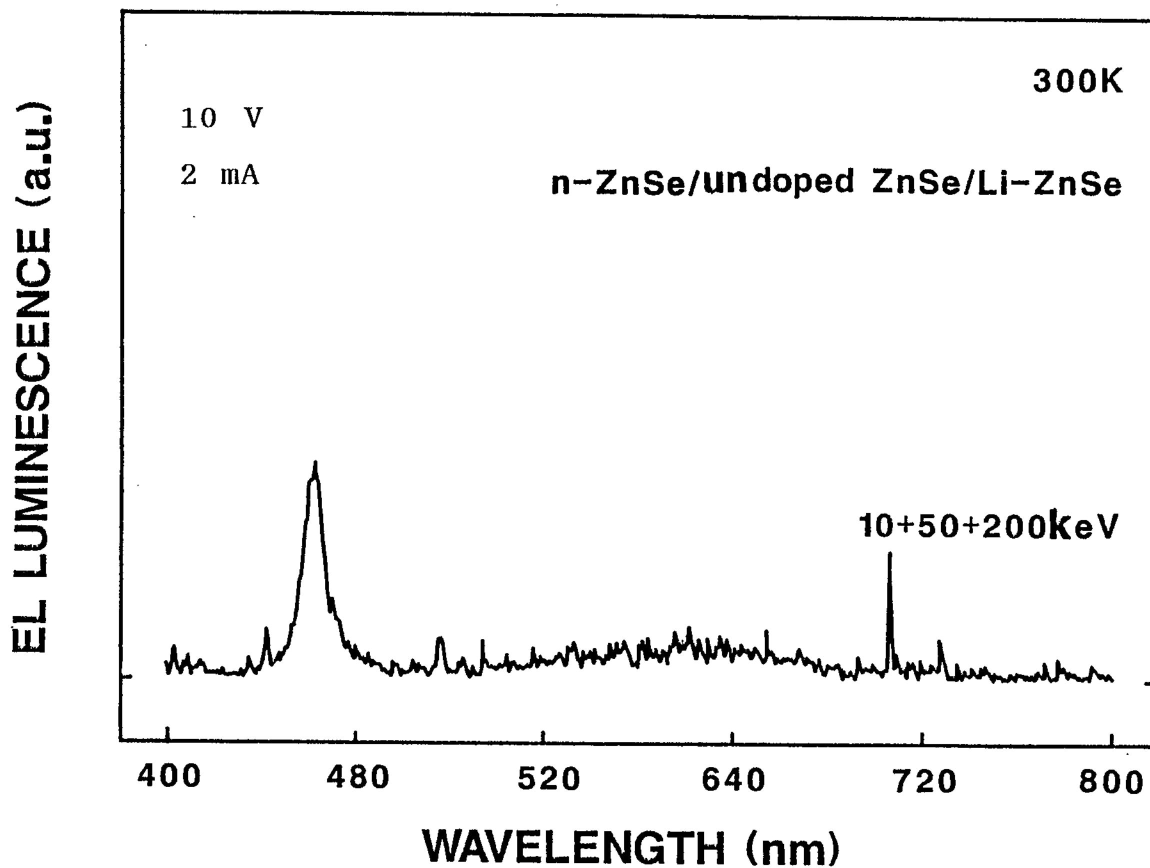

Fig.5.2.12. EL spectrum at 300 K of the B-LED (at 2 mA and 10 V).

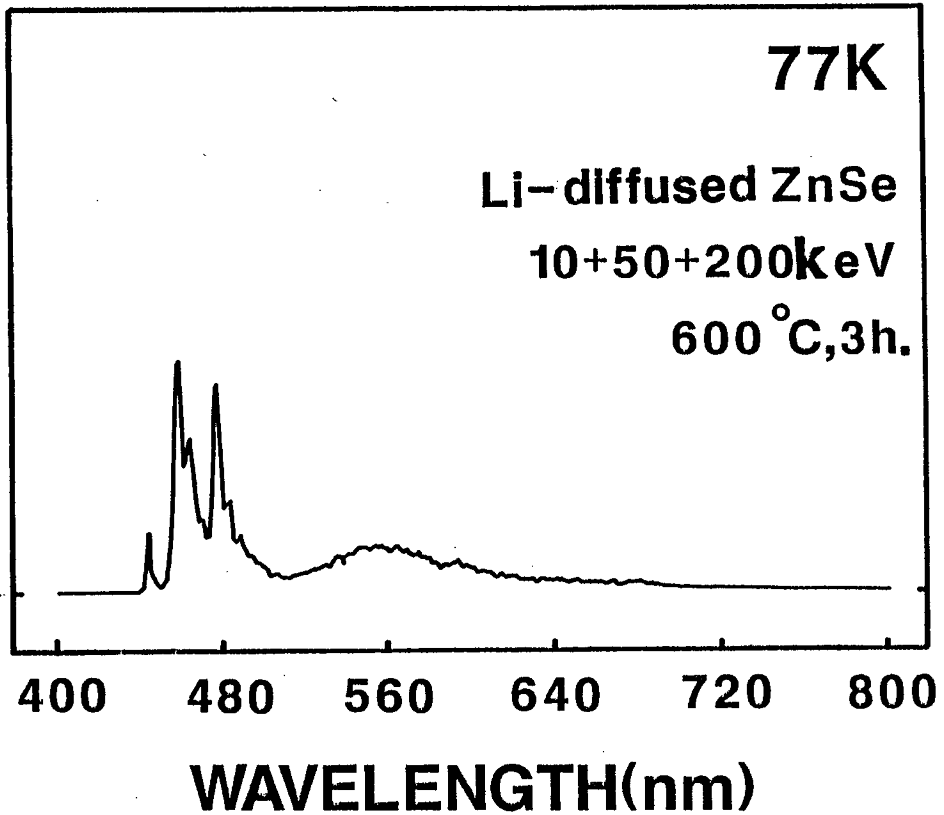

Fig.5.2.13. PL spectrum at 77 K of the diffused epilayer itself before fabricating the B-LED with nipp-type of device structure.

6. Conclusion

The ZnSe B-LED with pn junction has not been fabricated so far. I have discussed the reason why p-type ZnSe is not grown in the epitaxial growth and adopted MOVPE to overcome the compensation effect, since MOVPE could be run at low temperature (250 ^{o}C). To obtain a high quality undoped and subsequently p-type ZnSe, it is most important to grow the epilayers with high crystalline quality. The crystallographic property should be prominent and the residual impurity concentration must be low. Also, the crystalline quality is closely related to the lattice mismatching and growth conditions. We have investigated the effects of growth conditions on the crystalline quality both for undoped ZnSe heteroepilayers and for homoepilayers with complete lattice matching to find the optimum growth conditions. On the next stage, I have examined the thermal stability of the ZnSe epilayers grown at low temperatures. It is to apply the post-annealing procedure to ion implantation for p-type doping. It has been found that the crystalline quality of ZnSe epilayers is maintained even at 650 ^{o}C and still more to 700 ^{o}C by introducing the Zn vapor in the ambience. We have doped Li and Na impurities by ion implantation in the ZnSe epilayers and compared Li acceptor with Na acceptor in ZnSe. The radiation damage is related to the activation rate of acceptors, generation rate of SA centers and the crystalline quality. We have further doped Li impurities into ZnSe homoepilayers by ion implantation and tried a p-type conversion. Furthermore, Li is superior to Na as p-type

doping species in ZnSe because of the lightness of the radiation damage. We have fabricated a ZnSe B-LED with pn junction by growing n-type ZnSe on Li^{+}-implanted ZnSe and investigated the relation between the crystalline quality of n-type ZnSe and the device property. By improving the crystalline quality of n-type ZnSe, the blue emission is secured at 77 K from the B-LED. However, the EL emission has not been observed at 300 K. The reason of the failure is discussed. It is suggested that the crystalline quality of Li^{+}-implanted ZnSe epilayers near the pn junction is strongly related to EL property, since the crystalline quality of the implanted epilayer essentially determine the crystalline quality of the over-epilayer. The crystalline quality of the epilayers, accordingly, should be improved near the pn interface. A fatal part of the device using ion implantation is that pn interface is exposed to air. The crystalline quality at pn interface is thus unavoidably degraded. A new device structure ("nipp-type") is proposed. That is to interpose undoped ZnSe buffer epilayer on Li^{+}-implanted ZnSe before growing an n-type ZnSe epilayer. We utilize the buffer epilayer in diffusing Li impurities by annealing as a new pn interface. Since the pn interface can be maintained relatively clean, the white EL emission contains a dominant blue light emission spectrum at 300 K. It is thus of vital importance to keep the crystalline quality high near the pn interface to secure the strong blue light emission at 300 K.

The crystalline quality of the Li-diffused epilayer near the pn junction is yet to be improved. It is therefore possible to

develop the B-LED with high efficiency only by improving the crystalline quality near the pn interface.

7. Acknowledgements

I would like to thank Mr. Koyama, Dr. Yamashita, Dr.Tanaka and Professor Fujita (Department of Electrical Engineering, Kyoto University) for fruitful discussions and helpful corporations. Particularly, I would like to thank Mr. Koyama for the study of ZnSe crystal growth, who was in charge of ZnSe substrate preparation with keeping high crystalline quality. I would like to thank Professor Otsuka in Osaka University (Department of Physics, College of General Education) for some worthy advice, fruitful discussions and lead on this study and for the constitution of the thesis. Also, I am grateful to Professor Ohyama, Professor Hirata, Associate Professor Nakata (Department of Physics, College of General Education), and Professor Murase (Department of Physics, College of Physical Science) in Osaka university for fruitful discussions. Furthermore, I would like to thank Mr. Oka for ZnSe substrate preparation and Ms. Nagasaki, Mukae, Sakamoto, Katagai and Yamano for energetic assistance of PL measurement.

8. References

[1] K.Birus, in: Ergebinesse der exakten Naturwissenscaften, Band 20 (SprigerVerlag, Berlin, 1941)183.

[2] R.Z.Bachrach and D.G.Lorimor: Phys.Rev. B7(1973)700.

[3] K.Koga,T.Nakata and T.Niina: Extended Abstract 17 th Conf. SSDM(1985)249.

[4] L.Hoffman,G.Ziegler,D.Thesis and C.Weyrich: J.Appl.Phys. 52(1982)6962.

[5] W.L.Roth: "Physics and Chemistry of II-VI Compounds", ed. by M.Aven and J.S.Prener, North-Holland and Publishing Company, Amsterdam, Chap.3 (1967).

[6] E.Parthe: "Crystal Chemistry of Tetrahedral Structures", Gorden & Breach Sci.Publ. (1964).

[7] S.Fujita,H.Mimoto,H.Takabe and T.Noguchi: J.Cryst.Growth 47 (1979)326.

[8] D.R.Stull: Ind.Eng.Chem. 39(1947)717.

[9] R.A.Mcdonald et.al.: J.Chem.Eng.Data 4(1959)311.

[10] B.Ray ed.: "II-VI Semiconducting Compounds", (Benjamin Inc. New York).

[11] J.C.Phillips: "Bonds and Bands in Semiconductors", (Academic Press, New York and London, 1973) Chap.9, p.244.

[12] G.Mandel: Phys.Rev. 134(1964)A1073.

[13] G.Mandel, F.F.Morehead and P.R.Wagner: Phys.Rev. 136(1964) A826.

[14] F.A.Kroger: J.Phys.Chem.Solids 26(1965)1707.

[15] F.A.Kroger: J.Phys.Chem.Solids 26(1965)1717.

[16] H.Sato: J.Phys.Soc.Jpn. 21(1966)1481.

[17] Ph.Ged: J.Phys.Chem.Solids 40(1979)439.

[18] T.Mitsuyu,K.Ohkawa, and O.Yamazaki, Appl.Phys.Lett. 49(1986)1348.

[19] T.Yao and Y.Okada, Jpn.J.Appl.Phys. 25(1986)821.

[20] K.Yoneda,T.Toda,Y.Hishida and T.Niina: J.Cryst.Growth 67 (1984)125.

[21] M.Kitagawa,Y.Tomomura,K.Nakanishi,A.Suzuki and S.Nakajima: J.Cryst.Growth 101(1990)52.

[22] Y.Kawakami,T.Taguchi and A.Hiraki: J.Vacuum Sci.Technol. B5 (1987)1171.

[23] S.Fujita,Y.Tomomura and A.Sasaki: Jpn.J.Appl.Phys. 22 (1983)L583.

[24] S.Yamaga,A.Yoshikawa and H.Kasai: J.Cryst.Growth 86(1988) 252.

[25] T.Yokogawa,M.Ogura and T.Kajiwara: J.Appl.Phys. 62(1987) 2843.

[26] O.Kanehisa,M.Shiiki,M.Migita and H.Yamamoto: J.Cryst.Growth 86(1988)367.

[27] H.Ando,A.Taike,M.Konagai and K.Takahashi: J.Appl.Phys. 62 (1987)1251.

[28] V.P.Tanninen and T.O.Tuomi: Thin Solid Films 90(1982)339.

[29] Y.Ohki,Y.Toyoda,H.Kobayashi and I.Akasaki: Gallium Arsenide and Compounds: Inst.Phys.Conf.Ser. 63(1981)479.

[30] A.Shintani and S.Minagawa: J.Cryst.Growth 40(1974)1.

[31] H.M.Manasvit,F.M.Erdmann and S.I.Simpson: J.Electrochem. Soc. 118(1971)1864.

[32] M.Ilegems,R.Dingle and R.A.Logan: Bull.Am.Phys.Soc. 17 (1972)233.

[33] J.I.Pankov: IEEE Trans.Electron Devices ED-22(1975)721.

[34] J.I.Pankov,D.Richman,E.A.Miller and J.E.Berkeyheiser: J. Lumin. 4(1971)63.

[35] H.Hashimoto,H.Amano,N.Sawaki and I.Akasaki: Abstract 2nd Int.Conf.MOVPE,Sheffield,U.K.,1984,A3.4.

[36] G.Jacob,M.Boulou and D.Bois: J.Lumin. 17(1978)263.

[37] T.Yao,M.Ogura,S.Matsuoka and T.Morishita: Appl.Phys.Letters 43(1983)49.

[38] W.Stutius: J.Cryst.Growth 59(1982)1.

[39] T.Yao: J.Cryst.Growth 72(1985)31.

[40] R.N.Bhargava: J.Cryst.Growth 59(1982)1.

[41] S.Fujita, Y.Matsuda and A.Sasaki, J.Cryst.Growth 68(1984)231.

[42] A.Yoshikawa, K.Tanaka, S.Yamada and H.Kasai, Jpn.J.Appl.Phys. 32(1984)L424.

[43] P.J.Wright, R.J.M.Griffiths and B.Cockayne, J.Cryst.Growth 66(1984)26.

[44] H.Mitsuhashi, I.Mitsuishi, M.Mizuta and H.Kukimoto, Jpn.J.Appl.Phys. 24(1985)L578.

[45] A.Kamata, K.Hirahara, M.Kawachi and T.Beppu, The 17th Conference on Solid State Devices and Materials Extended Abstracts, Tokyo, 1985 (Business Center for Academic Societies Japan, Tokyo, 1985)p.233.

[46] S.Fujita, T.Yodo and A.Sasaki, J.Cryst.Growth 72(1985)27.

[47] W.Stutius, J.Appl.Phys. 53(1982)284.

[48] W.Stutius, Appl.Phys.Letters 40(1982)246.

[49] T.Yodo, H.Oka, T.Koyama and K.Yamashita, Jpn.J.Appl.Phys. 26(1987)L561.

[50] T.Yao, Y.Makita and S.Maekawa, Appl.Phys.Letters 35(1979)97.

[51] T.Yao and T.Okada, Jpn.J.Appl.Phys. 25(1986)821.

[52] W.L.Roth, in: Physics and Chemistry of II-VI compounds, Eds. M.Aven and J.S.Prener (North-Holland, Amsterdam, 1967) p.127.

[53] M.Neuberger, in: II-VI Semiconducting Compounds Data Tables (Electronic Properties Information Center, Hughes Aircraft Company, Culver City, CA, 1969).

[54] F.A.Ponce, W.Stutius and J.G.Werthern, Thin Solid Films 104 (1983)133.

[55] W.Stutius, J.Electron.Mater. 10(1981)95.

[56] P.J.Dean, Phys.Status Solidi(a) 81(1984)625.

[57] J.O.Williams, T.L.Ng, A.C.Wright, B.Cockayne and P.J.Wright, J.Crystal Growth 68(1984)237.

[58] P.J.Wright and B.Cockayne, J.Crystal Growth 59(1982)148.

[59] Y.Fujiwara, S.Shirakata, T.Nishino, Y.Hamakawa and S.Fujita, Jpn.J.Appl.Phys. 25(1986)1628.

[60] H.A.Mar and R.M.Park, J.Appl.Phys. 60(1986)1229.

[61] N.Maung and J.O.Williams, J.Cryst.Growth 86(1988)629.

[62] C.Werkhoven, B.J.Fitzpatrick, S.P.Herko, R.N.Bhargava and P.J.Dean, Appl.Phys.Letters 38(1981)540.

[63] P.Blanconnier,J.F.Hogrel,A.M.Jean-Louis and B.Sermage, J.Appl.Phys.52(1981)6895.

[64] R.M.Park, H .A.Mar and N.M.Salansky, J.Vac.Sci.Technol.B3(1985)1637.

[65] K.Menda, I.Takayasu, T.Minato and M.Kawashima, J.Cryst. Growth 86(1988)342.

[66] T.Koyama, T.Yodo, H.Oka, K.Yamashita and T.Yamazaki, J. Cryst.Growth 91(1988)639.

[67] T.Koda and S.Shionoya, Phys.Rev. 136(1964)A541.

[68] S.Shionoya, in: II-VI Semiconducting Compounds, Ed. D.G.Thomas (Benjamin, New York, 1967)p.1.

[69] T.Yodo, T.Koyama and K.Yamashita, J.Cryst.Growth 86 (1988)273.

[70] T.Taguchi and T.Yao, J.Appl.Phys. 56(1984)3002.

[71] H.Hartmann, R.Mach and B.Selle, in Current Topics in Materials Science, edited by E.Kaldis(North-Holland Publishing Company, Amsterdam, 1982), p.359.

[72] A.Aven and R.E.Halsted, Phys.Rev. A137(1965)228.

[73] M.Yamaguchi and T.Shigematsu, Jpn.J.Appl.Phys. 17 (1978)335.

[74] W.E.Martin, J.Appl.Phys. 44(1973)5639.

[75] M.Aven and E.L.Kreiger, J.Appl.Phys. 41(1970)1930.

[76] H.Bjerkeland and J.Holwech, Phys.Norv. 6(1972)139.

[77] A.K.Kun and R.J.Robinson, J.Electron.Mat. 5(1976)23.

[78] H.Hartmann, R.Mach and B.Selle, in Current Topics in Materials Science, edited by E. Kaldis (North-Holland Publishing Company, Amsterdam, 1982), p.357.

[79] A.S.Grove, Physics and Technology of Semiconductor Devices, 1 st ed. (John Wiley and Sons, Inc., New York, 1967), p.88.

[80] A.S.Grove, A.Roder and C.T.Sah, J.Appl.Phys. 36 (1965)802.
[81] M.Satoh and K.Igaki, Jpn.J.Appl.Phys. 22(1983)68.
[82] Shi-Min Haung, Y.Nozue and K.Igaki, Jpn.J.Appl.Phys. 22(1983)L420.
[83] T.Yodo, T.Koyama and K.Yamashita, J.Appl.Phys. 64(1988)2403.
[84] K.Ohkawa, T.Mitsuyu and O.Yamazaki, J.Appl.Phys. 62 (1987)3216.
[85] T.Niina, T.Minato and K.Yoneda, Jpn.J.Appl.Phys. 21 (1982)L387.
[86] B.Cockayne, P.J.Wright, M.S.Skolnick and A.D.Pitt, J. Cryst.Growth 72(1985)17.
[87] T.Yodo,T.Koyama, and K.Yamashita, J.Cryst.Growth 92(1988)196.
[88] Y.Horikoshi,M.Kawashima, and H.Yamaguchi, Jpn.J.Appl.Phys. 27,169(1988).
[89] K.Ohmi, I.Suemune, K.Kanda, Y.Kan and M.Yamanishi, Jpn.J.Appl.Phys. 26(1987)L2072.
[90] T.Yodo and K.Yamashita, Jpn.J.Appl.Phys. 27(1988)L903.
[91] T.Yodo and K.Yamashita, J.Cryst.Growth 93(1988)656.
[92] T.Yodo, T.Koyama and K.Yamashita, J.Appl.Phys. 65(1989)2728.
[93] L.Stock and W.Richter, J.Cryst.Growth 77(1986)144.
[94] H.Cheng, J.M.Depuydt, J.E.Potts and T.L.Smith, Appl.Phys. Letters 52(1988)147.
[95] J.Nishizawa, K.Itoh, Y.Okuno and F.Sakurai, J.Appl.Phys. 57(1985)2210.

[96] T.Yasuda, I.Mitsuishi and H.Kukimoto, Appl.Phys.Letters 52(1988)57.

[97] A.Ohki, N.Shibata and S.Zembutu, Jpn.J.Appl.Phys. 27(1988) L909.

[98] R.M.Park, H.A.Mar, and N.M.Salansky, J.Appl.Phys. 58(1985)1047.

[99] R.M.Park, J.Kleiman, H.A.Mar, and T.L.Smith, J. Appl.Phys. 63(1988)2851.

[100] A.Yoshikawa, S.Muto, S.Yamaga, and H.Kasai, Jpn.J. Appl.Phys. 27(1988)L260.

[101] M.Okajima, M.Kawachi, T.Sato, K.Hirahara, A.Kamata, and T.Beppu, Extended Abstract of the 18 th International Conference on Solid State Devices and materials, Tokyo, (1986)647.

[102] Y.S.Park, and B.K.Shin, J.Appl.Phys. 45(1974)1444.

[103] Y.S.Park, and C.H.Chung, Appl.Phys.Letters 18(1971)99.

[104] Z.L.Wu, J.L.Merz, C.J.Werkhoven, B.J.Fitzpatrick, and R.N.Bhargava, Appl.Phys.Letters 40(1982)345.

[105] J.S.Vermaak, and J.Petruzzello, J.Appl.Phys. 55 (1984)1215.

[106] G.F.Neumark, J.Appl.Phys. 51(1980)3383.

[107] H.Cheng, J.M.Depuydt, J.E.Pott, and M.A. Haase, J.Cryst. Growth 95(1989)512.

[108] J.Nishizawa, K.Itoh, Y.Okuno and F.Sakurai, J.Appl.Phys. 57 (1985) 2851.

[109] M.A.Haase, H.Cheng, J.M.Depuydt and J.E.Potts, J.Appl.Phys. 67 (1990) 448.

[110] A.Ohki, N.Shibata, K.Ando and S.Zembutu, J.Crystal Growth 93 (1988) 692.

[111] T.Yodo and K.Yamashita, Appl.Phys.Letters 54 (1989) 1778.

[112] P.J.Dean,B.J.Fitzpatrick and R.N.Bhargava, Phys.Rev. B26 (1982)2016.

9. Publication lists

[1] T.Yodo,H.Oka,T.Koyama and K.Yamashita: Japan.J.Appl.Phys. 26(1987)L561.
"Epitaxial Growth of High Quality ZnSe on GaAs Substrate by Atmospheric Pressure MOVPE Using Dimethyzinc and Hydrogen Selenide"

[2] T.Yodo,T.Koyama and K.Yamashita: J.Cryst.Growth 86(1988)273.
"GROWTH OF HIGH-QUALITY ZnSe BY MOVPE ON (100) ZnSe SUBSTRATE"

[3] T.Yodo,T.Koyama and K.Yamashita: J.Cryst.Growth 92(1988)196.
"DEPENDENCE OF SOURCE GAS MOLE RATIO ON CRYSTALLINE QUALITY OF ZnSe LAYERS GROWN ON (100) ZnSe SUBSTRATES BY ATMOSPHERIC PRESSURE METALORGANIC VAPOR PHASE EPITAXY"

[4] T.Yodo,T.Koyama and K.Yamashita: J.Appl.Phys. 64(1988)2403.
"High-quality epitaxial growth of ZnSe on (100) ZnSe by atmospheric pressure metalorganic vapor phase epitaxy"

[5] T.Yodo,T.Koyama,K.Ueda and K.Yamashita: J.Appl.Phys. 65(1989)2728.
"ZnSe homoepitaxial layers grown at very low temperatures by atmospheric pressure metalorganic vapor phase epitaxy"

[6] T.Yodo and K.Yamashita: Japan.J.Appl.Phys. 27(1988)L903.
"Effect of Heat Treatment on the Crystalline Quality of ZnSe Epilayers Grown by Metalorganic Vapor Phase Epitaxy"

[7] T.Yodo and K.Yamashita: J.Cryst.Growth 93(1988)656.
"THERMAL STABILITY OF ZnSe EPILAYER GROWN BY MOVPE"

[8] T.Yodo,K.Ueda and K.Yamashita: J.Cryst.Growth 99(1990)403.
"THERMAL STABILITY OF ZnSe HOMO- AND HETEROEPILAYERS GROWN AT LOW TEMPERATURES BY ATMOSPHERIC PRESSURE MOVPE"

[9] T.Yodo and K.Yamashita: Appl.Phys.Letters 53(1988)2403.
"Li-doped ZnSe epitaxial layers by ion implantation"

[10] T.Yodo and K.Yamashita: Appl.Phys.Letters 54(1989)1778.
"Na^{+}-implanted ZnSe epitaxial layers grown by atmospheric pressure metalorganic vapor phase epitaxy"

[11] T.Yodo,K.Ueda and K.Yamashita: J.Cryst.Growth 101(1990)289.
"p-TYPE DOPING BY ION IMPLANTATION INTO ZnSe EPITAXIAL LAYERS GROWN BY METALORGANIC VAPOR PHASE EPITAXY"

[12] T.Yodo,K.Ueda,K.Morio,K.Yamashita and S.Tanaka: J.Appl.Phys. 68(1990)3212.
"Photoluminescence study of Li- and Na-implanted ZnSe epitaxial layers grown by atmospheric pressure metalorganic vapor phase epitaxy"

[13] T.Yodo,K.Ueda,K.Morio,K.Yamashita and S.Tanaka: J.Appl.Phys. 68(1990)5674.
"Epitaxial growth of ZnS grown at low temperatures by atmospheric pressure metalorganic vapor phase epitaxy"

[14] T.Yodo,K.Ueda,K.Morio,K.Yamashita and S.Tanaka: J.Cryst.growth 107(1991) 659.
"High quality over-epilayer growth of ZnSe on Li^{+}-implanted ZnSe epilayers by atmospheric pressure MOVPE"